The Essential Roles of DNA Resection AND The Impact of Loss of Function NHEJ Mutations on DSB Repair In Human Somatic Cells

A DISSERTATION SUBMITTED TO THE FACULTY
OF THE UNIVERSITY OF MINESOTA
BY

EU HAN LEE

IN PARTIAL FULFILLMENT OF THE
REQUIREMENTS FOR THE DEGREE OF DOCTOR
OF PHILOSOPHY

Eric A. Hendrickson, Ph.D.
Advisor

March 2014

ACKNOWLEDGMENTS

With great pleasure I would like to express my gratitude to my advisor, Dr. Eric Hendrickson, for the support, guidance, and welcoming us into your home to break bread on numerous occasions. I am greatly indebted to my exam committee, Dr. Michel Sanders, Dr. Tom Hayes, Dr. Deanna Koepp, and Dr. Jeff Simon for their tremendous support in times of great struggle and their scientific feedback. I am also very appreciative of the efforts invested by the principal investigators and personnel in the BMBB/MCSB departments to train and support graduate students. As an international student, I am humbled by the generosity of the institutions in this country that have made graduate school a possibility for me.

I want to thank my dearest husband Dr. John Billig, I am grateful for all his support and understanding of the sacrifices I had to make in graduate school. Our pet dog Austin, who is always the first to greet me at the door, his unconditional love and his non-judgmental barks. I would like to thank my eccentric parents (in Malaysia) who don't always get me, but I love them for all they have done and for mixing up half their genomes that accounts for who I am today; and my sister who shares some of my genes. I also wish to thank my precious grandfather, aunts, and cousins who are scattered around in Asia/Pacific and US.

I want to thank the Sobeck laboratory for our daily scientific and non-scientific exchanges as well as their generosity for sharing reagents. It has been a great pleasure and an honor to collaborate with the Sobeck laboratory. I would also like to express my gratitude towards Dr. Tsuyoshi Kawabata from the Shima laboratory for sharing new protocols with me, as well as the Bielinsky laboratory for sharing their reagents. I am eternally grateful to Dr. Duncan Clarke for permitting me to use his confocal microscope.

I would also like to thank the participants of our Friday afternoon combined laboratory meetings (Bielinsky, Harris, Shima, Sobeck, and Hendrickson laboratories) for their scientific feedback. Last but not least, it has been a pleasure to work with current and previous Hendrickson laboratory members especially Dr. Sehyun Oh and Dr. Farjana Fattah with whom I have collaborated.

DEDICATION

To my husband, parents, family, Austin (pet dog),
Alan Turing, Rosalind Franklin,
and world peace.

ABSTRACT

DNA resection is a highly conserved biological process that protects the genome. It links DNA damage to checkpoint activation and is required for the homologous recombination (HR) pathway. The relatively recent discovery of CtIP, EXO1, and DNA2 as the nucleases responsible for DNA resection in the HR pathway, has generated significant interest in this field of DNA repair. The majority of studies depend upon "knockdowns" via the use of siRNA to address the function of CtIP, EXO1, and DNA2, and then usually only in the presence of exogenous DNA damage. With our conditionally-null knockout human cell lines, we find that CtIP, EXO1, and DNA2 are essential in human somatic cells and that they are required for normal DNA replication fork progression even in the absence of exogenous DNA damage. Furthermore, we find that CtIP, EXO1, and DNA2 are co-regulated and that they coordinately regulate the stability of FANCD2, BRCA2, Rad51, and CHK1. Current chemotherapeutic drugs work by inhibiting DNA replication. Since HR is required for the repair of damaged replication forks, the process of DNA resection is a promising drug target, either alone or in combination in combination with current chemotherapeutic drugs. Therefore, it is important that we understand the mechanisms and regulation of CtIP, EXO1, and DNA2.

The nonhomologous end-joining pathway (NHEJ) is subdivided into a Ku – dependent pathway {Classical NHEJ (C-NHEJ)} and a Ku-independent, {Alternative NHEJ (A-NHEJ)}. C-NHEJ repair normally dominates in human cells but how or why this happens has remained obscure. Using C- NHEJ loss-of-function mutant cell lines for Ku86, LIGIV, DNA-PK_{cs}, and XLF, we found that Ku86 uniquely and strongly represses the A-NHEJ pathway, which suggests that Ku86 regulates DSB repair by controlling pathway choice decisions.

Table of Contents

LIST OF FIGURES

CHAPTER II: The Impact of DNA Resection Mutants and The Regulation of CtIP, EXO1, and DNA2 in Human Somatic Cells.

LIST OF TABLES

CHAPTER II: The Impact Of DNA Resection Mutants And The Regulation Of CtIP, EXO1, And DNA2 In Human Somatic Cells.

CHAPTER I:

Introduction

Introduction

The human genome has been determined to be 3 billion base pairs in length and it encodes 20,000 genes that reside in 23 pairs of chromosomes. Impressively, all this DNA is contained within each and every one of the 3.7 x 10^{13} cells[1-6] that make up a human body. Ironically (and tragically), it only takes as little as one mutation of one gene in one cell to take life away.

In a multi-cellular organism, cells are organized into tissues and organs such that they regulate each other's growth and proliferation. In an environment where cells are required to proliferate, mitogens are secreted to signal cells in a G0 quiescent state to enter the cell cycle[1,7]. The active phases of the cell cycle consist of G1-, S-, G2- and M-phases[1]. In general, G1 cells prepare the cell to enter S-phase where DNA replication occurs to copy the genome only once[8]. When DNA replication is complete in S-phase, the cell enters the G2-phase where it ensures that replication and repair is complete before entering M-phase. In M-phase, the duplicated genome is first segregated equally into two portions that will eventually be transmitted to the two daughter cells[8].

DNA damage can occur in all phases of the cell cycle. Of the various forms of DNA damage, DNA double-stranded breaks (DSBs) pose the greatest threat to the cellular genome because they are lethal or mutagenic when unrepaired or misrepaired, respectively[1]. DSBs can arise exogenously from factors such as ionizing radiation (IR) exposure. Alternatively, DSBs can also arise from endogenous metabolic processes. One such process is DNA replication. When DNA replication forks stall for long periods of time they can collapse into DSBs[9,10]. To

manage such threats, the cell has evolved checkpoint mechanisms that arrest cell cycle progression to provide sufficient time to repair the DSBs. When these checkpoints fail, cell cycle progression with incomplete repair results in mutations and genomic instability[1,9,10]. Importantly, the cell is equipped with at least two DSB repair mechanisms: homologous recombination (HR) and nonhomologous end-joining (NHEJ) pathways. The HR pathway requires an intact template homologous to the broken chromosome for error-free repair[11]. In contrast, the NHEJ pathway does not require a homologous template but simply rejoins two ends of broken DNA together; however, unfortunately NHEJ is often error prone, which can result in mutagenesis[12].

One of the major mechanistic distinctions between HR and NHEJ is that HR generally requires extensive resection of the DNA ends whereas C-NHEJ requires little or no resection. DNA resection is a conserved biological process that is also linked to checkpoint activation. A trio of nucleases CtIP, EXO1, and DNA2 are implicated in DNA resection and are presumed to generate the single-stranded DNA (ssDNA) ends that are required for the HR repair of DSBs[13-16]. Besides being required for DSB repair, the essential function(s) and regulation of these nucleases has not been thoroughly investigated in human cells and will be addressed in this study.

The Most Lethal Form Of DNA Damage: DNA Double-Stranded Breaks (DSBs)

On a daily basis, a cell is confronted by numerous exogenous and endogenous events that cause DNA damage that includes ssDNA breaks, the formation of bulky adducts, mismatched base pairing, and DNA DSBs. DSBs hold the greatest threat to cellular survival and fitness because they can trigger either cell death or genomic instability, respectively[1]. Reactive oxidative species (ROS) from endogenous metabolites or exogenous sources, such as IR, randomly breaks sugar-phosphate bonds on the backbones of both DNA strands. When the breaks occur close enough to each other, the strands can separate into two free ends, which is classified as a DSB[17].

Not all DSBs are random, nor harmful however. Thus, programmed DSBs are also produced during V(D)J recombination which is required for antibody diversification in developing T- and B- cells of our immune system[18]. Programmed DSBs in the immune system rely on the C-NHEJ pathway for repair, and mutations in any of the genes that compromise the C-NHEJ pathway result in patients with severe combined immunodeficiency syndromes (SCID)[19].

DNA replication is a major source of endogenous (and decidedly unwanted) DSBs[9,10]. Replication forks can spontaneously stall when they encounter lesions or regions that are difficult to replicate. Highly repetitive regions in the human genome are often difficult to replicate. These include trinucleotide repeats (TNRs), telomeres, LINE, or ALU repeat elements that can transiently form complex DNA structures at periods when they become single-stranded[20-22]. During DNA

replication, these transient complex DNA structures, such as hairpins, triplex and quadruplex DNA can trigger replication fork stalling[2,4-6]. During DNA replication, these transient complex DNA structures, such as hairpins, triplex and quadruplex DNA can trigger replication fork stalling[2-6]. Stalled forks are stabilized and then restarted by the ATR-CHK1 signaling pathway[9-11,23], which involve the HR and Fanconi anemia pathways[24,25]. Importantly, if the stalled forks are not repaired or restarted in a timely fashion, endonucleases can cleave exposed ssDNA replication forks, which results in the formation of a DSB[9,10,26,27].

Regardless of the source, DSBs must be repaired; otherwise, they lead to mutations, genomic instability or cell death[28]. To counter this threat, organisms have evolved specialized DNA repair pathways to fix the damaged DNA. DSB repair is a challenging process because it is no simple task to accurately rejoin two ends of DNA that are in motion. Metaphorically speaking, DSB repair would be as challenging as accurately joining two ends of a broken thread, without using knots. In human cells, DSBs are repaired by the NHEJ[12,29] or the HR pathways[11]. These two DSB repair pathways are mechanistically distinct. NHEJ directly re-ligates the broken ends of DNA in a manner that can be error prone[2,12] thus leading to the loss of genetic information. In contrast, HR repairs DSBs by "copying" genetic information that was lost at the site of the DSB from an undamaged homologous template for repair. As a result, HR repair is generally an error-free repair pathway that restores genetic information[11].

Cell Cycle Checkpoints

Since the genome is constantly challenged with DNA damage, cells are equipped with G1-, S-, and G2-checkpoints to sense DNA damage and delay the progression of the cell cycle[30]. Checkpoints essentially extend the cell cycle phase where DNA damage has occurred and hence they provide the cell with a window of time to repair the damaged DNA before moving on to the next cell cycle phase[1,9,31] . A cell that proceeds to the next cell cycle phase with incomplete repair will suffer from genomic instability, mutations, and even apoptosis[30]. The ATM-CHK2 and ATR-CHK1 pathways primarily govern cell cycle checkpoints by sensing the DNA damage, transmitting the signal to arrest the cell cycle and then facilitating DNA repair[1,32]. The ATM-CHK2 pathway is primarily responsive to DSBs while the ATR-CHK1 pathway is extremely responsive to DNA damage with exposed tracts of ssDNA such as occurs at stalled DNA replication forks[9].

DNA damage in G1 triggers G1 checkpoint activation. How DNA damage is sensed is still biochemically vague. What is clear, however, is that sensing activates ATM, which, in turn phosphorylates and activates p53. The phosphorylation of p53, an established tumor suppressor, extends the half-life of the p53 protein and increases its transcriptional activity for various target genes[30]. To arrest the cell cycle, p53 increases the transcription of p21/CIP1[30]. As p21/CIP1 levels increase in the cell, it deactivates Cdk2/Cylin E to arrest the cells in G1 and prevent the transition into S-phase. NHEJ repairs the majority of G1-phase DSBs by default

because there are no sister chromatids for the HR pathway[12,33]. Once the damage is repaired, the cell resumes its cell cycle progression.

The S-phase checkpoint is considerably more complicated than the G1-checkpoint. Safeguarding a genome that is actively doubling in size is intuitively, a complex process. In S-phase, an estimated 30,000 to 50,000 origins of replication are initiated, which translates to 60,000 to 100,000 replication forks[34]. Damaged or stalled replication forks are complex DNA structures with vulnerable, naked ssDNA, which can collapse into dangerous DSBs if these structures continue to persist[9]. Clearly, it is in the cell's best interest to repair and restart these forks in a timely fashion. Furthermore, if the cell transitions into the G2/M phase with incomplete DNA repair and/or replication, the cell will suffer from mutations, loss of genetic information and genomic instability. The S-phase checkpoint safeguards the cell genome by providing the cell time to repair and complete replication by delaying S-phase progression[23,35].

Although the details of fork re-start/repair need to be elucidated, many of the general steps are already known. At stalled replication forks, stretches of naked ssDNA are exposed and subsequently coated by RPA. RPA-coated ssDNA, in turn, recruits TOPBP1, Rad17, and the 9-1-1 complex, whose job it is to mediate the recruitment of ATR-ATRIP[9,35]. Claspin, which is normally associated with moving replication forks, mobilizes from stalled forks to interact with ATR-ATRIP and mediate the phosphorylation of the CHK1 kinase at serine 345 and serine 317[36-38]. Phosphorylated CHK1 is the direct activator of the S-phase checkpoint. Similar to the G1-checkpoint, S-phase checkpoint prevents progression into G2/M-phase by

inhibiting S- to G2-phase promoting factors. In this case, Cdc25A and Cdc25C are phosphorylated by CHK1, which signals them for protein degradation and sequestration by 14-3-3, respectively[32]. In a situation where stalled forks collapses into DSBs, the ATM-CHK2 pathway is also activated which further prolongs the S-phase delay[9].

After DNA replication is complete, the cell enters the G2-phase where it prepares itself for cell division in the mitotic (M-) phase. In M-phase, the cell segregates its newly duplicated genome and physically pinches itself in two, producing a daughter cell with an identical set of genes. The G2/M-checkpoint surveys the genome one final time for any unrepaired damage[31]. Both the ATR-CHK1 and ATM-CHK2 pathways activate the G2/M checkpoints by upregulating factors that deactivate the Cdc25 family of phosphatases, which promote cell cycle progression as described above. As a result, Cdk1/Cyclin B, the cyclin-dependent kinase, which promote G2/M progression remains inactive, thereby arresting the cell in G2[32]. When cells arrest in either S- or G2/M-phases the HR pathway is the preferred mechanism to repair damaged DNA because sister chromatids are available after DNA replication[33]. Moreover, damaged and stalled DNA replication forks are complex structures that require the precision of HR to repair and restart, without losing any genetic information[26].

DNA Replication: How The Cell Copies And Protects Its Genome

When a cell is prompted to enter the active cell cycle to proliferate, it must duplicate all 3 billion base pairs of genetic material, through DNA replication. DNA replication is a critical biological process that occurs in the S-phase of cell cycle with the purpose of making a "copy" of its genome. The genome must be copied with the highest fidelity; otherwise, harmful mutations may be passed on to the future generations[8,39].

In the G1-phase, the cell prepares for DNA replication. It is during G1 that ORCS, Cdt1 and Cdc6 proteins load the MCM2-7 helicase complexes on to unique sequences called replication origins. Together, ORC, Cdt1, Cdc6, and MCM2-7 are called the pre-replication complex (or PreRC) and any origin bound by preRC is considered licensed[8]. The purpose of licensing is to ensure that chromosomes are replicated once and only once per cell cycle and to potentiate the origins for the initiation of DNA replication. As the cell enters S-phase, the Dbf4-dependent kinase (DDK) is activated, which in turn phosphorylates the MCM subunits to load Cdc45 and Treslin. Next, activated cyclin-dependent kinase (CDK) phosphorylates Treslin and RecQ4 facilitating the binding of TopBP1 which then recruits the Go-ichi-ni-san (GINS) helicase complex and polymerase-ε, the DNA polymerase that extends RNA primers on the leading strand[40]. Finally, polymerase-α:primase, the polymerase that synthesizes RNA primers on template; and pol-δ, the lagging strand DNA polymerase that extends the RNA primers[40], arrive at the origin. DNA replication initiates when two replisomes emerge and travel away from each other [8,39,41].

DNA Replication Barriers: Repetitive Regions

The genomic landscape of a human cell is wrought with obstacles for a traveling replication fork. Highly repetitive regions in the human genome, including trinucleotide repeats (TNRs), telomeres, LINEs, SINEs, DNA transposons, and ALU repeat elements transiently form complex DNA structures when they become single-stranded[20-22]. During DNA replication, these complex DNA structures, such as hairpins, triplex and quadruplex DNA become barriers to DNA replication and trigger replication fork stalling[2,4-6]. In addition, common fragile sites (CFS) are late replicating, AT rich regions that are prone to breakage when cells are under replication stress or when ATR function is compromised[42-44]. Recently, a second class of CFS termed early replicating common fragile sites (ERCFs) was discovered. As their name implies, ERCFs are early replicating regions that are GC-enriched regions (including LINEs, SINEs, ALUs and tRNAs) that are prone to breakage during DNA replication[45]. Similar to CFSs, ERCFs are more prone to break if ATR is inhibited[42-44]. The presence of these fragile sites strongly suggest that the volatility of DNA replication is currently underestimated.

Importantly, stalled replication forks are detrimental to the cell. They must be repaired and restarted in a timely manner; otherwise, the prolonged stalling will lead to collapse of a fork into a dangerous DSB. At stalled replication forks, stretches of naked ssDNA are exposed and are subsequently coated by RPA, which in turn recruits TOPBP1, Rad17, and the 9-1-1 complex to mediate the recruitment of ATR-ATRIP[9,35]. Claspin, which is normally associated with an active replication fork,

detaches from stalled forks and localizes with ATR-ATRIP to mediate the phosphorylation of the CHK1 kinase at serine 345 and serine 317[36-38], which directly activates the S-phase checkpoint.

Stalled forks are stabilized and then restarted by ATR-CHK1 signaling[9-11,23], which activates the HR and FA pathways[24,25].

Homologous Recombination (HR)

In contrast to NHEJ, which can simply fuse the ends of DSB together, the HR pathway requires an undamaged template that is homologous to the site of damaged DNA in order to enact repair. Not surprisingly, the HR pathway is upregulated in the late S and G2 phases of the mammalian cell cycle where sister chromatids are available[33,46]. HR repair normally occurs with high fidelity such that it can restore any genetic information that might be lost at the site of DNA damage.

The HR pathway was originally identified in yeast (*S. cerevisiae*) and it is well conserved in higher organisms. The RAD50 epistasis group - RAD50, RAD51, RAD52, RAD54, RAD55, RAD57, RAD59, MRE11, and XRS2 - whose products are the core components of the HR machinery, was found through a reverse genetic screen for radiosensitive mutants[47]. In humans, the HR pathway is more complicated but nonetheless orthologs of the RAD50 epistasis group have been identified. However, additional factors such as BRCA1, BRCA2, Rad51 homologs (Rad51C, Rad51B, Rad51D, and DMC1), and Rad54 homologs (Rad54B, and Rad54L) expand the repertoire of the human HR machinery[11,33].

HR repair begins with an essential 5'>3' DNA resection step of the ends of a DSB, facilitated by the MRN (Mre11, Rad50, and Nbs1) complex that generate 3'-ssDNA[33]. RPA is then recruited to coat the ssDNA, which simultaneously protects the ssDNA from degradation and activates the DNA damage checkpoint via ATR-ATRIP recruitment as described above. BRCA2 is then recruited to the site of damage where it displaces RPA for Rad51, forming a nucleoprotein filament[11]. The nucleoprotein filament (Rad51-ssDNA) is stabilized by Rad54, which also subsequently aids the homology search for an undamaged homologous template correct template[48]. Rad54 facilitates the nucleoprotein filament's invasion of the undamaged homologous template, and displaces one of the template strands to form a D-loop heteroduplex[48]. Here, DNA polymerases extend the invading strand and via DNA replication recover any lost genetic information suffered at the DSB[40]. When extension of the invading strand is complete, the newly synthesized (nascent) DNA strand is ligated back to the native strand where the break originally occurred by DNA Ligase I(LIGI)[11].

DNA End Resection

DNA resection is a highly conserved biological process that generates ssDNA from dsDNA and is catalyzed by nucleases. DNA resection is a critical process that links DNA damage to cell cycle checkpoint activation, which is key to the survival and fitness of an organism[15,16,49-67]. Furthermore, DNA resection is required for HR and for generating ssDNA that forms protective t-loops at the ends of

chromosomes[68]. The mechanism of DNA resection at the ends of a DSB, the first step of HR, had been unclear for a long period of time. Within the past 6 years, a plethora of studies have emerged, identifying CtIP (SAE2 in yeast), EXO1 and DNA2 as the trio of nucleases involved in the DNA resection of DSBs[15,16,49-67].

The resection pathway was initially delineated in yeast as a 2-tiered process. At a DSB SAE2 (CtIP in humans) and the MRX complex (the MRN complex in humans) begins the resection process by minimally resecting the ends by 100bp[56,58]. This minimal processing is followed by long-range resection facilitated either by EXO1 or DNA2 and it can extend over kb lengths[54,55,66]. As a result, long 3'-overhangs of ssDNA are generated that can be utilized by the HR machinery to complete the repair.

Importantly, the impairment of DNA resection results in human disease and cancer. Mutations in human CtIP were found in Seckel and Jawad syndrome patients that suffer from microcephaly and various developmental disorders[69]. Additionally, CtIP is overexpressed in several breast cancer cell lines[70] suggesting that DNA resection may have a role in cancer cells. Consequently, DNA resection appears to be important for human health and more investigation on this process seems warranted. Importantly, these nucleases could potentially serve as novel cancer drug targets, in strategies that could augment current chemotherapeutic treatments.

CtIP

Human CtIP (C-terminal interacting protein) was originally identified from a yeast-2-hybrid screen for genes that interact with CtBP (C-terminal binding protein), which binds to the human adenovirus E1A transforming factor[71]. Thus, the function of CtIP was first described to likely be be that of a transcription factor. Subsequently, however, it has been shown to have a role in regulating the cell cycle[72-74]. It was first associated with the HR repair pathway when it was reported that CtIP binds to BRCA1 (a key HR factor), and that it is phosphorylated by ATM[75,76]. The current understanding of CtIP as a nuclease was only discovered 6 years ago when Sartori *et al.* reported that CtIP localizes to sites of DSBs and is required for resection. Furthermore, detailed studies of DNA resection by SAE2 in yeast corroborated the findings that CtIP is a factor required for DNA resection.

The human CtIP locus is located on Chromosome 18, and the protein is encoded by 19 exons. The first codon is non-coding but the remaining 18 exons encode for the ~100 kDa, full-length CtIP protein of 897 amino acids (a.a). CtIP dimerizes into a functional dimer through a coiled-coil (CC) domain located at its N-terminus[77]. Yeast CtIP, SAE2, is reported to be an endonuclease and its nuclease domain resides in the C-terminus. Human CtIP is weakly conserved with SAE2; however, the C-termini of CtIP and SAE2 do share significant homology[16]. In spite of this homology, it is still unclear whether CtIP possesses intrinsic nuclease activity. What is clear is that its interaction with the MRN complex stimulates resection[57]. Furthermore, the significant divergence of the N-terminal domains of CtIP from

SAE2 suggests that CtIP has evolved to adopt more specialized functions in order to manage the larger and more complicated genomes of higher organisms.

CtIP interacts with the MRN complex[14,57] and localizes to sites of DSBs[14,52,53,57] to mediate further resection by EXO1[51] and DNA2[51,63]. However, CtIP appears to have additional functions apart from facilitating DSB resection. Thus, CtIP has been reported to interact with BRCA1[73,74,78], Rb[72], PCNA[79], CDK2[50], and ATM[14,73]; indicating a role for CtIP in the DNA damage response (DDR) signaling pathway and checkpoint regulation.

CtIP is an essential gene in mice and it has been suggested to carry out essential functions in cells cycle regulation with Rb[80]. In a recent study, two human CtIP mutations that result in CtIP C-terminal truncations were identified in Seckel (SCKL2) and Jawad (J) syndrome patients[69] (characterized by mirocephaly and developmental defects). The SCKL2 and J mutations are presumed to be hypormorphic in mediating DNA resection. However, they still possess their Rb-interacting domain at the N-terminus[52,72] strongly suggesting that CtIP may be essential in humans, similar to mice.

EXO1

Human EXO1 is highly conserved with yeast EXO1. Human EXO1 is located on Chromosome 1 and consists of 13 coding (from a total of 15) exons. The EXO1 locus encodes for two isoforms, EXO1b and EXO1a. EXO1b is 803 a.a. long with a molecular weight of ~100 kDa. EXO1a is the product of an alternative splice site

located in the boundary of exons 14 and 15. The variant transcript results in a frameshift and uses an upstream stop codon resulting in the EXO1a isoform, which is 43 a.a. shorter than EXO1b. The EXO1 isoforms have not been reported to carry out separate functions; however, more investigation is warranted.

The human EXO1 is a member of the Rad2 structure-specific family of nucleases that possess 5'-3' endonucleolytic and exonucleolytic activities[81]. The endonucleolytic activity of EXO1 is capable of incising 5'-flap structures by using a common nuclease mechanism that bends DNA at nicks or gaps to expose the flap structures[82], whereas its 5'-3' exonucleolytic activity is highly processive and is capable of to generating kb long stretches of ssDNA[60,83,84]. Moreover, EXO1 is a multitasking nuclease[85]; it was originally described as the nuclease utilized in the mismatch repair pathway to excise patches of mismatched DNA[86-90]. However, multiple subsequent studies demonstrate the far-reaching involvement of EXO1 in DNA replication[91], HR[51], checkpoint activation[92], nucleotide excision repair (NER)[92] and telomere maintenance[68].

The involvement of EXO1 in DDR was demonstrated in studies showing tight coordinate regulation of EXO1 during replication stress[11,67,93,94]. When DNA replication is inhibited by hydroxyurea or aphidicolin treatment, EXO1b is phosphorylated by ATR, which signals for its ubiquitylation and proteasomal degradation; a process mediated by 14-3-3 proteins that specifically recognize phosphorylated EXO1[94,95]. The degradation of EXO1 in response to DNA damage is postulated to prevent extensive DNA resection at the damage site.

EXO1 is an important player in DSB repair and is required for IR resistance and genomic stability. Currently, EXO1 is heavily studied for its direct role in the long-range resection of DSBs, a process which is essential for the HR pathway. *In vitro* studies have shown that EXO1 is involved with two distinct DNA resection machineries. EXO1 can resect DNA in complexes with BLM, MRN and either with RPA or hSSB1 (SOSS1)[60,83,84]. hSSB1 is a newly discovered ssDNA binding protein that is required for IR resistance and genomic stability[96]. It has similar functions to RPA except that hSSB1 binds and stabilizes DNA with distinct kinetics[97] and does not co-localize with RPA[96]. hSSB1 was shown to enhance (in comparison to RPA) the exonucleolytic activity of EXO1 and the affinity of EXO1 for DNA ends. The different ssDNA structures stabilized by RPA or hSSB1 are thought to regulate the kinetics of resection by EXO1[84]. This suggests that the recruitment of RPA or SSB1 to the damage site may constitute a new mechanism to tailor resection products in response to the various types of DNA damage and repair.

In addition to DNA resection, EXO1 has been gaining attention as a key player in the process of DNA replication. Very recently, it was reported to travel intimately with the replication fork in study that isolated proteins on nascent DNA by mass spectrometry (iPOND-MS) [91]. Furthermore, EXO1 physically associates with PCNA through its (PCNA interacting protein motif) PIP box domain. The exact function of EXO1 in DNA replication is unclear and further investigation is warranted.

In mice, EXO1 was reported to play a significant role in telomere maintenance; murine EXO1 tailors ssDNA or G-overhangs such that they can form

the t-loop structures[68] that protect telomeres. EXO1 knockout mice are viable[2,98,99]; however, it is not known if this is also the case for humans.

DNA2

The human DNA2 locus is located on chromosome 10 and encodes 21 coding exons. The full-length protein is 1060 a.a. with a mass of ~140 kDa, and it is a member of the helicase and nuclease family of proteins that are highly conserved among various species[100]. The helicase domain of hDNA2 is located in the N-terminus, while the endonuclease domain is found on the C-terminus of the protein[100]. Human DNA2 has not been very well characterized; however much has been learned from yeast models. Yeast DNA2 was initially described as a flap endonuclease that excises 5'-flap ssDNA structures resulting from the displacement of Okazaki fragments during Polymerase δ extension[101,102]. The excision by yeast DNA2 leaves behind ~6 nt long flaps, which are further processed by FEN-1 to create ligatable nicks to be sealed by LIGI[101,102]. More recently, studies have shown that yeast DNA2 functions synergistically with EXO1 in DNA resection of DSBs (downstream of SAE2)[55].

DNA2 is an essential gene in yeast due to its requirement in DNA replication[103] but it is not known if it is essential for human cells or mice. Human DNA2 also has helicase and endonuclease domains in the N- and C-termini, respectively; confusingly however, human DNA2 *in vitro* is devoid of helicase activity and only has active endonucleolytic activity[100]. In human cells, DNA2 is

found in the mitochondria, where it maintains mitochondrial DNA stability, and in the nucleus, where it is required for genomic stability[104].

In vitro studies have reported that human DNA2 makes up a third DNA resection machinery. hDNA2 resects DNA in a complex with RPA, BLM and MRN and processively clips off 30-40 nt pieces of ssDNA[60,97]. Interestingly, RPA serves to guide the DNA resection of hDNA2 in the 5'-3' direction; and in contrast to EXO1, hDNA2 is not stimulated by hSSB1[97]. Furthermore, human DNA2 was recently reported to be involved in HR-mediated repair of damaged replication forks[63]. The regulation of these resection machines and their preferences for various types of DNA damage requires further investigation.

The vast majority of studies on CtIP[14,24,25,52,53,57], EXO1[9,10,26,51,67,93,105], and DNA2[11,16,51,63,106] function are based on transiently knocking down CtIP, EXO1, and DNA2, followed by examining the cell's responses to DNA damaging agents. Inasmuch information that these studies provide, we still do not know if CtIP and EXO1 are essential genes in human cells. It is important to know whether CtIP and EXO1 are essential in humans because if they are essential, it would most certainly mean they have essential functions in addition to responding and repairing artificially-induced DNA damage.

The Fanconi Anemia (FA) Pathway

The cellular genome is susceptible to DNA modifications resulting from exposure to various environmental factors, chemotherapeutic agents, or reactive metabolic products produced endogenously. Interstrand crosslinks (ICLs) are a modification where covalent bonds are formed between bases of both strands. DNA replication forks stall when they encounter ICLs[107]. The replication machinery cannot separate the covalently linked DNA and requires the FA pathway to resolve the ICLs and restart the stalled fork; otherwise, ICLs are lethal if left unresolved. The FA pathway was discovered in FA patients who suffer from bone marrow failure and cancer predisposition. Unfortunately, FA is a heritable, recessive, genomic instability syndrome and FA patients begin suffering at very young ages. FA patient cells are highly sensitive to DNA replication inhibitors such as hydroxyurea (HU), and aphidicolin (APH) and especially sensitive to ICL agents such as cisplatin and mitomycin C (MMC). When challenged with these compounds, FA patient cells are highly susceptible to chromosomal aberrations that are mediated by the NHEJ pathway[108,109].

Residing upstream in the FA pathway is an 8-membered, core complex comprised of FANCA, B, C, E, F, G, L, and M, which functions as a ubiquitin ligase. When a replication fork encounters an ICL, it stalls and the ATR-CHK1 pathway is activated. ATR subsequently phosphorylates the core complex, which in turn monoubiquitylates FANCD2/FANCI that is located centrally in the FA pathway. As a result, FANCD2 dissociates from FANCI and localizes to the site of damage where it

recruits downstream FA components[110,111]: FAN1 (Fanconi Anemia nuclease 1), FANCP (Slx4), FANCD1 (BRCA2), FANCO, FANCJ (BACH1/BRIP) and FANCN (PALB2). The downstream components make incisions on one strand to unhook the ICL, which separates the DNA strands such that a DSB is created on one chromatid, and a gap with the ICL lesion on the other chromatid. Ironically, the cell is now left with an ICL lesion and a DSB to repair. In order to repair the resulting ICL lesion, translesion polymerases are recruited to bypass the lesion and fill in the gap; and the DSB is subsequently repaired by the HR pathway, which uses the newly repaired sister chromatid as the homologous template[107,112].

The HR pathway is intimately connected to the FA pathway. In the HR pathway, BRCA1 is required to interact with BRCA2, through PALB2, in order for Rad51 to be recruited onto DNA. The identification of FANCD1 (BRCA2) and FANCN (PALB2) in the FA pathway[113], and a study reporting that Rad51 is involved in ICL repair[114] clearly show the interaction between the HR and FA pathways. However, it is not clear how these pathways are regulated and further investigation is warranted.

The NHEJ Pathways

NHEJ is another DSB repair pathway that is mechanistically distinct from the HR pathway[12]. In contrast to HR, NHEJ generally simply religates the two ends of broken DNA together and does not require a homologous template for repair. NHEJ repair has the advantage of speed over HR; however, it is error prone. In human

cells NHEJ is the primary DSB repair pathway and evolutionarily, it has been argued that this is so because the large human genome contains many non-coding regions that can buffer the errors derived from NHEJ repair in exchange for faster repair. In contrast, in yeast, HR is the predominant DSB repair pathway because with a concise and intron-less yeast genome, they cannot "afford" the errors that NHEJ would generate.

NHEJ exists as two, biochemically and mechanistically distinct sub pathways: a main "classic" end-joining pathway (C-NHEJ) and one interchangeably referred to as microhomology-mediated end joining (MMEJ)[115-117], alternative NHEJ (A-NHEJ), or backup NHEJ (B-NHEJ)[118,119] (hereafter referred to as A-NHEJ). Neither of these NHEJ sub pathways are precise; the C-NHEJ repair mechanism involves minimal DNA end processing, whereas A-NHEJ mechanistically results in deletions per force that are often accompanied by microhomology at the repair junction.

The C-NHEJ pathway consists of at least 7 components; Ku70, Ku86, DNA-PK_{cs}, Artemis, XRCC4, XLF and LIGIV. This is an important pathway because it is essential for the development of the immune system where it repairs DSB intermediates during V(D)J recombination and class switch recombination for antibody diversification, telomere maintenance, and genome maintenance[12]. In the event of a DSB, Ku is thought to be the first protein to bind to both ends of the DNA. Ku70 and Ku86 are highly expressed in mammalian cells and they form a heterodimer (Ku). Ku possesses a torroidal shape that fits snuggly on to ends of DNA duplexes with a high dissociation constant in the range of ~10 nM[12,29]. Once bound to DNA, Ku protects the vulnerable DNA ends from nucleolytic degradation

and recruits DNA-PK_{cs}, a phosphoinositol-3-like family serine/threonine protein kinase[120]. Ku and DNA-PK_{cs} assembled on the DNA end constitute DNA-dependent protein kinase complex (DNA-PK). The assembly of DNA-bound DNA-PK, activates the kinase activity of the DNA-PK_{cs} catalytic subunit, which in turn recruits the nuclease Artemis to trim the ends of the broken DNA[12]. In particular, the nuclease activity of Artemis opens the hairpins of V(D)J recombination intermediates in order to generate DNA ends that are compatible for ligation. In the final step, another trimeric complex that consists of LIGIV, XLF and XRCC4 ligates the ends of the break together[121].

The C-NHEJ pathway is a metaphorical double-edged sword. Although C-NHEJ plays a role in maintaining genomic stability, there are several studies that report that C-NHEJ also contributes to genomic instability. For example, the inhibition of DNA-PK reduces genomic instability of BRCA2- and BRCA1-deficient cells[122,123]. Moreover, the inactivation of C-NHEJ (Ku or LIGIV) in BRCA1- or FANC-deficient cells reduces the frequency of abnormal chromosomes[124,125].

In contrast to C-NHEJ and HR, the mechanism and regulation of A-NHEJ is unclear. However, it is known that the signature motif of A-NHEJ repair is microhomology at the repair junctions and that the reaction is "Ku independent"[126]. The microhomology that is observed in A-NHEJ repair junctions is thought to result from DNA resection of the DSB ends to generate 3' ssDNA with regions of microhomology (generally a few nucleotides), which are subsequently used for ligation [127]. Therefore, if a break occurs in a stretch of nucleotides between two regions of microhomology, A-NHEJ will delete the stretch of nucleotides and one of

the regions of microhomology and leave behind just one of the original microhomology regions at the repair junction.

A-NHEJ is thought to be a minor pathway of NHEJ because it is usually detected only in the absence of C-NHEJ[128]. Early efforts to characterize end joining properties in mammalian cells identified two classes of repair junctions: one with simple ligations, and another with microhomology[129,130]. Studies in yeast showed that in the absence of Ku, cells employ an alternative repair mechanism that can still mediate joining with microhomology in the repair junctions[117,128]. Subsequently, *in vitro* data demonstrated that a Ku-independent, alternative end joining pathway was indeed present and responsible for the microhomology at the repair junctions[131,132].

In recent years, the A-NHEJ pathway has been gaining interest as a key player in genomic stability. Transgenic mice with targeted knockouts for Ku70, Ku80, XRCC4, or LIGI, in a p53-deficient background have increased incidence of tumors; furthermore, the translocations found in these tumors bear the signature motif of A-NHEJ (microhomology)[133,134]. Another study involving mouse embryonic stem cells with a translocation reporter system also reported that the majority of translocations had microhomology sequences at the repair junctions[135]. Most compellingly, microhomology signatures have been found at the breakpoints of chromosomal rearrangements in primary human cancer cells[127,136]; though it is important to note that A-NHEJ is likely not solely responsible for such events. These findings have spurred an interest in identifying the components of the A-NHEJ pathway. Currently, it is known that poly (ADP-ribose) polymerase-1 (PARP-1), X-

ray cross complementing 1 (XRCC1), DNA ligase III (LIGIII), polynucleotide kinase (PNK) as well as Flap endonuclease 1 (Fen-1)[115,116,119,132,137,138] are likely involved; however, further investigation to identify other factors is warranted.

The Choice Between HR or NHEJ

In mammalian cells, NHEJ is the predominant pathway and is active in all phases of the cell cycle, whereas HR is predominantly active in the S- and G2-phases. Currently, it is thought that the choice between HR and NHEJ is regulated at the level of end resection[139]. Thus, C-NHEJ is preferred when there is little to no resection, A-NHEJ when there is modest resection, whereas HR requires the most extensive resection[16,33,118,128,140,141].

In S- and G2-phases when HR is active, CDKs modulates the activity of resection factors by phosphorylation in order to bias the pathway choice towards HR repair of DSBs[49,50,56,142,143]. In contrast, the p53 binding protein 1 (53BP1) also plays a significant role in pathway choice when NHEJ is used for the repair of DSBs. At DSBs in G1, 53BP1 recruits PTIP and RIF1, which, in turn represses the recruitment of BRCA1-CtIP. The repression of BRCA1-CtIP essentially blocks the DNA resection that is necessary for HR, and perforce promotes NHEJ. Conversely, in the S- and G2-phases, the activation of BRCA1-CtIP by CDKs prevents the accumulation of 53BP1 at DSBs[122,123,144-147]. These studies provide evidence that repair pathway choice is a complex process, but one that generally revolves around the access of DNA resection factors to the DNA ends.

Recombinant Adeno-Associated Virus (rAAV) and Gene Targeting

Adeno-associated virus (AAV) is a small (20 to 25 nm in diameter), nonenveloped, 4.7 kb single-stranded DNA (ssDNA) virus belonging to the *Parvoviridae* family[148]. It is estimated that 50 to 90% of the human population is seropositive for AAV[149]; however, there is no conclusive evidence for any association of AAV with disease or pathology. To date, six AAV serotypes have been identified in primates (AAV-1 to AAV-6) and only AAV type 2 (AAV-2) isolated from humans[150].

AAV is a defective virus dependent on the presence of a helper virus, usually adenovirus or herpesvirus, for replication. The AAV genome is encapsidated as a ssDNA molecule of 4680 bases with inverted terminal repeat (ITR) sequences of 145 bases at each end. The viral genome contains two open reading frames (ORFs) that encode for the proteins Rep (replication) and Cap (capsid). Three promoters have been found: p5, p19, and p40 [151]. Along with alternative splicing and through the use of different initiation codons, AAV can generate 4 Rep and 3 Cap proteins, each with specialized functions. The ITRs are *cis*-acting elements required for replication, packaging and integration of the AAV genome into the genome of the host[150].

Since AAV does not inflict human diseases, it was touted as the next vehicle for gene therapy. As a result, a recombinant form of AAV (rAAV) was developed that is not capable of carrying out a lytic infection. The rAAV genome was constructed by "gutting" the AAV genome (i.e. rep and cap) and replacing them with sequences in

place for the gene of interest between the two ITRs[149,152,153], such that the resultant chimeric virus will have a packaging capacity around the size of the AAV genome, between 4.1 to 4.9 kb.

A unique feature of modifying the genome of rAAV is that it is quite efficient at knocking out genes in human cells by utilizing the host's HR pathway. The overall gene targeting frequency is 3%, or 3 correct targeting events in every 100 productive transductions or genomic integrations[154,155]. rAAV mediated gene targeting is 100-fold more efficient compared to traditional transfection methods[154]. rAAV methodology is both simple and expeditious; the entire experiment to knock out a gene can take as little as 2 months. A simple protocol driven almost exclusively by PCR to construct the targeting vectors and viral stocks enhanced the ease of working with rAAV vectors. Additionally, the rAAV targeting (homology) arms are short enough (< 1.0 kb) to enable screening the resulting clones by PCR instead of Southern blots, once again expediting the targeting process, and the homology arms can be modified to "flox" exons of interest. In recent years rAAV has gained popularity to generate knockout human cell lines in many fields of study[155].

The first generation of rAAV knockout vectors were constructed with a promoter-driven, NEO selection cassette[154,156]. In a correct gene targeting event, the rAAV vector utilizes the HR pathway to locate the correct locus and replace the exon of interest with the PGK:NEO selection cassette to yield a correctly targeted, G418 resistant clone. The downside of this generation of vectors was that promoter-driven NEO selection cassette conferred G418-resistance to rAAV vectors that integrate randomly in the genome. Since the majority of the integration events are

random, this vector creates a large pool of non-targeted, G418 resistant clones. As a result, the population of correctly targeted clones is highly diluted in the selection process, and lowers the efficiency of screening.

To enrich for correctly-targeted, G418-resistant clones in the screening process, the synthetic exon promoter trap (SEPT) knockout vector was developed[157]. The SEPT vector does not have a promoter; instead, it is constructed with a splice acceptor upstream of an internal ribosomal entry site (IRES) sequence to express NEO. Therefore, the SEPT vector only confers G418 resistance to clones that are correctly targeted or when the vector fortuitously integrates into random ORFs. The SEPT vector effectively enriches for correctly targeted clones by eliminating the numerous random integration events that do not occur in ORFs. With the SEPT vector, the average targeting frequency is increased by 6-fold compared to the promoter-driven knockout vectors[157].

The Human HCT116 Cell Line

The cell line of our choice is the human colorectal adenocarcinoma HCT116 cell line. This cell line has 46 chromosomes with intact p53[158]. HCT116 is MLH1-deficient which renders it mismatch repair defective[159]. Since MMR generally impedes gene targeting, the HCT116 cell line is particularly amenable to this technology. There are over 40 reports of successful gene targeting having been carried out HCT116 cells, allowing for an assessment of the null phenotype[155]. The ease of knocking out genes in this cell line has provided our laboratory with

countless isogenic mutant cell lines that are essentially as powerful as yeast genetic models.

Summary

In summary, human cells have evolved multiple DNA DSB repair pathways: HR, C-NHEJ, and A-NHEJ. HR repair requires extensive DNA resection and a homologous template in the form of an undamaged sister chromatid that can result in error-free repair. In contrast, the C- and A-NHEJ pathways simply rejoin the two ends of broken DNA together and do not require a homologous template for repair.

Recent studies report that CtIP, EXO1, and DNA2 are the nucleases that resect DNA DSBs. These studies depend on siRNA knockdowns and only address response to exogenous DNA damaging agents, and they fail to address gene function in an otherwise unperturbed cell nor do they test their essential functions[51-53,57,63,94,160,161]. To fill this void, I have constructed genetic models in human somatic cells that are conditionally null for CtIP, EXO1 and DNA2. With these cell lines, I made novel observations: 1) CtIP, EXO1 and DNA2 are all essential in human cells, 2) CtIP and EXO1 are intimately involved in DNA replication, 3) CtIP, EXO1, and DNA2 are coregulated, and 4) CtIP, EXO1, and DNA2 coordinately regulate BRCA2, Rad51, FANCD2, and CHK1.

In a second project, I characterized differences in C-NHEJ and A-NHEJ. The Ku-dependent C-NHEJ repair is by no means precise due to minimal end processing of DSBs, whereas the A-NHEJ repair mechanism involves greater end processing

that is often accompanied by microhomology at the repair junction[118,128,140]. In this study, we have found that Ku is a unique C-NHEJ factor that actively represses the A-NHEJ pathway.

The HR and NHEJ pathways must be carefully regulated. DSBs or DNA damage that arise during DNA replication are preferably repaired by HR because it is error-free; however, cells compromised for HR or FA are susceptible to NHEJ to repair these DSBs[1,122-125]. Alas, the resulting NHEJ repair, while fixing the immediate problem often leads to chromosomal aberrations that are ultimately detrimental to the cell[113,125,139,162]. In this study, we show by genetically inactivating CtIP and EXO1 that the absence of DNA resection results in 53BP1 being heavily recruited to chromatin, which allows NHEJ to dictate DSB repair. As a result we observe extremely high rates of chromosomal aberrations. Together, these studies indicate that HR and NHEJ are regulated by DNA resection.

References:

1. Goodarzi, A. A. & Jeggo, P. A. The repair and signaling responses to DNA double-strand breaks. *Adv. Genet.* **82,** 1–45 (2013).
2. Bentley, J., Diggle, C. P., Harnden, P., Knowles, M. A. & Kiltie, A. E. DNA double strand break repair in human bladder cancer is error prone and involves microhomology-associated end-joining. *Nucleic Acids Res* **32,** 5249–5259 (2004).
3. Bianconi, E. *et al.* An estimation of the number of cells in the human body. *Ann. Hum. Biol.* **40,** 463–471 (2013).
4. Fouché, N., Ozgür, S., Roy, D. & Griffith, J. D. Replication fork regression in repetitive DNAs. *Nucleic Acids Res* **34,** 6044–6050 (2006).
5. Voineagu, I., Narayanan, V., Lobachev, K. S. & Mirkin, S. M. Replication stalling at unstable inverted repeats: interplay between DNA hairpins and fork stabilizing proteins. *Proc Nat Acad of Sci* **105,** 9936–9941 (2008).
6. Gerhardt, J. *et al.* The DNA replication program is altered at the Fmr1 locus in fragile x embryonic stem cells. *Mol Cell* **53,** 1–13 (2013).
7. Malumbres, M. & Barbacid, M. Cell cycle, CDKs and cancer: a changing paradigm. *Nat Rev Cancer* **9,** 153–166 (2009).
8. DePamphilis, M. L., de Renty, C. M., Ullah, Z. & Lee, C. Y. 'the octet': eight protein kinases that control mammalian DNA replication. *Front Physiol* **3,** 1–20 (2012).
9. Cimprich, K. A. & Cortez, D. ATR: an essential regulator of genome integrity. *Nat Rev Mol Cell Biol* **9,** 616–627 (2008).
10. Lopes, M. *et al.* The DNA replication checkpoint response stabilizes stalled replication forks. *Nature* **412,** 557–561 (2001).
11. San Filippo, J., Sung, P. & Klein, H. Mechanism of eukaryotic homologous recombination. *Annu Rev Biochem* **77,** 229–257 (2008).
12. Lieber, M. R. The mechanism of double-strand DNA break repair by the nonhomologous DNA end-joining pathway. *Annu Rev Biochem* **79,** 181–211 (2010).
13. Longhese, M. P., Bonetti, D., Manfrini, N. & Clerici, M. Mechanisms and regulation of DNA end resection. *EMBO J* **29,** 2864–2874 (2010).
14. You, Z. & Bailis, J. M. DNA damage and decisions: CtIP coordinates DNA repair and cell cycle checkpoints. *Trends in Cell Biology* **20,** 402–409 (2010).
15. Huertas, P. DNA resection in eukaryotes: deciding how to fix the break. *Nat Struct Mol Biol* **17,** 11–16 (2010).
16. Mimitou, E. P. & Symington, L. S. DNA end resection: many nucleases make light work. *DNA Repair (Amst)* **8,** 983–995 (2009).
17. Pierce, A. J. *et al.* Double-strand breaks and tumorigenesis. *Trends in Cell Biology* **11,** S52–59 (2001).
18. Verkaik, N. S. *et al.* Different types of V(D)J recombination and end-joining defects in DNA double-strand break repair mutant mammalian cells. *Eur J Immunol* **32,** 701–709 (2002).
19. Hakem, R. DNA-damage repair; the good, the bad, and the ugly. *EMBO J* **27,** 589–605 (2008).

20. Anand, R. P. *et al.* Overcoming natural replication barriers: differential helicase requirements. *Nucleic Acids Res* **40,** 1091–1105 (2012).
21. Maizels, N. Dynamic roles for G4 DNA in the biology of eukaryotic cells. *Nat Struct Mol Biol* **13,** 1055–1059 (2006).
22. Mirkin, S. M. Expandable DNA repeats and human disease. *Nature* **447,** 932–940 (2007).
23. Branzei, D. & Foiani, M. The checkpoint response to replication stress. *DNA Repair (Amst)* **8,** 1038–1046 (2009).
24. Chaudhury, I., Sareen, A., Raghunandan, M. & Sobeck, A. FANCD2 regulates BLM complex functions independently of FANCI to promote replication fork recovery. *Nucleic Acids Res* **41,** 6444–6459 (2013).
25. Petermann, E., Orta, M. L., Issaeva, N., Schultz, N. & Helleday, T. Hydroxyurea-stalled replication forks become progressively inactivated and require two different RAD51-mediated pathways for restart and repair. *Mol Cell* **37,** 492–502 (2010).
26. Branzei, D. & Foiani, M. Maintaining genome stability at the replication fork. *Nat Rev Mol Cell Biol* **11,** 208–219 (2010).
27. Ragland, R. L. *et al.* RNF4 and PLK1 are required for replication fork collapse in ATR-deficient cells. *Genes Dev* **27,** 2259–2273 (2013).
28. Mahaney, B. L., Meek, K. & Lees-Miller, S. P. Repair of ionizing radiation-induced DNA double-strand breaks by non-homologous end-joining. *Biochem J* **417,** 639–650 (2009).
29. Hendrickson, E. A., Huffman, J. L. & JA, T. Structural aspects of Ku and the DNA-dependent protein kinase complex. New York: Taylor and Francis Group. *DNA damage recognition …* 629–684 (2006).
30. Kastan, M. B. & Bartek, J. Cell-cycle checkpoints and cancer. *Nature* **432,** 316–323 (2004).
31. Löbrich, M. & Jeggo, P. A. The impact of a negligent G2/M checkpoint on genomic instability and cancer induction. *Nat Rev Cancer* **7,** 861–869 (2007).
32. Smith, J., Tho, L. M., Xu, N. & Gillespie, D. A. The ATM-Chk2 and ATR-Chk1 pathways in DNA damage signaling and cancer. *Adv. Cancer Res.* **108,** 73–112 (2010).
33. Symington, L. S. & Gautier, J. Double-strand break end resection and repair pathway choice. *Annu Rev Genet* **45,** 247–271 (2011).
34. Méchali, M. Eukaryotic DNA replication origins: many choices for appropriate answers. *Nat Rev Mol Cell Biol* **11,** 728–738 (2010).
35. Errico, A. & Costanzo, V. Mechanisms of replication fork protection: a safeguard for genome stability. *Crit Rev Biochem Mol Bio* **47,** 222–235 (2012).
36. Chini, C. C. S. Human Claspin is required for replication checkpoint control. *J Biol Chem* **278,** 30057–30062 (2003).
37. Chini, C. C. S., Wood, J. & Chen, J. Chk1 is required to maintain claspin stability. *Oncogene* **25,** 4165–4171 (2006).
38. Petermann, E., Helleday, T. & Caldecott, K. W. Claspin promotes normal replication fork rates in human cells. *Mol. Biol. Cell* **19,** 2373–2378 (2008).
39. Mendez, J. Temporal regulation of DNA replication in mammalian cells. *Crit*

Rev Biochem Mol Bio **44,** 343–351 (2009).
40. Lange, S. S., Takata, K.-I. & Wood, R. D. DNA polymerases and cancer. *Nat Rev Cancer* **11,** 96–110 (2011).
41. Thu, Y. M. & Bielinsky, A. K. Enigmatic roles of Mcm10 in DNA replication. *Trends Biochem Sci* **38,** 184–194 (2013).
42. Durkin, S. G. & Glover, T. W. Chromosome fragile sites. *Annu Rev Genet* **41,** 169–192 (2007).
43. Cimprich, K. A. Fragile sites: breaking up over a slowdown. *Curr Biol* **13,** R231–R233 (2003).
44. Casper, A. M., Nghiem, P., Arlt, M. F. & Glover, T. W. ATR regulates fragile site stability. *Cell* **111,** 779–789 (2002).
45. Barlow, J. H. *et al.* Identification of early replicating fragile sites that contribute to genome instability. *Cell* **152,** 620–632 (2013).
46. Mao, Z., Bozzella, M., Seluanov, A. & Gorbunova, V. DNA repair by nonhomologous end joining and homologous recombination during cell cycle in human cells. *Cell Cycle* **7,** 2902–2906 (2008).
47. Krogh, B. O. & Symington, L. S. Recombination proteins in yeast. *Annu Rev Genet* **38,** 233–271 (2004).
48. Mazin, A. V., Mazina, O. M., Bugreev, D. V. & Rossi, M. J. Rad54, the motor of homologous recombination. *DNA Repair (Amst)* **9,** 286–302 (2010).
49. Wang, H. *et al.* The interaction of CtIP and Nbs1 connects CDK and ATM to regulate HR-mediated double-strand break repair. *PLoS Genet* **9,** e1003277 (2013).
50. Buis, J., Stoneham, T., Spehalski, E. & Ferguson, D. O. Mre11 regulates CtIP-dependent double-strand break repair by interaction with CDK2. *Nat Struct Mol Biol* **19,** 246–252 (2012).
51. Eid, W. *et al.* DNA end resection by CtIP and exonuclease 1 prevents genomic instability. *EMBO Rep* **11,** 962–968 (2010).
52. You, Z. *et al.* CtIP links DNA double-strand break sensing to resection. *Mol Cell* **36,** 954–969 (2009).
53. Huertas, P. & Jackson, S. P. Human CtIP mediates cell cycle control of DNA end resection and double strand break repair. *J Biol Chem* **284,** 9558–9565 (2009).
54. Mimitou, E. P. & Symington, L. S. Sae2, Exo1 and Sgs1 collaborate in DNA double-strand break processing. *Nature* **455,** 770–774 (2008).
55. Zhu, Z., Chung, W.-H., Shim, E. Y., Lee, S. E. & Ira, G. Sgs1 helicase and two nucleases Dna2 and Exo1 resect DNA double-strand break ends. *Cell* **134,** 981–994 (2008).
56. Huertas, P., Cortés-Ledesma, F., Sartori, A. A., Aguilera, A. & Jackson, S. P. CDK targets Sae2 to control DNA-end resection and homologous recombination. *Nature* **455,** 689–692 (2008).
57. Sartori, A. A. *et al.* Human CtIP promotes DNA end resection. *Nature* **450,** 509–514 (2007).
58. Takeda, S., Nakamura, K., Taniguchi, Y. & Paull, T. T. Ctp1/CtIP and the MRN complex collaborate in the initial steps of homologous recombination. *Mol Cell* **28,** 351–352 (2007).

59. Peng, G. *et al.* Human nuclease/helicase Dna2 alleviates replication stress by promoting DNA end resection. *Cancer Res* 1–12 (2012). doi:10.1158/0008-5472.CAN-11-3152
60. Nimonkar, A. V. *et al.* BLM-DNA2-RPA-MRN and EXO1-BLM-RPA-MRN constitute two DNA end resection machineries for human DNA break repair. *Genes Dev* **25,** 350–362 (2011).
61. Mimitou, E. P. & Symington, L. S. Ku prevents Exo1 and Sgs1-dependent resection of DNA ends in the absence of a functional MRX complex or Sae2. *EMBO J* **29,** 3358–3369 (2010).
62. Ira, G. *et al.* DNA end resection, homologous recombination and DNA damage checkpoint activation require CDK1. *Nature* **431,** 1011–1017 (2004).
63. Karanja, K. K., Cox, S. W., Duxin, J. P., Stewart, S. A. & Campbell, J. L. DNA2 and EXO1 in replication-coupled, homology-directed repair and in the interplay between HDR and the FA/BRCA network. *Cell Cycle* **11,** 3983–3996 (2012).
64. Hodgson, A. *et al.* Mre11 and Exo1 contribute to the initiation and processivity of resection at meiotic double-strand breaks made independently of Spo11. *DNA Repair (Amst)* **10,** 138–148 (2011).
65. Nicolette, M. L. *et al.* Mre11–Rad50–Xrs2 and Sae2 promote 5′ strand resection of DNA double-strand breaks. *Nat Struct Mol Biol* **17,** 1478–1485 (2010).
66. Marrero, V. A. & Symington, L. S. Extensive DNA end processing by Exo1 and Sgs1 inhibits break-induced replication. *PLoS Genet* **6,** e1001007 (2010).
67. Bolderson, E. *et al.* Phosphorylation of Exo1 modulates homologous recombination repair of DNA double-strand breaks. *Nucleic Acids Res* **38,** 1821–1831 (2010).
68. Wu, P., Takai, H. & de Lange, T. Telomeric 3′ overhangs derive from resection by Exo1 and Apollo and fill-in by POT1b-associated CST. *Cell* **150,** 39–52 (2012).
69. Qvist, P. *et al.* CtIP mutations cause Seckel and Jawad syndromes. *PLoS Genet* **7,** e1002310 (2011).
70. Wu, G. & Lee, W.-H. CtIP, a multivalent adaptor connecting transcriptional regulation, checkpoint control and tumor suppression. *Cell Cycle* **5,** 1592–1596 (2006).
71. Schaeper, U., Subramanian, T., Lim, L., Boyd, J. M. & Chinnadurai, G. Interaction between a cellular protein that binds to the C-terminal region of adenovirus E1A (CtBP) and a novel cellular protein is disrupted by E1A through a conserved PLDLS motif. *J Biol Chem* **273,** 8549–8552 (1998).
72. Meloni, A. R., Smith, E. J. & Nevins, J. R. A mechanism for Rb/p130-mediated transcription repression involving recruitment of the CtBP corepressor. *Proc Natl Acad Sci USA* **96,** 9574–9579 (1999).
73. Li, S. Binding of CtIP to the BRCT repeats of Brca1 involved in the transcription regulation of p21 is disrupted upon DNA damage. *J Biol Chem* **274,** 11334–11338 (1999).
74. Yu, X., Wu, L. C., Bowcock, A. M., Aronheim, A. & Baer, R. The C-terminal (BRCT) domains of BRCA1 interact in vivo with CtIP, a protein implicated in the CtBP pathway of transcriptional repression. *J Biol Chem* **273,** 25388–

25392 (1998).
75. Yu, X. & Chen, J. DNA damage-induced cell cycle checkpoint control requires CtIP, a phosphorylation-dependent binding partner of BRCA1 C-terminal domains. *Mol Cell Biol* **24,** 9478–9486 (2004).
76. Lee, W.-H. *et al.* Functional link of BRCA1 and ataxia telangiectasia gene product in DNA damage response : Article : Nature. *Nature* **406,** 210–215 (2000).
77. Dubin, M. J. Dimerization of CtIP, a BRCA1- and CtBP-interacting Protein, Is mediated by an N-terminal coiled-coil Motif. *J Biol Chem* **279,** 26932–26938 (2004).
78. Barber, L. J. & Boulton, S. J. BRCA1 ubiquitylation of CtIP: Just the tIP of the iceberg? *DNA Repair (Amst)* **5,** 1499–1504 (2006).
79. Gu, B. & Chen, P.-L. Expression of PCNA-binding domain of CtIP, a motif required for CtIP localization at DNA replication foci, causes DNA damage and activation of DNA damage checkpoint. *Cell Cycle* **8,** 1409–1420 (2009).
80. Chen, P.-L. *et al.* Inactivation of CtIP leads to early embryonic lethality mediated by G1 restraint and to tumorigenesis by haploid insufficiency. *Mol Cell Biol* **25,** 3535–3542 (2005).
81. Wilson, D. M. *et al.* Hex1: a new human Rad2 nuclease family member with homology to yeast exonuclease 1. *Nucleic Acids Res* **26,** 3762–3768 (1998).
82. Orans, J. *et al.* Structures of human exonuclease 1 DNA complexes suggest a unified mechanism for nuclease family. *Cell* **145,** 212–223 (2011).
83. Nimonkar, A. V., Ozsoy, A. Z., Genschel, J., Modrich, P. & Kowalczykowski, S. C. Human exonuclease 1 and BLM helicase interact to resect DNA and initiate DNA repair. *Proc Natl Acad Sci USA* **105,** 16906–16911 (2008).
84. Richard, D. J. *et al.* hSSB1 rapidly binds at the sites of DNA double-strand breaks and is required for the efficient recruitment of the MRN complex. *Nucleic Acids Res* **39,** 1692–1702 (2011).
85. Tran, P. T., Erdeniz, N., Symington, L. S. & Liskay, R. M. EXO1-A multi-tasking eukaryotic nuclease. *DNA Repair (Amst)* **3,** 1549–1559 (2004).
86. Liberti, S. E. *et al.* Bi-directional routing of DNA mismatch repair protein human exonuclease 1 to replication foci and DNA double strand breaks. *DNA Repair (Amst)* **10,** 73–86 (2011).
87. Marti, T. M., Mansour, A. A., Lehmann, E. & Fleck, O. Different frameshift mutation spectra in non-repetitive DNA of MutSalpha- and MutLalpha-deficient fission yeast cells. *DNA Repair (Amst)* **2,** 571–580 (2003).
88. Sun, X., Zheng, L. & Shen, B. Functional alterations of human exonuclease 1 mutants identified in atypical hereditary nonpolyposis colorectal cancer syndrome. *Cancer Res* **62,** 6026–6030 (2002).
89. Jäger, A. C. *et al.* HNPCC mutations in the human DNA mismatch repair gene hMLH1 influence assembly of hMutLalpha and hMLH1-hEXO1 complexes. *Oncogene* **20,** 3590–3595 (2001).
90. Schmutte, C. *et al.* Human exonuclease I interacts with the mismatch repair protein hMSH2. *Cancer Res* **58,** 4537–4542 (1998).
91. López-Contreras, A. J. *et al.* A proteomic characterization of factors enriched at nascent DNA molecules. *Cell Rep* **3,** 1105–1116 (2013).

92. Sertic, S. *et al.* Human exonuclease 1 connects nucleotide excision repair (NER) processing with checkpoint activation in response to UV irradiation. *Proc Natl Acad Sci USA* **108,** 13647–13652 (2011).
93. Morin, I. *et al.* Checkpoint-dependent phosphorylation of Exo1 modulates the DNA damage response. *EMBO J* **27,** 2400–2410 (2008).
94. Engels, K., Giannattasio, M., Muzi-Falconi, M., Lopes, M. & Ferrari, S. 14-3-3 Proteins regulate exonuclease 1–dependent processing of stalled replication forks. *PLoS Genet* **7,** e1001367 (2011).
95. Andersen, S. D. *et al.* 14-3-3 checkpoint regulatory proteins interact specifically with DNA repair protein human exonuclease 1 (hEXO1) via a semi-conserved motif. *DNA Repair (Amst)* **11,** 267–277 (2012).
96. Richard, D. J. *et al.* Single-stranded DNA-binding protein hSSB1 is critical for genomic stability. *Nat Rev Mol Cell Biol* **453,** 677–681 (2008).
97. Yang, S.-H. *et al.* The SOSS1 single-stranded DNA binding complex promotes DNA end resection in concert with Exo1. *EMBO J* **9,** 126–139 (2012).
98. Schaetzlein, S. *et al.* Exonuclease-1 deletion impairs DNA damage signaling and prolongs lifespan of telomere-dysfunctional mice. *Cell* **130,** 863–877 (2007).
99. Wei, K. Inactivation of Exonuclease 1 in mice results in DNA mismatch repair defects, increased cancer susceptibility, and male and female sterility. *Genes Dev* **17,** 603–614 (2003).
100. Masuda-Sasa, T., Imamura, O. & Campbell, J. L. Biochemical analysis of human Dna2. *Nucleic Acids Res* **34,** 1865–1875 (2006).
101. Bae, S. H. Coupling of DNA Helicase and Endonuclease Activities of Yeast Dna2 Facilitates Okazaki Fragment Processing. *J Biol Chem* **277,** 26632–26641 (2002).
102. Kao, H. I. Dna2p helicase/nuclease Is a tracking protein, like FEN1, for flap cleavage during Okazaki fragment maturation. *J Biol Chem* **279,** 50840–50849 (2004).
103. Lee, K. H. *et al.* The endonuclease activity of the yeast Dna2 enzyme is essential in vivo. *Nucleic Acids Res* **28,** 2873–2881 (2000).
104. Zheng, L. *et al.* Human DNA2 is a mitochondrial nuclease/helicase for efficient processing of DNA replication and repair intermediates. *Mol Cell* **32,** 325–336 (2008).
105. Cotta-Ramusino, C. *et al.* Exo1 processes stalled replication forks and counteracts fork reversal in checkpoint-defective cells. *Mol Cell* **17,** 153–159 (2005).
106. Mimitou, E. P. & Symington, L. S. DNA end resection- unraveling the tail. *DNA Repair (Amst)* **10,** 344–348 (2011).
107. Kottemann, M. C. & Smogorzewska, A. Fanconi anaemia and the repair of Watson and Crick DNA crosslinks. *Nature* **493,** 356–363 (2013).
108. Kee, Y. & D'Andrea, A. D. Molecular pathogenesis and clinical management of Fanconi anemia. *J Clin Invest* **122,** 3799–3806 (2012).
109. Moldovan, G.-L. & D'Andrea, A. D. How the fanconi anemia pathway guards the genome. *Annu Rev Genet* **43,** 223–249 (2009).
110. Sobeck, A., Stone, S., Landais, I., de Graaf, B. & Hoatlin, M. E. The Fanconi

Anemia Protein FANCM Is Controlled by FANCD2 and the ATR/ATM Pathways. *J Biol Chem* **284,** 25560–25568 (2009).
111. Sareen, A., Chaudhury, I., Adams, N. & Sobeck, A. Fanconi anemia proteins FANCD2 and FANCI exhibit different DNA damage responses during S-phase. *Nucleic Acids Res* **40,** 8425–8439 (2012).
112. Garner, E. & Smogorzewska, A. Ubiquitylation and the Fanconi anemia pathway. *FEBS Letters* **585,** 2853–2860 (2011).
113. Roy, R., Chun, J. & Powell, S. N. BRCA1 and BRCA2: different roles in a common pathway of genome protection. *Nat Rev Cancer* **12,** 68–78 (2011).
114. Long, D. T., Räschle, M., Joukov, V. & Walter, J. C. Mechanism of RAD51-dependent DNA interstrand cross-link repair. *Science* **333,** 84–87 (2011).
115. Boboila, C. *et al.* Robust chromosomal DNA repair via alternative end-joining in the absence of X-ray repair cross-complementing protein 1 (XRCC1). *Proc Natl Acad Sci USA* **109,** 2473–2478 (2012).
116. Liang, L. *et al.* Human DNA ligases I and III, but not ligase IV, are required for microhomology-mediated end joining of DNA double-strand breaks. *Nucleic Acids Res* **36,** 3297–3310 (2008).
117. Kramer, K. M., Brock, J. A., Bloom, K., Moore, J. K. & Haber, J. E. Two different types of double-strand breaks in Saccharomyces cerevisiae are repaired by similar RAD52-independent, nonhomologous recombination events. *Mol Cell Biol* **14,** 1293–1301 (1994).
118. Nussenzweig, A. & Nussenzweig, M. C. A backup DNA repair pathway moves to the forefront. *Cell* **131,** 223–225 (2007).
119. Wang, M. *et al.* PARP-1 and Ku compete for repair of DNA double strand breaks by distinct NHEJ pathways. *Nucleic Acids Res* **34,** 6170–6182 (2006).
120. Meek, K., Dang, V. & Lees-Miller, S. P. DNA-PK: the means to justify the ends? *Adv. Immunol.* **99,** 33–58 (2008).
121. Ellenberger, T. & Tomkinson, A. E. Eukaryotic DNA ligases: structural and functional insights. *Annu Rev Biochem* **77,** 313–338 (2008).
122. Bunting, S. F. *et al.* 53BP1 inhibits homologous recombination in Brca1-deficient cells by blocking resection of DNA breaks. *Cell* **141,** 243–254 (2010).
123. Bunting, S. F. *et al.* BRCA1 Functions independently of homologous recombination in DNA interstrand crosslink repair. *Mol Cell* **46,** 125–135 (2012).
124. Patel, A. G., Sarkaria, J. N. & Kaufmann, S. H. Nonhomologous end joining drives poly(ADP-ribose) polymerase (PARP) inhibitor lethality in homologous recombination-deficient cells. *Proc Natl Acad Sci USA* **108,** 3406–3411 (2011).
125. Pace, P. *et al.* Ku70 Corrupts DNA repair in the absence of the Fanconi anemia pathway. *Science* **329,** 219–223 (2010).
126. Fattah, F. *et al.* Ku regulates the non-homologous end joining pathway choice of DNA double-strand break repair in human somatic cells. *PLoS Genet* **6,** e1000855 (2010).
127. McVey, M. & Lee, S. E. MMEJ repair of double-strand breaks (director's cut): deleted sequences and alternative endings. *Trends Genet* **24,** 529–538

(2008).
128. Boulton, S. Identification of a Saccharomyces cerevisiae Ku80 homologue: roles in DNA double strand break rejoining and in telomeric maintenance. *Nucleic Acids Res* **24,** 4639–4648 (1996).
129. Roth, D. B. & Wilson, J. H. Nonhomologous recombination in mammalian cells: role for short sequence homologies in the joining reaction. *Mol Cell Biol* **6,** 4295–4304 (1986).
130. Roth, D. B., Porter, T. N. & Wilson, J. H. Mechanisms of nonhomologous recombination in mammalian cells. *Mol Cell Biol* **5,** 2599–2607 (1985).
131. Daley, J. M. & Wilson, T. E. Rejoining of DNA double-strand breaks as a function of overhang length. *Mol Cell Biol* **25,** 896–906 (2005).
132. Wang, H. *et al.* Biochemical evidence for Ku-independent backup pathways of NHEJ. *Nucleic Acids Res* **31,** 5377–5388 (2003).
133. Difilippantonio, M. J. *et al.* Evidence for replicative repair of DNA double-strand breaks leading to oncogenic translocation and gene amplification. *J Exp Med* **196,** 469–480 (2002).
134. Zhu, C. *et al.* Unrepaired DNA breaks in p53-deficient cells lead to oncogenic gene amplification subsequent to translocations. *Cell* **109,** 811–821 (2002).
135. Weinstock, D. M. A model of oncogenic rearrangements: differences between chromosomal translocation mechanisms and simple double-strand break repair. *Blood* **107,** 777–780 (2006).
136. Tsai, A. G. *et al.* Human chromosomal translocations at CpG sites and a theoretical basis for their lineage and stage specificity. *Cell* **135,** 1130–1142 (2008).
137. Audebert, M., Salles, B. & Calsou, P. Involvement of poly(ADP-ribose) polymerase-1 and XRCC1/DNA ligase III in an alternative route for DNA double-strand breaks rejoining. *J Biol Chem* **279,** 55117–55126 (2004).
138. Liang, L. *et al.* Modulation of DNA end joining by nuclear proteins. *J Biol Chem* **280,** 31442–31449 (2005).
139. Bunting, S. F. & Nussenzweig, A. End-joining, translocations and cancer. *Nat Rev Cancer* **13,** 443–454 (2013).
140. Haber, J. E. Alternative endings. *Proc Natl Acad Sci USA* **105,** 405–406 (2008).
141. Ma, J.-L., Kim, E. M., Haber, J. E. & Lee, S. E. Yeast Mre11 and Rad1 proteins define a Ku-independent mechanism to repair double-strand breaks lacking overlapping end sequences. *Mol Cell Biol* **23,** 8820–8828 (2003).
142. Ferretti, L. P., Lafranchi, L. & Sartori, A. A. Controlling DNA-end resection: a new task for CDKs. *Front Genet* **4,** 99 (2013).
143. Cerqueira, A. *et al.* Overall Cdk activity modulates the DNA damage response in mammalian cells. *J Cell Biol* **187,** 773–780 (2009).
144. Di Virgilio, M. *et al.* Rif1 prevents resection of DNA breaks and promotes immunoglobulin class switching. *Science* **339,** 711–715 (2013).
145. Callén, E. *et al.* 53BP1 Mediates Productive and Mutagenic DNA Repair through Distinct Phosphoprotein Interactions. *Cell* **153,** 1266–1280 (2013).
146. Escribano-Díaz, C. *et al.* A cell cycle-dependent regulatory circuit composed of 53bp1-Rif1 and Brca1-ctip controls DNA repair pathway choice. *Semin.*

Cell Dev. Biol. (2013).
147. Zimmermann, M., Lottersberger, F., Buonomo, S. B., Sfeir, A. & de Lange, T. 53BP1 regulates DSB repair using Rif1 to control 5' end resection. *Science* **339,** 700–704 (2013).
148. Berns, K. I. & Giraud, C. Biology of adeno-associated virus. *Curr. Top. Microbiol. Immunol.* **218,** 1–23 (1996).
149. Chirmule, N. *et al.* Immune responses to adenovirus and adeno-associated virus in humans. *Gene Ther* **6,** 1574–1583 (1999).
150. Lai, C. M., Lai, Y. K. Y. & Rakoczy, P. E. Adenovirus and adeno-associated virus vectors. *DNA Cell Biol* **21,** 895–913 (2002).
151. Berns, K. I. & Linden, R. M. The cryptic life style of adeno-associated virus. *Bioessays* **17,** 237–245 (1995).
152. Berns, K. I. & Giraud, C. Adenovirus and adeno-associated virus as vectors for gene therapy. *Ann N Y Acad Sci* **772,** 95–104 (1995).
153. Daya, S. & Berns, K. I. Gene therapy using adeno-associated virus vectors. *Clinical Microbiology Reviews* **21,** 583–593 (2008).
154. Russell, D. W. & Hirata, R. K. Human gene targeting by viral vectors. *Nat Genet* **18,** 325–330 (1998).
155. Hendrickson, E. A. Gene targeting in human somatic cells. *Sourcebook of Models for Biomedical Research* 509–525 (2008). doi:10.1007/978-1-59745-285-4_53
156. Kohli, M., Rago, C., Lengauer, C., Kinzler, K. W. & Vogelstein, B. Facile methods for generating human somatic cell gene knockouts using recombinant adeno-associated viruses. *Nucleic Acids Res* **32,** e3 (2004).
157. Topaloglu, O., Hurley, P. J., Yildirim, O., Civin, C. I. & Bunz, F. Improved methods for the generation of human gene knockout and knockin cell lines. *Nucleic Acids Res* **33,** e158 (2005).
158. Bunz, F. *et al.* Requirement for p53 and p21 to sustain G2 arrest after DNA damage. *Science* **282,** 1497–1501 (1998).
159. Aebi, S. *et al.* Loss of DNA mismatch repair in acquired resistance to cisplatin. *Cancer Res* **56,** 3087–3090 (1996).
160. Yuan, J. & Chen, J. N-Terminus of CtIP is critical for homologous recombination-mediated double-strand break repair. *J Biol Chem* **284,** 31746–31752 (2009).
161. Yun, M. H. & Hiom, K. CtIP-BRCA1 modulates the choice of DNA double-strand-break repair pathway throughout the cell cycle. *Nature* **459,** 460–463 (2009).
162. Adamo, A. *et al.* Preventing nonhomologous end joining suppresses DNA repair defects of Fanconi anemia. *Mol Cell* **39,** 25–35 (2010).

CHAPTER II:
The Impact Of DNA Resection Mutants And The Regulation Of CtIP, EXO1, And DNA2 In Human Somatic Cells

A version of this chapter is to be submitted for publication in the near future.

Homologous recombination begins with an essential step where the ends of a double-stranded break are resected to generate long tracts of ssDNA. In human cells, several studies have identified that CtIP and EXO1 are required for the resection of DSBs. CtIP also plays a major role in the DNA damage response pathway and together with the EXO1 exonuclease, it facilitates extensive resection to expose long tracks of ssDNA, which drives the HR repair process. To date, the majority of studies on CtIP and EXO1 function rely on siRNA knockdown and subsequent exposure to DNA damaging agents. Inasmuch as we have learned from these studies, they are nonetheless predicated on a cell's response to DNA damaging agents and they fail to address the essential functions of CtIP and EXO1 in an unperturbed cell. The construction of human cells conditionally-null for CtIP, EXO1, and DNA2 have helped us further understand the functions of these genes. In the absence of CtIP or EXO1, replication forks stall and collapse into DSBs even without the presence of DNA damaging agents. We also find that CtIP, EXO1, and DNA2 are co-regulated and that they coordinately regulate the protein levels of FANCD2, BRCA2, Rad51, and CHK1.

Introduction

DNA double-stranded breaks (DSBs) are the most lethal form of DNA lesions for a cell and they must be repaired if the cell is to survive. In human cells, DSBs are repaired by the non-homologous end joining (NHEJ)[1,2] or homologous recombination (HR) pathways[3]. These two DSB repair pathways are mechanistically distinct. NHEJ directly re-ligates two broken ends of DNA[1,3] and can be error prone[4] resulting in the loss of genetic information, whereas the HR pathway requires homologous templates for repair and is generally error-free[3].

The genomic landscape of a human cell is wrought with obstacles for an active replication fork. Highly repetitive regions in the human genome, including trinucleotide repeats (TNRs), telomeres, LINE, SINE, DNA transposons, and ALU repeat elements transiently form complex DNA structures at periods when they become single-stranded[5-7]. During DNA replication, these complex DNA structures, such as hairpins, triplex and quadruplex DNA become barriers to DNA replication and they can trigger replication fork stalling[4,8-10]. For example, common fragile sites (CFS) are late replicating, AT-rich repetitive regions that are prone to breakage when cells are under replication stress or when ATR function is compromised[11-13]. Recently, a second class of CFS described as Early replicating common fragile sites (ERCFs) was discovered. As their name implies, ERCFs are early replicating regions. Most are GC enriched (LINE, SINE, ALU and tRNA) sequences that are prone to breakage during DNA replication[14]. Similar to CFs, ERCFs are more prone to break if ATR is inhibited[11-13]. The presence of these fragile sites suggests that the volatility of DNA replication is currently underestimated.

In HR, DNA resection is an essential step that occurs at DSB ends to unveil 3'-overhang stretches of single-stranded DNA that are required to complete the repair[3,15,16]. This resection pathway was initially delineated in yeast (*Saccharomyces cerevisiae*) as a 2-tiered process. SAE2 (CtIP in humans) and the MRX complex (MRN complex in humans) comprised of Mre11, Rad50 and Xrs2 (Nbs1 in humans), begins the resection process at the DSBs with a minimal resection[17,18] of 100 bp, followed by long-range resection facilitated by EXO1 and DNA2 to extend over kb in length[19-21]. DNA2[19-21] is essential in yeast because it also carries out an essential function in Okazaki fragment processing[22-24] whereas SAE2 and EXO1 are not required for survival.

In humans, it also well understood that CtIP (CtBP interacting protein)[25] is an important HR factor[26]. CtIP interacts with the MRN complex[27,28] and localizes to sites of DSBs[27-30] to mediate further resection by EXO1[31] and DNA2[31,32]. However, CtIP appears to have additional functions from apart from DSB resection. Human CtIP is the most divergent protein of all the resection factors described above and it has been shown to interact with BRCA1[33-35], Rb[36], PCNA[37], CDK2[38], and ATM[28,34] emphasizing roles of CtIP in the DNA damage response (DDR) signaling pathway and checkpoint regulation.

CtIP is an essential gene in mice, where it was suggested to carry out an essential function in cell cycle regulation with Rb[39]. In a recent study, two human CtIP mutations that result in CtIP C-terminal truncations were identified in Seckel (SCKL2) and Jawad (J) syndrome patients[40] (characterized by microcephaly and developmental defects). The SCKL2 and J mutations are thought to be hypomorphic

in mediating DNA resection. However, they still possess the Rb-interacting domain at their N-terminus strongly suggesting that CtIP maybe essential in humans, similar to mice[30,36].

EXO1 is a multitasking nuclease[41]. EXO1 plays a role in telomere maintenance by tailoring G-overhangs for t-loop structure formation[42] in mice, and it is also a well-established factor in the mismatch repair (MMR) pathway[43-47]. Moreover, EXO1 is reported to be involved in DNA replication from studies showing tight regulation of EXO1 during replication stress[1,48-50 3,51,52], and in a recent study, EXO1 was reported to travel intimately with the replication fork in an isolation of proteins on nascent DNA – mass spectrometry (iPOND-MS) study[1,3,53]. EXO1 is not essential in mice[4,54,55] but it is unknown if this is also the case for humans. Typically, the lethality of a mouse gene directly translates to their human counterparts; however, exceptions do occur. For instance, Ku86 null mice are viable[3,56], whereas Ku86 null human cells do not survive[5-7,57,58].

In vitro studies suggest that DNA2 and EXO1 can operate as 3 distinct forms of resection machines. Initially, two studies reported that both DNA2 and EXO1 individually interact with BLM, MRN, and RPA to resect dsDNA[4,8-10,59,60], thereby suggesting that there are two redundant DSB resection complexes. However, another study described a third resection machine in which human single strand binding protein (hSSB1) and MRN were demonstrated to specifically activate the nuclease activity of EXO1, but not DNA2[3,61-64]. The regulation of these resection complexes and their potential preferences for different types of DNA damage requires further investigation.

Human DNA2 has not been very well characterized; however, much has been learned from yeast. Yeast DNA2 was initially described as a flap endonuclease that excises 5'-flap ssDNA structures resulting from the displacement of Okazaki fragments during Polymerase δ extension. The excision by DNA2 leaves behind ~6 nt long flaps which are further processed by FEN-1 to create ligatable nicks to be sealed by DNA ligase I or LIGI[65]. More recently, studies have shown that yeast DNA2 is a nuclease, downstream of SAE2 (CtIP in human), which functions synergistically with EXO1 in the resection of DSBs[21]. EXO1 can provide partial compensation in the absence of DNA2; however, the contrary is not true, indicating that DNA2 may play an accessory role in DSB resection[21]

Human DNA2 possesses canonical helicase and endonuclease domains in its N- and C-termini, respectively. However, human DNA2 *in vitro* is devoid of helicase activity and only has active endonucleolytic activity[66]. In human cells, DNA2 is found in mitochondria, where it is required for mitochondrial DNA stability, and the nucleus, where it is required for genomic stability[67].

The vast majority of studies on CtIP[27-30,68,69], EXO1[31,48,50,51,63,64,70], and DNA2[3,15,16,31,32] have been based on transiently knocking down CtIP, EXO1, and DNA2, followed by examining the cell's responses to DNA damaging agents. Inasmuch information as these studies provide, it is unknown whether CtIP and EXO1 are essential genes in human cells and what their precise roles in DNA replication and repair may be.

To further investigate the functions of CtIP and EXO1 in otherwise unperturbed cells, we constructed HCT116 cell lines that are conditionally-null for

CtIP and EXO1. This powerful genetic model allowed us to make observations of cellular behavior in the absence of these essential genes. After inactivating CtIP and EXO1 by Cre-mediated recombination of the "Floxed" allele, the CtIP and EXO1-null cells have a time window of 5-7 days before completely dying off. This provides us with a generous window of time to observe the temporal dynamics of DNA repair factors and cellular behavior. In the absence of DNA damaging agents or DNA replication inhibitors, the inactivation of CtIP or EXO1 cannot rescue replication forks that stall in repetitive regions where breakage-prone CFs and ERCFs reside. Ultimately, the stalled forks collapse into DSBs. For the first time, we also show that CtIP and EXO1 are co-regulated, and that they also regulate the stability of FANCD2 and several important HR factors including BRCA2, Rad51, CHK1, and DNA2. We argue that CtIP and EXO1 are essential for replication forks to overcome naturally occurring barriers.

Results

Construction of human conditional CtIP-, EXO1-, and DNA2-null somatic cell lines

The majority of studies on CtIP, EXO1, and DNA2 rely solely on their transient inactivation by siRNA knockdown and then measure the cells' response to DNA damaging agents. Although siRNA methods swiftly lead to important findings, they fail to address the essential functions of CtIP and EXO1 in an unperturbed cell. Therefore, we derived HCT116 cells that are conditionally-null for CtIP, EXO1 and DNA2.

The conditional $CtIP^{Flox/-}$ and $EXO1^{Flox/-}$ HCT116 cell lines were constructed with the aid of recombinant adeno-associated virus (rAAV)-mediated gene targeting technology[17,18,71]. In order to inactivate CtIP and EXO1, we used a synthetic exon promoter trap (SEPT):Neo selection cassette[19-21,72] strategy to target exons 2 and 3 of the CtIP and EXO1 genomic loci, respectively. These exons were specifically chosen because their loss creates frameshift mutation, in the open reading frame after Cre-mediated excision.

To target the first CtIP and EXO1 alleles, rAAV targeting vectors were designed with 3 loxP sites sequentially flanking the exon(s) and the SEPT:Neo selection cassette (Fig. 1A). The correctly targeted G418 resistant clones ($CtIP^{Neo/+}$ and $EXO1^{Neo/+}$) were transiently transfected with a PGK driven, Cre-expressing plasmid (pPGK Cre) to remove the SEPT:Neo cassette and restore expression of the "Floxed" allele, $CtIP^{F/+}$ and $EXO1^{F/+}$ (Fig. 1B). For the second round knockout, we

utilized non-conditional knockout vectors designed with 2 loxP sites to flank the SEPT:Neo cassette. The correctly targeted clones (CtIP$^{F/Neo}$ and EXO1$^{F/Neo}$, Fig. 1C) were transiently transfected with pPGK Cre to derive the CtIP$^{F/-}$ and EXO1$^{F/-}$ null HCT116 cell lines (Fig. 1D).

DNA2 is triploid in the HCT116 cell line and all three alleles were targeted with a rAAV targeting vector designed with 3 loxP sites sequentially flanking the exon and the SEPT:Neo selection cassette (Fig. 1G). After the first round of targeting, correctly targeted G418 resistant clones (DNA2$^{Neo/+/+}$, Fig. 1H) were transiently transfected with a pPGKCre to remove the SEPT:Neo cassette and restore expression of the "Floxed" allele, DNA2$^{F/+/+}$ (Fig. 1I). The desired DNA2$^{F/+/+}$ clone was identified and subsequently targeted at a second allele to generate a DNA2$^{F/Neo/+}$ cell line. DNA2$^{F/Neo/+}$ cells were transiently transfected with pPGKCre (Fig. 1J) and clones were identified that had undergone a single Cre recombination event that had completely excised the "Floxed" exon and SEPT:Neo cassette on the second targeted allele (DNA2$^{F/-/+}$, Fig. 1K). The third and final allele in DNA2$^{F/-/+}$ cells was targeted in a similar fashion as the second round. Correctly targeted DNA2$^{F/-/Neo}$ clones (Fig. 1L) were identified and Cre'd for a "true" conditional DNA2$^{F/-/-}$ null cell line (Fig. 1M).

Finally, we established a Cre-Estrogen Receptor (CreERt2) inducible system by stably integrating a CreERt2-expressing plasmid into the CtIP$^{F/-}$, EXO1$^{F/-}$, and DNA2$^{F/-/-}$ (Figs. 1E & 1N) cell lines via PiggyBac transposition. The characterization of CtIP$^{-/-}$, EXO1$^{-/-}$, and DNA2$^{-/-/-}$ null cells is conveniently achieved by adding

tamoxifen to CtIP$^{F/-}$:CreERt2, EXO1$^{F/-}$:CreERt2, and DNA2$^{F/-/-}$:CreERt2 cells in culture to synchronously induce the excision of the nuclear "Floxed" exons.

CtIP and EXO1 are required for survival in human somatic cells

CtIP is an essential gene in mice[19-21,39]. CtIP$^{-/-}$ embryos die at D4.0, where they arrest in G0-phase, thus making it impossible to characterize any CtIP$^{-/-}$ mouse embryonic fibroblasts (MEFs). In contrast, EXO1$^{-/-}$ mice are viable with phenotypes of sterility and cancer predisposition[22-24,39]. In most cases the lethality of a gene in mice implies a similar phenotype for its human ortholog, hence leading us to postulate that CtIP, but not EXO1, might be essential in human somatic cells. However, exceptions do exist such as Ku86, where Ku86-null mice are alive[25,56] but Ku86-null human cells do not survive[26,57,58].

To induce the excision of "floxed" exons in the CtIP$^{F/-}$:CreERt2 and EXO1$^{F/-}$:CreERt2 cell lines, a final concentration of 10 nM tamoxifen was added to the cultures. Whole cell extracts were then prepared from the indicated time points to monitor CtIP and EXO1 expression levels by western analysis. After 3 days of tamoxifen exposure, CtIP (Fig. 2A) and EXO1 (Fig. 2B) protein levels were undetectable in the CtIP$^{F/-}$:CreERt2 and EXO1$^{F/-}$:CreERt2 cells respectively. In contrast, cells treated with just EtOH (carrier) as controls, maintained their respective expression of CtIP and EXO1 (Fig. 2A & 2B) throughout the duration of the experiment. Thus, CtIP$^{F/-}$:CreERt2 and EXO1$^{F/-}$:CreERt2 are efficiently converted into CtIP- and EXO1-null cells after the CreERt2 fusion protein is induced by tamoxifen. The CtIP$^{F/-}$:CreERt2 and EXO1$^{F/-}$:CreERt2 cells display a proliferation

pattern similar to WT:CreERt2 in the absence of tamoxifen (Fig. 2C). In contrast, CtIP$^{F/-}$:CreERt2 and EXO1$^{F/-}$:CreERt2 failed to proliferate like WT:CreERt2 cells in the presence of tamoxifen (Fig. 2D). Therefore, human somatic cells cannot survive without CtIP or EXO1.

When the cells stopped growing after tamoxifen treatment we noticed that the nuclei of CtIP- and EXO1- null cells shared morphological phenotype similar to X-ray irradiated cells, in which their nuclei dramatically increased in size due to severe DNA damage (data not shown). Consistent with this observation: the DNA damage marker p53 was highly elevated in tamoxifen-treated CtIP$^{F/-}$:CreERt2 and EXO1$^{F/-}$:CreERt2 cells (Fig. 2A and 2B). This is a strong indicator that DNA damage is accumulating in the absence of CtIP and EXO1.

Since the HCT116 cell line are MLH1-deficient[73], we were concerned that the lethality of CtIP and EXO1 may be synthetic with MLH1. Therefore, we established MLH1 expressing CtIP$^{F/-}$:CreERt2 and EXO1$^{F/-}$:CreERt2 cells (Fig. 1SC). After treating CtIP$^{F/-}$:CreERt2 + MLH1 and EXO1$^{F/-}$:CreERt2 + MLH1 cells with tamoxifen, we observed an identical lack of proliferation in the MTS colormetric assay (Fig. S1B), alongside with the diminishing protein levels of CtIP and EXO1 (Fig. S1C). Thus, CtIP and EXO1 are still essential in MLH1-expressing cells, and they are not synthetically lethal with the absence of MLH1.

In summary, we have shown that the CreERt2 inducible system is functional such that CtIP and EXO1 are inactivated in response to tamoxifen. We also established that human somatic cells do not survive the absence of CtIP or EXO1 and

accumulate DNA damage as measured by the up-regulation of p53 levels. Importantly, all of this occurred without any external sources of genotoxins.

Loss of CtIP or EXO1 induces chromosomal aberrations

Since damaged DNA presumably accumulates (Figs. 2A & 2B) in the absence of CtIP and EXO1, we sought to assess the effects of this absence on genomic stability by karyotype analysis. For this experiment, we used $CtIP^{F/-}$:CreERt2 and $EXO1^{F/-}$:CreERt2 cells that were immediately exposed to tamoxifen (day 0) as controls and compared them to cells exposed to tamoxifen for 1 day and the last possible time points when the samples can yield metaphase spreads for analysis (7 days for CtIP and 5 days for EXO1).

At day 0, the karyotypes of $CtIP^{F/-}$:CreERt2 appear normal with diploid chromosomes, minimal breaks and no evidence of chromosomal fragmentation (Fig. 3A & Table 1). However, after one day of tamoxifen treatment, chromosomal breaks in the CtIP-null cells become more frequent, and metaphases with >15 breaks appeared in 13% of the analyzed metaphases (Fig. 3A & Table 1). Congruent with increased breaks, we found quantifiable chromosome fragments (1 to 15) in 70% of the metaphases and 13% additional metaphases that were too fragmented to quantify. We also observed increased aneuploidy, where 60% of the metaphases had 47 to 60 chromosomes and 13% of the metaphases were tetraploid. After 7 days of tamoxifen treatment, the chromosomal abnormalities of CtIP-null cells are more severe as metaphases with >15 breaks and severely fragmented chromosomes doubled from 13% to 27%. Additionally, aneuploidy was more severe with an

increase to 17% tetraploid metaphases and 7% octaploid metaphases (Fig. 3A & Table 1).

Similarly at day 0, EXO1$^{F/-}$:CreERt2 cells appeared normal with diploid chromosomes, minimal breaks and no evidence of chromosomal fragmentation (Fig. 3B & Table 2). After one day of tamoxifen treatment, the chromosomal abnormalities in EXO1-null cells were more severe than CtIP-null cells with 75% of the metaphases containing >15 breaks and fragments were detected in all metaphases. Furthermore, 60% of the daylong tamoxifen-treated EXO1$^{F/-}$:CreERt2 cells were extremely fragmented while the remaining 40% had <15 fragments, and all metaphases were in the diploid range. After 5 days of tamoxifen treatment, all EXO1-null metaphases had >15 breaks and extremely fragmented chromosomes. In addition, 70% of the metaphases were tetraploid (Fig. 3 & Table 2).

Radial structures are rare forms of chromosomal fusions commonly seen in Fanconi Anemia patient cells treated with replication inhibitors[74]. Control CtIP$^{F/-}$:CreERt2 and EXO1$^{F/-}$:CreERt2 cells did not exhibit any radial chromosomes. However, 16% of tamoxifen-treated CtIP$^{F/-}$:CreERt2 cells acquired 1 to 3 radials, and 3% had more than 3 radials after 1 or 7 days respectively of tamoxifen treatment. In the EXO1$^{F/-}$:CreERt2 cells, we found that radial structures occurred at even higher frequency than CtIP$^{F/-}$:CreERt2 cells. After one day of tamoxifen exposure, 45% of the EXO1$^{F/-}$:CreERt2 cells acquired 1 to 3 radials and after 5 days, 50% of the cells had acquired 1 to 3 radials and 20% had more than 3 radials. Thus, the loss of CtIP or EXO1 results not only in chromosomal fragmentations, but also in fusions and radial structures.

CtIP and EXO1 regulate global DNA replication

CtIP and EXO1 have mainly been described as resection factors in DNA damage repair. However, CtIP has been implicated in regulation of the cell cycle because: i) CtIP is cell cycle regulated gene, which peaks during S and G2 phases[27-30,75], ii) CtIP interacts with Rb[31,36,76], a major cell cycle regulator, and iii) CtIP-null MEFs arrest in G0[31,32,39]. And recently, EXO1 was found to be intimately associated with replication forks in an iPOND-MS study[33-35,53].

Using asynchronous CtIP$^{F/-}$:CreERt2 and EXO1$^{F/-}$:CreERt2 cells, we analyzed cell cycle profiles of cells via an EdU incorporation assay that lacked CtIP or EXO1 to determine whether CtIP and EXO1 play direct roles in DNA replication. EtOH-treated WT:CreERt2, CtIP$^{F/-}$:CreERt2, and EXO1$^{F/-}$:CreERt2 cells appeared to maintain normal cell cycle profiles with distinct G1-, S- and G2-phases throughout the duration of the experiment (Fig. 4A, 4B, & 4C).

In stark contrast, the cell cycle profiles of tamoxifen-treated CtIP$^{F/-}$:CreERt2 and EXO1$^{F/-}$:CreERt2 cells were severely altered compared to tamoxifen-treated WT:CreERt2 cells and their EtOH-treated counterparts (Fig. 4). A day after CtIP$^{F/-}$:CreERt2 (Fig. 4D & Fig. S3F) and EXO1$^{F/-}$:CreERt2 cells were treated with tamoxifen, (Fig 4E & Fig S3F) virtually all of the cells occupied G2-phase. Eventually, the entire populations of CtIP- and EXO1-null cells become aneuploid such that they exceed 4N DNA content (Figs. 4D & 4F). During the acquisition process, we could not resolve cells with a DNA content that surpassed the linear detection threshold, indicating that there were cells with potentially 8N+ DNA content. Therefore, we

acquired data in logarithmic scale to identify missing populations of aneuploid cells. Indeed, after 7 days of tamoxifen treatment, the majority of CtIP- and EXO1-null cells were detected with 8N DNA content (Figs. S2D & S2F). Interestingly, we also observed 16N DNA content in cells lacking CtIP but not EXO1.

From these experiments we conclude that CtIP and EXO1 are required for the regulation of normal DNA replication and cell cycle progression. In the absence of CtIP or EXO1, continuous DNA replication without concomitant mitosis occurs until cells accumulate abnormally large amounts of DNA ranging from 8N to 16N.

CtIP and EXO1 are required for normal replication tract length

It was clear that DSBs are occurring endogenously in CtIP- or EXO1-null cells as evidenced by the accumulation of chromosomal aberrations (Fig. 3) and elevated p53 levels (Fig. 2). Moreover, the DSBs in these cells must originate from endogenous sources since the cells were not exposed to any DNA damaging agents. Importantly, DNA damage such as DSBs, lesions, and crosslinks can spontaneously occur during DNA replication in S-phase. Stalled replication forks that do not get reinitiated will collapse into DSBs that can result in chromosomal aberrations [36,64] [13,37] [38,62,63]. Furthermore, rodent cells defective for HR (BRCA2-deficient and dominant negative Rad51 expression in V79 hamster cells) suffer from slower replication fork velocities[77], and CHK1-deficient cells suffer from shorter replication tract lengths[78]. In conjunction with our data showing and continued DNA synthesis (Fig. 4), these studies in aggregate strongly hinted at DNA replication as the source

of DNA damage in the absence of CtIP and EXO1. In other words, we hypothesized that CtIP or EXO1 are required for normal DNA replication progression.

We assessed the direct impact of the loss of CtIP and EXO1 on DNA replication through a dual-labeled DNA fiber analysis. In this experiment, we compared DNA replication tract lengths in CtIP$^{F/-}$:CreERt2 and EXO1$^{F/-}$:CreERt2 cells treated with tamoxifen for 2 and 3 days to DNA replication tract lengths of their EtOH-treated counterparts and WT:CreERt2 cells. Replication tracts were first labeled with digoxigenin-dUTP (red) for 15 min followed by EdU (green) for 30 min. Tract lengths of the second label (green) that followed the first label (red) were used as a relative measure of replication velocity (Fig. 5D).

WT:CreERt2 cells produced median tract lengths of 15.9 μm whereas tract lengths of EtOH-treated CtIP$^{F/-}$:CreERt2 and EXO1$^{F/-}$:CreERt2 cells were significantly shorter, with median tract lengths of 14.4 μm ($p < 0.001$) and 11.8 μm ($p < 0.0001$), respectively (Fig. 5D). Therefore, cells that lack one allele of CtIP and EXO1 are haploinsufficient for DNA replication with slower replication fork velocities. Strikingly, after 2 days of tamoxifen treatment, the median tract lengths of CtIP$^{F/-}$:CreERt2 measured 7.9 μm (Fig. 5B) and EXO1$^{F/-}$:CreERt2 measured 7.2 μm (Fig. 5C), which were 2-fold shorter (Fig. 5D) than WT:CreERt2 tract lengths. After 3 days of tamoxifen treatment, replication tracts were severely shortened to median lengths of 3.0 μm in CtIP$^{F/-}$:CreERt2 (Fig. 5B) and 2.8 μm in EXO1$^{F/-}$:CreERt2 (Fig. 5C).

The fiber analysis demonstrated that replication forks have drastically reduced velocities in the absence of CtIP and EXO1. To extend these studies, we

analyzed chromatin fractions for PCNA by western analysis. In the WT:CreERt2 and EtOH-treated cells; we observed that the unmodified PCNA was the majority species in the chromatin (Fig. 5E). Strikingly, when the CtIP$^{F/-}$:CreERt2 and EXO1$^{F/-}$:CreERt2 cells were exposed to tamoxifen, their unmodified PCNA drastically shifted toward the larger, modified PCNA species over the course of the experiment. Previous experiments show that PCNA ubiquitylation functions as a 'code' for DNA damage to alert the cell of the different types of defects that arise during DNA replication[79], which is correlated with our findings.

In toto, these data suggest that CtIP and EXO1 are normally closely associated with the replication fork and PCNA for normal DNA replication progression. The notion that CtIP and EXO1 maybe closely associated with replication forks is not unfounded because CtIP associates with PCNA during replication[37,40] and EXO1 is associate with nascent DNA strands[30,36,53]. We extend these observations to show that the absence of CtIP or EXO1 directly impacts on DNA replication fork progression.

The loss of CtIP and EXO1 leads to stalled replication forks and DSBs

CtIP- and EXO1-null cells experience severe DNA replication defects (Fig. 5). Here, we sought for other markers at the whole cell level to confirm the presence of DNA damage and replication fork stalling. Additionally, we also took advantage of a

relatively large time window before the cell dies to acquire a temporal view of the dynamics of these markers in cells lacking CtIP and EXO1.

The phosphorylated form of H2AX (γH2AX) is a marker of DNA DSBs[41,80,81]. WT:CreERt2 cells on average possessed only 2 γH2AX foci per cell whereas CtIP$^{F/-}$:CreERt2 and EXO1$^{F/-}$:CreERt2 cells treated with EtOH had an average of 5 and 6 foci per cell, respectively. This observation confirmed the haploinsufficiency we observed earlier with fork progression (Fig. 5). In stark contrast, CtIP$^{F/-}$:CreERt2 cells possessed a range from 16 to 27 γH2AX foci per cell over a 5 day course of tamoxifen treatment and EXO1$^{F/-}$:CreERt2 cells scored even higher with a range from 23 to 25 gH2AX foci per cell. These numbers are significantly higher compared to WT:CreERt2 or even camptothecin (CPT) treated cells. The γH2AX foci persisted throughout the course of the experiment indicating that many DSBs remain unrepaired consistent with the breaks and fragments observed in the karyotype analysis we described above (Fig. 3 and Table 1).

53BP1 is a major NHEJ mediator[42,82,83] and it is an antagonist of the CtIP activity required for HR[43-47,84,85]. 53BP1 is responsible for the genotoxic NHEJ-mediated repair that results in chromosomal abnormalities[86] and it is proposed to inhibit HR by opposing CtIP-mediated end-resection[83-85]. Since the lack of CtIP or EXO1 apparently renders HR defective, we hypothesized that 53BP1 may now have free reign to mediate DSB repair in CtIP- and EXO1-null cells.

WT:CreERt2 and EtOH-treated CtIP$^{F/-}$:CreERt2 cells averaged less than 1 53BP1 focus per cell. The EtOH-treated EXO1$^{F/-}$:CreERt2 cells in contrast, which also have the most γH2AX foci amongst the controls, scored significantly higher with

3.5 53BP1 foci per cell (Figs. 6A and 6B) After a day of tamoxifen treatment, the CtIP$^{F/-}$:CreERt2 cells scored 6 foci per cell whereas EXO1$^{F/-}$:CreERt2 increased dramatically reaching a peak of 24 foci per cell. With increasing lengths of tamoxifen treatment, the average 53BP1 foci in CtIP$^{F/-}$:CreERt2 cells climbed to 11 per cell after 3 days and peaked at 14 per cell after 5 days. Conversely, EXO1$^{F/-}$:CreERt2 cells displayed a different trend, where the average 53BP1 foci gradually decreased to 13 and 11 per cell after 3 and 5 days, respectively of tamoxifen treatment (Figs 6A and 6B).

To support this immunofluorescence (IF) data, we prepared whole cell extracts (WCE) and chromatin fractions in order to assess chromatin recruitment patterns. Over the course of this experiment, 53BP1 recruitment to the chromatin increased after tamoxifen treatment in the CtIP$^{F/-}$:CreERt2 cells, whereas the opposite occurs in EXO1$^{F/-}$:CreERt2 cells. This trend in chromatin recruitment strongly mirrors the IF data (Figs. 6A & 6B).

So far, we have shown that CtIP- and EXO1-null cells suffer extensive DNA DSBs in addition to very short replication tract lengths. Moreover, the majority of the chromatin-bound PCNA in these cells is modified, consistent with the presence of high levels of lesions at the replication forks. Thus, we next wanted to determine whether DNA replication is the source of the DSBs. FANCD2 is a component of the Fanconi Anemia (FA) pathway that forms nuclear foci at stalled forks, which is required for restarting stalled replication forks[68,87]. In addition, RPA, another key HR factor, also forms foci in stalled replication forks[88,89]. Therefore, we analyzed

FANCD2 and RPA foci to evaluate if persistent stalled forks occurred in CtIP- and EXO1-null cells.

WT:CreERt2 cells averaged 1 FANCD2 focus per cell whereas both CtIP$^{F/-}$:CreERt2 and EXO1$^{F/-}$:CreERt2 cells treated with EtOH had an average of 2 FANCD2 foci per cell (Figs. 6A & 6C). This increase in FANCD2 foci is again consistent with earlier observations of haploinsufficiency in these cell lines. In comparison, WT:CreERt2 exposed to hydroxyurea had an average of 7 FANCD2 foci per cell. After a day of tamoxifen treatment, we observed that FACND2 foci reached their peaks in CtIP$^{F/-}$:CreERt2 and EXO1$^{F/-}$:CreERt2 cells with 5 and 7 FANCD2 foci per cell. After 3 and 5 days of tamoxifen treatment, a steep reduction of FANCD2 foci to less than 1 focus per cell was observed in both CtIP$^{F/-}$:CreERt2 and EXO1$^{F/-}$:CreERt2 cells.

We observed the same dynamics for RPA foci. Control WT:CreERt2 cells averaged less than 1 RPA focus per cell, whereas both CtIP$^{F/-}$:CreERt2 and EXO1$^{F/-}$:CreERt2 cells treated with EtOH had an average of 1.6 and 2.8 FANCD2 foci, respectively, per cell. WT:CreERt2 exposed to hydroxyurea exhibited 6.8 RPA foci per cell, consistent with HU's well-documented ability to stall replication forks[90]. After a day of tamoxifen treatment, RPA foci also reached their peaks in CtIP$^{F/-}$:CreERt2 and EXO1$^{F/-}$:CreERt2 cells with 6.5 and 7.3 RPA foci per cell. After 3 and 5 days of tamoxifen treatment, RPA foci in CtIP$^{F/-}$:CreERt2 cells declined to 4 and 2.7 foci, respectively. EXO1$^{F/-}$:CreERt2 cells experienced an even steeper decline after 3 and 5 days of tamoxifen treatment with averages of 1.2 and less than 1 focus per cell, respectively.

The chromatin recruitment patterns of FANCD2, RPA, and 53BP1 were identical to the foci dynamics of the respective proteins (Fig. 6G). Interestingly, FANCD2 protein levels in the WCE and chromatin fractions dropped below detection levels in CtIP- and EXO-null cells (Figs. 6F & 6G), suggesting that CtIP and EXO1 may regulate FANCD2 expression or stability (see also below). In contrast, RPA and 53BP1 levels in WCE were abundant and their expression/stability did not seem to be diminished (Figs. 6F & 6G).

Collectively, these observations suggested that the inactivation of CtIP or EXO1 triggers DNA replication fork stalling. And since the forks cannot be restarted, the stalled forks may persist for a few days and then collapse into DSBs that are improperly repaired by NHEJ.

CtIP and EXO1 are co-regulated and they coordinately regulate HR factors

Using western analysis of WCE and chromatin fractions, we were surprised to observe coordinate regulation of CtIP and EXO1 (Figs. 6F & 6G). Thus, in $CtIP^{F/-}$:CreERt2 cells treated with tamoxifen not only is CtIP depleted, but also EXO1 (Fig. 6F). An identical, loss of CtIP expression was also observed in EXO1-null cells (Fig. 6F). Additionally, we also observed that FANCD2 levels were dependent on the levels of CtIP and EXO1 (Fig. 6F). These observations suggested that DNA resection may directly regulate HR via the coordinate co-regulation of key HR factors. Thus, we next determined whether this stability effect could be extended to other HR factors that act downstream of FANCD2.

CtIP$^{F/-}$:CreERt2 and EXO1$^{F/-}$:CreERt2 cells were treated with tamoxifen and then harvested after 1, 3, 5, and 7 days to prepare WCE (Fig. 7A). These extracts were first probed for CtIP and EXO1 expression. As expected, both proteins were responsive to tamoxifen and their expression levels dropped below detection levels over the course of the experiment (Fig. 7A).

Surprisingly, after 3 days of tamoxifen treatment, FANCD2, BRCA2, and Rad51 were also barely detectable in CtIP$^{F/-}$:CreERt2 and EXO1$^{F/-}$:CreERt2 cells (Fig. 7A). We then asked if this coordinate regulation could be extended to DNA2 because like CtIP and EXO1, it is required for DSB resection. In the CtIP-null cells, DNA2 was rapidly degraded to levels below detection, similar to Rad51, BRCA2, and FANCD2. Conversely, in EXO1-null cells, we observed DNA2 was shifted to a larger species that persisted at day 3 and 5 after EXO1 inactivation and was then undetectable (together with CtIP) at the latest time point (Day 7). This suggests that the stability of DNA2 is also dependent on CtIP and EXO1.

The loss of CtIP or EXO1 triggers replication fork stalling and, in theory, should activate the ATR-CHK1 checkpoint. Very unexpectedly, however, CHK1 protein levels were downregulated in a dramatic fashion similar to FANCD2, BRCA2, and RAD51 in both CtIP- and EXO1-null cells (Fig. 7A). ATR levels were downregulated to below WT:CreERt2 levels in CtIP-null cells while ATR levels were not affected in the EXO1-null cells until CtIP expression dropped below detection levels (Fig. 7A). Furthermore, the mediator of ATR-CHK1 signaling, Claspin[91,92], was also degraded, which is consistent with studies showing that CHK1 regulates Claspin levels[93]. The loss of CHK1[94] and Claspin[95,96] expression, and the reduction in ATR

(Fig. 7A) levels indicated that the cells are under prolonged genotoxic stress from stalled replication forks and cannot recover from checkpoint activation.

Stalled forks that collapse into DSBs signal that damage through the ATM-CHK2 pathway. Importantly, CtIP- and EXO1-null cells had elevated total CHK2 levels and phosphorylated CHK2 ($Threonine_{68}$)[97] (Fig. 7B), and ATM was also upregulated and activated shown by the phosphorylation of ATM at $Serine_{1981}$[98] (Fig. 7B). Supporting our earlier conclusion that HR is disabled and that the DSBs are being repaired by NHEJ, the expression of the key NHEJ factor, Ku86, remained steady (Fig. 7A).

We next investigated whether a proteasomal degradation pathway was responsible for the rapid downregulation of HR factors in the absence of CtIP and EXO1. Cells treated with EtOH or tamoxifen for 24 hr followed by 1 uM of MG132, a well-documented proteasome inhibitor[99] or DMSO (control). WCE were prepared in the following 12- and 24-hr time points. In the controls, cells that were treated with EtOH and MG132 showed that the proteins of interest accumulated over time whereas DMSO-treated cells maintained normal protein levels. In both $CtIP^{F/-}$:CreERt2 and $EXO1^{F/-}$:CreERt2 cells treated with tamoxifen, we observed that FANCD2, BRCA2, Rad51, and CHK1 are likely regulated through the proteasomal degradation pathway because their protein levels were rescued -at least partially- in the presence of MG132 but not in DMSO (Fig. 7C). These results demonstrate that FANCD2, BRCA2, Rad51, and CHK1 are rapidly degraded by the proteasome when persistently stalled replication forks induced by the absence of DNA resection cannot be restarted.

The co-regulation and coordinate regulation of CtIP, EXO1, and DNA2

DNA2 is an additional important DNA resection factor. We also constructed a $DNA2^{F/-/-}$:CreERt2 conditionally-null HCT116 cell line and showed that DNA2 is also an essential gene in human somatic cells (data not shown). We used this cell line to investigate whether loss of DNA2 would also impact the stability of CtIP, EXO1, and HR factors. We prepared WCE from $DNA2^{F/-/-}$:CreERt2, $CtIP^{F/-}$:CreERt2, and $EXO1^{F/-}$:CreERt2 cells that were treated with tamoxifen after 1, 3, and 5 days. Consistently, the protein levels of CtIP, EXO1, and DNA2 in the corresponding conditionally-null cell lines diminished to levels below detection after tamoxifen treatment; indicating that the inducible CreERt2 system was functional (Fig. 8A).

As previously observed (Fig. 7A), we saw an immediate downregulation of CtIP protein levels after inactivating EXO1. In striking contrast, the inactivation of DNA2 led to an increase in CtIP protein levels at day 1, which then followed by the los of CtIP expression at days 3 and 5. Upon the inactivation of DNA2 and CtIP with tamoxifen, EXO1 protein levels were immediately downregulated to undetectable levels by day 3. Additionally, the inactivation of DNA2 also resulted in the rapid degradation of BRCA2, FANCD2, Rad51 and CHK1 protein levels.

To extended analysis of the novel phenotypes of coordinate regulation, we also characterized GM637 cells, which is an immortalized but otherwise normal, human fibroblast cell line[100]. In this cell line, we individually knocked down CtIP, EXO1, and DNA2 by siRNA and found that CtIP, EXO1, and DNA2 are indeed co-

regulated. Additionally, the protein levels of FANCD2 were also rapidly degraded after knocking down CtIP, EXO1, or DNA2 (Fig. 8C). This experiment shows that the regulatory functions of CtIP, EXO, and DNA2 are not specific to the HCT116 cell line.

In aggregate, our findings suggest that CtIP, EXO1, and DNA2 are co-regulated. The regulation pattern observed between them are slightly different such that: 1) CtIP inactivation leads to rapid degradation of EXO1 and DNA2, 2) EXO1 inactivation leads to a slower degradation of CtIP and DNA2 protein levels, and 3) DNA2 inactivation leads to an increase uniquely in CtIP expression followed by the rapid degradation of both CtIP and EXO1. Furthermore, we also show that CtIP, EXO1, and DNA2 are epistatic in human cells in the sense that their inactivation results in the similar and synchronous degradation of BRCA2, FANCD2, Rad51, and CHK1.

Finally, the chromatin recruitment patterns of HR factors in CtIP-, EXO1- and DNA2-null cells were inspected because the global protein levels from the WCE do not always reflect chromatin recruitment. As expected, the diminishing presence of CtIP, EXO1 and DNA2 in the chromatin of the corresponding conditionally-null cell lines indicated that the inducible CreERt2 system was functional upon tamoxifen treatment (Fig. 8D).

The chromatin recruitment of CtIP was much stronger in DNA2 heterozygous cells compared to EXO1 heterozygous cells. The complete inactivation of DNA2, however, resulted in decreased recruitment of CtIP at day 1, which became barely detectable at the remaining time points. In contrast, we observed moderate

chromatin recruitment of CtIP 1 day after EXO1 inactivation, although recruitment at later time points was undetectable.

The chromatin recruitment of EXO1 was significantly different between CtIP- and DNA2-null cells (Fig. 8D). Upon inactivation of CtIP, moderate EXO1 recruitment was observed only at day 1 but not at the later time points. Interestingly, the inactivation of DNA2 triggered a heavy recruitment of EXO1 to the chromatin at day 1, which was followed by a gradual decrease at days 3 and 5. Despite the decrease, the chromatin levels of EXO1 were still well above the level of detection. In contrast to what had been observed with WCEs, DNA2 was recruited and persisted in the chromatin fractions of CtIP- and EXO1-null cells throughout the duration of the experiment.

The fates of FANCD2, BRCA2, and Rad51 were similar to their corresponding WCE protein levels such that they were not present (or degraded) in the chromatin fractions of CtIP-, EXO1-, and DNA2-null cells by day 3 and thereafter (Fig. 8E). This observation further corroborates the dogma that BRCA2, FANCD2, and Rad51 are HR factors that reside downstream of resection.

In summary, the inactivation of DNA2 initially triggers heavy recruitment of EXO1 to the chromatin, which then gradually decreases over time. In contrast, the inactivation of EXO1 triggers recruitment of DNA2 to the chromatin at steady levels over time. This suggests that the two nucleases downstream of CtIP may mutually compensate for the loss of each other. The invariability of each single mutant, however, indicates that whatever compensation is occurring is insufficient to support viability.

Discussion

We have constructed three novel and powerful genetic models using human somatic cells that are conditionally-null (with inducible CreERt2 system) for CtIP, EXO1, or DNA2. With these cell lines, we discovered that CtIP, EXO1, and DNA2 are essential genes in the HCT116 cell line. The HCT116 cell line is also MLH1 deficient[73] and we were concerned that the lethality of CtIP and EXO may be synthetic with MLH1. To address this concern, we showed that MLH1-expressing HCT116 cells still do not survive without CtIP and EXO1, thereby excluding the possibility that CtIP and EXO1 are synthetically lethal with MLH1. Given that CtIP and EXO1 are essential for survival, we deduced that they carry out essential function(s) even in the absence of exogenous DNA damage. These studies have revealed essential function(s) for these genes and also uncovered a novel regulation of the HR pathway by CtIP and EXO1 in human somatic cells.

CtIP and EXO1 are required to maintain genomic stability

CtIP and EXO1 maintain genomic stability[31]. Thus, when CtIP and EXO1 were knocked-down the cells were more susceptible to radial chromosome formation when exposed to DNA damaging agents[31,83]. We showed here that cells completely lacking CtIP or EXO1 suffer from elevated levels of chromosomal breaks, fragmentations, and aneuploidy as well as radials. One of the more compelling aspects of our study is that $CtIP^{F/-}$:CreERt2 and $EXO1^{F/-}$:CreERt2 cells were never exposed to DNA damaging agents, showing that all these chromosomal abnormalities were manifested endogenously. It is also perhaps important to point

out that during the analysis we noticed many fusion events that were too complex to analyze and omitted from the dataset. Therefore, our results strongly supported the argument that CtIP and EXO1 maintain genome stability and led us to postulate that CtIP and EXO1 have essential roles in DNA replication.

CtIP, EXO1, and CHK1 are epistatic in regulating DNA replication

The inactivation of CtIP or EXO1 triggered continued DNA synthesis that resulted in cells containing an extremely high DNA content. The maximum DNA content peaked at approximately 16N in CtIP-null cells and 8N EXO1-null cells, which was in agreement with the karyotype analyses showing octaploid chromosomes only in CtIP-null cells. Extending our studies on DNA replication, we showed that replication fork tract lengths drastically decreased in a time-dependent manner in CtIP- and EXO1-null cells. Interestingly, we also observed that the inactivation of CtIP or EXO1 causes rapid CHK1 degradation (Fig. 7A).

We argue that the replication phenotypes and the CHK1 loss in the absence of CtIP and EXO1 are correlated events. Supporting our argument, similar DNA replication phenotypes have been reported as a result of CHK1 deficiency. Previous studies showed that the inhibition of CHK1 in human cells causes increased DNA replication initiation[101] and checkpoint mutants in yeast lead to continued DNA synthesis and increased breaks[102]. Moreover, DT40 CHK1$^{-/-}$ cells, replication fork progression is severely impaired with severely short replication tract lengths[78]. Collectively, these data support our argument that CtIP, EXO1, and CHK1 are

epistatic in a pathway that regulates DNA replication initiation, fork progression and that they contribute to genome stability.

CtIP and EXO1 are closely associated with the replication fork to prevent replication fork collapse and mutagenic NHEJ repair

Highly repetitive regions in the human genome, including trinucleotide repeats (TNRs), telomeres, LINE, SINE, DNA transposons, and ALU repeat elements transiently form complex DNA structures at periods when they become single-stranded[5-7] such that they can become barriers to DNA replication and thus trigger replication fork stalling[4,8-10]. CFs and ERCFs reside in these repetitive regions and are prone to breakage during DNA replication[14] and they break more so when ATR is inhibited[11-13]. Furthermore, previous studies reported that: i) CtIP is tethered to PCNA at the replication fork to survey for replication associated damages and activate checkpoints, ii) PCNA promotes processive resection by EXO1 *in vitro*, iii) EXO1 is associated with nascent DNA strands during replication.

Together, our experiments and previous studies, suggest that in CtIP- and EXO1-null cells replication forks stall at highly repetitive regions and then collapse into DSBs. Therefore, CtIP and EXO1 are likely working in concert with the replication forks to prevent fork stalling when they encounter complex DNA structures at repetitive regions.

In both CtIP and EXO1-null cells, FANCD2 and RPA foci formation and chromatin recruitment dynamics were similar, where they initially peaked and then diminished in a time dependent manner. Additionally, PCNA was modified and

subsequently accumulated over time in the chromatin fractions of CtIP- and EXO1-null cells. Together, these events indicate that the absence of CtIP and EXO1 strongly triggers the stalling of replication forks that then persist over days because they cannot restart. Since this event coincides with high levels of γH2AX foci and increasing CHK2 and ATM activation, we also argue that the stalled forks eventually collapse to form DSBs.

CtIP and 53BP1 compete for DSBs[83] and 53BP1 is modulated by ATM to and performs toxic NHEJ repairs[86] that result in chromosomal radials and fusions. With the HR pathway disabled in CtIP- and EXO1-null cells and the concomitant activation of ATM-CHK2, 53BP1[103,104] may now be free to monopolize all the DSBs for NHEJ repair which result in the chromosomal aberrations[86] that we observed in the karyotype analysis of CtIP- and EXO1-null cells (Fig. 3).

Regulatory functions of CtIP, EXO1, and DNA2

We show here that CtIP, EXO1, and DNA2 are co-regulated. The loss of CtIP, EXO1, or DNA2 ultimately results in the downregulation of the other two proteins. As surprising, CtIP, EXO1, and DNA2 also coordinately regulate FANCD2, BRCA2, Rad51, and CHK1 expression. Thus, the inactivation of CtIP, EXO1, or DNA2 triggers the simultaneous degradation of FANCD2, BRCA2, Rad51, and CHK1 that was mediated by the proteasome. The loss of these proteins essentially renders the HR[3,16,105] and FA pathways inactive. These observations demonstrate that the FA and HR pathways are closely connected by DNA resection.

The influence of CHK1 on DNA replication

CHK1 plays a significant role in DNA replication. In human cells, CHK1 inhibition causes increased replication initiation [101]. Another study in human cells also showed that prolonged genotoxic stress leads to CHK1 degradation[94]. Furthermore, DT40 CHK1$^{-/-}$ cells have very short DNA replication tracts and present with cell cycle defects[78]. Lastly, Rad53 (i.e., CHK1) mutants in yeast suffered with continued DNA synthesis and increased breaks[102]. Claspin is the mediator for the ATR-CHK1 signaling and it is regulated by CHK1 protein levels[91-93]. Like CHK1, Claspin also influences replication fork progression [106].

CHK1 degradation is a normal response to replication stress. When CHK1 is activated it must be degraded in order for the cell to terminate the checkpoint and recover. The degradation process was teased apart when cells were exposed to prolonged genotoxic stress where it was then observed that CHK1 was degraded by the proteasome[94]. Claspin shares a similar fate with CHK1 after checkpoint activation[96] and Claspin protein levels are regulated by CHK1. Unlike CHK1, Claspin is expressed in S- and G2- phases and degraded upon entry into mitosis[96]. In our CtIP- and EXO1-null human cells CHK1 as well as Claspin is degraded in concert with severely shortened DNA replication tract lengths. We argue that the inactivation of CtIP or EXO1 triggers replication fork stalling that results in a Claspin-mediated CHK1 activation. Since the stalled replication forks cannot restart, CHK1 and Claspin are constantly activated and degraded. As a result, checkpoint termination and cell cycle progression cannot take place. Finally, without ATR-CHK1, the stalled replication forks are destabilized[63,70 64] and collapse into DSBs[107].

Claspin degradation can also be caused as a byproduct of mitotic entry. This seems unlikely, to be relevant to our data, however because CtIP- and EXO1-null cells no longer proliferate and the robust CHK2 activation (Fig. 7A) indicates that the cells are arrested.

Summary

In an unperturbed S-phase, a replication forks eventually run into repetitive regions that causes them to stall. Through Claspin, the ATR-CHK1 pathway is activated which in turn, stabilizes the stalled forks and recruits replication fork restart factors including FANCD2, BRCA2, and Rad51. CtIP and EXO1 are also closely associated with the replication forks, presumably through docking on to PCNA. The close proximity of CtIP and EXO1 permits swifter action on the stalled forks for end resection that creates access for FANCD2, BRCA2, and Rad51 to restart the stalled forks in timely manner. However, in the absence of CtIP and EXO1, stalled replication forks are unable to restart because the FANCD2, BRCA2 and Rad51 cannot correctly access the stalled forks. As the stalled forks persist over time, CHK1 and Claspin is under constant activation and degradation with no time to recover their protein levels. As a result, ATR cannot stabilize the stalled forks without CHK1 and the forks are now susceptible to fork collapse.

Materials and Methods

Cell culture

The wild-type HCT116 cell line and mutant derivatives were cultured in McCoy's 5A medium containing 10% fetal bovine serum, 100 U/ml penicillin/streptomycin in a humidified incubator with 5% CO_2 at 37 ^{o}C. Applicable cell lines were selected in 0.5 to 1 mg/ml G418 concentrations during gene targeting selection and 1ug/mL of puromycin for the selection of stable CreERt2 expressing cells. To induce stalled replication forks and DSBs, cells were exposed to 1 mM hydroxyurea for 24 hr, and 10 uM camptothecin for 4 hr, respectively. CreERt2 was induced by 5 nM of tamoxifen to excise floxed alleles in the nucleus.

CreERt2 and MLH1 expression vector construction

PB/SB-CG-DEST (Puro) has been described[108]. Cre-ER ^{t2} was PCR amplified from pCAG-CreER^{t2} (Addgene, Plasmid 14797) with HincII and AvrII sites engineered into the forward and reverse primers, respectively. The purified CreER^{t2} PCR product was digested with HincII and AvrII (New England BioLabs) and ligated into pENTR221 with compatible SnaBI and XbaI restriction sites. LR clonase reaction (Invitrogen) was then performed using PB/SB-CG-DEST (Puro) and pENTR221- Cre-ER, following the manufacturer's instructions. A MLH1 cDNA was PCR amplified from pCEP9 MLH1 (Addgene, Plasmid16458) with primers containing attB1 and attB2 sites. The MLH1 PCR product was first cloned into pDONR221 via a BP clonase reaction, and subsequently cloned into PB/SB-CG-DEST (Neo) via a LR clonase reaction according to the manufacturer's instructions.

rAAV knockout vector construction and rAAV production

rAAV knockout vector construction as well as rAAV production was carried out according to methodologies and procedures as described[109]. PCR products were amplified from wild-type HCT116 genomic DNA with the Phusion Polymerase Enzyme (Thermo Scientific). Primer sequences are shown in table S1.

Genomic DNA isolation and PCR screening

To screen for correctly targeted clones, genomic DNA was isolated in a 96-well format with DirectLysis–PCR Reagent (ViagenBiotech). A homemade Taq polymerase was used in the screening PCR, and screening primers are available upon request.

Immunostaining

Cells were grown in chamber slides. After two rinses with 1X PBS, cells were fixed in 4% paraformaldehyde for 10 min. Cells were permeabilized with ice-cold 0.1% Triton X-100, CSK buffer (10 mM HEPES-KOH, pH 7.4, 300 mM sucrose, 100 mM NaCl, 3 mM MgCl2) 10 min, washed twice with 0.1% Tween 20, 1X PBS (PBST). Permeabilized cells were blocked with 5% fish skin gelatin or 5% BSA, 1X PBS, 0.1% Tween 20 for 1 hr, and incubated with primary antibody and incubated for 30 min at RT, or overnight at 4°C. Cells were washed 3 x 5 min with 0.1% Tween 20, 1X PBS and incubated with secondary antibodies for 30 min at room temperature. Cells were washed 3 x 5 min with PBST again, incubated in 2 ug/mL DAPI for 3 min, dried

and mounted on to cover slips (No. 1 thickness) with ProLong® Gold Antifade Reagent (P36934) from Life Technologies. All washes were carried out with gentle shaking. Slides were viewed with Zeiss Axioplan 2 confocal microscope at 60X. Images and foci were analyzed with FIJI.

Cell viability assay

Cells were seeded at 400 cells/well in 96-well plates the day before exposing cells to 5 nM Tamoxifen or an equivalent volume of EtOH. Cell viability was measured at the indicated time points with the CellTiter 96® AQueous One Solution Cell Proliferation Assay from Promega according to manufacturer's instructions. Wavelengths were measure at 492 nm on a Wallac plate reader.

DNA fiber assays

Prior to labeling replicating forks with digoxigenin-dUTP (Dig-dUTP), cells were treated with a hypotonic buffer solution (10 mM HEPES, 30 mM KCl, pH 7.4) to allow efficient transport of dig-dUTP into the nucleus. Cells were incubated with 100 mM Dig-dUTP for 15 min, followed by 50 uM EdU. After labeling, cells were harvested with a 10-fold excess of unlabeled cells, fixed (3:1 methanol:acetic acid fixative solution) and dropped onto slides. Slides were dipped in cell lysis solution and DNA fibers were stretched by gravity. For visualization, Dig-dUTP was stained with a primary sheep anti-digoxigenin antibody from Roche, followed by a secondary Alexa Fluor® 594 Donkey anti-sheep IgG (H+L) antibody from Life Technologies. Incorporated EdU was first labeled with a biotin via click reaction,

followed by streptavidin, Alexa Fluor® 488 conjugate. Slides were viewed on a Zeiss Axioplan 2 confocal microscope and replication tract lengths were measure with FIJI. Tract length results are takes from two experiments (N=100/experiment). Error bars represent the standard error of the mean and significance was determined by the Mann-Whitney test, where $P < 0.001$, and $P < 0.0001$ are ***, and ****, respectively.

Whole cell extract (WCE) preparation and chromatin fractionation of human cells

For WCE preparation, cells were trypsinized and washed with 1X PBS. The cell pellets were suspended in cell lysis buffer (in 10 mM Tris pH 7.4, 150 mM NaCl, 1% NP-40, 0.5% sodium deoxycholate, 1 mM EDTA, 1 mM DTT, complete protease inhibitor cocktail tablets by Roche). For chromatin fractions, cell pellets were resuspended in CSK buffer (10 mM HEPES-KOH, pH 7.4, 300 mM sucrose, 100 mM NaCl, 3 mM MgCl2, complete protease inhibitor cocktail tablets by Roche) and prepared as described[110].

Karyotype analysis

Karyotype analysis was sourced to the Cytogenomics Shared Resource at the University of Minnesota.

EdU incorporation assay

Cells were incubated with 10uM EdU for 40 min for EdU incorporation. 400,000 cells were harvested and labeled with the Click-iT® EdU Alexa Fluor® 647 Flow Cytometry Assay Kit (Life Technologies), according to a described modified procedure [111].

Immunoblotting and antibodies

20-27 ug of WCE and chromatin samples were separated on 4-15% gradient gels (Bio-Rad) and transferred on to PVDF membranes (GE Healthcare). Membranes were blocked with 5% nonfat powdered milk (Amresco) for 1 hr, and probed with primary antibodies over night at 4°C with gentle rocking. Horseradish peroxidase-conjugated secondary antibodies and ECL Prime detection solution (GE Healthcare) were used to detect protein bands. Membranes were stripped with Restore Western Blot Stripping Buffer (Thermo Scientific). A List of antibodies is shown in Table S3.

Figure Legends

Figure 1. Construction of conditional CtIP and EXO1-null cell lines

Scheme for inactivating CtIP and EXO1. (A) Partial diagrams of the human CtIP and EXO1 loci. Numbered rectangles represent exons and solid triangles depict loxP sites. Conditional rAAV knockout vectors were designed to target exons 2 and 3 of CtIP and EXO1, respectively. Correctly targeted clones, (B) CtIP$^{Neo/+}$ and EXO1$^{Neo/+}$ clones were transiently transfected with a Cre-expressing plasmid (+PGK Cre) to excise the SEPT:Neo cassette. (C) G418 sensitive CtIP$^{F/+}$ and EXO1$^{F/+}$ clones retaining the "floxed" exon were identified and subjected to a second round of gene targeting with a non-conditional knockout vector (SEPT:Neo). The SEPT:Neo cassette in the (D) CtIP$^{F/Neo}$ and EXO1$^{F/Neo}$ null cell lines was again excised by pPGK-Cre transient transfection to yield "floxed" conditional (E) CtIP$^{F/-}$ and EXO1$^{F/-}$ null cell lines. (F) The inducible CreERt2 recombinase system was established by stably introducing a CreERt2-expressing plasmid via PiggyBac transposition. Scheme for inactivating DNA2. (G) Partial diagram of the human DNA2 locus. Numbered rectangles represent exons and solid triangles depict loxP sites. Conditional rAAV knockout vectors were designed to target exon 2 of DNA2. Correctly targeted clones, (H) DNA2$^{Neo/+/+}$ clones were transiently transfected with a Cre-expressing plasmid (+PGK Cre) to excise the SEPT:Neo cassette. (I) G418 sensitive DNA2$^{F/+/+}$ clones retaining the "floxed" exon were identified and subjected to a second round of gene targeting with the same conditional knockout vector. (J) The SEPT:Neo cassette in DNA2$^{F/Neo/+}$ cell lines was excised again by pPGK-Cre transient transfection to yield (K) DNA2$^{F/-/+}$ null cell lines. (L) The third allele was knocked

out in a similar fashion with the same conditional knockout vector and (M) excision of the SEPT:Neo cassette in DNA2$^{F/-/Neo}$ yielded a conditional DNA2$^{F/-/-}$ null cell line. (N) The inducible CreERt2 recombinase system was established by stably introducing a CreERt2-expressing plasmid via PiggyBac transposition.

Figure 2. CtIP and EXO1 are essential in human somatic cells

Tamoxifen induces the loss of CtIP and EXO1 expression. A-B) Cells were plated the day before adding EtOH or tamoxifen. Cells were harvested for whole cell extract (WCE) preparation after 1, 3, 5 and 7 days post-tamoxifen or EtOH exposure and separated on a 4 to 15% polyacrylamide gel. The membrane was immunoblotted with antibodies against CtIP, EXO1 and p53. Cells do not grow without CtIP and EXO1. Cells were plated on 96-well plates at 500 cells per well in triplicate the day before adding EtOH (C) or tamoxifen (D) and cell growth was measured via a MTS colormetric assay.

Figure 3. CtIP and EXO1 are required for genomic stability

The loss of CtIP and EXO1 induces severe chromosomal aberrations. A) Representative karyotypes of $CtIP^{F/-}$:CreERt2 cells and B) $EXO1^{F/-}$:CreERt2 cells in a time course exposure to tamoxifen. Red arrows indicate chromosomal breaks and blue arrows represent radials. Chromosome fragments are labeled with a red f.

Figure 4. CtIP and EXO1 regulate DNA replication

Increased DNA replication initiation in the absence of CtIP and EXO1. Cells were plated the day before adding EtOH or tamoxifen. On the indicated time points, cells were incubated with EdU for 40 mins and harvested for staining accordingly to the manufacturer's instructions. EdU was labeled with Alexa-Fluor 647 to measure nucleotide incorporation and propidium idodide (PI) was used to measure DNA content. On the X-axis: PI and Y-axis: EdU Alexa Fluor 647. A) WT:CreERt2, B) $CtIP^{F/-}$:CreERt2 and C) $EXO1^{F/-}$:CreERt2 cells in EtOH for 7 days. Cell cycle profiles of A) WT:CreERt2, B) $CtIP^{F/-}$:CreERt2 and C) $EXO1^{F/-}$:CreERt2 cells treated with EtOH for 7 days. Cell cycle profiles of C) WT:CreERt2, D) $CtIP^{F/-}$:CreERt2 and E) $EXO1^{F/-}$:CreERt2 cells treated with tamoxifen.

Figure 5. CtIP and EXO1 are required for normal DNA replication tract lengths

Loss of CtIP and EXO1 severely reduces DNA replication fork velocities. Dual labeling of DNA fibers. A) Cells were plated in 48-well plates the day before tamoxifen or EtoH treatment. After 2 and 3 days the cells were first labeled with Digoxigenin-dUTP for 15 min and then with EdU for 30 min. Digoxigenin-dUTP was stained with Alexa-Fluor 594 (red) and EdU was stained with Alexa-Fluor 488 (Green). Representative images of dual-labeled fibers and their median replication tract lengths (Med) in microns from (B) WT:CreERt2 cells, (C) $CtIP^{F/-}$:CreERt2 and (D) $EXO1^{F/-}$:CreERt2 cells treated with EtOH or tamoxifen. (E) Box plots of replication tract lengths from a total 200 fibers (from two independent experiments). The Mann-Whitney test show that replication tract lengths in $CtIP^{F/-}$:CreERt2 and $EXO1^{F/-}$:CreERt2 cells treated with EtOH or tamoxifen are significantly shorter than those of WT:CreERt2 cells.

Figure 6. Inactivation of CtIP and EXO1 triggers severe replication fork stalling

Inactivation of CtIP and EXO1 induces DSBs and DNA damage foci associated with replication fork stalling. A) Cells were grown in 4-well chamber slides and treated with EtOH or tamoxifen the next day. At the indicated time points, cells were fixed with paraformaldehyde and stained with the appropriate antibodies. γH2AX and 53BP1 foci were induced by incubating WT: Cre ERt2 cells with 10 uM Camptothecin (CPT) for 4 hr; FANCD2 and RPA foci were induced by incubating WT: Cre ERt2 cells with 1 mM hydroxyurea for 24 hr. Foci were scored from a total of 400 nuclei from two independent experiments and bars represent average foci per cell. B) Representative images of γH2AX in red, C) 53BP1 foci in red, D) FANCD2 in green and E) RPA in red. Images in blue represent DAPI staining of nuclear DNA. F) Western analysis of whole cell extracts (WCE) and G) chromatin fractions prepared from cells at the indicated time points and conditions.

Figure 7. CtIP and EXO1 levels are mutually dependent and they regulate HR factors

A) Cells were plated on 10 cm dishes and treated with EtOH or 10 uM tamoxifen the next day. Cells were harvested after 1, 3, 5, and 7 days after tamoxifen treatment or 7 days after EtOH treatment for whole cell extract preparation (WCE). WCE was electrophoresed on a 4-15% polyacrylamide gel and immunoblotted with antibodies against CtIP and EXO1. The membrane was stripped and reprobed with antibodies against the indicated HR and DNA replication factors. CtIP and EXO1 regulate CHK1 and other cell cycle related factors. B) The same membrane from above was stripped and reprobed for CHK1 and other cell-cycle checkpoint related proteins. The 26S proteasome complex degrades the proteins regulated by CtIP and EXO1. C) Cells were plated on 10 cm dishes and allowed to grow overnight before adding 10 uM of tamoxifen or EtOH. 24 hr later 1 mM MG132 or DMSO was added to the plates that still contain 10uM Tamoxifen or DMSO. After 12 and 24 hr post MG132 exposure, cells were harvested for WCE preparation. WCE were separated on a 4 to 15% polyacrylamide gel and probed for the indicated proteins of interest.

Figure 8. Coordinate regulation of CtIP, EXO1 and DNA2

CtIP, EXO1 and DNA2 are co regulated. A) WCE from WT HCT116 and the indicated derivatives were separated on a 4 to 15% polyacrylamide gradient gel and immunoblotted with antibodies against CtIP, and subsequently stripped and reprobed for EXO1 and DNA2. B) CtIP, EXO1, and DNA2 coordinately regulate BRCA2, FANCD2, Rad51 and CHK1. The co-regulation of CtIP, EXO1, and DNA2 is not specific to the HCT116 cell line. C) CtIP, EXO1 and DNA2 are co-regulated in normal cells (GM637 fibroblasts), and coordinately regulate FANCD2 protein levels. The loss of CtIP, EXO1 and DNA2 triggers chromatin recruitment of DNA repair factors. D) Chromatin fractions from wild-type HCT116 cells and derivatives were separated on a 4 to 15% polyacrylamide gradient gel and probed with the appropriate antibodies. F) CtIP, EXO1, and DNA2 coordinately regulate BRCA2, FANCD2, Rad51 and CHK1.

Table 1. Quantitation of chromosomal aberrations in tamoxifen-treated CtIP$^{F/-}$:CreERt2 cells

Final time points of the indicated cell lines were chosen based on availability of metaphases for analysis. Metaphases were scored for breaks, chromosome fragments, aneuploidy, and radial structures. All values are represented as percentage of metaphases analyzed.

Table 2. Quantitation of chromosomal aberrations in tamoxifen-treated $EXO1^{F/-}$:CreERt2 cells

Final time points of the indicated cell lines were chosen based on availability of metaphases for analysis. Metaphases were scored for breaks, chromosome fragments, aneuploidy, and radial structures. All values are represented as percentage of metaphases analyzed.

Figure 1

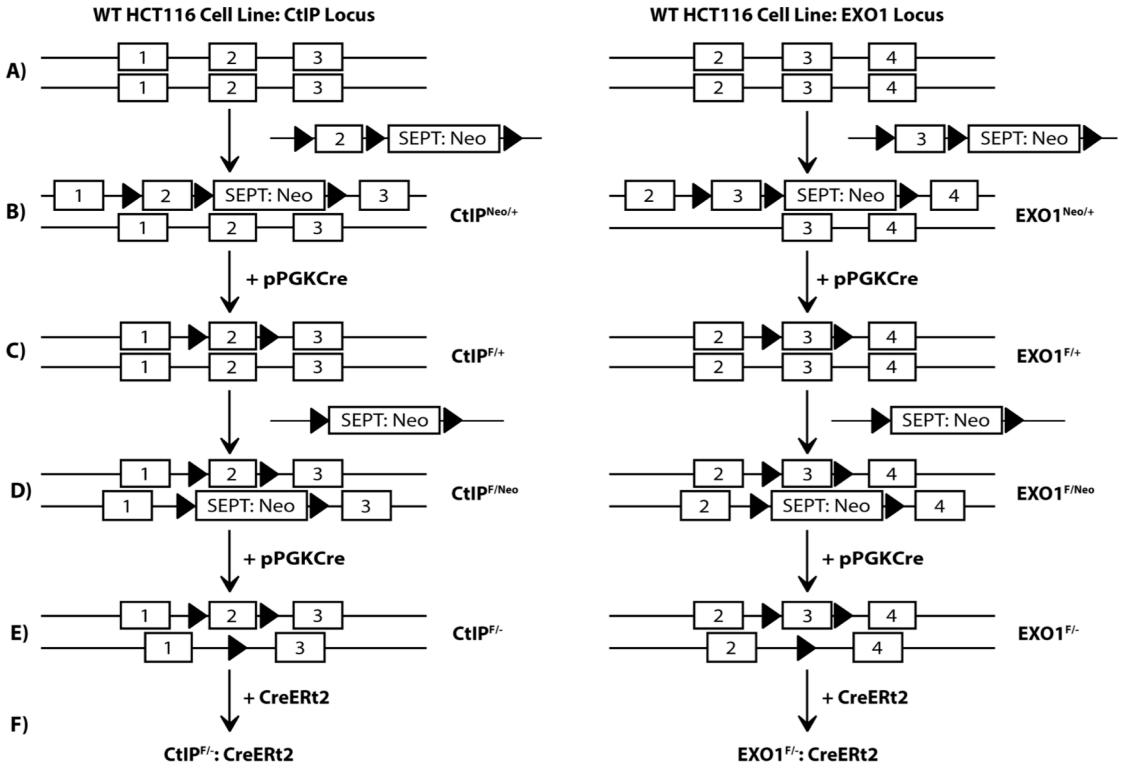
WT HCT116 Cell Line: CtIP Locus
WT HCT116 Cell Line: EXO1 Locus
A)
B)
C)
D)
E)
F)
SEPT: Neo
+ pPGKCre
+ CreERt2
CtIP^Neo/+
CtIP^F/+
CtIP^F/Neo
CtIP^F/-
CtIP^F/-: CreERt2
EXO1^Neo/+
EXO1^F/+
EXO1^F/Neo
EXO1^F/-
EXO1^F/-: CreERt2

Figure 1

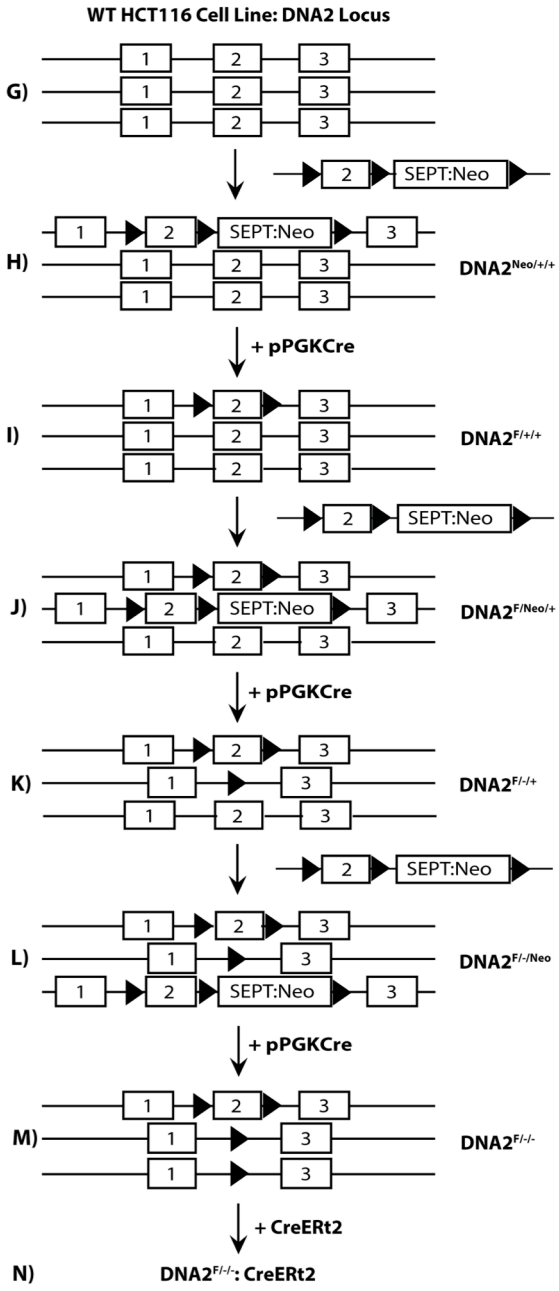
WT HCT116 Cell Line: DNA2 Locus
G)
H)
DNA2Neo/+/+
+ pPGKCre
I)
DNA2F/+/+
J)
DNA2F/Neo/+
+ pPGKCre
K)
DNA2F/-/+
L)
DNA2F/-/Neo
+ pPGKCre
M)
DNA2F/-/-
+ CreERt2
N)
DNA2F/-/-: CreERt2
SEPT:Neo

Figure 2

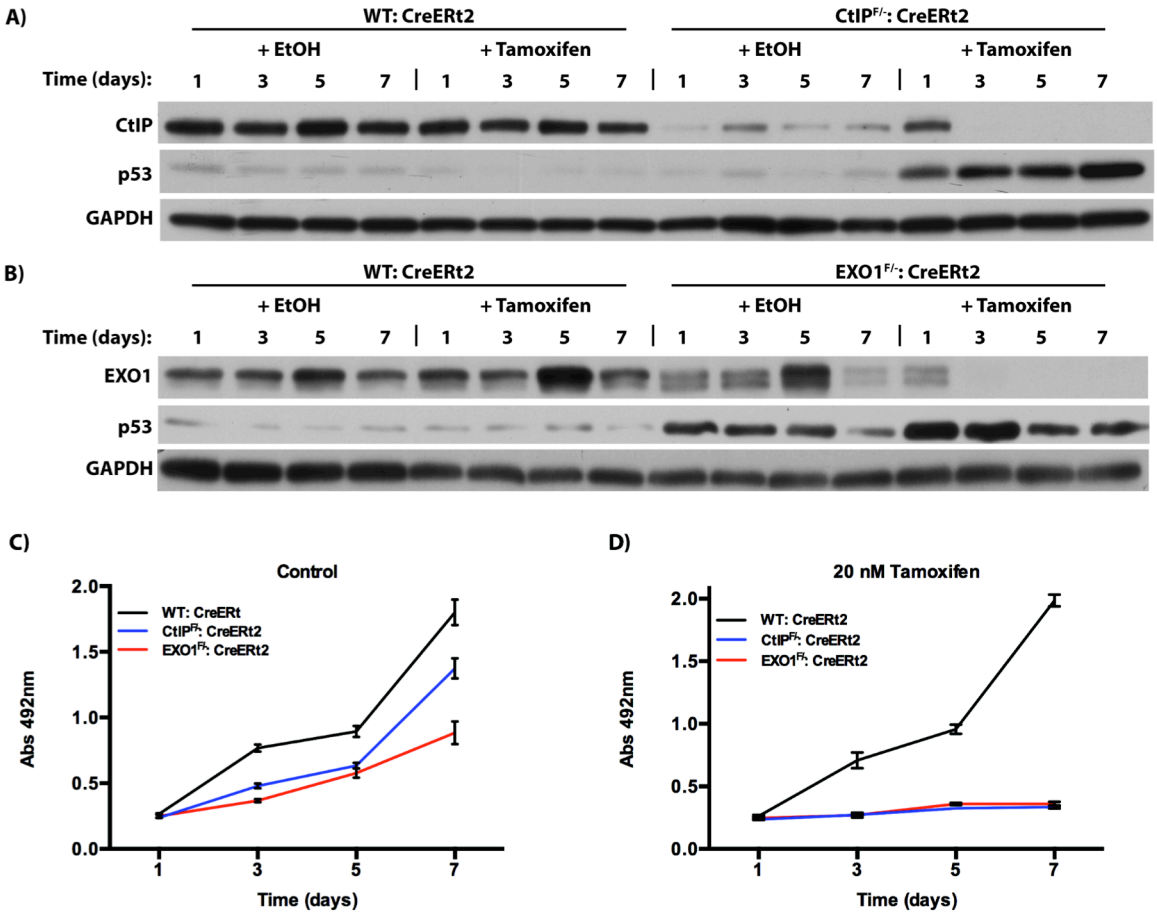
A)
WT: CreERt2
CtIP F/-: CreERt2
+ EtOH
+ Tamoxifen
Time (days): 1 3 5 7 1 3 5 7 1 3 5 7 1 3 5 7
CtIP
p53
GAPDH
B)
WT: CreERt2
EXO1 F/-: CreERt2
+ EtOH
+ Tamoxifen
Time (days): 1 3 5 7 1 3 5 7 1 3 5 7 1 3 5 7
EXO1
p53
GAPDH
C)
Control
WT: CreERt
CtIP F/-: CreERt2
EXO1 F/-: CreERt2
Abs 492nm
Time (days)
D)
20 nM Tamoxifen
WT: CreERt2
CtIP F/-: CreERt2
EXO1 F/-: CreERt2
Abs 492nm
Time (days)

Figure 3

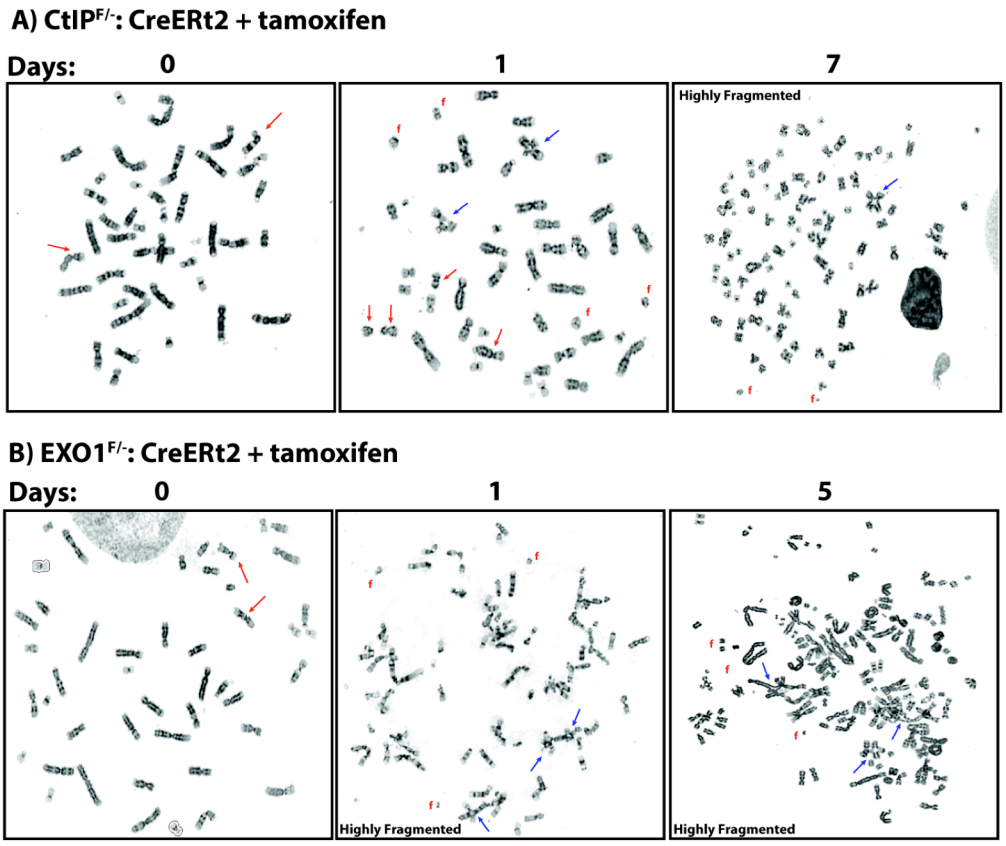
A) CtIP$^{F/-}$: CreERt2 + tamoxifen
Days: 0
1
7
Highly Fragmented
B) EXO1$^{F/-}$: CreERt2 + tamoxifen
Days: 0
1
5
Highly Fragmented
Highly Fragmented

Table 1

Table 1: Karyotype analyses of CtIP mutants

CtIP$^{F/-}$: CreERt2				
Days after tamoxifen treatment		**0**	**1**	**7**
Breaks	0	66.7	0.0	6.7
	1-3	30.0	36.7	43.3
	4-15	3.3	50.0	23.3
	>15	0.0	13.3	26.7
Fragments	0	0.0	20.0	46.7
	Present < 15	0.0	70.0	26.7
	Highly Fragmented	0.0	13.3	26.7
Chromosomes (Count)	43-46	100.0	26.7	60.0
	>47-60	0.0	60.0	16.7
	Tetraploid	0.0	13.3	16.7
	Octaploid	0.0	0.0	6.7
Radials	0	100.0	80.0	83.3
	1-3	0.0	16.7	13.3
	>3	0.0	3.3	3.3
	Total Metaphases Anlayzed	**30**	**30**	**30**

Values represented as percentage of total metaphases analyzed

Table 2

Table 2: Karyotype analyses of EXO1 mutants

EXO1$^{F/-}$: CreERt2				
Days after tamoxifen treatment		**0**	**1**	**5**
Breaks	0	66.7	0.0	0.0
	1-3	26.7	0.0	0.0
	4-15	6.7	25.0	0.0
	>15	0.0	75.0	100.0
Fragments	0	100.0	0.0	0.0
	Present < 15	0.0	40.0	0.0
	Highly Fragmented	0.0	60.0	100.0
Chromosomes (Count)	43-46	90.0	100.0	0.0
	>47-60	10.0	0.0	30.0
	Tetraploid	0.0	0.0	70.0
	Octaploid	0.0	0.0	0.0
Radials	0	100.0	55.0	30.0
	1-3	0.0	45.0	50.0
	>3	0.0	0.0	20.0
	Total Metaphases Anlayzed	**30**	**20**	**10**

Values represented as percentage of total metaphases analyzed

Figure 4

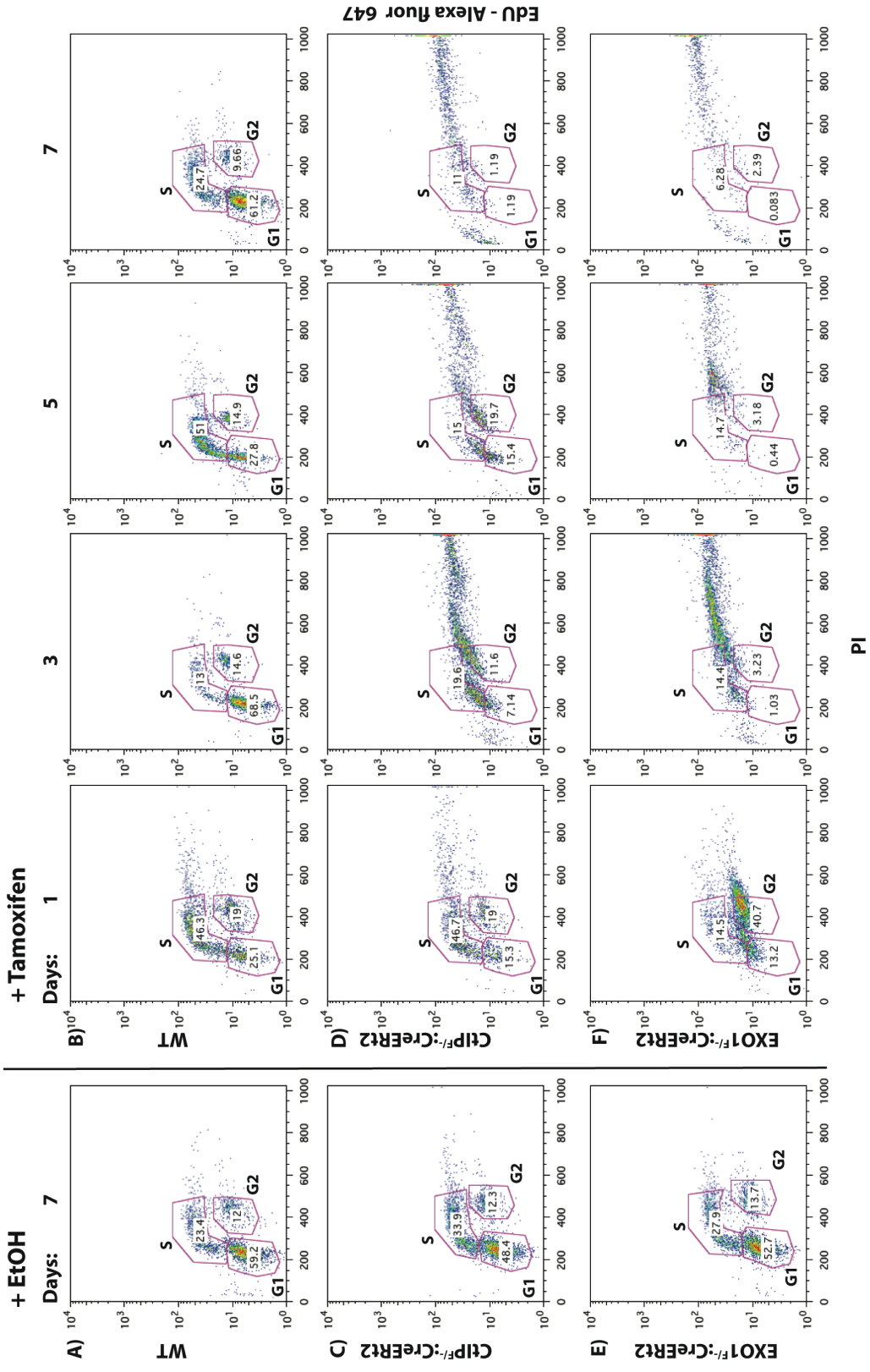
+ EtOH
+ Tamoxifen
Days: 7
Days: 1
3
5
7
A)
B)
C)
D)
E)
F)
WT
Ctip F/-:CreERt2
EXO1 F/-:CreERt2
S
G1
G2
EdU - Alexa fluor 647
PI

Figure 5

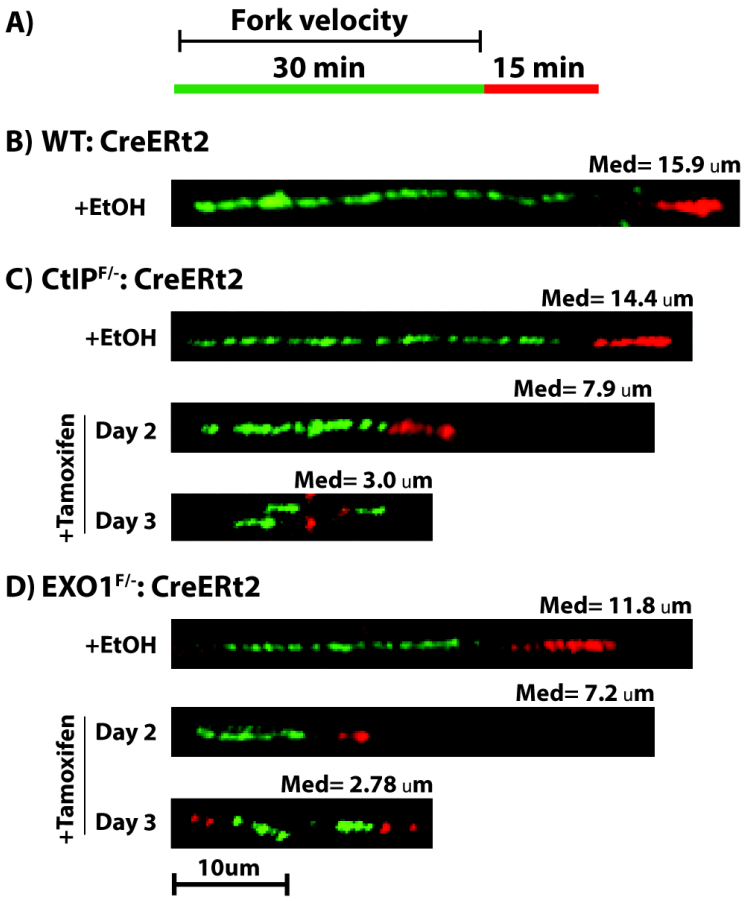
A)
Fork velocity
30 min
15 min
B) WT: CreERt2
Med= 15.9 um
+EtOH
C) CtIP F/-: CreERt2
Med= 14.4 um
+EtOH
Med= 7.9 um
+Tamoxifen
Day 2
Med= 3.0 um
Day 3
D) EXO1 F/-: CreERt2
Med= 11.8 um
+EtOH
Med= 7.2 um
+Tamoxifen
Day 2
Med= 2.78 um
Day 3
10um

Figure 5

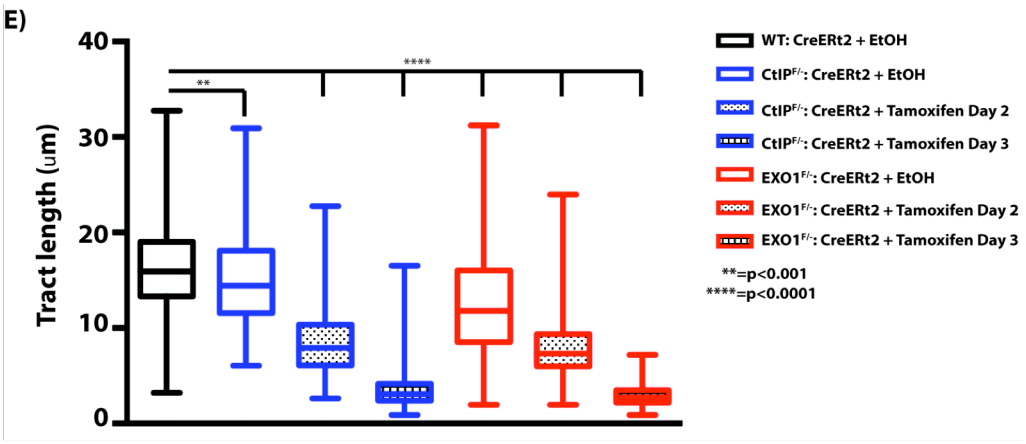
E)
Tract length (um)
40
30
20
10
0
**
****
WT: CreERt2 + EtOH
CtIP F/-: CreERt2 + EtOH
CtIP F/-: CreERt2 + Tamoxifen Day 2
CtIP F/-: CreERt2 + Tamoxifen Day 3
EXO1 F/-: CreERt2 + EtOH
EXO1 F/-: CreERt2 + Tamoxifen Day 2
EXO1 F/-: CreERt2 + Tamoxifen Day 3
**=p<0.001
****=p<0.0001

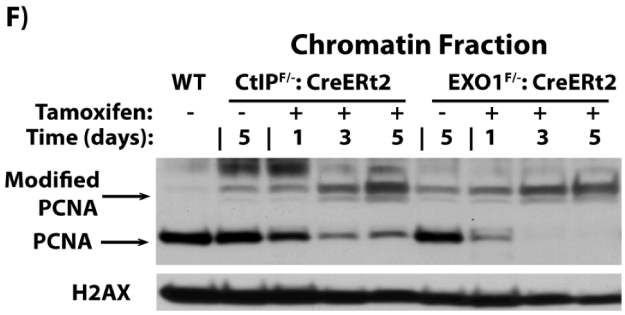
F)
Chromatin Fraction
WT
CtIP F/-: CreERt2
EXO1 F/-: CreERt2
Tamoxifen: - - + + + - + + +
Time (days): | 5 | 1 3 5 | 5 | 1 3 5
Modified PCNA
PCNA
H2AX

Figure 6

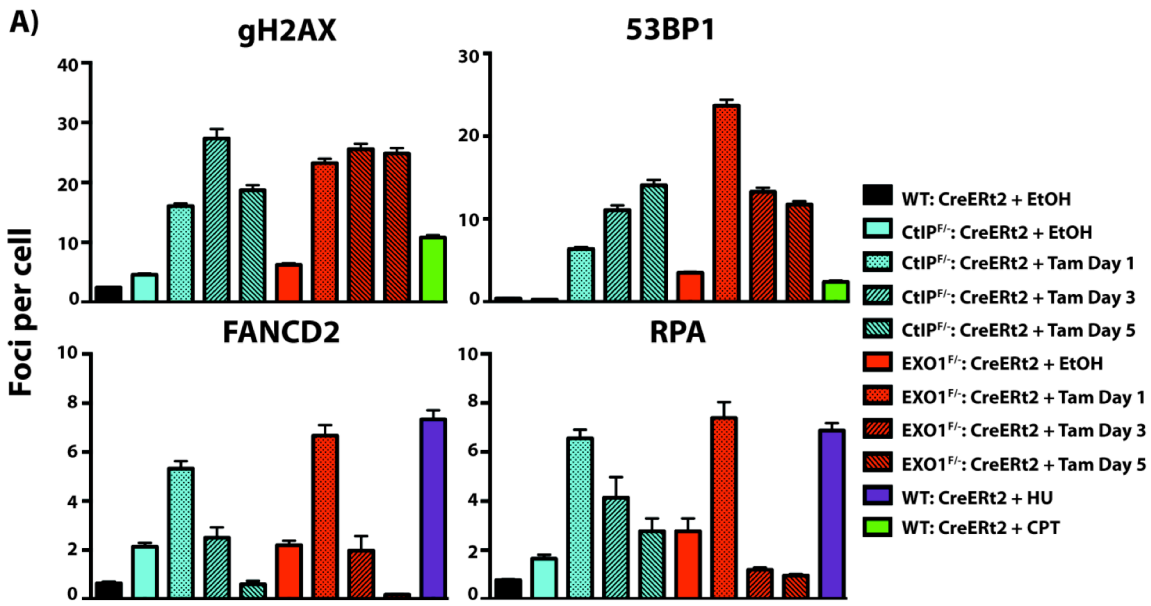
A)
gH2AX
53BP1
FANCD2
RPA
Foci per cell
WT: CreERt2 + EtOH
CtIP F/-: CreERt2 + EtOH
CtIP F/-: CreERt2 + Tam Day 1
CtIP F/-: CreERt2 + Tam Day 3
CtIP F/-: CreERt2 + Tam Day 5
EXO1 F/-: CreERt2 + EtOH
EXO1 F/-: CreERt2 + Tam Day 1
EXO1 F/-: CreERt2 + Tam Day 3
EXO1 F/-: CreERt2 + Tam Day 5
WT: CreERt2 + HU
WT: CreERt2 + CPT

Figure 6

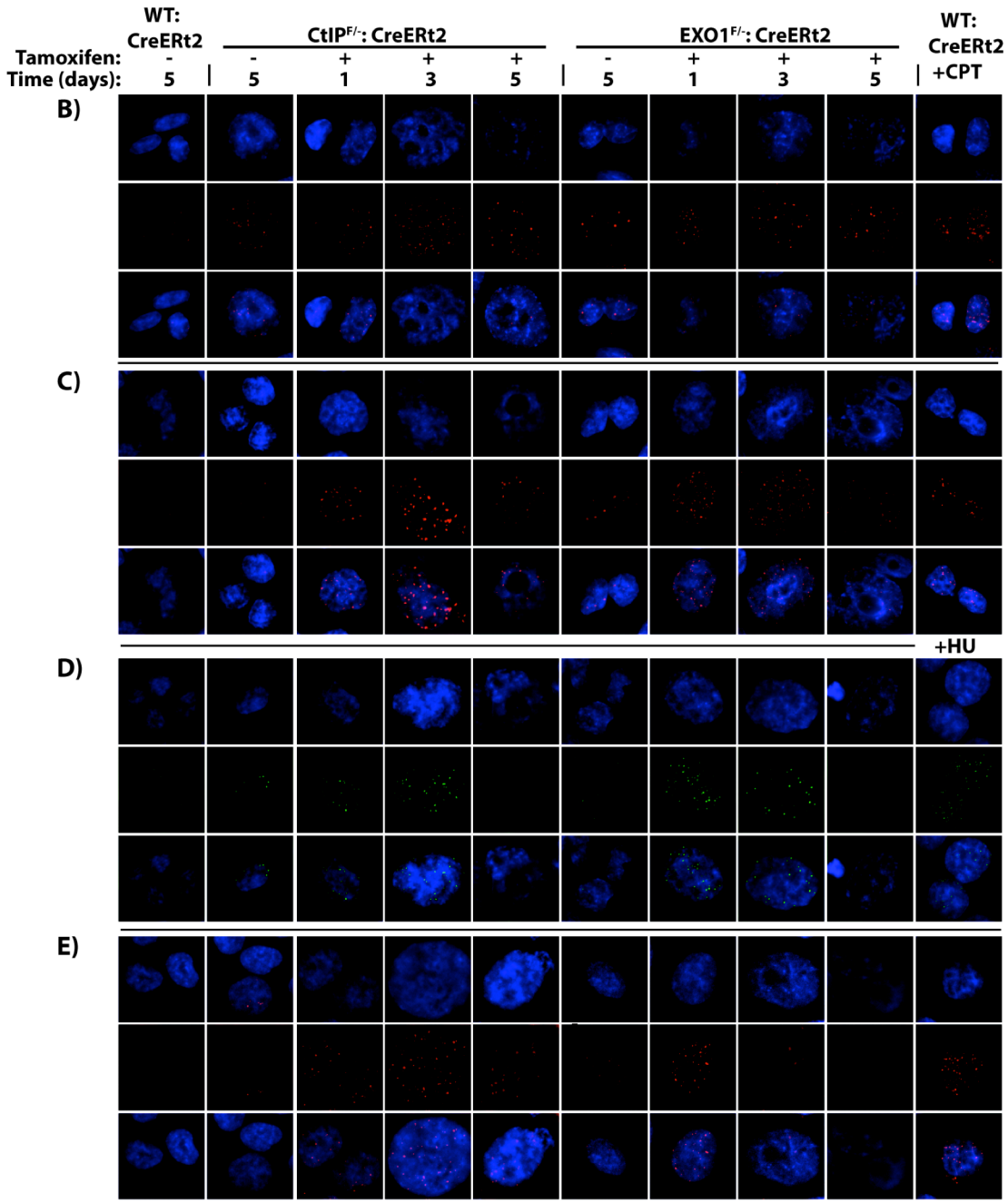
WT: CreERt2
CtIP F/-: CreERt2
EXO1 F/-: CreERt2
WT: CreERt2 +CPT
Tamoxifen: - - + + + - + + +
Time (days): 5 5 1 3 5 5 1 3 5
B)
C)
D)
E)
+HU
DAPI
gH2AX
53BP1
FANCD2
RPA
Merge

Figure 6

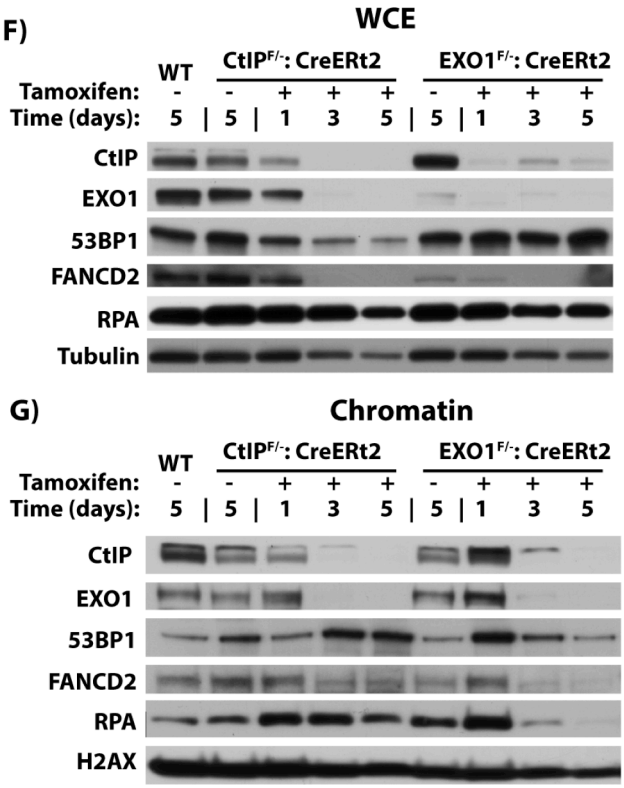
F)
WCE
WT
CtIP F/-: CreERt2
EXO1 F/-: CreERt2
Tamoxifen: - - + + + - + + +
Time (days): 5 | 5 | 1 3 5 | 5 | 1 3 5
CtIP
EXO1
53BP1
FANCD2
RPA
Tubulin
G)
Chromatin
WT
CtIP F/-: CreERt2
EXO1 F/-: CreERt2
Tamoxifen: - - + + + - + + +
Time (days): 5 | 5 | 1 3 5 | 5 | 1 3 5
CtIP
EXO1
53BP1
FANCD2
RPA
H2AX

Figure 7

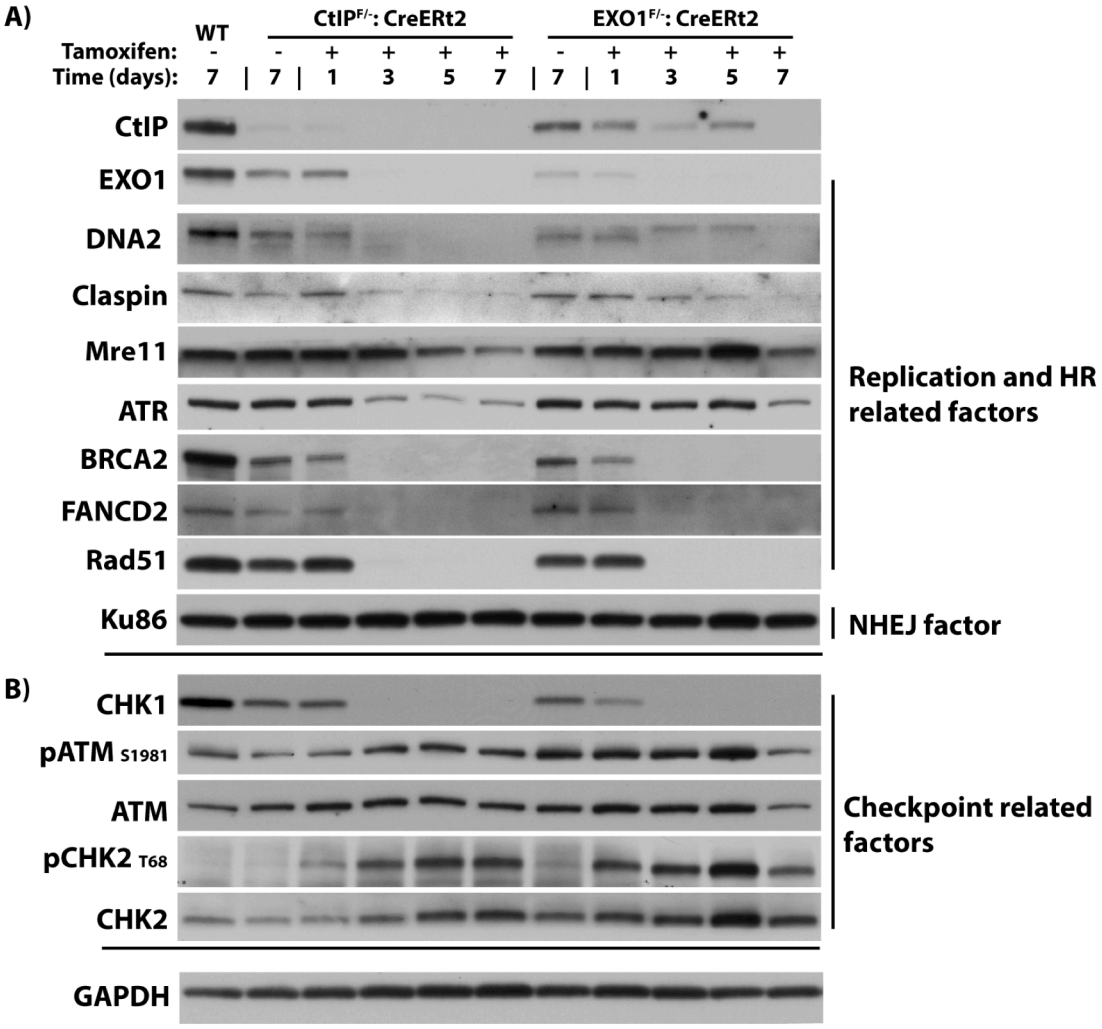
A)
WT
CtIP F/-: CreERt2
EXO1 F/-: CreERt2
Tamoxifen: - - + + + + - + + + +
Time (days): 7 | 7 | 1 3 5 7 | 7 | 1 3 5 7
CtIP
EXO1
DNA2
Claspin
Mre11
ATR
BRCA2
FANCD2
Rad51
Ku86
Replication and HR related factors
NHEJ factor
B)
CHK1
pATM S1981
ATM
pCHK2 T68
CHK2
Checkpoint related factors
GAPDH

Figure 7

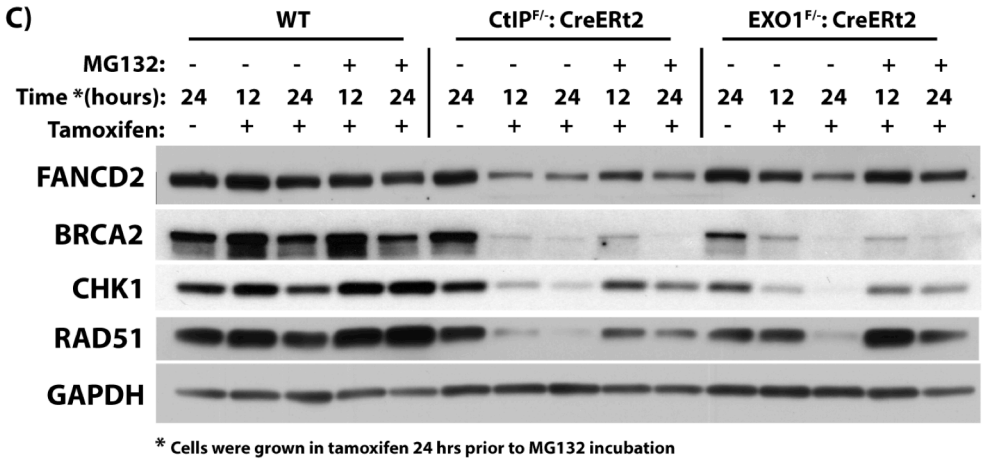
C)
WT
CtIP F/-: CreERt2
EXO1 F/-: CreERt2
MG132: - - - + + - - - + + - - - + +
Time *(hours): 24 12 24 12 24 24 12 24 12 24 24 12 24 12 24
Tamoxifen: - + + + + - + + + + - + + + +
FANCD2
BRCA2
CHK1
RAD51
GAPDH
* Cells were grown in tamoxifen 24 hrs prior to MG132 incubation

Figure 8

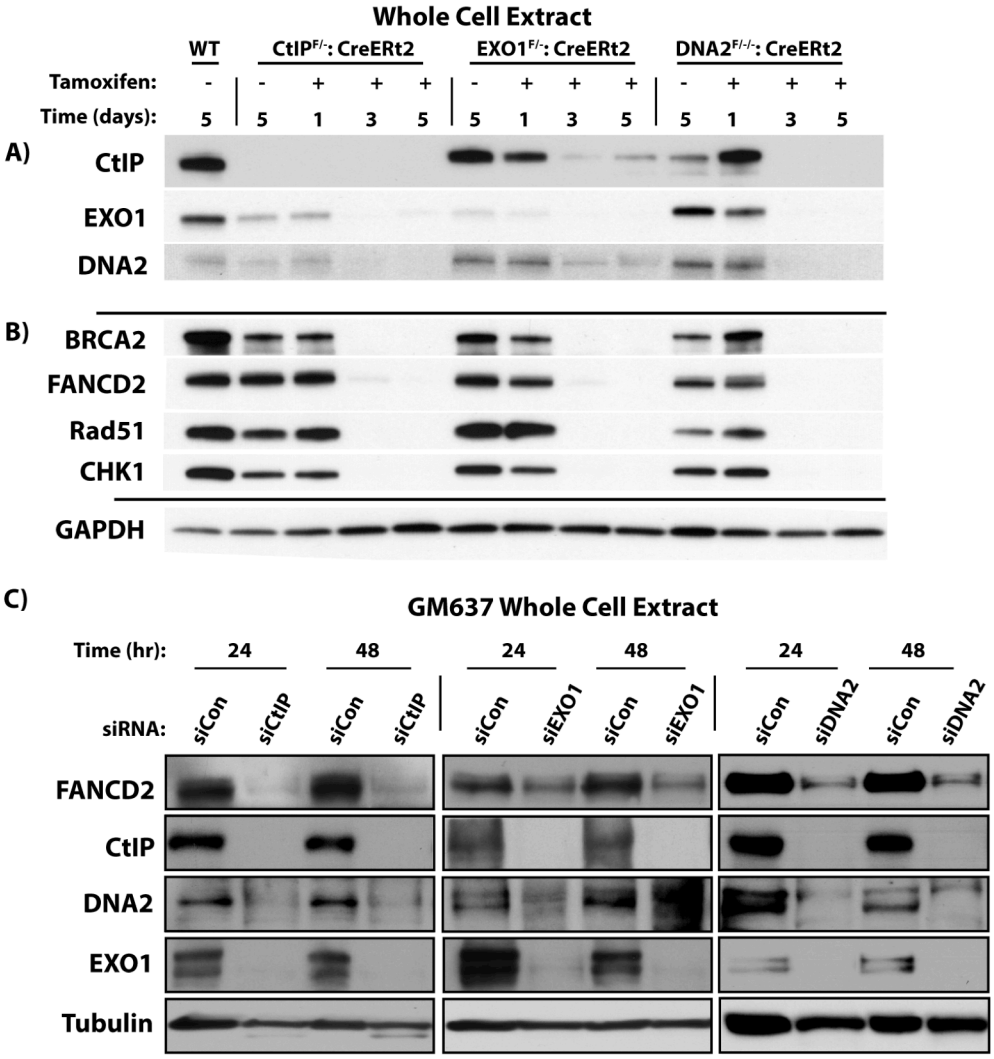
Whole Cell Extract
WT
CtIP F/-: CreERt2
EXO1 F/-: CreERt2
DNA2 F/-/-: CreERt2
Tamoxifen:
Time (days):
A)
CtIP
EXO1
DNA2
B)
BRCA2
FANCD2
Rad51
CHK1
GAPDH
C)
GM637 Whole Cell Extract
Time (hr):
siRNA:
siCon
siCtIP
siEXO1
siDNA2
FANCD2
CtIP
DNA2
EXO1
Tubulin

Figure 8

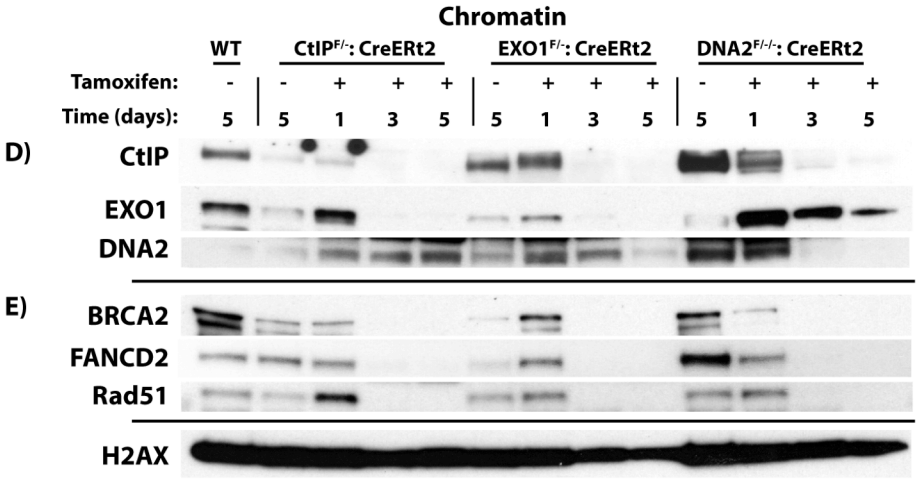
Chromatin
WT
CtIP F/-: CreERt2
EXO1 F/-: CreERt2
DNA2 F/-/-: CreERt2
Tamoxifen: - - + + + - + + + - + + +
Time (days): 5 5 1 3 5 5 1 3 5 5 1 3 5
D)
CtIP
EXO1
DNA2
E)
BRCA2
FANCD2
Rad51
H2AX

Supplementary Figure Legends

Supplementary Figure 1. CtIP and EXO1 are not synthetically lethal with MLH1.

MLH1-expressing cells cannot survive without CtIP or EXO1. A) $CtIP^{F/-}$:CreERt2 and $EXO1^{F/-}$:CreERt2 cells stably expressing MLH1 were plated on 96-well plates at 500 cells per well in triplicates the day before adding EtOH (A) or tamoxifen (B). Cell growth was measured via MTS colormetric assay at the indicated time points.

Supplementary Figure 2. Loss of CtIP and EXO1 disrupts the cell cycle.

Loss of CtIP and EXO1 severely disrupts a normal cell cycle. Data from the EdU incorporation assay are plotted in the form of histograms for a different view of DNA content. After 7 days of EtOH treatment, WT: CreERt2 (Fig. S2A), $CtIP^{F/-}$:CreERt2 (Fig. S2B) and $EXO1^{F/-}$:CreERt2 (Fig. S2C) have normal G1 and G2 peaks. However, in the presence of tamoxifen $CtIP^{F/-}$:CreERt2 (Fig. S2B) and $EXO1^{F/-}$:CreERt2 (Fig. S2C) cells gradually lose their G1 and G2 peaks and indiscriminate peaks representing DNA content >4N begin to arise at day 3, and by day 7 the histograms appear disordered with DNA content exceeding the linear range of detection. As we expected, WT:CreERt2 (Fig. S2B) have normal cell cycle profiles throughout the duration of the experiment.

Supplementary Figure 3. Loss of CtIP and EXO1 leads to continued DNA synthesis and aneuploidy.

Data from the EdU incorporation assay were acquired in logarithmic scale to include missing events. After 7 days of EtOH treatment, WT:CreERt2 (Fig. S2A), $CtIP^{F/-}$:CreERt2 (Fig. S2B) and $EXO1^{F/-}$:CreERt2 (Fig. S2C) have normal G1 and G2 peaks. However, in the presence of tamoxifen $CtIP^{F/-}$:CreERt2 (Fig. S2B) and $EXO1^{F/-}$:CreERt2 (Fig. S2C) cells gradually lose their G1 and G2 peaks and indiscriminate peaks representing DNA content >4N begin to arise at day 3, and by day 7 the histograms appear disordered with DNA content exceeding the linear range detection. As we expected, WT:CreERt2 (Fig. S2B) have normal cell cycle profiles throughout the duration of the experiment.

Supplementary Table 1. rAAV knockout vector construction

Primer sequences used to construct knockout vectors for CtIP, EXO1, and DNA2. PCR products of the indicated Fragment 1 and Fragment 2 primer pairs are fused to generate the left homology arms that contain a "Floxed" allele of all conditional knockout vectors. PCR products were cloned into TOPO cloning vectors, digested to reveal compatible sticky ends and finally ligated appropriately as described[109].

Supplementary Table 2. List of antibodies for western analyses and immunofluorescence

Supplementary Figure 1

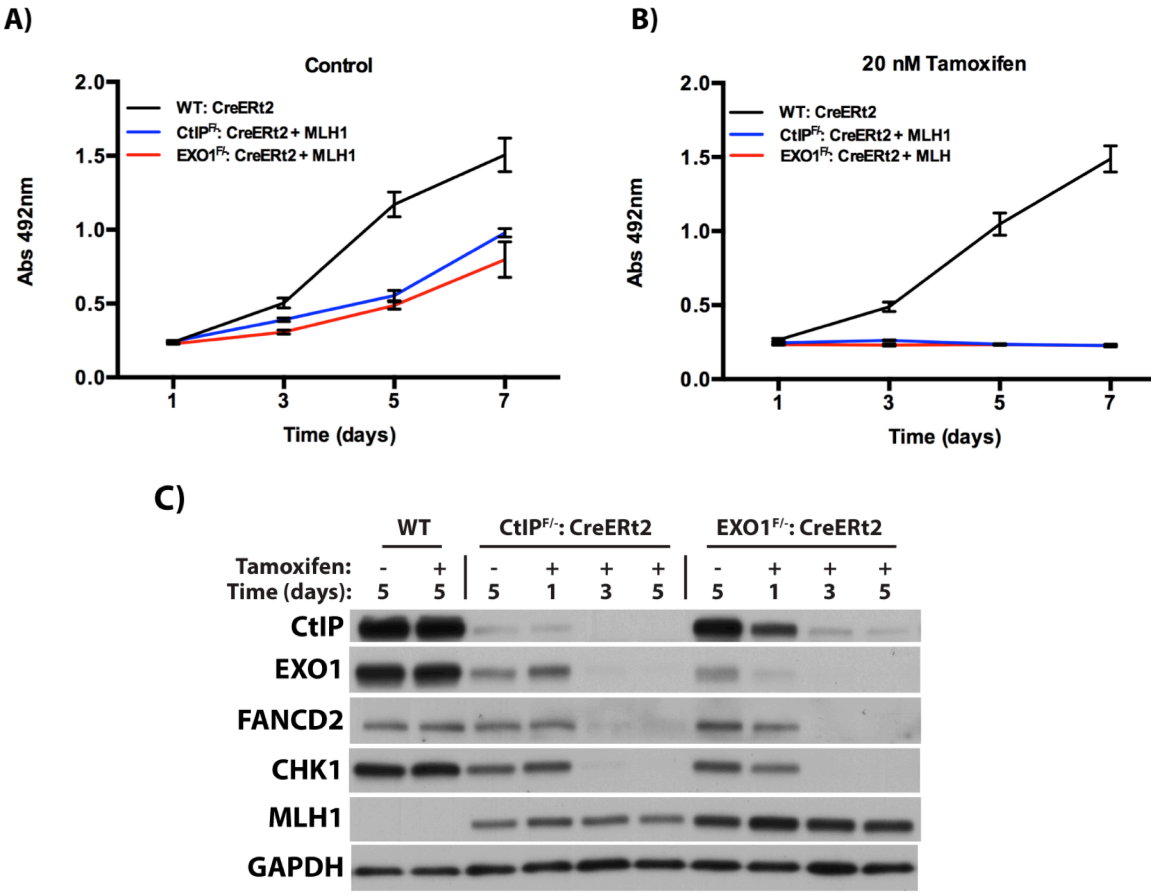

Supplementary Figure 2

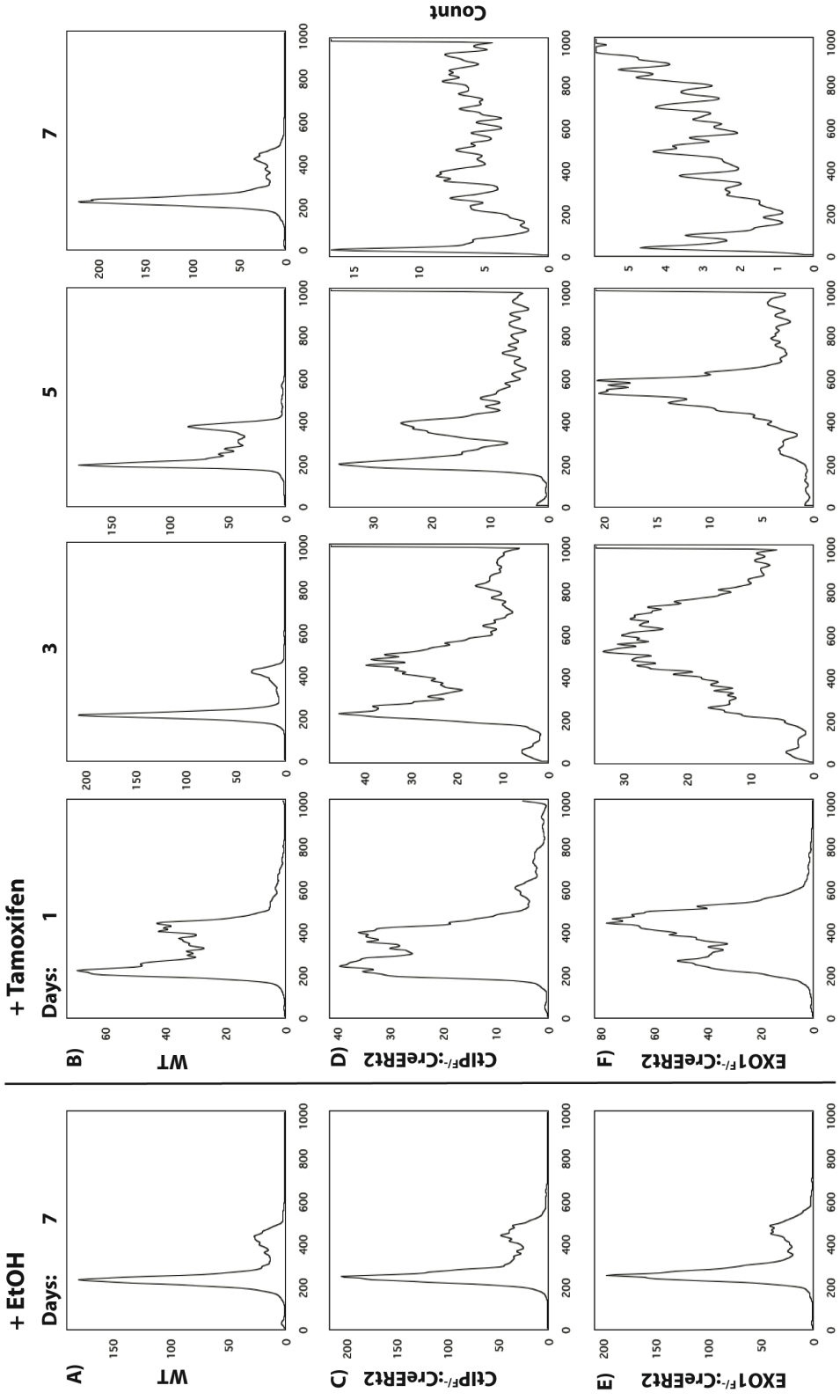

Supplementary Figure 3

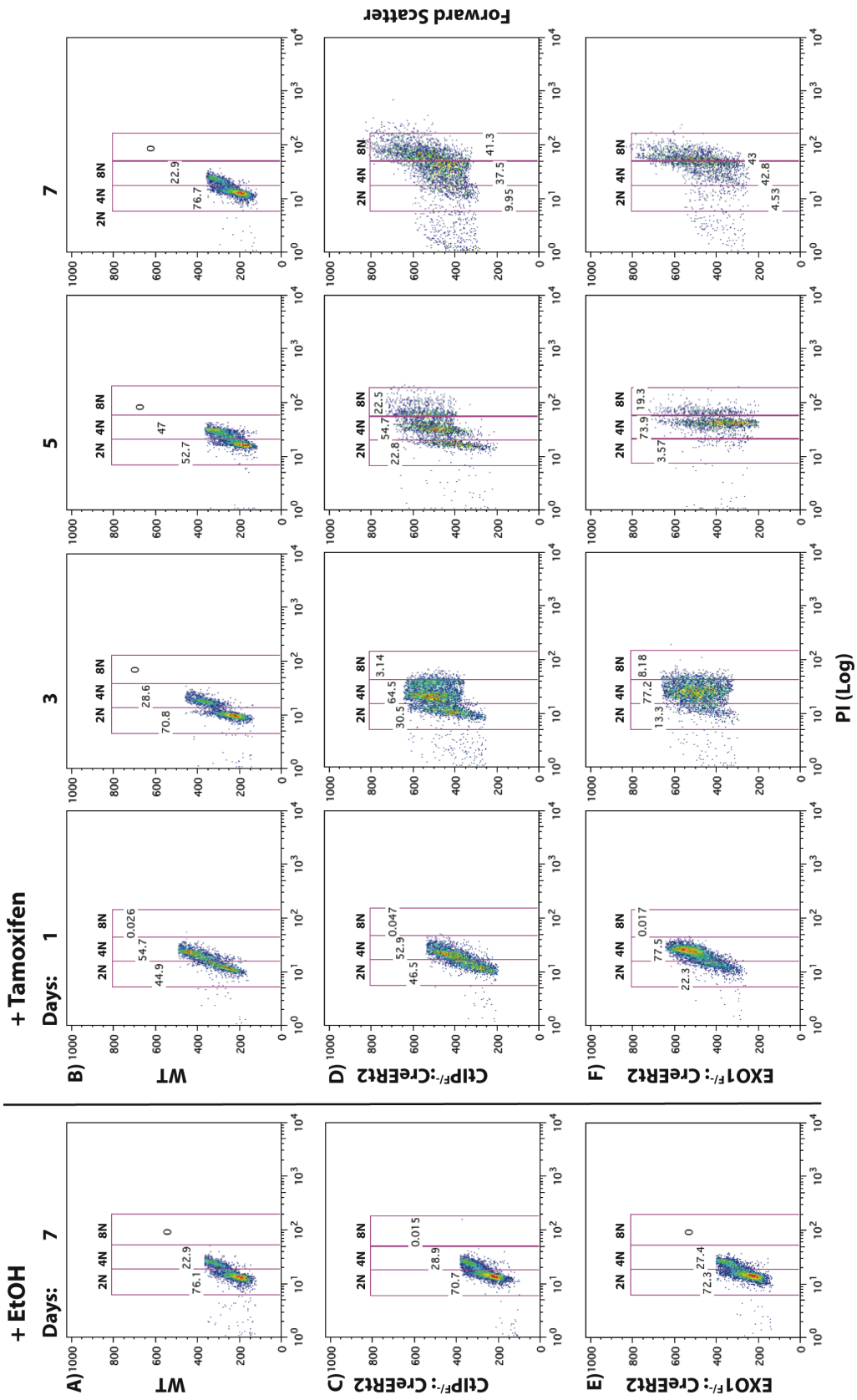

Table S1

Vector Construction Primers	
CtIP Conditional Knockout Vector	
CtIP CKO LHA Frag1 Not1 Fwd	5' atacatacgcggccgccctttattctaagagaggcatgaa 3'
CtIP CKO LHA Frag1 LoxP Rev	5'cgtataatgtatgctatacgaagttatcatttttagaatttggga -ggggaagg 3'
CtIP CKO LHA Frag2 LoxP Fwd	5' cgtatagcatacattatacgaagttatctgggcttgtgtt -tcatcctg 3'
CtIP CKO LHA Frag2 XbaI Rev	5'ggtattgcttctagacaaagccactacagtctcaacaa 3'
CtIP CKO RHA ECoRI Fwd	5'agcaataccgaattcttgttgagactgtagtggctttg 3'
CtIP CKO RHA NotI Rev	5' atacatacgcggccgcgatcagctgggcacagca 3'
CtIP Straight Knockout Vector	
CtIP SKO LHA Not1 Fwd	5' atacatacgcggccgcccagctcatatttagtttctgga 3'
CtIP SKO LHA XbaI Rev	5' ggtattgcttctagacacaagcccagatatcctca 3'
CtIP SKO RHA EcoRI Fwd	5' agcaataccgaattctagtggctttgtatacctttgtatgac 3'
CtIP SKO RHA NotI Rev	5' atacatacgcggccgcgatcagctgggcacagcagc 3'
EXO1 Conditional Knockout Vector	
EXO1 CKO LHA Frag1 Not1 Fwd	5'atacatacgcggccgcctctgtatagaaagggcttagg 3'
EXO1 CKO LHA Frag1 LoxP Rev	5'cgtataatgtatgctatacgaagttatgactgcagtggcc -tatatc 3'
EXO1 CKO LHA Frag2 LoxP Fwd	5' cgtatagcatacattatacgaagttatggactccaagct -ttctctt 3'
EXO1 CKO LHA Frag2 XbaI Rev	5' atacatactctagaaaaaaggcactgtaggtctc 3'
EXO1 CKO RHA ECoRI Fwd	5' agcaataccgaattcgagtatcaagacactgatggac 3'
EXO1 CKO RHA NotI Rev	5' atacatacgcggccgcgaactacttgaccctccaag 3'
EXO1 Straight Knockout Vector	
EXO1 SKO LHA Not1 Fwd	5' atacatacgcggccgcgacagagggataaagtgaagat 3'
EXO1 SKO LHA XbaI Rev	5' atacatactctagaatactacctctaatgccacttg 3'
EXO1 SKO RHA EcoRI Fwd	5' agcaataccgaattcgggtacagaaaacatactgcta 3'
EXO1 SKO RHA NotI Rev	5' atacatacgcggccgccttgatcccatgagatagtaac 3'
DNA2 Conditional Knockout Vector	
DNA2 CKO LHA Frag1 Not1 Fwd	5' ataagaatgcggccgcctctacccaaagtgtggtatgtg 3'
DNA2 CKO LHA Frag1 LoxP Rev	5' cgtataatgtatgctatacgaagttatgtaaacgtattaggga -ggcttc 3'
DNA2 CKO LHA Frag2 LoxP Fwd	5' cgtatagcatacattatacgaagttatcgtttacatgtagga -acctaagc 3'
DNA2 CKO LHA Frag2 XbaI Rev	5' gctctagagctagcactgccacctcatag 3'
DNA2 CKO RHA ECoRI Fwd	5' ccggaattccttcgaatcttgttcagggctta 3'
DNA2 CKO RHA NotI Rev	5' atagtttagcggccgcaatattcaggccaagcacagtag 3'

CKO: Conditional Knockout, SKO: Straight Knockout, Frag: Fragment, LHA: Left Homology arm, RHA: Right Homology Arm

Table S2

Antibody	Cat. No./Clone	Manufacturer	Application
RPA	9H8	**AbCam**	WB/IF
53BP1	ab36823		WB/IF
EXO1	ab95012		WB
CtIP	ab70163		WB
GAPDH	ab9484		WB
DNA2	ab96488		WB
γH2AX	A300-081A	**Bethyl Scientific**	IF
H2AX	A300-082A		WB
BRCA2	Ab-1	**Calbiochem**	WB
ATM	Phospho CHK1/2 Sampler Kit #9931	**Cell Signaling Technolgies**	WB
pATM S1981			WB
CHK2			WB
pCHK2 T68			WB
ATR	27095		WB
FANCD2	100-182	**Novus Biologicals**	IF
PCNA	FL261	**Santa Cruz Biotechnologies**	WB
14-3-3σ	C18		WB
Cdc25C	H-6		WB
CHK1	G-4		WB
Claspin	Q20		WB
FANCD2	Fl17		WB
Ku86	B11		WB
MRE11	C16		WB
Rad51	H92		WB

WB: Western Blot, IF: Immunofluorescence

I would like to thank Dr. Tsuyoshi Kawabata from the laboratory of Dr. Naoko Shima for sharing new protocols, Dr. Alexandra Sobeck and her lab members for sharing their reagents, and Dr. Duncan Clarke for his generous permission to access his microscopy equipment. We would also like to acknowledge the Flow Cytometry Core Facility and cytogenetic analyses performed in the Cytogenomics Shared Resource at the University of Minnesota with support from the comprehensive Masonic Cancer Center NIH Grant #P30 CA077598-09.

References

1. Hendrickson, E. A., Huffman, J. L. & Tainer J.A, T. Structural aspects of Ku and the DNA-dependent protein kinase complex. editors. New York: Taylor and Francis Group. pp. *DNA damage recognition.* 629–684 (2006).
2. Lieber, M. R. The mechanism of double-strand DNA break repair by the nonhomologous DNA end-joining pathway. *Annu Rev Biochem* **79,** 181–211 (2010).
3. San Filippo, J., Sung, P. & Klein, H. Mechanism of eukaryotic homologous recombination. *Annu Rev Biochem* **77,** 229–257 (2008).
4. Bentley, J., Diggle, C. P., Harnden, P., Knowles, M. A. & Kiltie, A. E. DNA double strand break repair in human bladder cancer is error prone and involves microhomology-associated end-joining. *Nucleic Acids Res* **32,** 5249–5259 (2004).
5. Anand, R. P. *et al.* Overcoming natural replication barriers: differential helicase requirements. *Nucleic Acids Res* **40,** 1091–1105 (2012).
6. Maizels, N. Dynamic roles for G4 DNA in the biology of eukaryotic cells. *Nat Struct Mol Biol* **13,** 1055–1059 (2006).
7. Mirkin, S. M. Expandable DNA repeats and human disease. *Nature* **447,** 932–940 (2007).
8. Fouché, N., Ozgür, S., Roy, D. & Griffith, J. D. Replication fork regression in repetitive DNAs. *Nucleic Acids Res* **34,** 6044–6050 (2006).
9. Voineagu, I., Narayanan, V., Lobachev, K. S. & Mirkin, S. M. Replication stalling at unstable inverted repeats: interplay between DNA hairpins and fork stabilizing proteins. *Proc Nat Acad of Sci* **105,** 9936–9941 (2008).
10. Gerhardt, J. *et al.* The DNA replication program is altered at the Fmr1 locus in fragile x embryonic stem cells. *Mol Cell* **53,** 1–13 (2013).
11. Durkin, S. G. & Glover, T. W. Chromosome fragile sites. *Annu Rev Genet* **41,** 169–192 (2007).
12. Cimprich, K. A. Fragile sites: breaking up over a slowdown. *Curr Biol* **13,** R231–R233 (2003).
13. Casper, A. M., Nghiem, P., Arlt, M. F. & Glover, T. W. ATR regulates fragile site stability. *Cell* **111,** 779–789 (2002).
14. Barlow, J. H. *et al.* Identification of early replicating fragile sites that contribute to genome instability. *Cell* **152,** 620–632 (2013).
15. Mimitou, E. P. & Symington, L. S. DNA end resection: many nucleases make light work. *DNA Repair (Amst)* **8,** 983–995 (2009).
16. Mimitou, E. P. & Symington, L. S. DNA end resection- unraveling the tail. *DNA Repair (Amst)* **10,** 344–348 (2011).
17. Takeda, S., Nakamura, K., Taniguchi, Y. & Paull, T. T. Ctp1/CtIP and the MRN complex collaborate in the initial steps of homologous recombination. *Mol Cell* **28,** 351–352 (2007).
18. Huertas, P., Cortés-Ledesma, F., Sartori, A. A., Aguilera, A. & Jackson, S. P. CDK targets Sae2 to control DNA-end resection and homologous recombination. *Nature* **455,** 689–692 (2008).
19. Mimitou, E. P. & Symington, L. S. Sae2, Exo1 and Sgs1 collaborate in DNA

double-strand break processing. *Nature* **455,** 770–774 (2008).
20. Marrero, V. A. & Symington, L. S. Extensive DNA end processing by Exo1 and Sgs1 inhibits break-induced replication. *PLoS Genet* **6,** e1001007 (2010).
21. Zhu, Z., Chung, W.-H., Shim, E. Y., Lee, S. E. & Ira, G. Sgs1 helicase and two nucleases Dna2 and Exo1 resect DNA double-strand break ends. *Cell* **134,** 981–994 (2008).
22. Maga, G. Okazaki fragment processing: Modulation of the strand displacement activity of DNA polymerase delta by the concerted action of replication protein A, proliferating cell nuclear antigen, and flap endonuclease-1. *Proc Natl Acad Sci USA* **98,** 14298–14303 (2001).
23. Lee, K. H. *et al.* The endonuclease activity of the yeast Dna2 enzyme is essential in vivo. *Nucleic Acids Res* **28,** 2873–2881 (2000).
24. Budd, M. E., Antoshechkin, I. A., Reis, C., Wold, B. J. & Campbell, J. L. Inviability of a DNA2 deletion mutant is due to the DNA damage checkpoint. *Cell Cycle* **10,** 1690–1698 (2011).
25. Schaeper, U., Subramanian, T., Lim, L., Boyd, J. M. & Chinnadurai, G. Interaction between a cellular protein that binds to the C-terminal region of adenovirus E1A (CtBP) and a novel cellular protein is disrupted by E1A through a conserved PLDLS motif. *J Biol Chem* **273,** 8549–8552 (1998).
26. Yu, X. & Chen, J. DNA damage-induced cell cycle checkpoint control requires CtIP, a phosphorylation-dependent binding partner of BRCA1 C-terminal domains. *Mol Cell Biol* **24,** 9478–9486 (2004).
27. Sartori, A. A. *et al.* Human CtIP promotes DNA end resection. *Nature* **450,** 509–514 (2007).
28. You, Z. & Bailis, J. M. DNA damage and decisions: CtIP coordinates DNA repair and cell cycle checkpoints. *Trends in Cell Biology* **20,** 402–409 (2010).
29. Huertas, P. & Jackson, S. P. Human CtIP mediates cell cycle control of DNA end resection and double strand break repair. *J Biol Chem* **284,** 9558–9565 (2009).
30. You, Z. *et al.* CtIP links DNA double-strand break sensing to resection. *Mol Cell* **36,** 954–969 (2009).
31. Eid, W. *et al.* DNA end resection by CtIP and exonuclease 1 prevents genomic instability. *EMBO Rep* **11,** 962–968 (2010).
32. Karanja, K. K., Cox, S. W., Duxin, J. P., Stewart, S. A. & Campbell, J. L. DNA2 and EXO1 in replication-coupled, homology-directed repair and in the interplay between HDR and the FA/BRCA network. *Cell Cycle* **11,** 3983–3996 (2012).
33. Yu, X., Wu, L. C., Bowcock, A. M., Aronheim, A. & Baer, R. The C-terminal (BRCT) domains of BRCA1 interact in vivo with CtIP, a protein implicated in the CtBP pathway of transcriptional repression. *J Biol Chem* **273,** 25388–25392 (1998).
34. Li, S. Binding of CtIP to the BRCT repeats of Brca1 involved in the transcription regulation of p21 is disrupted upon DNA damage. *J Biol Chem* **274,** 11334–11338 (1999).
35. Barber, L. J. & Boulton, S. J. BRCA1 ubiquitylation of CtIP: Just the tIP of the iceberg? *DNA Repair (Amst)* **5,** 1499–1504 (2006).
36. Meloni, A. R., Smith, E. J. & Nevins, J. R. A mechanism for Rb/p130-mediated

transcription repression involving recruitment of the CtBP corepressor. *Proc Natl Acad Sci USA* **96,** 9574–9579 (1999).
37. Gu, B. & Chen, P.-L. Expression of PCNA-binding domain of CtIP, a motif required for CtIP localization at DNA replication foci, causes DNA damage and activation of DNA damage checkpoint. *Cell Cycle* **8,** 1409–1420 (2009).
38. Buis, J., Stoneham, T., Spehalski, E. & Ferguson, D. O. Mre11 regulates CtIP-dependent double-strand break repair by interaction with CDK2. *Nat Struct Mol Biol* **19,** 246–252 (2012).
39. Chen, P.-L. *et al.* Inactivation of CtIP leads to early embryonic lethality mediated by G1 restraint and to tumorigenesis by haploid insufficiency. *Mol Cell Biol* **25,** 3535–3542 (2005).
40. Qvist, P. *et al.* CtIP mutations cause Seckel and Jawad syndromes. *PLoS Genet* **7,** e1002310 (2011).
41. Tran, P. T., Erdeniz, N., Symington, L. S. & Liskay, R. M. EXO1-A multi-tasking eukaryotic nuclease. *DNA Repair (Amst)* **3,** 1549–1559 (2004).
42. Wu, P., Takai, H. & de Lange, T. Telomeric 3′ overhangs derive from resection by Exo1 and Apollo and fill-in by POT1b-associated CST. *Cell* **150,** 39–52 (2012).
43. Liberti, S. E. *et al.* Bi-directional routing of DNA mismatch repair protein human exonuclease 1 to replication foci and DNA double strand breaks. *DNA Repair (Amst)* **10,** 73–86 (2011).
44. Marti, T. M., Mansour, A. A., Lehmann, E. & Fleck, O. Different frameshift mutation spectra in non-repetitive DNA of MutSalpha- and MutLalpha-deficient fission yeast cells. *DNA Repair (Amst)* **2,** 571–580 (2003).
45. Sun, X., Zheng, L. & Shen, B. Functional alterations of human exonuclease 1 mutants identified in atypical hereditary nonpolyposis colorectal cancer syndrome. *Cancer Res* **62,** 6026–6030 (2002).
46. Jäger, A. C. *et al.* HNPCC mutations in the human DNA mismatch repair gene hMLH1 influence assembly of hMutLalpha and hMLH1-hEXO1 complexes. *Oncogene* **20,** 3590–3595 (2001).
47. Schmutte, C. *et al.* Human exonuclease I interacts with the mismatch repair protein hMSH2. *Cancer Res* **58,** 4537–4542 (1998).
48. Cotta-Ramusino, C. *et al.* Exo1 processes stalled replication forks and counteracts fork reversal in checkpoint-defective cells. *Mol Cell* **17,** 153–159 (2005).
49. Lieber, M. R. The mechanism of human nonhomologous DNA end joining. *J Biol Chem* **283,** 1–5 (2008).
50. Morin, I. *et al.* Checkpoint-dependent phosphorylation of Exo1 modulates the DNA damage response. *EMBO J* **27,** 2400–2410 (2008).
51. Bolderson, E. *et al.* Phosphorylation of Exo1 modulates homologous recombination repair of DNA double-strand breaks. *Nucleic Acids Res* **38,** 1821–1831 (2010).
52. Engels, K., Giannattasio, M., Muzi-Falconi, M., Lopes, M. & Ferrari, S. 14-3-3 Proteins regulate exonuclease 1–dependent processing of stalled replication forks. *PLoS Genet* **7,** e1001367 (2011).
53. López-Contreras, A. J. *et al.* A proteomic characterization of factors enriched

at nascent DNA molecules. *Cell Rep* **3,** 1105–1116 (2013).
54. Schaetzlein, S. *et al.* Exonuclease-1 deletion impairs DNA damage signaling and prolongs lifespan of telomere-dysfunctional mice. *Cell* **130,** 863–877 (2007).
55. Wei, K. Inactivation of Exonuclease 1 in mice results in DNA mismatch repair defects, increased cancer susceptibility, and male and female sterility. *Genes Dev* **17,** 603–614 (2003).
56. Nussenzweig, A. *et al.* Requirement for Ku80 in growth and immunoglobulin V(D)J recombination. *Nature* **382,** 551–555 (1996).
57. Li, G., Nelsen, C. & Hendrickson, E. A. Ku86 is essential in human somatic cells. *Proc Natl Acad Sci USA* **99,** 832–837 (2002).
58. Wang, Y., Ghosh, G. & Hendrickson, E. A. Ku86 represses lethal telomere deletion events in human somatic cells. *Proc Natl Acad Sci USA* **106,** 12430–12435 (2009).
59. Nimonkar, A. V., Ozsoy, A. Z., Genschel, J., Modrich, P. & Kowalczykowski, S. C. Human exonuclease 1 and BLM helicase interact to resect DNA and initiate DNA repair. *Proc Natl Acad Sci USA* **105,** 16906–16911 (2008).
60. Nimonkar, A. V. *et al.* BLM-DNA2-RPA-MRN and EXO1-BLM-RPA-MRN constitute two DNA end resection machineries for human DNA break repair. *Genes Dev* **25,** 350–362 (2011).
61. Yang, S.-H. *et al.* The SOSS1 single-stranded DNA binding complex promotes DNA end resection in concert with Exo1. *EMBO J* **9,** 126–139 (2012).
62. Branzei, D. & Foiani, M. The checkpoint response to replication stress. *DNA Repair (Amst)* **8,** 1038–1046 (2009).
63. Cimprich, K. A. & Cortez, D. ATR: an essential regulator of genome integrity. *Nat Rev Mol Cell Biol* **9,** 616–627 (2008).
64. Lopes, M. *et al.* The DNA replication checkpoint response stabilizes stalled replication forks. *Nature* **412,** 557–561 (2001).
65. Bae, S. H. Coupling of DNA Helicase and Endonuclease Activities of Yeast Dna2 Facilitates Okazaki Fragment Processing. *J Biol Chem* **277,** 26632–26641 (2002).
66. Masuda-Sasa, T., Imamura, O. & Campbell, J. L. Biochemical analysis of human Dna2. *Nucleic Acids Res* **34,** 1865–1875 (2006).
67. Duxin, J. P. *et al.* Human Dna2 is a nuclear and mitochondrial DNA maintenance protein. *Mol Cell Biol* **29,** 4274–4282 (2009).
68. Chaudhury, I., Sareen, A., Raghunandan, M. & Sobeck, A. FANCD2 regulates BLM complex functions independently of FANCI to promote replication fork recovery. *Nucleic Acids Res* **41,** 6444–6459 (2013).
69. Petermann, E., Orta, M. L., Issaeva, N., Schultz, N. & Helleday, T. Hydroxyurea-stalled replication forks become progressively inactivated and require two different RAD51-mediated pathways for restart and repair. *Mol Cell* **37,** 492–502 (2010).
70. Branzei, D. & Foiani, M. Maintaining genome stability at the replication fork. *Nat Rev Mol Cell Biol* **11,** 208–219 (2010).
71. Russell, D. W. & Hirata, R. K. Human gene targeting by viral vectors. *Nat Genet* **18,** 325–330 (1998).

72. Kohli, M., Rago, C., Lengauer, C., Kinzler, K. W. & Vogelstein, B. Facile methods for generating human somatic cell gene knockouts using recombinant adeno-associated viruses. *Nucleic Acids Res* **32,** e3 (2004).
73. Hawn, M. T. *et al.* Evidence for a connection between the mismatch repair system and the G2 cell cycle checkpoint. *Cancer Res* **55,** 3721–3725 (1995).
74. Kee, Y. & D'Andrea, A. D. Molecular pathogenesis and clinical management of Fanconi anemia. *J Clin Invest* **122,** 3799–3806 (2012).
75. Liu, F. & Lee, W.-H. CtIP activates its own and cyclin D1 promoters via the E2F/RB pathway during G1/S progression. *Mol Cell Biol* **26,** 3124–3134 (2006).
76. Wu, G. & Lee, W.-H. CtIP, a multivalent adaptor connecting transcriptional regulation, checkpoint control and tumor suppression. *Cell Cycle* **5,** 1592–1596 (2006).
77. Daboussi, F. *et al.* A homologous recombination defect affects replication-fork progression in mammalian cells. *J Cell Sci* **121,** 162–166 (2008).
78. Petermann, E. *et al.* Chk1 requirement for high global rates of replication fork progression during normal vertebrate S phase. *Mol Cell Biol* **26,** 3319–3326 (2006).
79. Moldovan, G.-L., Pfander, B. & Jentsch, S. PCNA, the maestro of the replication fork. *Cell* **129,** 665–679 (2007).
80. Bonner, W. M. *et al.* GammaH2AX and cancer. *Nat Rev Cancer* **8,** 957–967 (2008).
81. Nakamura, A. J., Rao, V. A., Pommier, Y. & Bonner, W. M. The complexity of phosphorylated H2AX foci formation and DNA repair assembly at DNA double-strand breaks. *Cell Cycle* **9,** 389–397 (2010).
82. Dimitrova, N., Chen, Y.-C. M., Spector, D. L. & de Lange, T. 53BP1 promotes non-homologous end joining of telomeres by increasing chromatin mobility. *Nature* **456,** 524–528 (2008).
83. Bunting, S. F. *et al.* 53BP1 inhibits homologous recombination in Brca1-deficient cells by blocking resection of DNA breaks. *Cell* **141,** 243–254 (2010).
84. Escribano-Díaz, C. *et al.* A cell cycle-dependent regulatory circuit composed of 53bp1-Rif1 and Brca1-ctip controls DNA repair pathway choice. *Semin. Cell Dev. Biol.* (2013).
85. Zimmermann, M., Lottersberger, F., Buonomo, S. B., Sfeir, A. & de Lange, T. 53BP1 regulates DSB repair using Rif1 to control 5' end resection. *Science* **339,** 700–704 (2013).
86. Callén, E. *et al.* 53BP1 Mediates Productive and Mutagenic DNA Repair through Distinct Phosphoprotein Interactions. *Cell* **153,** 1266–1280 (2013).
87. Andreassen, P. R., D'Andrea, A. D. & Taniguchi, T. ATR couples FANCD2 monoubiquitination to the DNA-damage response. *Genes Dev* **18,** 1958–1963 (2004).
88. Zou, L. & Elledge, S. J. Sensing DNA damage through ATRIP recognition of RPA-ssDNA complexes. *Science* **300,** 1542–1548 (2003).
89. Byun, T. S., Pacek, M., Yee, M.-C., Walter, J. C. & Cimprich, K. A. Functional uncoupling of MCM helicase and DNA polymerase activities activates the

ATR-dependent checkpoint. *Genes Dev* **19,** 1040–1052 (2005).
90. Petermann, E. & Helleday, T. Pathways of mammalian replication fork restart. *Nat Rev Mol Cell Biol* **11,** 683–687 (2010).
91. Chini, C. C. S. Human Claspin is required for replication checkpoint control. *J Biol Chem* **278,** 30057–30062 (2003).
92. Chini, C. C. S. & Chen, J. Claspin, a regulator of Chk1 in DNA replication stress pathway. *DNA Repair (Amst)* **3,** 1033–1037 (2004).
93. Chini, C. C. S., Wood, J. & Chen, J. Chk1 is required to maintain claspin stability. *Oncogene* **25,** 4165–4171 (2006).
94. Zhang, Y.-W. *et al.* Genotoxic stress targets human Chk1 for degradation by the ubiquitin-proteasome pathway. *Mol Cell* **19,** 607–618 (2005).
95. Peschiaroli, A. *et al.* SCFbetaTrCP-mediated degradation of Claspin regulates recovery from the DNA replication checkpoint response. *Mol Cell* **23,** 319–329 (2006).
96. Mailand, N., Bekker-Jensen, S., Bartek, J. & Lukas, J. Destruction of Claspin by SCFbetaTrCP restrains Chk1 activation and facilitates recovery from genotoxic stress. *Mol Cell* **23,** 307–318 (2006).
97. Ward, I. M., Wu, X. & Chen, J. Threonine 68 of Chk2 is phosphorylated at sites of DNA strand breaks. *J Biol Chem* **276,** 47755–47758 (2001).
98. Bakkenist, C. J. & Kastan, M. B. DNA damage activates ATM through intermolecular autophosphorylation and dimer dissociation. *Nature* **421,** 499–506 (2003).
99. Lee, D. H. & Goldberg, A. L. Proteasome inhibitors: valuable new tools for cell biologists. *Trends in Cell Biology* **8,** 397–403 (1998).
100. Schwarz, S. B. *et al.* The effect of radio-adaptive doses on HT29 and GM637 cells. *Radiat Oncol* **3,** 12 (2008).
101. Syljuåsen, R. G. *et al.* Inhibition of human Chk1 causes increased initiation of DNA replication, phosphorylation of ATR targets, and DNA breakage. *Mol Cell Biol* **25,** 3553–3562 (2005).
102. Sabatinos, S. A., Green, M. D. & Forsburg, S. L. Continued DNA Synthesis in Replication Checkpoint Mutants Leads to Fork Collapse. *Mol Cell Biol* **32,** 4986–4997 (2012).
103. Wang, B. 53BP1, a Mediator of the DNA Damage Checkpoint. *Science* **298,** 1435–1438 (2002).
104. DiTullio, R. A. *et al.* 53BP1 functions in an ATM-dependent checkpoint pathway that is constitutively activated in human cancer. *Nat. Cell Biol.* **4,** 998–1002 (2002).
105. Symington, L. S. & Gautier, J. Double-strand break end resection and repair pathway choice. *Annu Rev Genet* **45,** 247–271 (2011).
106. Petermann, E., Helleday, T. & Caldecott, K. W. Claspin promotes normal replication fork rates in human cells. *Mol. Biol. Cell* **19,** 2373–2378 (2008).
107. Ragland, R. L. *et al.* RNF4 and PLK1 are required for replication fork collapse in ATR-deficient cells. *Genes Dev* **27,** 2259–2273 (2013).
108. Rahrmann, E. P. *et al.* Forward genetic screen for malignant peripheral nerve sheath tumor formation identifies new genes and pathways driving tumorigenesis. *Nat Genet* **45,** 756–766 (2013).

109. Rago, C., Vogelstein, B. & Bunz, F. Genetic knockouts and knockins in human somatic cells. *Nat Protoc* **2,** 2734–2746 (2007).
110. Ge, X. Q., Jackson, D. A. & Blow, J. J. Dormant origins licensed by excess Mcm2-7 are required for human cells to survive replicative stress. *Genes Dev* **21,** 3331–3341 (2007).
111. Hamelik, R. M. & Krishan, A. Click-iT assay with improved DNA distribution histograms. *Cytometry A* **75,** 862–865 (2009).

CHAPTER III:
Ku Regulates The Pathway Choice Of DNA Double-Strand Break Repair In Human Somatic Cells

My Contributions to this chapter

Figure 1

Figure 3

Figure 4

Figure 6

Figure 8

Figure S1

This chapter is a replicate of a pubcication in *PLoS Genetics*, e1000855 (2010).
Farjana J. Fattah, **Eu Han Lee**, Natalie Weisensel, Yongbao Wang, Natalie Lichter and Eric A. Hendrickson. Ku regulates the non-homologous end joining pathway choice of DNA double-strand break repair in human somatic cells.

The repair of DNA double-strand breaks (DSBs) is critical for the maintenance of genomic integrity and viability for all organisms. Mammals have evolved at least two genetically discrete ways to mediate DNA DSB repair: homologous recombination (HR) and non-homologous end joining (NHEJ). In mammalian cells, most DNA DSBs are preferentially repaired by NHEJ. Recent work has demonstrated that NHEJ consists of at least two sub-pathways - the main Ku heterodimer-dependent or "classic" NHEJ (C-NHEJ) pathway and an "alternative" NHEJ (A-NHEJ) pathway, which usually generates microhomology-mediated signatures at the repair junctions. In our study, recombinant adeno-associated virus knockout vectors were utilized to construct a series of isogenic human somatic cell lines deficient in the core C-NHEJ factors (Ku, DNA-PK_{cs}, XLF, and LIGIV) and the resulting cell lines were characterized for their ability to carry out DNA DSB repair. The absence of DNA-PK_{cs}, XLF or LIGIV resulted in cell lines that were profoundly impaired in DNA DSB repair activity. Very unexpectedly, Ku86-null cells showed wild-type levels of DNA DSB repair activity that was dominated by microhomology joining events indicative of A-NHEJ. Correspondingly, A-NHEJ DNA DSB repair activity could also be efficiently de-repressed in LIGIV- and DNA-PK_{cs}-null cells by subsequently reducing the level of Ku70. These studies demonstrate that in human cells C-NHEJ is the major DNA DSB repair pathway and, more importantly, they show that Ku is the critical C-NHEJ factor that regulates DNA DSB repair pathway choice.

Author Summary

Humans utilize at least two major pathways to repair DNA double-strand breaks (DSBs): homologous recombination (HR) and non-homologous end joining (NHEJ) and there are at least two genetically discrete sub-pathways of NHEJ: classic-NHEJ (C-NHEJ) and alternative-NHEJ (A-NHEJ). Since the products generated by each of these three repair (sub)pathways differ substantially from one another, it is biologically critical that certain DNA DSBs are repaired by certain DNA DSB repair pathways. How this pathway choice is made was unclear. In this study, knockout human cell lines that are defective in core C-NHEJ factors were generated. These cell lines are by-and-large extremely deficient in DNA DSB repair, proving that C-NHEJ is the major DNA DSB repair pathway in human cells. Unexpectedly, cell lines reduced for the C-NHEJ factors Ku70 or Ku86, carried out proficient DNA DSB repair because of hyperactive A-NHEJ. In published work [1] and work that is in press [2], we have also demonstrated that Ku suppresses HR throughout the genome and at telomeres, respectively. Collectively, these data imply that Ku ensures that C-NHEJ is the major DNA DSB repair pathway by two mechanisms; *i*) enabling C-NHEJ and *ii*) by actively suppressing HR and A-NHEJ. Thus, Ku is the critical regulator of DNA DSB repair pathway choice in human somatic cells.

Introduction

One of the most harmful lesions a cell can encounter is a DNA double-strand break (DSB). In all organisms, efficient repair of these DNA DSBs is critical for the maintenance of genomic integrity and viability [3]. Unfortunately, DNA DSBs are frequently generated endogenously during normal cellular processes such as DNA replication, lymphoid V(D)J or class-switch recombination and are induced exogenously by the exposure to a variety of genotoxic agents such as ionizing radiation or chemotherapeutics [4]. Cells have conspired to meet this demand on their genetic material with the evolution of two mechanistically distinct pathways to repair DNA DSBs: homologous recombination (HR), which takes advantage of either a homologous chromosome or a sister chromatid to join the broken DNA ends [5] and non-homologous end joining (NHEJ), a process that directly joins the DNA DSB with little or no sequence homology between the broken ends [4]. In bacteria and lower eukaryotes, HR dominates the DNA DSB repair events whereas in higher eukaryotes, and especially in mammals, NHEJ is the preferred pathway for DNA DSB repair. NHEJ consists of at least two genetically and biochemically distinct sub-pathways: a main — "classic" — end-joining pathway (C-NHEJ) and one interchangeably referred to as microhomology-mediated end joining (MMEJ) [6], alternative NHEJ (A-NHEJ), or backup NHEJ (B-NHEJ) [7,8] (hereafter referred to as A-NHEJ). C-NHEJ, while by no means precise, results in minimal DNA end processing, whereas A-NHEJ mechanistically results in deletions per force that are often accompanied by microhomology at the repair junction {[9,10]; reviewed by [8,11]}.

There are at least seven proteins required for C-NHEJ: Ku70, Ku86, the DNA dependent protein kinase catalytic subunit (DNA-PK_{cs}), Artemis, X-ray cross complementing 4 (XRCC4), XRCC4-like factor (XLF) and DNA ligase IV (LIGIV) {reviewed by [12]}. The basic mechanism of C-NHEJ has been worked out in great detail. Ku70 and Ku86 form a heterodimer (Ku) that contains an internal cavity, which Ku uses to bind to and encircle broken DNA ends [13]. Ku, besides protecting DNA ends from exonucleolytic attack, also recruits DNA-PK_{cs}, a phosphoinositol-3-like family serine/threonine protein kinase [14]. Together, Ku70, Ku86 and DNA-PK_{cs} form the DNA-dependent protein kinase complex (DNA-PK) and the assembly of this trimeric complex on the ends of double-stranded DNA activates the kinase activity of DNA-PK_{cs}. DNA-PK_{cs}, in turn, phosphorylates and activates the nuclease Artemis, which facilitates "cleaning up" of the ends. As a final step, ligation of the broken ends is catalyzed by the trimeric LIGIV complex, which consists of the catalytic core, DNA LIGIV, and its two accessory factors, XLF and XRCC4.

In contrast to C-NHEJ, the mechanism, the regulation, and the factors involved in A-NHEJ remain elusive. Mechanistically, it is believed that during A-NHEJ both broken ends are resected 5'-to-3' on one strand to generate 3'-single-stranded overhangs containing regions of microhomology (generally a few nucleotides), which are then used to mediate the repair event. Because of this reaction pathway, deletion of the sequences between the microhomologies occurs as does deletion of one of the blocks of (micro)homology. Moreover, the remaining block of microhomology always resides at the precise site of repair and can be used as a landmark to define such repair events [8,11].

A-NHEJ was not thought to be a very robust nor a particularly important DNA DSB repair pathway because it could usually only be detected in the absence of C-NHEJ. Indeed, one of the first descriptions of A-NHEJ came with the observation that of the few NHEJ DNA DSB repair events that could be detected in Ku86-deficient budding yeast, they occurred mostly between short direct repeats [9]. Since then, there have been similar reports in fission yeast [15], frogs [16] and several mammalian systems [17,18,19,20,21] including humans [22]. The significance of — and parallel interest in — A-NHEJ increased with the demonstration that A-NHEJ could substitute at reasonable levels for C-NHEJ during DNA DSB repair events in murine lymphoid class switch recombination [23,24] and during certain types of aberrant V(D)J recombination reactions [25]. Moreover, A-NHEJ has been implicated in the generation of large deletions and other genomic rearrangements in murine cells [26,27]. Similarly, microhomology has been found at the recombination junctions of radiation-induced genomic rearrangements [28,29] implying that even radiation-induced DNA DSBs can be repaired by A-NHEJ. Lastly, microhomologies are frequently detected at breakpoints for chromosomal deletions and translocations in human cancer cells [30,31]. These observations have propelled many laboratories to identify the factors required for A-NHEJ. These studies have implicated poly (ADP-ribose) polymerase-1 (PARP-1), X-ray cross complementing 1 (XRCC1), DNA ligase III (LIGIII), polynucleotide kinase (PNK) as well as Flap endonuclease 1 (Fen-1) [7,16,32,33,34] but it is clear that additional factors await identification.

One of the most compelling questions in the DNA DSB repair field is how pathway choice is determined. That is, once a chromosome breaks, how does the cell determine whether HR, C-NHEJ or A-NHEJ will mediate its repair? Since each of these repair pathways produces a discretely distinct product, including some which have been implicated in human cancer, the answer to this question seems especially biologically important. Several laboratories have suggested that the relative abundance of factors, binding affinities for DNA ends, cell type specificity and/or cell cycle phases may impact upon this decision {reviewed in [35]}. These issues are complicated even more in human somatic cells where the impact of loss-of-function mutations on some of the C-NHEJ genes has distinctly different phenotypes than are observed in other mammals. In particular, Ku70 and Ku86 have evolved an essential telomere maintenance function that does not seem to be evident in any other mammalian systems studied to date [1,36,37]. Interestingly, Ku seems to exert this function by repressing the HR-mediated disassembly of telomeres [2] suggesting that pathway choice is critical for naturally occurring double-stranded DNA ends as well as broken ones.

To begin to experimentally address some of these issues we have generated a series of human somatic cell lines genetically engineered using recombinant adeno-associated virus (rAAV)-mediated gene targeting [38,39,40] to contain reduced levels of the C-NHEJ factors Ku70, Ku86, DNA-PK_{cs}, XLF and LIGIV. We hypothesized that in the presence of reduced or no C-NHEJ activity the frequency and regulation of A-NHEJ in human cells could be assessed. To this end we utilized two *in vivo* plasmid end joining assays that have been employed to study end joining in

mammalian cells [34,41,42] to demonstrate that null mutations in DNA-PK$_{cs}$, XLF or LIGIV resulted in a severe reduction in the frequency of productive DNA DSB repair. The small number of repair events that did occur in these null cell lines were hallmarked by the heavy usage of microhomology. Thus, these studies confirmed that C-NHEJ is the predominate NHEJ pathway operative inside human somatic cells and in its absence small amounts of A-NHEJ can be detected. Very surprisingly, and in stark contrast to the results with DNA-PK$_{cs}$, XLF and LIGIV-null cell lines, DNA DSB repair activity was actually slightly elevated in Ku86 conditionally-null cell lines. These repair events appeared, once again, to be heavily biased towards microhomology-mediated repair. This result suggested that Ku86 actively suppresses A-NHEJ in human somatic cells. This hypothesis was confirmed by using molecular and genetic approaches to reduce the levels of Ku70 in cell lines that were null for either DNA-PK$_{cs}$ or LIGIV and which resulted in cell lines that had regained a robust DNA DSB repair activity that was mediated by microhomology. Together, these studies demonstrate that Ku (Ku70 and Ku86) is the critical regulator of DNA DSB repair pathway choice in human somatic cells.

Results

Strategy and cell lines

To elucidate the role of C-NHEJ factors in DNA DSB repair, we made use of an extrachromosomal reporter assay system {[34,42]; Figure 1}. This assay permits, in addition to the generation of defined DNA DSBs, a detailed follow up of the repair of the reporter plasmid. In this assay, end joining is measured by the reconstitution of green fluorescent protein (GFP) expression [42]. The reporter pEGFP-Pem1-Ad2 consists of the GFP gene engineered such that it is interrupted by a 2.4 kb intron derived from the rat Pem1 gene (Figure 1A). An exon derived from adenovirus (Ad) has been introduced into the middle of the intron and it is flanked on both sides by *HindIII* and *I-SceI* restriction enzyme recognition sequences. In un-digested or partially-digested plasmids, GFP is not expressed because the Ad exon is efficiently incorporated into the GFP mRNA (Figure 1C). Digestion of the plasmid either with *HindIII* or *I-SceI* at the flanking sites generates a linear plasmid lacking the adenoviral exon with either compatible 5'-overhanging cohesive ends or incompatible ends, respectively (Figure 1B). The *HindIII* sites are arranged such that cohesive 4-bp overlapping ends are generated, whereas the *I-SceI* sites are arranged in an inverted orientation, which demands that some sort of processing must occur before the ends can be rejoined. Thus, the impact of loss-of-function NHEJ gene mutations on these aspects of end joining can be individually assessed. Due to the buffering capacity of the intron, end joining by the cellular repair apparatus of transfected, linearized plasmid usually re-constitutes GFP expression, even when extensive additions or deletions of nucleotides have occurred (Figure

1C). As a result, a wide spectrum of end joining events can be detected and quantitated by FACS (fluorescently activated cell sorting). As a transfection control, cells are always co-transfected with a pCherry expression plasmid, and the data are expressed as the percentage of cherry-positive cells that are also green-positive. Lastly, pEGFP-Pem1-Ad2 contains a bacterial origin of replication and an antibiotic resistance gene permitting the plasmids to be recovered from human cells and rescued in *E. coli*. Consequently, the structure of the repair junctions, which provides mechanistic insight into the type of repair that was utilized, can be identified by DNA sequencing.

This assay system was used to interrogate a series of isogenic human HCT116 cell lines. HCT116 is a human adenocarcinoma somatic tissue culture cell line. It is diploid, is wild-type for all of the major DNA DSB and checkpoint genes and has a stable karyotype [40]. The derivative cell lines had been engineered using rAAV gene targeting to be reduced or deficient in the expression of most of the C-NHEJ factors, namely: Ku70 [1,43], Ku86 [2,36], DNA-PK_{cs} [44], XLF (Fattah *et al*., unpublished) or LIGIV (Oh *et al*., unpublished).

LIGIV is the only C-NHEJ gene that is haploinsufficient for plasmid DNA end joining *in vivo*

When *HindIII*- or *I-SceI*-linearized pEGFP-Pem1-Ad2 plasmid was introduced into the parental HCT116 cell line, intracellular circularization allowing GFP expression could easily be detected and quantitated by flow cytometry (Figure 2). When the same experiment was carried out with the C-NHEJ heterozygous cell lines,

significant repair activity was always observed (Figure 2). Averaged over four experiments, the Ku70, Ku86, DNA-PK_{cs} and XLF heterozygous cell lines showed only a slightly reduced ability to repair this DNA DSB that was not significantly different from wild-type (Figure 3). In contrast, the $LIGIV^{+/-}$ cell line possessed only ~65% the repair capacity of the parental cell line and was reproducibly haploinsufficient (Figures 2 and 3). In no case was a significant difference in repair frequency between the repair of *HindIII*- or *I-SceI*-plasmid observed (Figure 3). While the FACS analysis (Figures 2 and 3) measured repair frequency, the repaired plasmids could also be analyzed molecularly. In particular, the *HindIII*-cleaved substrate contained 4 bp compatible overhangs that essentially constituted a stretch of microhomology (Figure 1B). If these sequences are used to mediate the repair event, they generate a slightly smaller plasmid that contains a single *HindIII* restriction enzyme recognition site where there use to be two. Consequently, the recovered, repaired *HindIII*-linearized pEGFP-Pem1-Ad2 plasmids were re-digested with *HindIII* before gel electrophoresis, and the frequency of plasmids that had reconstituted a single *HindIII* site ("perfect joins") was determined. $Ku70^{+/-}$, $Ku86^{+/-}$ (Table S1), DNA-$PK_{cs}^{+/-}$ (Table S3), $XLF^{+/-}$ (Table S5) and $LIGIV^{+/-}$ (Table S7) cells perfectly rejoined an average of ~37% of the substrates, which was slightly higher than the 23% perfect rejoining observed in wild-type cells (summarized in Figure S1 and Figure 6B). Thus, even though the repair activity was not substantially affected by the loss of one allele of any of the C-NHEJ genes tested, the repair profiles shifted towards microhomology-mediated joining. In several instances, perfectly joined plasmids (as assessed by restriction digest and gel electrophoresis) were sequenced

and without exception the existence of the expected single *HindIII* site was confirmed (data not shown). Lastly, plasmids for those *HindIII*-linearized substrates that did not perfectly rejoin and 30 plasmids for the *I-SceI*-linearized substrate (which can not perfectly rejoin) were sequenced. This analysis demonstrated that the size of the accompanying deletions (Figures S3 and S4), the frequency of microhomology usage, and the frequency of insertions was, with a few interesting exceptions (see the Discussion), comparable to that observed in wild-type cells (Tables S2, S4, S6 and S8 and Figures S1 and S2). From these experiments, we concluded that the reduction by one allele of most C-NHEJ factors is generally aphenotypic for DNA end joining whereas LIGIV is haploinsufficient, implying that LIGIV may be a limiting C-NHEJ factor in human somatic cells.

The absence of DNA-PK$_{cs}$, XLF and LIGIV greatly reduces DNA repair activity

In rodents, cells deficient in any of the C-NHEJ components are generally very deficient in joining virtually all types of DNA DSBs [3]. To test whether C-NHEJ-deficient human cells are also impaired in end joining, we repeated the above experiment in DNA-PK$_{cs}$-, XLF- and LIGIV-null cell lines. In all three cases, the frequency of end joining was greatly reduced (Figure 4). On average, DNA-PK$_{cs}$- and XLF-null cell lines were diminished by an order-of-magnitude and showed only about 10% the repair activity observed in the parental cell line (Figure 3). The LIGIV-null cell line was always the most profoundly affected cell line and performed end-joining only a few percent above background. The fact that XLF-null cells were

reproducibly more active than the LIGIV-null cells is consistent with XLF playing an important, but not essential, role in DNA DSB ligation. We next attempted — as a proof-of-principle — to functionally rescue the XLF-null line to confirm that the loss of end-joining activity was due specifically to the respective targeted knockout mutations in these cell lines. A XLF cDNA was stably introduced via retroviral infection into the XLF-null cell line, and a subclone expressing wild-type levels of XLF protein was isolated (data not shown). This cell line showed an end-joining activity that was 90% of wild-type (Figure 3) directly demonstrating that the absence of XLF was responsible for the phenotype of the null cells. In conclusion, these experiments demonstrated that C-NHEJ is the major NHEJ repair pathway in human somatic cells, and in its absence only low (albeit detectable - see below) levels of end joining can occur.

The absence of Ku changes the repair profile, but not the repair activity

Primates are unique in that, in contrast to every other species examined to date, the Ku genes have evolved to become essential [1,2,36], due to their ability to suppress lethal HR-mediated telomere recombination [2]. Consequently, human cell lines that are null for either Ku70 [1] or Ku86 [36] are not viable. We have, however, constructed a "conditionally-null" ($Ku86^{flox/-}$) cell line for Ku86. This cell line has been engineered through rAAV gene targeting technology to contain only a singly functional "floxed" allele of Ku86 [2]. In the presence of the Cre recombinase, the floxed allele is excised and the cells become null for Ku expression. Importantly,

the loss of Ku86 is essentially complete in 4 to 5 days and although the cells will ultimately succumb, they generally don't do so for approximately 2 weeks [2]. Thus, the day 4 to day 14 window was used to assess the ability of the cells to perform end joining. Consequently, $Ku86^{flox/-}$ cells were either infected with a control adenovirus (AdCMV) or an adenovirus expressing Cre (AdCre). At 4, 5 and 6 days post-infection, a portion of the cells were processed for Western analysis, which confirmed that the levels of Ku86 protein were greatly diminished in the AdCre-treated cells compared to the control AdCMV-treated cells (Figure 5A). The levels of Ku86 never go to zero because a minor portion of the cells are either not productively infected with the adenoviral vector and/or they do not efficiently undergo Cre-mediated recombination [2]. At 120 hr post adenovirus infection, the cells were transfected with pEGFP-Pem1-Ad2 and 24 hr later the cells were analyzed by FACS analysis. Very unexpectedly, $Ku86^{flox/-}$ +AdCre cells performed end joining at a wild-type frequency (Figure 5B). Indeed, in four independent experiments the "Ku86-null" cells reproducibly seemed to have even slightly higher levels of end joining activity than wild-type cells, regardless of whether *HindIII*- or *I-SceI*-linearized substrates were used (Figure 3).

We were perplexed by this result until we considered the possibility that although the frequency of end-joining was not altered in Ku86-null cells the repair profile might be. To experimentally test this hypothesis, the repaired *HindIII*-cleaved pEGFP-Pem1-Ad2 substrate plasmids were recovered from Ku86-null cells and analyzed by agarose gel electrophoresis following *HindIII* re-digestion for perfect rejoining. In the parental and heterozygous cell lines this type of repair

event was observed in about 30% of the repaired plasmids (Figs. 6A and 6B). In striking contrast, ~80% of all the plasmids recovered from Ku86-null cells had reconstituted a single *HindIII* site (Figures 6A and 6B). Thus, while the overall repair frequency in Ku86-null cells was not significantly different from wild-type cells, the repair profile was heavily shifted to one that utilized more microhomology.

Microhomology-mediated end joining also dominates in the absence of DNA-PK$_{cs}$, XLF and LIGIV

Although end joining was greatly reduced in DNA-PK$_{cs}$-, XLF- and LIGIV-null cell lines (Figure 4), it was not zero. Given the above results with Ku86-null cells, we next tested whether the residual repair in these other C-NHEJ-null cell lines was also heavily biased towards microhomology. Indeed, although there were far fewer repair events in these three cell lines in comparison to Ku86-null cells, they were nonetheless predominantly (70 to 80%) mediated by microhomology (Figure 6B). Thus, DNA-PK$_{cs}$-, XLF- and LIGIV-null cell lines had an identical repair profile to Ku86-null cells (Figure 6B), but carried out only 1 to 10% as many repair events as Ku86-null cells.

A-NHEJ is negatively regulated by Ku in human somatic cells

The above results suggested that Ku normally actively suppresses A-NHEJ. In Ku's presence, even when C-NHEJ is inactivated by mutations in DNA-PK$_{cs}$, XLF or LIGIV, A-NHEJ is apparently still strongly suppressed (Figure 4). In contrast, in Ku's absence, A-NHEJ is "unleashed" and rescues the repair activity of the cells (Figure 5).

Interestingly, there is precedent for this model in the literature. Thus, mouse cell lines deficient for Ku86 repair *I-SceI*-induced DNA DSBs with a frequency similar to that of wild-type cells but with a repair profile that is biased towards microhomology [45]. Moreover, the ionizing radiation sensitivity of LIGIV-deficient chicken DT40 cells can be rescued by the deletion of Ku70 [46]. Perhaps most impressively, LIGIV deficiency in the mouse results in embryonic lethality and this can be rescued by the deletion of Ku86 [47]. Although, repair profiles were not assessed in the latter two studies, they are consistent with the absence of Ku de-repressing A-NHEJ to the point where the phenotypes could be rescued.

To investigate if this paradigm could be extended to human cells we directly tested whether the strong repair defects of DNA-PK_{cs}- and the very severe defects of LIGIV-null cells could be rescued by reducing the amount of Ku in these cell lines. A combination of genetic and molecular approaches was utilized to achieve a significant knockdown of Ku, a highly abundant protein. Thus, rAAV gene targeting was first used to functionally inactivate one Ku70 allele in DNA-PK_{cs}- and LigIV-null cell lines. DNA-$PK_{cs}^{-/-}$:$Ku70^{+/-}$ and $LIGIV^{-/-}$:$Ku70^{+/-}$ cell lines have ~50% the level of Ku70 protein compared to wild-type cells (Figure 7B; [1,43]) and this reduction in Ku very slightly rescued the repair deficiencies of either cell line (compare panel 5 with panel 6 and panel 8 with panel 9 in Figure 7A; Figure 7C). siRNA against Ku70 was then used to reduce the level of Ku protein to ~5% of wild-type (+ siRNA, Figure 7B). Impressively, DNA-$PK_{cs}^{-/-}$ and $LIGIV^{-/-}$ cells showed wild-type and greatly enhanced, respectively, end-joining activity (compare panel 5 with panel 7 and panel 8 with panel 10 in Figure 7A; Figure 7C), directly demonstrating that a

reduction in Ku can "reanimate" a cell that appears "dead" for DNA DSB repair. Importantly, the end joining occurring in these Ku-reduced cell lines was predominately microhomology mediated (Tables S3, S4, S7 and S8). Moreover, these data provide a plausible molecular mechanistic explanation for the earlier genetic results obtained in chickens and mice.

Microhomology-mediated A-NHEJ predominates in C-NHEJ deficient cells

To confirm and extend the above results, we utilized a reporter assay that is biased towards detecting A-NHEJ events. pDVG94 is designed such that the relative efficiency of C-NHEJ versus A-NHEJ events can be assessed [41,48]. When pDVG94 is digested with *AfeI* and *EcoRV* it results in a blunt-ended linear substrate with a 6-bp repeat at both ends (Figure 8A). C-NHEJ can rejoin these ends and yield a wide variety of junctions but A-NHEJ almost exclusively generates a single product in which the 2 repeats have been reduced to 1, which simultaneously generates a novel *BstXI* restriction enzyme recognition site (Figure 8A). Thus, linearized pDVG94 plasmid was transfected into the mutant cell lines and 48 hr later repaired plasmids were recovered, purified and then used as substrates for PCR using a 5'-radiolabeled PCR primer (Figure 8B). The relative level of A-NHEJ is subsequently determined by quantification of the *BstXI*-digested PCR products where a 180 bp product represents the repaired plasmid and a cleaved 120 bp product is diagnostic of microhomology-mediated end joining (Figure 8B). The parental cell line, $Ku86^{flox/-}$ and $Ku86^{flox/-}$ infected with AdCMV cell lines carried out only a few percent of

microhomology-mediated end joining in this assay (Figure 8C). In contrast, Ku86-null cells showed on average 45% microhomology use (Figure 8C). Although this assay cannot be used to determine the absolute frequency of the individual repair events, it confirmed that in the absence of Ku, microhomology-mediated events became easily detectable.

This phenotype was even more evident in the DNA-PK_{cs}- (Figure 8D), XLF- (Figure 8E) and LIGIV- (Figure 8F) null cell lines. In the absence of one of these three factors, the frequency of microhomology-mediated end joining was virtually 100%. Importantly, the re-introduction of a wild-type DNA-PK_{cs} or XLF cDNA into their respective null cell line, partially and completely, respectively, reverted the repair events to a C-NHEJ spectrum. Again, the degree of repair complementation was directly related to the degree of complementing protein expression achieved in these cell lines (data not shown).

These experiments demonstrated that in the presence of Ku, but the absence of other C-NHEJ factors that virtually all of the end joining in human cells is carried out by microhomology-mediated processes. In contrast, in the presence of the other C-NHEJ factors but in the absence of Ku, some, but not all, of the end joining occurs using microhomology.

Ku protects DNA ends from degradation

In every metabolic reaction (*e.g.*, DNA DSB repair, V(D)J recombination, telomere maintenance, *etc*.) that Ku participates in, and in every organism that such reactions have been characterized, Ku's absence is marked by hyper-resection of the

relevant DNA ends [13]. To determine if this aspect of Ku's absence is conserved in human cells extensive sequencing was carried out of pEGFP-Pem1-Ad2 plasmids recovered from wild type and Ku86-null cells. A significant increase in deletion size in Ku86-null cells compared to wild-type cells was observed. In wild-type cells the median deletion size was 595 bp whereas in Ku86-null cells it was 1158 bp for *HindIII*-linearized plasmids (Table S1 and Figure S3). This same trend was also observed in *I-SceI*-linearized plasmids as the median deletion size was 1097 bp in Ku86-null cells in comparison to 321 bp in wild type cells (Table S2 and Figure S4). When the same analysis was carried out for DNA-PK_{cs}-null (Tables S3 and S4), XLF-null (Tables S5 and S6) and LIGIV-null (Tables S7 and S8) cell lines less degradation of the DNA ends compared to wild-type cells was observed (Figures S3 and S4). In summary, the presence or absence of Ku in human somatic cells carried with it a hyper-resection phenotype that was identical to that observed for Ku-dependent reactions in all other species.

Discussion

We have utilized rAAV knockout technology to construct a powerful reagent: a series of isogenic human cell lines that are defective for genes required for the C-NHEJ-mediated branch of DNA DSB repair. We used these cell lines along with several informative reporter systems to demonstrate that wild-type human cells vastly prefer to utilize C-NHEJ over A-NHEJ for end joining reactions. Unexpectedly, the absence of the proximal C-NHEJ factor Ku, resulted in cells that still carried out robust levels of end joining, suggesting that Ku normally suppresses other end joining pathways. This model was supported by the construction of double mutant cell lines, which demonstrated that the reduction of Ku in a cell that was incapable of carrying out C-NHEJ still resulted in high levels of end joining. Thus, these studies demonstrate that Ku is the critical regulator for determining pathway choice in human somatic cells.

Ku, the "mother" of all DNA DSB repair inhibitors?

Ku is a heavily researched DNA repair factor and the majority of studies rightfully concentrate on some aspect of Ku's ability to positively facilitate the myriad of repair and recombination reactions that require C-NHEJ. In this and related studies, we have recently documented that Ku has an additional and hitherto underappreciated function — it is a powerful inhibitor for all the other DNA DSB repair pathways. Specifically, we have demonstrated that in Ku is an essential repressor of HR-mediated aberrant telomere recombination. In the absence of Ku, the HR apparatus can apparently gain access to the telomeric ends and generate

lethal telomeric shortening [2]. Thus, Ku can inhibit HR specifically at telomeres. Moreover, in a study that characterized generalized rAAV-mediated gene targeting — a process that requires HR — for loci scattered throughout the genome we demonstrated that the absence of Ku results in a ~10-fold increase in correct gene targeting [1]. Importantly, the increase in correct gene targeting came at no expense to random integrations. These data strongly suggested that the reduction of Ku in human somatic cells de-repressed HR enough to facilitate much higher levels of gene targeting while simultaneously allowing other repair pathways to carry out random integrations at wild-type levels. This conclusion is completely supported by the data provided in this present study. Thus, here we have documented that in the absence of Ku, A-NHEJ is greatly up-regulated. Together, these studies have revealed that Ku can inhibit HR at telomeres, and it can inhibit HR and A-NHEJ throughout the genome. Moreover, this work and the work of Fattah *et al*. [1] make the strong prediction that the random rAAV integrations observed in Ku-deficient cells are mediated by A-NHEJ.

How does Ku orchestrate all this inhibition?

Many models can be envisioned for how Ku suppresses A-NHEJ. One possibility is that Ku, via direct protein:protein interaction, sequesters a key A-NHEJ factor from performing its function. In a Ku-deficient cell, this factor would be free to facilitate A-NHEJ. A good candidate for such a putative factor exists. Thus, a bevy of independent laboratories have demonstrated that PARP-1 interacts with Ku [49,50,51,52,53]. And a PARP-1 interaction domain has been defined in the Ku70

subunit at AA243-261 [52]. This model predicts that a cell expressing a Ku70 incapable of interacting with PARP-1 (*e.g.*, mutated at residues AA243-261) would phenocopy the Ku loss-of-function mutations and we are attempting to construct such a cell line. A second, and in our minds, likelier possibility, is that Ku controls A-NHEJ by regulating access to the substrate; namely, a dsDNA end. We prefer this model because not only does Ku repress A-NHEJ but it also represses HR at internal loci [1] and at telomeres [2]. While it is possible that Ku mediates all of this repression by physically binding to and inhibiting/sequestering a different protein or proteins for each reaction, it seems simpler if Ku simultaneously regulates all three processes by regulating access to the substrate for all of these pathways: double-stranded DNA ends. Specifically, we propose that in order to be channeled into a particular pathway (HR, A-NHEJ or C-NHEJ), that pathway's DNA binding factor (probably RAD52, PARP-1 and Ku, respectively) needs to bind onto the ends of the break and subsequently recruit their pathway's associated factors. We posit that Ku generally gets to the ends of a dsDNA break faster and/or with higher affinity than RAD52 or PARP-1 and once there it blocks their access, such that repair is fated to occur by C-NHEJ. This model is by no means novel and has been proposed by a myriad of investigators and was broached at least a decade ago [54], although it still remains largely untested. In this regard, a cell line that expressed a double-stranded DNA end binding Ku mutant would be predicted to be incapable of repressing either HR or A-NHEJ and the construction of such a cell line is underway. Lastly, this model, in particular, could explain the differences between mice and humans. In mice, the levels of Ku/DNA-PK are much lower than they are in humans

and consequently there might be a "fair fight" between Ku, Rad52 and PARP-1 over who gets to a broken end. In contrast, in human cells where the levels of Ku/DNA-PK are about 50-fold higher [13,55], Ku has become the "bully" and essentially dominates pathway choice.

Is there evidence for yet another sub-pathway of NHEJ?

In this study we have interrogated our mutant cell lines with two structurally similar, but fundamentally different, types of DNA ends. In one of them (*HindIII*-linearized pEGFP-Pem1-Ad2) a region of pre-existing microhomology was presented to the cell. In the other (*I-SceI*-linearized pEGFP-Pem1-Ad2 and linearized pDVG94) some processing by the cell was required to reveal the microhomology. Microhomology-mediated end joining of the *HindIII*-linearized pEGFP-Pem1-Ad2 plasmid could be detected in the wild-type parental cells (Figure 2 and Tables S1, S3, S5 and S7). This perfect end joining increased in Ku heterozygotes and became the predominate reaction product in Ku- reduced/null cell lines. These results can be most simply interpreted if Ku inhibits A-NHEJ and as the level of Ku is reduced the levels of A-NHEJ reciprocally rise. The data generated using the two repair substrates that required processing suggests that this model is, however, over-simplified. Thus, as the level of Ku was reduced in the various cell lines the frequency of microhomology-mediated end joining increased with *I-SceI*-linearized pEGFP-Pem1-Ad2 and linearized pDVG94, but so did other end joining activities. This was most evident in the experiments using pDVG94 where ~55% of the repaired plasmids in a Ku-null cell did not use microhomology to repair the

plasmid (Figure 8C). Sequencing of these events and those derived from *I-SceI*-linearized pEGFP-Pem1-Ad2 did not reveal any novel repair signatures and most events looked indistinguishable from typical C-NHEJ products (Table S2). Together, these studies suggest that there may be at least one additional NHEJ pathway that is distinguishable from C-NHEJ and A-NHEJ by its lack of requirement for Ku and its lack of microhomology use, respectively. Needless to say, these products could also be accounted for by A-NHEJ if it does not have an absolute requirement for microhomology. The construction of humans cell lines that are doubly defective for C-NHEJ and A-NHEJ should genetically address this issue.

The power of rAAV-mediated human somatic cell genetics

Advances in the DNA DSB repair field have come predominately from studies on yeast and genetically modified mice. There are instances, C-NHEJ foremost among them, however, where the phenotypes of yeast and mice mutants do not accurately recapitulate the corresponding phenotypes observed in humans. Since ultimately we wish to apply what we have learned in model systems to the study of humans in the clinic, a potentially more appropriate model system is the use of human somatic cells in culture. There are, of course, attendant limitations to using human cells in culture and the requisite caution needs to be taken in extrapolating cell culture results to patients in the clinic. It is, however, also reasonable to expect that the physiology of human cells in culture may reflect more accurately the basic biochemical process of human patients than, say, rodent cells *in vivo* might. The strength of the rodent system stems predominately from the ability to make

targeted alterations of individual genes using the technology of HR [56]. This technology exists for human somatic cells as well [39,40,57]. Overall, at least 73 different genes have been functionally inactivated in a total of 43 different human somatic cell lines {[40] and unpublished data}. To our knowledge, however, this is one of the first reports of the systematic inactivation of a large number of genes involved in a single pathway. Importantly, we have shown that it is possible to make simple knockouts, conditional knockouts and double mutant human somatic cell lines with relative ease. The general utility of rAAV-mediated gene targeting may thus be of interest for investigators working on biological problems that cannot be adequately modeled in, for example, the mouse.

Materials and Methods

Cell culture

The human wild-type HCT116 cell line and its derivatives were cultured in McCoy's 5A medium containing 10% fetal bovine serum, 100 U/ml penicillin, and 100 U/ml streptomycin in a humidified incubator with 5% CO_2 at 37 ^{o}C. Cell lines derived from correct gene targeting were propagated under G418 (1 mg/ml) selection. Cell lines carrying exogenous cDNA expression vectors (either XLF or DNA-PK_{cs}) were grown in 2 mg/ml of puromycin.

Cell lines

The wild-type human HCT116 cell line was obtained from the ATCC. The derivative $Ku70^{+/-}$ [43], $Ku86^{+/-}$ [36], $Ku86^{flox/-}$ [2], DNA-$PK_{cs}^{+/-}$ and DNA-$PK_{cs}^{-/-}$ [44] cell lines have been described. Derivatives of $Ku70^{+/-}$ cells treated with Ku70 RNAi (SMARTPool oligonucleotides; Dharmacon) or stably expressing shRNA vectors directed against Ku70 have also been described [1]. The $XLF^{+/-}$ and $XLF^{-/-}$ (Fattah *et al*., manuscript in preparation) and the $LIGIV^{+/-}$ and $LIGIV^{-/-}$ (Oh *et al*., manuscript in preparation) cell lines were generated by rAAV gene targeting. Similarly, compound mutant cell lines (*e.g*., $Ku70^{+/-}$:$LIGIV^{-/-}$) were generated using the rAAV targeting technology described elsewhere [40].

Treatment of $Ku86^{flox/-}$ cells with Cre

To generate Ku86-null cells, the $Ku86^{flox/-}$ cells were plated onto a 6-well plate at a density of 5 X 10^4 cells per well and allowed to attach for 18 hr. Adenoviral infection

was carried out by adding 2 ml of fresh media containing 5 X 10^8 virus particles of either a control (AdCMV) or experimental (AdCre) adenoviral stock to each well [2]. After 4 days (96 hr) of incubation the cells were re-plated into 6-well plates and allowed to incubate for another 24 hr before the cells were transfected with linearized NHEJ substrates (see below). Flow cytometry was then carried out after an additional incubation for 24 hr.

The end-joining assay, transfection and FACS analysis

The *in vivo* end-joining reporter plasmid pEGFP-Pem1-Ad2 (Figure 1) has been described [34,42]. Prior to transfection, the pEGFP-Pem1-Ad2 plasmid was digested with *Hind*III or *I-Sce*I (NEB) for 8 to 12 hr to generate different types of DNA ends. A pCherry plasmid (Clontech) was co-transfected with linearized pEGFP-Pem1-Ad2 as a control of transfection efficiency. The cell line under analysis was subcultured a day before transfection and was ~60 to 70% confluent for transfection. Transfections were performed using Lipofectamine 2000 (Invitrogen) according to manufacture's instructions. Green (EGFP) and red (Cherry) fluorescence was measured by fluorescence-activated flow cytometry (FACS) 24 hr later [34]. For FACS analysis cells were harvested, washed in 1X PBS and fixed using 2% paraformaldehyde. FACS analysis was performed on a FACSCalibur instrument (BD Biosciences). For the HCT116 cell line a red-versus-green standard curve was derived with varying amount of cherry and green plasmids to avoid measurements near the plateau region. The values of repaired events is reported as a ratio of cells that were double positive for red and green fluorescence over total cells that are

only positive for red fluorescence. This ratio normalizes the repair events to the transfection controls. The values for all the mutants are reported as a percent repair of wild-type cells.

Plasmid rescue

The repaired NHEJ reporter pEGFP-Pem1-Ad2 substrates were rescued from human cells using a Qiagen mini-preparation protocol, transformed into *E. coli* (TOP10) and colonies carrying the repaired plasmids were selected on LB plates containing 30 mg/ml of kanamycin. The fidelity of NHEJ repair events was examined by digesting the plasmid DNA from individual colonies with the restriction enzyme *Hind*III prior to agarose gel electrophoresis. Precise junctional information was obtained by DNA sequencing using a variety of primers (sequences available upon request) located upstream and downstream of the Ad2 exon sequence. Those events that had not restored the original restriction site were always analyzed by sequencing. For *I-Sce*I-digested substrate, all the repair products were directly sequenced, as incompatible *I-Sce*I sites should not restore the original restriction site(s).

Microhomology assay

The microhomology assay was performed as described [41]. In brief, 2.5 mg of *EcoRV*- (NEB) and *AfeI*- (NEB) digested plasmid pDVG94 were transfected into cells that were ~60% confluent, in 6 well plates, using Lipofectamine 2000 (Invitrogen) according to manufacturer's instruction. The transfection efficiencies of wild-type HCT116 and the derivative mutant cell lines were determined using the plasmid

pEGFP-Pem1 as described above. After transfection (48 hr), plasmid DNA was recovered using a modified Qiagen mini-preparation protocol. Repaired pDVG94 plasmid was PCR amplified using primer FM30 and a 5'-radiolabeled primer DAR5 [41]. The PCR product was digested with *BstXI* (NEB). Restriction fragments were separated by electrophoresis along with undigested PCR product in a 6% polyacrylamide gel in TBE buffer. The gel was subsequently dried and exposed to film. The bands representing the undigested (180 bp) or digested (120 bp) PCR products were quantified using ImageQuant software.

The authors are indebted to Dr. V. Gorbunova (University of Rochester, NY), Dr. G. Illiakis (University of Duisburg-Essen Medical School, Germany) and Dr. D. van Gent (Erasmus University, Netherlands) and members of their laboratories who were extremely generous with their reagents and advice. We would like to acknowledge the assistance of the Flow Cytometry Core Facility of the Masonic Cancer Center, a comprehensive cancer center designated by the National Cancer Institute, supported in part by P30 CA77598. We thank Drs. Anja-Katrin Bielinsky (University of Minnesota, MN) and Katheryn Meek (Michigan State University, MI) for their helpful comments on the manuscript. We are indebted to Brian Ruis and Sehyun Oh (University of Minnesota, MN) for access to their DNA-PK_{cs} and LIGIV mutant cell lines, respectively. These studies were supported in part by National Institutes of Health grants GM069576 and HL079559 to E.A.H.

Author Contributions

The author(s) have made the following declaration about their contributions: Conceived and designed the experiments: FF and EAH. Performed the experiments: FF EHL NW YW NL. Analyzed the data: FF EHL NW EAH. Contributed reagents/material/analysis tools: YW. Wrote the paper: FF NW EAH.

References

1. Fattah FJ, Lichter NF, Fattah KR, Oh S, Hendrickson EA (2008) Ku70, an essential gene, modulates the frequency of rAAV-mediated gene targeting in human somatic cells. Proc Natl Acad Sci U S A 105: 8703-8708.
2. Wang Y, Ghosh G, Hendrickson EA (2009) Ku86 represses lethal telomere deletion events in human somatic cells. Proc Natl Acad Sci U S A in press.
3. Hakem R (2008) DNA-damage repair; the good, the bad, and the ugly. EMBO J 27: 589-605.
4. Cahill D, Connor B, Carney JP (2006) Mechanisms of eukaryotic DNA double strand break repair. Front Biosci 11: 1958-1976.
5. Li X, Heyer WD (2008) Homologous recombination in DNA repair and DNA damage tolerance. Cell Res 18: 99-113.
6. McVey M, Lee SE (2008) MMEJ repair of double-strand breaks (director's cut): deleted sequences and alternative endings. Trends Genet 24: 529-538.
7. Wang H, Perrault AR, Takeda Y, Qin W, Iliakis G (2003) Biochemical evidence for Ku-independent backup pathways of NHEJ. Nucleic Acids Res 31: 5377-5388.
8. Nussenzweig A, Nussenzweig MC (2007) A backup DNA repair pathway moves to the forefront. Cell 131: 223-225.
9. Boulton SJ, Jackson SP (1996) Identification of a Saccharomyces cerevisiae Ku80 homologue: roles in DNA double strand break rejoining and in telomeric maintenance. Nucleic Acids Res 24: 4639-4648.
10. Ma JL, Kim EM, Haber JE, Lee SE (2003) Yeast Mre11 and Rad1 proteins define a Ku-independent mechanism to repair double-strand breaks lacking overlapping end sequences. Mol Cell Biol 23: 8820-8828.
11. Haber JE (2008) Alternative endings. Proc Natl Acad Sci U S A 105: 405-406.
12. Lieber MR, Lu H, Gu J, Schwarz K (2008) Flexibility in the order of action and in the enzymology of the nuclease, polymerases, and ligase of vertebrate non-homologous DNA end joining: relevance to cancer, aging, and the immune system. Cell Res 18: 125-133.
13. Hendrickson EA, Huffman JL, Tainer JA (2006) Structural aspects of Ku and the DNA-dependent protein kinase complex. In: Seide W, Kow YW, Doetsch P, editors. DNA Damage Recognition. New York: Taylor and Francis Group. pp. 629-684.
14. Meek K, Dang V, Lees-Miller SP (2008) DNA-PK: the means to justify the ends? Adv Immunol 99: 33-58.
15. Manolis KG, Nimmo ER, Hartsuiker E, Carr AM, Jeggo PA, et al. (2001) Novel functional requirements for non-homologous DNA end joining in *Schizosaccharomyces pombe*. EMBO J 20: 210-221.
16. Gottlich B, Reichenberger S, Feldmann E, Pfeiffer P (1998) Rejoining of DNA double-strand breaks in vitro by single-strand annealing. Eur J Biochem 258: 387-395.
17. Kabotyanski EB, Gomelsky L, Han JO, Stamato TD, Roth DB (1998) Double-strand break repair in Ku86- and XRCC4-deficient cells. Nucl Acids Res 26: 5333-5342.
18. Feldmann E, Schmiemann V, Goedecke W, Reichenberger S, Pfeiffer P (2000) DNA double-strand break repair in cell-free extracts from Ku80-deficient

cells: implications for Ku serving as an alignment factor in non-homologous DNA end joining. Nucl Acids Res 28: 2585-2596.
19. Guirouilh-Barbat J, Huck S, Bertrand P, Pirzio L, Desmaze C, et al. (2004) Impact of the KU80 pathway on NHEJ-induced genome rearrangements in mammalian cells. Mol Cell 14: 611-623.
20. Guirouilh-Barbat J, Rass E, Plo I, Bertrand P, Lopez BS (2007) Defects in XRCC4 and KU80 differentially affect the joining of distal nonhomologous ends. Proc Natl Acad Sci U S A 104: 20902-20907.
21. Wu W, Wang M, Wu W, Singh SK, Mussfeldt T, et al. (2008) Repair of radiation induced DNA double strand breaks by backup NHEJ is enhanced in G2. DNA Repair (Amst) 7: 329-338.
22. Bentley J, Diggle CP, Harnden P, Knowles MA, Kiltie AE (2004) DNA double strand break repair in human bladder cancer is error prone and involves microhomology-associated end-joining. Nucleic Acids Res 32: 5249-5259.
23. Soulas-Sprauel P, Le Guyader G, Rivera-Munoz P, Abramowski V, Olivier-Martin C, et al. (2007) Role for DNA repair factor XRCC4 in immunoglobulin class switch recombination. J Exp Med 204: 1717-1727.
24. Yan CT, Boboila C, Souza EK, Franco S, Hickernell TR, et al. (2007) IgH class switching and translocations use a robust non-classical end-joining pathway. Nature 449: 478-482.
25. Corneo B, Wendland RL, Deriano L, Cui X, Klein IA, et al. (2007) Rag mutations reveal robust alternative end joining. Nature 449: 483-486.
26. Ferguson DO, Sekiguchi JM, Chang S, Frank KM, Gao Y, et al. (2000) The nonhomologous end-joining pathway of DNA repair is required for genomic stability and the suppression of translocations. Proc Natl Acad Sci U S A 97: 6630-6633.
27. Difilippantonio MJ, Zhu J, Chen HT, Meffre E, Nussenzweig MC, et al. (2000) DNA repair protein Ku80 suppresses chromosomal aberrations and malignant transformation. Nature 404: 510-514.
28. Morris T, Thacker J (1993) Formation of large deletions by illegitimate recombination in the HPRT gene of primary human fibroblasts. Proc Natl Acad Sci U S A 90: 1392-1396.
29. Nohmi T, Suzuki M, Masumura K, Yamada M, Matsui K, et al. (1999) Spi(-) selection: An efficient method to detect gamma-ray-induced deletions in transgenic mice. Environ Mol Mutagen 34: 9-15.
30. Canning S, Dryja TP (1989) Short, direct repeats at the breakpoints of deletions of the retinoblastoma gene. Proc Natl Acad Sci U S A 86: 5044-5048.
31. Smanik PA, Furminger TL, Mazzaferri EL, Jhiang SM (1995) Breakpoint characterization of the ret/PTC oncogene in human papillary thyroid carcinoma. Hum Mol Genet 4: 2313-2318.
32. Audebert M, Salles B, Calsou P (2004) Involvement of poly(ADP-ribose) polymerase-1 and XRCC1/DNA ligase III in an alternative route for DNA double-strand breaks rejoining. J Biol Chem 279: 55117-55126.
33. Liang L, Deng L, Chen Y, Li GC, Shao C, et al. (2005) Modulation of DNA end joining by nuclear proteins. J Biol Chem 280: 31442-31449.

34. Wang M, Wu W, Wu W, Rosidi B, Zhang L, et al. (2006) PARP-1 and Ku compete for repair of DNA double strand breaks by distinct NHEJ pathways. Nucleic Acids Res 34: 6170-6182.
35. Shrivastav M, De Haro LP, Nickoloff JA (2008) Regulation of DNA double-strand break repair pathway choice. Cell Res 18: 134-147.
36. Li G, Nelsen C, Hendrickson EA (2002) Ku86 is essential in human somatic cells. Proc Natl Acad Sci U S A 99: 832-837.
37. Myung K, Ghosh G, Fattah FJ, Li G, Kim H, et al. (2004) Regulation of telomere length and suppression of genomic instability in human somatic cells by Ku86. Mol Cell Biol 24: 5050-5059.
38. Kohli M, Rago C, Lengauer C, Kinzler KW, Vogelstein B (2004) Facile methods for generating human somatic cell gene knockouts using recombinant adeno-associated viruses. Nucl Acids Res 32: e3.
39. Rago C, Vogelstein B, Bunz F (2007) Genetic knockouts and knockins in human somatic cells. Nat Protoc 2: 2734-2746.
40. Hendrickson EA (2008) Gene targeting in human somatic cells. In: Conn PM, editor. Source Book of Models for Biomedical Research. Totowa, NJ: Humana Press, Inc. pp. 509-525.
41. Verkaik NS, Esveldt-van Lange RE, van Heemst D, Bruggenwirth HT, Hoeijmakers JH, et al. (2002) Different types of V(D)J recombination and end-joining defects in DNA double-strand break repair mutant mammalian cells. Eur J Immunol 32: 701-709.
42. Seluanov A, Mittelman D, Pereira-Smith OM, Wilson JH, Gorbunova V (2004) DNA end joining becomes less efficient and more error-prone during cellular senescence. Proc Natl Acad Sci U S A 101: 7624-7629.
43. Fattah KR, Ruis BL, Hendrickson EA (2008) Mutations to Ku reveal differences in human somatic cell lines. DNA Repair (Amst) 7: 762-774.
44. Ruis BL, Fattah KR, Hendrickson EA (2008) The catalytic subunit of DNA-dependent protein kinase regulates proliferation, telomere length, and genomic stability in human somatic cells. Mol Cell Biol 28: 6182-6195.
45. Schulte-Uentrop L, El-Awady RA, Schliecker L, Willers H, Dahm-Daphi J (2008) Distinct roles of XRCC4 and Ku80 in non-homologous end-joining of endonuclease- and ionizing radiation-induced DNA double-strand breaks. Nucleic Acids Res 36: 2561-2569.
46. Adachi N, Ishino T, Ishii Y, Takeda S, Koyama H (2001) DNA ligase IV-deficient cells are more resistant to ionizing radiation in the absence of Ku70: Implications for DNA double-strand break repair. Proc Natl Acad Sci U S A 98: 12109-12113.
47. Karanjawala ZE, Adachi N, Irvine RA, Oh EK, Shibata D, et al. (2002) The embryonic lethality in DNA ligase IV-deficient mice is rescued by deletion of Ku: implications for unifying the heterogeneous phenotypes of NHEJ mutants. DNA Repair (Amst) 1: 1017-1026.
48. Lou Z, Chen BP, Asaithamby A, Minter-Dykhouse K, Chen DJ, et al. (2004) MDC1 regulates DNA-PK autophosphorylation in response to DNA damage. J Biol Chem 279: 46359-46362.

49. Ruscetti T, Lehnert BE, Halbrook J, Le Trong H, Hoekstra MF, et al. (1998) Stimulation of the DNA-dependent protein kinase by poly(ADP-ribose) polymerase. J Biol Chem 273: 14461-14467.
50. Ariumi Y, Masutani M, Copeland TD, Mimori T, Sugimura T, et al. (1999) Suppression of the poly(ADP-ribose) polymerase activity by DNA-dependent protein kinase in vitro. Oncogene 18: 4616-4625.
51. Galande S, Kohwi-Shigematsu T (1999) Poly(ADP-ribose) polymerase and Ku autoantigen form a complex and synergistically bind to matrix attachment sequences. J Biol Chem 274: 20521-20528.
52. Pleschke JM, Kleczkowska HE, Strohm M, Althaus FR (2000) Poly(ADP-ribose) binds to specific domains in DNA damage checkpoint proteins. J Biol Chem 275: 40974-40980.
53. Sartorius CA, Takimoto GS, Richer JK, Tung L, Horwitz KB (2000) Association of the Ku autoantigen/DNA-dependent protein kinase holoenzyme and poly(ADP-ribose) polymerase with the DNA binding domain of progesterone receptors. J Mol Endocrinol 24: 165-182.
54. Van Dyck E, Stasiak AZ, Stasiak A, West SC (1999) Binding of double-strand breaks in DNA by human Rad52 protein. Nature 398: 728-731.
55. Finnie NJ, Gottlieb TM, Blunt T, Jeggo PA, Jackson SP (1995) DNA-dependent protein kinase activity is absent in xrs-6 cells: implications for site-specific recombination and DNA double-strand break repair. Proc Natl Acad Sci U S A 92: 320-324.
56. DeChiara TM (2001) Gene targeting in ES cells. Methods Mol Biol 158: 19-45.
57. Konishi H, Lauring J, Garay JP, Karakas B, Abukhdeir AM, et al. (2007) A PCR-based high-throughput screen with multiround sample pooling: application to somatic cell gene targeting. Nat Protoc 2: 2865-2874.

Figure Legends

Figure 1. Reporter substrate for analysis of NHEJ

A cartoon of the reporter construct (pEGFP-Pem1-Ad2). (A) The construct is essentially a GFP cassette whose expression is driven by CMV promoter and terminated by the SV40 polyA sequence. "G" is separated from "FP" by a 2.4 kb intron containing an exon (Ad) from adenovirus that is flanked by *HindIII* and *I-SceI* restriction sites. Splice donor (SD) and splice acceptor (SA) sites are shown. (B) Restriction sites used to introduce DNA DSBs. Digestion with *HindIII* generates compatible cohesive ends. Because *I-SceI* has a nonpalindromic 18-bp recognition site, cleavage of the two inverted *I-SceI* sites generates incompatible ends. (C) Due to the presence of the Ad-exon into the middle of the Pem1 intron, the Ad exon is efficiently spliced into the middle of the GFP ORF, inactivating the GFP activity and thus making the starting substrate GFP negative. Both sides of the Ad exon have *HindIII/I-SceI* restriction sites. Cleavage with either of these endonucleases removes the Ad exon and upon successful intracellular plasmid circularization GFP expression is restored and can be quantitated by flow cytometry.

Figure 2. NHEJ in the parental HCT116 and C-NHEJ mutant (heterozygous) cell lines

The indicated cell lines were transfected with *HindIII*- (Top panels) or *I-SceI*- (Bottom panels) linearized pEGFP-Pem1-Ad2 together with a supercoiled pCherry plasmid (to monitor transfection efficiency). The number in the top right corner corresponds to the percentage of cells that turned green after 24 hr as a percentage of the cells productively transfected.

Figure 3. The impact of C-NHEJ mutations on end joining

Four independent experiments comparable to those depicted in Figures 2 and 4 were performed and the average percent repair relative to wild type is shown with the standard deviation.

Figure 4. The loss of C-NHEJ greatly reduces end joining

The indicated cell lines were transfected with *HindIII*- (Top panels) or I-*SceI*- (Bottom panels) linearized pEGFP-Pem1-Ad2 plasmid together with a pCherry plasmid. The cells were analyzed by FACS 24 hr post transfection. The number of cells that were doubly EGFP (horizontal) and pCherry (vertical) positive versus the number that were pCherry positive was determined. For a given experiment the data are shown as percent repair in the upper right-hand corner of each plot.

Figure 5. Ku86-null cells show wild-type levels of end joining activity

(A) Western blot analysis shows that the expression of Cre (AdCre) in $Ku86^{flox/-}$ cells results in the reduction of Ku86 expression. AdCMV is a negative control adenoviral vector. (B) the indicated cell lines were transfected with either HindIII- (Top panels) or I-SceI- (bottom panels) linearized pEGFP-Pem1-Ad2 plasmid. All symbols are as in Figure 4.

Figure 6. The absence of Ku86 results in predominately microhomology-based end joining

(A) *HindIII*-linearized pEGFP-Pem1-Ad2 plasmids were recovered from either WT HCT116, Ku86$^{+/-}$ or Ku86$^{-/-}$ cells, propagated through *E. coli* and then analyzed for retention of a single *HindIII* restriction site ("perfect rejoining") by *HindIII* restriction enzyme digestion analysis. The asterisks indicate those plasmids where perfect rejoining occurred. (B) The results of four or more experiments similar to those depicted in (A) were combined and summarized. *N.B*. The re-expression of a WT DNA-PK$_{cs}$ or XLF cDNA (+cDNA) in their respective null cell lines reduced the frequency of perfect rejoining back to WT levels, confirming the specificity of the effect.

Figure 7. The reduction of Ku results in elevated levels of end joining in C-NHEJ mutant cell lines

(A) FACS profiles using the pEGFP-Pem1-Ad2 reporter substrate are shown for the indicated cell lines. The profiles for the Top and Bottom panels were generated using *HindIII*- and *I-SceI*-linearized plasmids, respectively. The percent of the substrate that was repaired is shown in the right-hand corner of each profile. (B) Western blot analyses demonstrate a reduction in Ku protein levels. Western blots for extracts derived from the indicated cell lines are shown using antibodies against either Ku86, Ku70 or (as a loading control) tubulin (Tub). Each of the blots was quantitated using a phosphoimager and the level of a particular Ku subunit relative to the amount expressed in the parental cell line is indicated below each blot. (C) Four independent experiments comparable to those depicted in panel A were performed and the average percent repair is shown with the standard deviation.

Figure 8. Independent confirmation of microhomology-mediated end joining in C-NHEJ mutant cell lines

(A) Reporter substrate biased for use by microhomology-directed NHEJ (A-NHEJ). The reporter has been designed such that cleavage with *Eco47III* and *EcoRV* results in a blunt-ended linear substrate with 6-bp direct repeats (boxes) at both ends. C-NHEJ joining will result in the retention of some of both repeats whereas A-NHEJ should generate a single repeat, which is a substrate for *BstXI*. This figure is excerpted from Verkaik *et al*., 2002, Eur. J. Immunol., 32:701. (B) The experimental scheme for analysis of the plasmids recovered from transfected cells. The plasmids were subjected to PCR using one radiolabeled (asterisk) primer. The PCR products were then subjected to *BstXI* restriction enzyme digestion. (C-F) Left Panels: Autoradiograms of representative microhomology assays using the indicated cell lines. The size of the primary PCR product (180 bp) and the *BstXI* cleavage product (120 bp) are indicated. Right Panels: Three independent experiments similar to the ones shown on the left were quantitated with a phosphoimager and averaged.

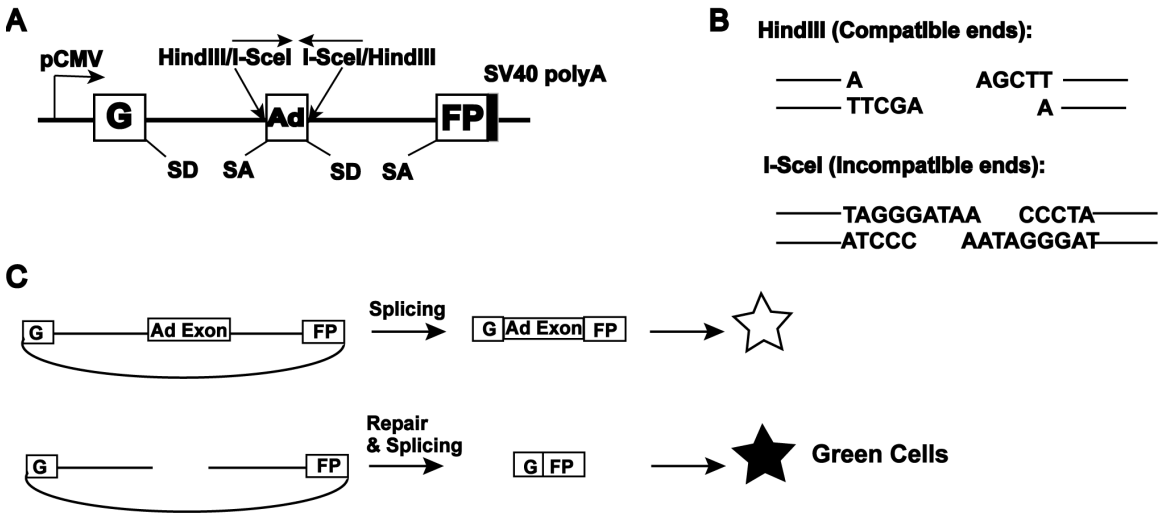
A
pCMV
HindIII/I-SceI
I-SceI/HindIII
SV40 polyA
G
Ad
FP
SD
SA
SD
SA
B
HindIII (Compatible ends):
A
AGCTT
TTCGA
A
I-SceI (Incompatible ends):
TAGGGATAA
CCCTA
ATCCC
AATAGGGAT
C
G
Ad Exon
FP
Splicing
G
Ad Exon
FP
G
FP
Repair
& Splicing
G
FP
Green Cells

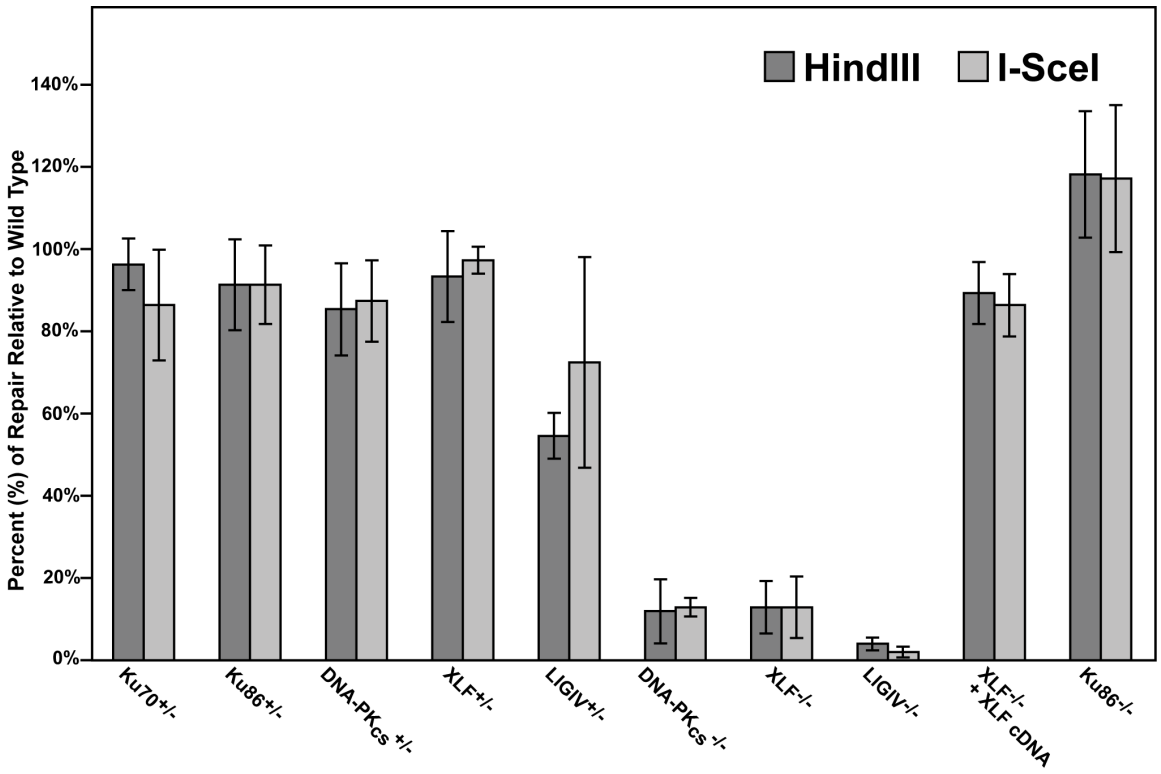
HindIII
I-SceI
Percent (%) of Repair Relative to Wild Type
140%
120%
100%
80%
60%
40%
20%
0%
Ku70+/-
Ku86+/-
DNA-PKcs +/-
XLF+/-
LIGIV+/-
DNA-PKcs -/-
XLF-/-
LIGIV-/-
XLF-/- + XLF cDNA
Ku86-/-

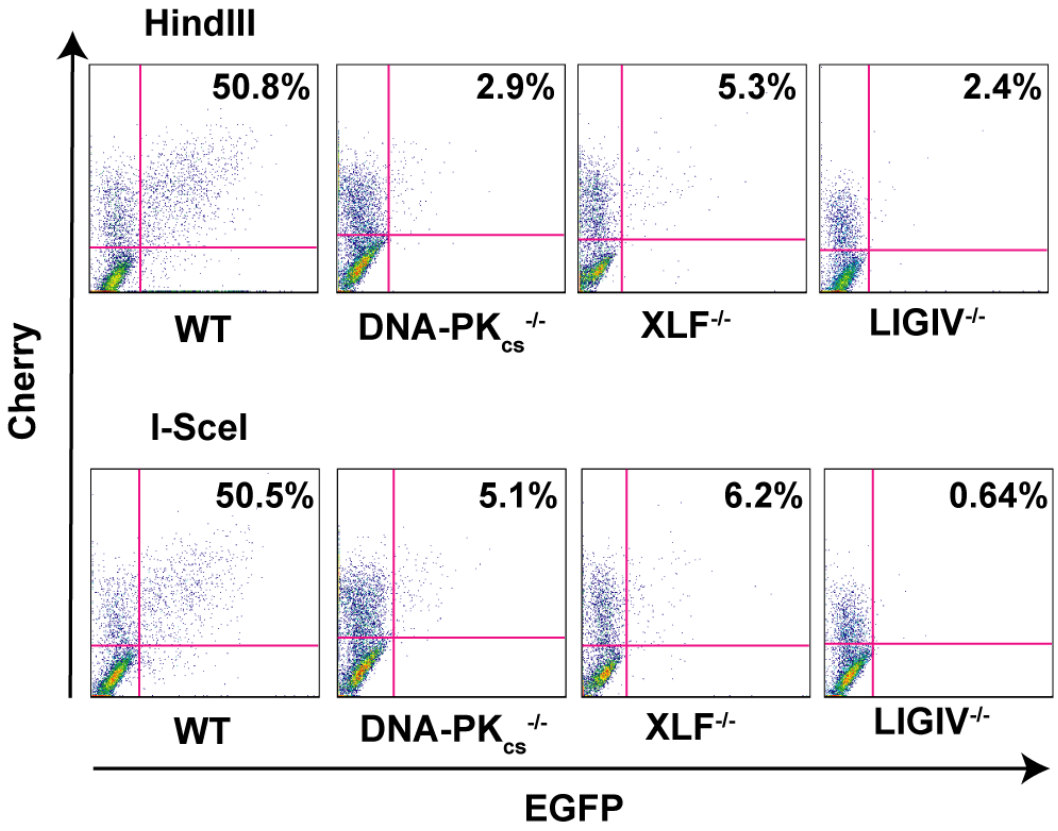
HindIII
50.8%
2.9%
5.3%
2.4%
WT
DNA-PKcs-/-
XLF-/-
LIGIV-/-
Cherry
I-SceI
50.5%
5.1%
6.2%
0.64%
WT
DNA-PKcs-/-
XLF-/-
LIGIV-/-
EGFP

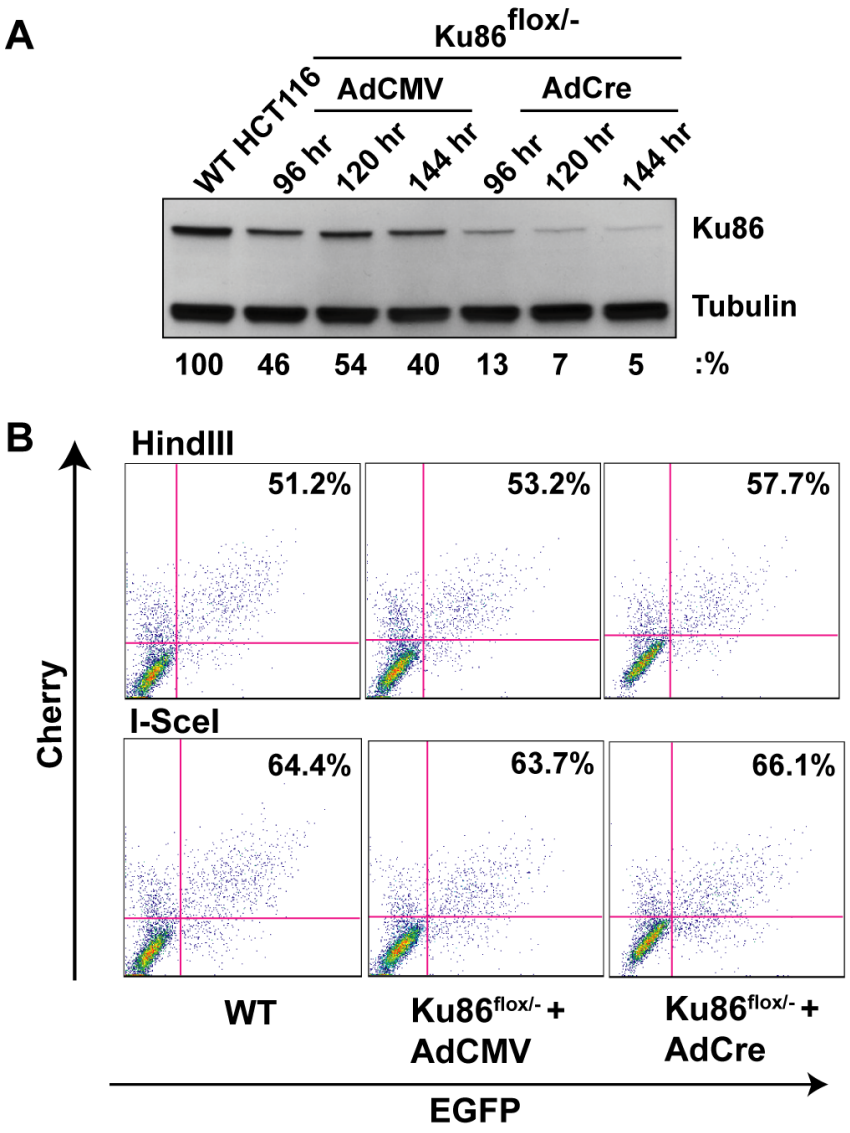
A
Ku86flox/-
AdCMV
AdCre
WT HCT116
96 hr
120 hr
144 hr
96 hr
120 hr
144 hr
Ku86
Tubulin
100 46 54 40 13 7 5 :%
B
HindIII
51.2%
53.2%
57.7%
I-SceI
64.4%
63.7%
66.1%
Cherry
WT
Ku86flox/- + AdCMV
Ku86flox/- + AdCre
EGFP

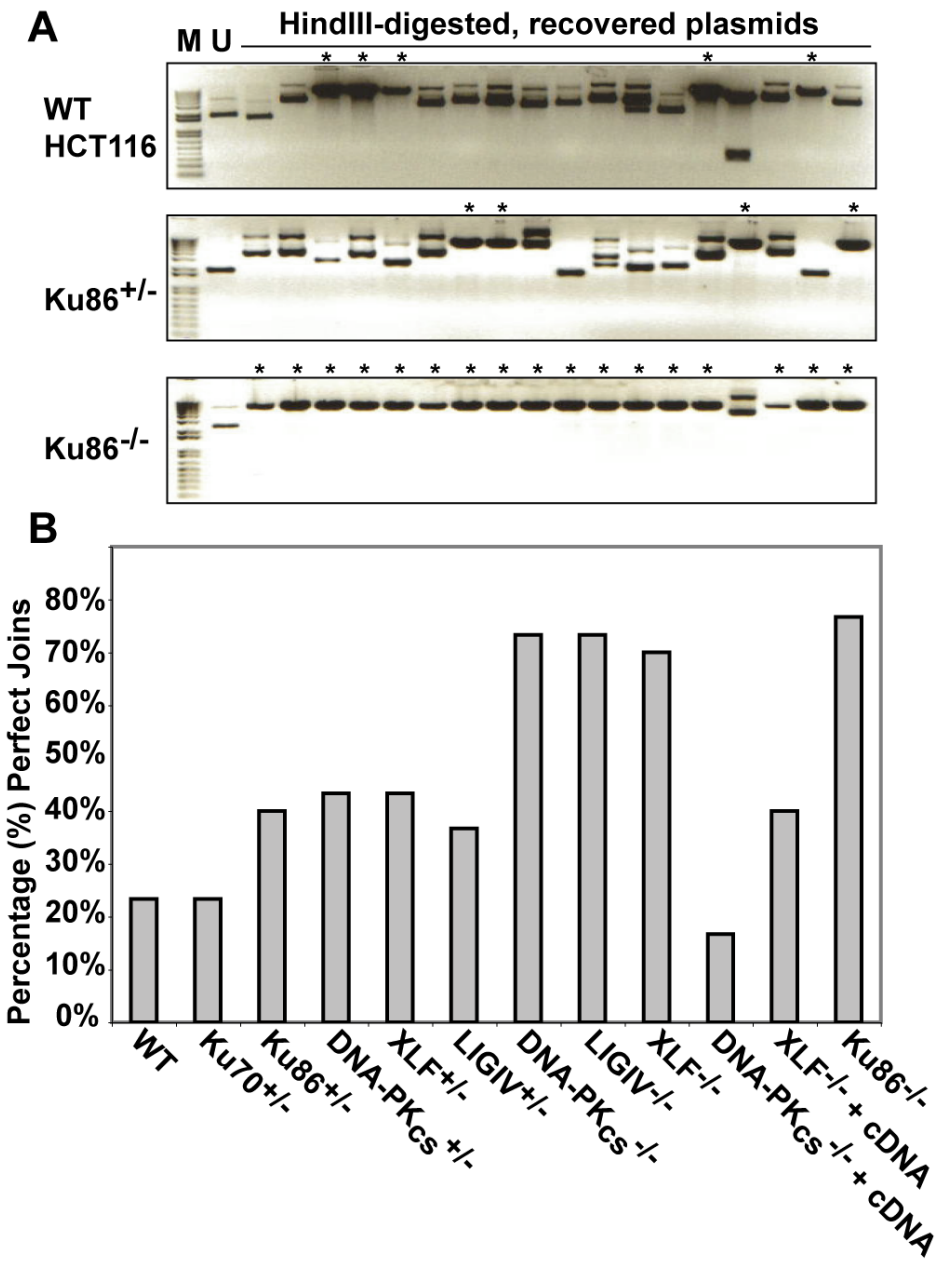
A
M U
HindIII-digested, recovered plasmids
WT HCT116
Ku86+/-
Ku86-/-
B
Percentage (%) Perfect Joins
80%
70%
60%
50%
40%
30%
20%
10%
0%
WT
Ku70+/-
Ku86+/-
DNA-PKcs +/-
XLF+/-
LIGIV+/-
DNA-PKcs -/-
LIGIV-/-
XLF-/-
DNA-PKcs -/- + cDNA
XLF-/- + cDNA
Ku86-/-

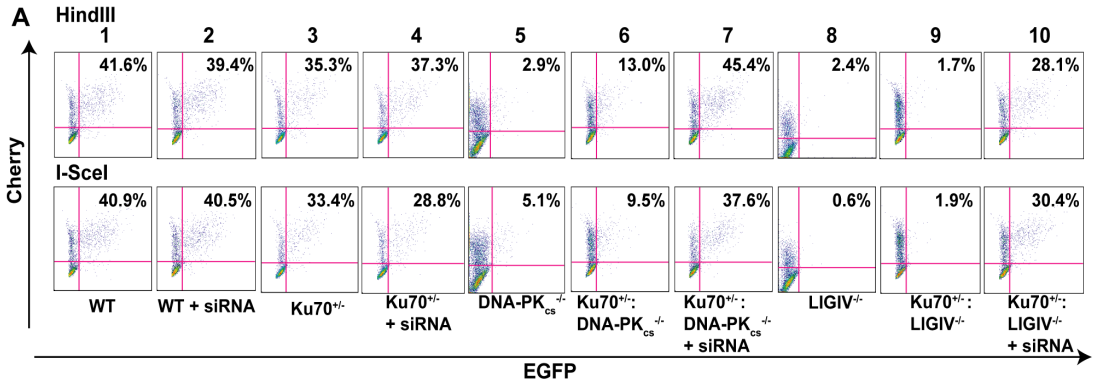
A
HindIII
1
2
3
4
5
6
7
8
9
10
41.6%
39.4%
35.3%
37.3%
2.9%
13.0%
45.4%
2.4%
1.7%
28.1%
I-SceI
40.9%
40.5%
33.4%
28.8%
5.1%
9.5%
37.6%
0.6%
1.9%
30.4%
Cherry
WT
WT + siRNA
Ku70+/-
Ku70+/- + siRNA
DNA-PKcs-/-
Ku70+/-: DNA-PKcs-/-
Ku70+/-: DNA-PKcs-/- + siRNA
LIGIV-/-
Ku70+/-: LIGIV-/-
Ku70+/-: LIGIV-/- + siRNA
EGFP

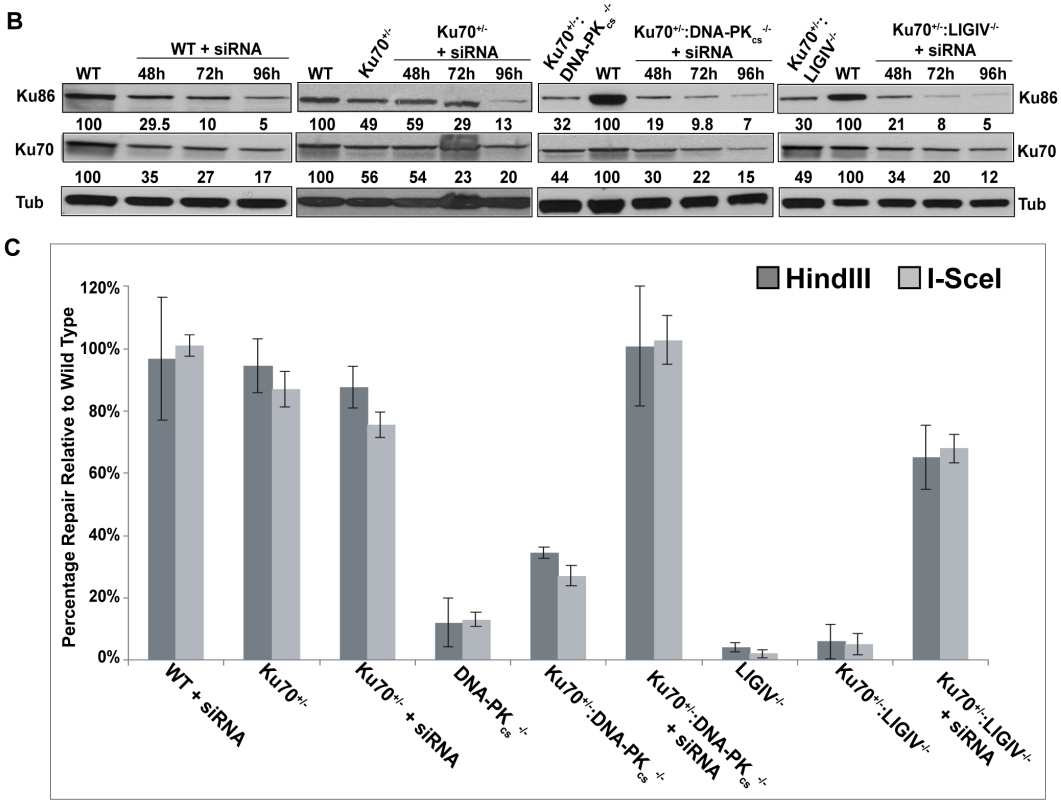
B
WT + siRNA
Ku70+/-
Ku70+/- + siRNA
Ku70+/-:DNA-PKcs-/-
Ku70+/-:DNA-PKcs-/- + siRNA
Ku70+/-:LIGIV-/-
Ku70+/-:LIGIV-/- + siRNA
WT 48h 72h 96h WT 48h 72h 96h WT 48h 72h 96h WT 48h 72h 96h WT 48h 72h 96h
Ku86
100 29.5 10 5 100 49 59 29 13 32 100 19 9.8 7 30 100 21 8 5
Ku70
100 35 27 17 100 56 54 23 20 44 100 30 22 15 49 100 34 20 12
Tub
C
HindIII
I-SceI
Percentage Repair Relative to Wild Type
120%
100%
80%
60%
40%
20%
0%
WT + siRNA
Ku70+/-
Ku70+/- + siRNA
DNA-PKcs-/-
Ku70+/-:DNA-PKcs-/-
Ku70+/-:DNA-PKcs-/- + siRNA
LIGIV-/-
Ku70+/-:LIGIV-/-
Ku70+/-:LIGIV-/- + siRNA

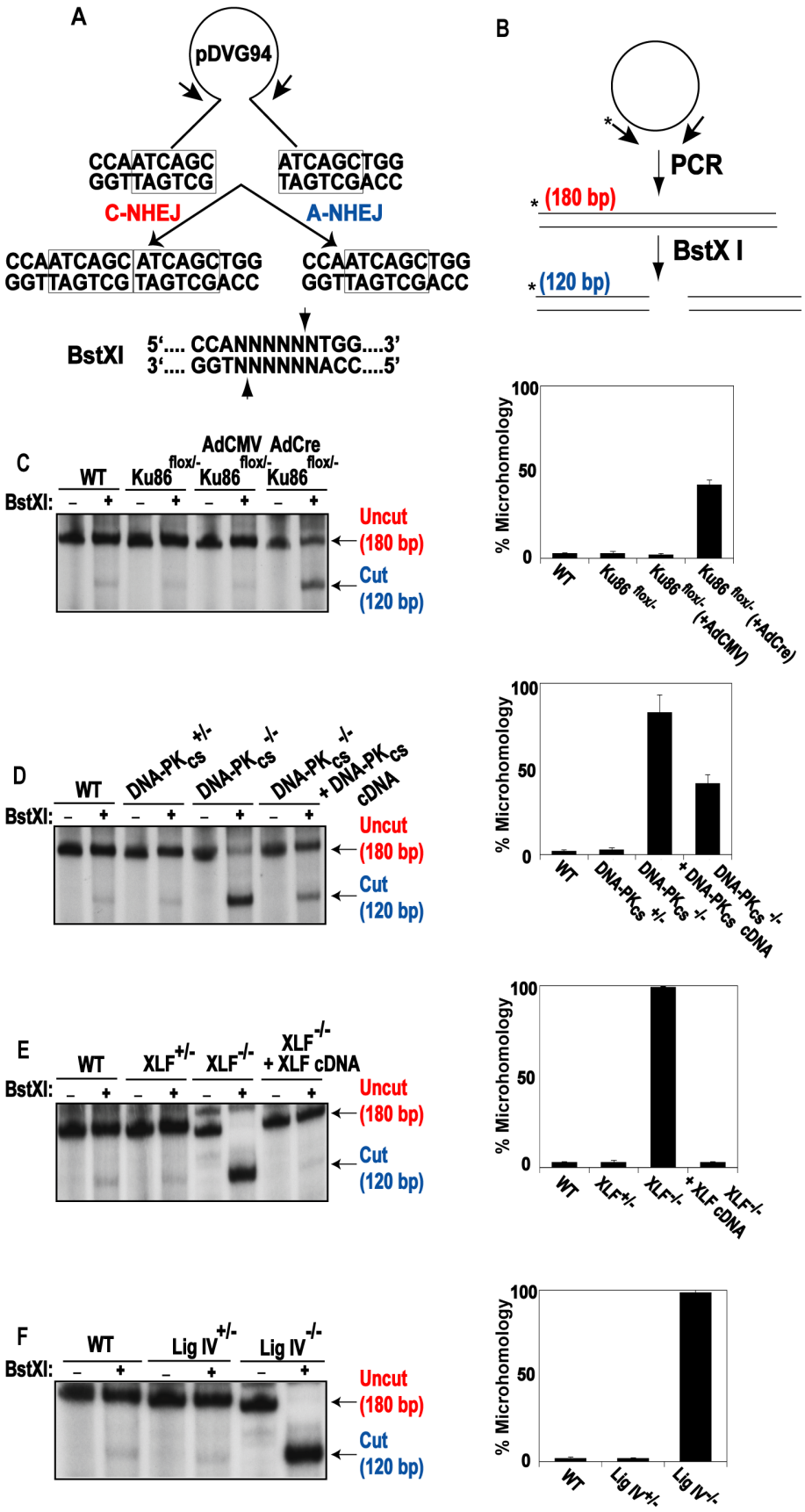
A
pDVG94
CCAATCAGC
GGTTAGTCG
ATCAGCTGG
TAGTCGACC
C-NHEJ
A-NHEJ
CCAATCAGC ATCAGCTGG
GGTTAGTCG TAGTCGACC
CCAATCAGCTGG
GGTTAGTCGACC
BstXI
5'.... CCANNNNNTGG....3'
3'.... GGTNNNNNACC....5'
B
PCR
* (180 bp)
BstX I
* (120 bp)
C
AdCMV AdCre
WT
Ku86 flox/-
Ku86 flox/-
Ku86 flox/-
BstXI: – + – + – + – +
Uncut
(180 bp)
Cut
(120 bp)
% Microhomology
100
50
0
WT
Ku86 flox/-
Ku86 flox/- (+AdCMV)
Ku86 flox/- (+AdCre)
D
WT
DNA-PKcs +/-
DNA-PKcs -/-
DNA-PKcs -/- + DNA-PKcs cDNA
BstXI: – + – + – + – +
Uncut
(180 bp)
Cut
(120 bp)
% Microhomology
100
50
0
WT
DNA-PKcs +/-
DNA-PKcs -/-
+ DNA-PKcs cDNA
DNA-PKcs -/- cDNA
E
WT
XLF+/-
XLF-/-
XLF-/- + XLF cDNA
BstXI: – + – + – + – +
Uncut
(180 bp)
Cut
(120 bp)
% Microhomology
100
50
0
WT
XLF+/-
XLF-/-
+ XLF cDNA
XLF-/-
F
WT
Lig IV+/-
Lig IV-/-
BstXI: – + – + – +
Uncut
(180 bp)
Cut
(120 bp)
% Microhomology
100
50
0
WT
Lig IV+/-
Lig IV-/-

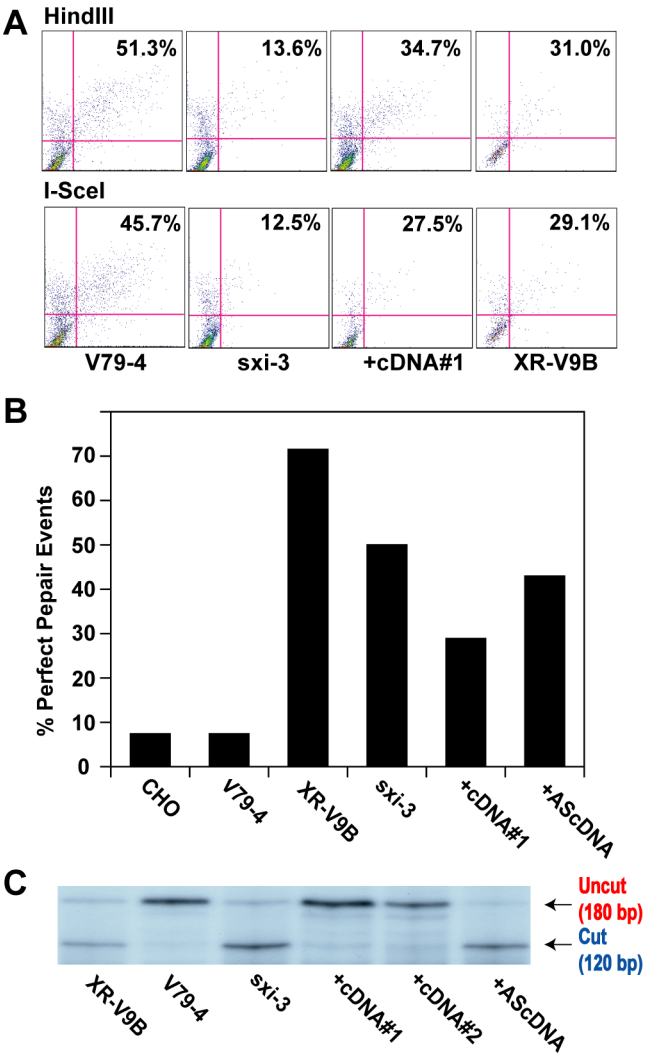
A
HindIII
51.3%
13.6%
34.7%
31.0%
I-SceI
45.7%
12.5%
27.5%
29.1%
V79-4
sxi-3
+cDNA#1
XR-V9B
B
% Perfect Pepair Events
0
10
20
30
40
50
60
70
CHO
V79-4
XR-V9B
sxi-3
+cDNA#1
+AScDNA
C
Uncut
(180 bp)
Cut
(120 bp)
XR-V9B
V79-4
sxi-3
+cDNA#1
+cDNA#2
+AScDNA

Supporting Figure Legends

Supporting Figure S1. Repair efficiency of heterozygous cell lines.

The indicated cell lines were transfected with HindIII- (Top panels) or I-SceI- (Bottom panels) linearized pEGFP-Pem1- Ad2 together with a supercoiled pCherry plasmid (to monitor transfection efficiency). The number in the top right corner corresponds to the percentage of cells that turned green after 24 hr as a percentage of the cells productively transfected.

Supporting Figure S2. Repair junction analysis of *HindIII* - linearized plasmids for perfect joins.

The data presented individually in Tables S1, S3, S5, and S7 using the HindIII-linearized pEGFP-Pem1-Ad2-lenearized plasmid was consolidated into 4 categories: perfect joins (dark rectangles), imperfect joins (light gray rectangles), microhomology (white rectangles), and insertions (dark gray rectangles) and is presented as the percentage of total events for each of the indicated cell lines.

Supporting Figure S3. Repair junction analysis of *I-SceI* - linearized plasmids for perfect joins.

The data presented individually in Tables S2, S4, S6, and S8 using the I-SceI-linearized pEGFP-Pem1-Ad2-lenearized plasmid was consolidated into 3 categories: imperfect joins (light gray rectangles), microhomology (white rectangles) and insertions (dark gray rectangles) and is presented as the percentage of total events for each of the indicated cell lines. N.B. Perfect joining is not possible with this substrate.

Supporting Figure S4. Sequence analysis of repair junctions of *HindIII* - linearized plasmids for deletions.

The data presented individually in Tables S1, S3, S5, and S7 using the *HindIII*-linearized pEGFP-Pem1-Ad2-lenearized plasmid was analyzed only for deletions. Each dot represents an individual data point and some dots overlap. The mean (dark rectangle) and the median (gray rectangle) are shown for each of the indicated cell lines.

Supporting Figure S5. Sequence analysis of repair junctions of *HindIII* - linearized plasmids for deletions.

The data presented individually in Tables S2, S4, S6, and S8 using the I-SceI-linearized pEGFP-Pem1-Ad2-lenearized plasmid was analyzed only for deletions. Each dot represents an individual data point and some dots overlap. The mean (dark rectangle) and the median (gray rectangle) are shown for each of the indicated cell lines.

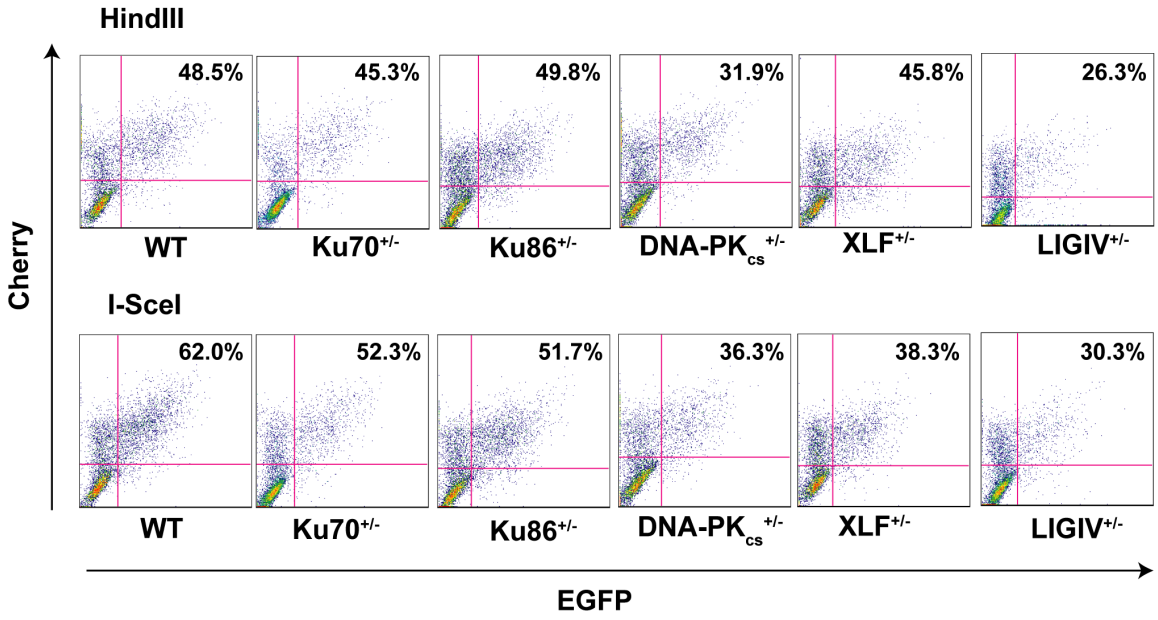
HindIII
48.5%
45.3%
49.8%
31.9%
45.8%
26.3%
WT
Ku70+/-
Ku86+/-
DNA-PKcs+/-
XLF+/-
LIGIV+/-
I-SceI
62.0%
52.3%
51.7%
36.3%
38.3%
30.3%
WT
Ku70+/-
Ku86+/-
DNA-PKcs+/-
XLF+/-
LIGIV+/-
Cherry
EGFP

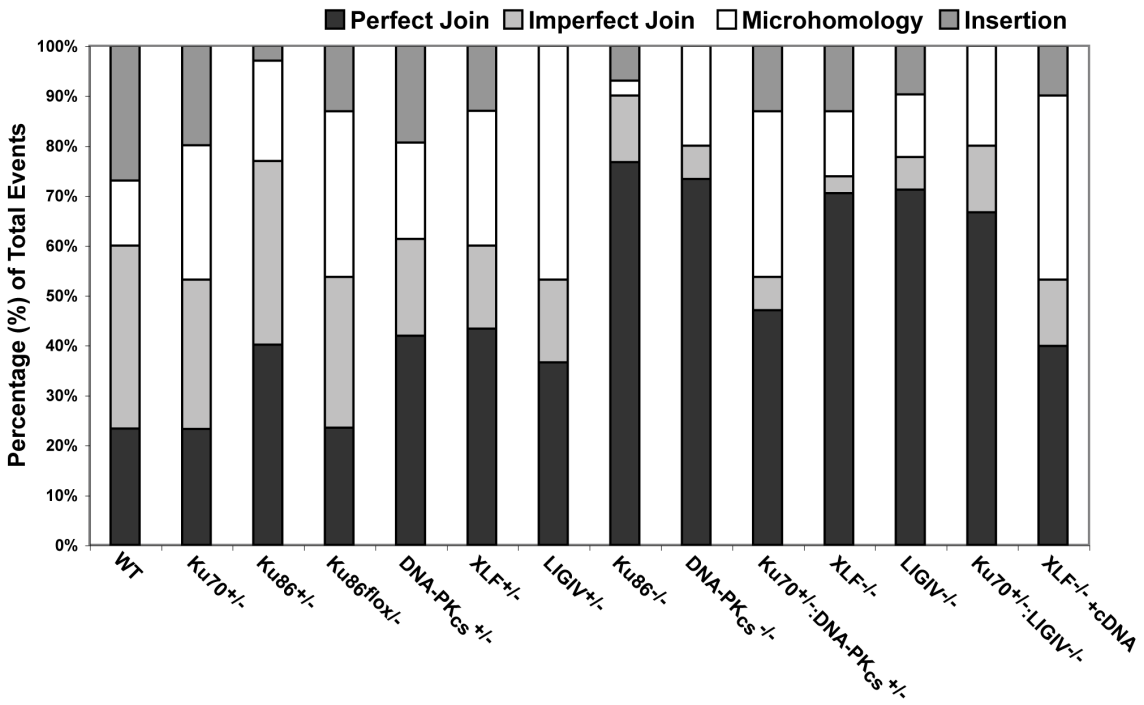
Perfect Join
Imperfect Join
Microhomology
Insertion
Percentage (%) of Total Events
100%
90%
80%
70%
60%
50%
40%
30%
20%
10%
0%
WT
Ku70+/-
Ku86+/-
Ku86flox/-
DNA-PKcs +/-
XLF+/-
LIGIV+/-
Ku86-/-
DNA-PKcs -/-
Ku70+/-:DNA-PKcs +/-
XLF-/-
LIGIV-/-
Ku70+/-:LIGIV-/-
XLF-/- +cDNA

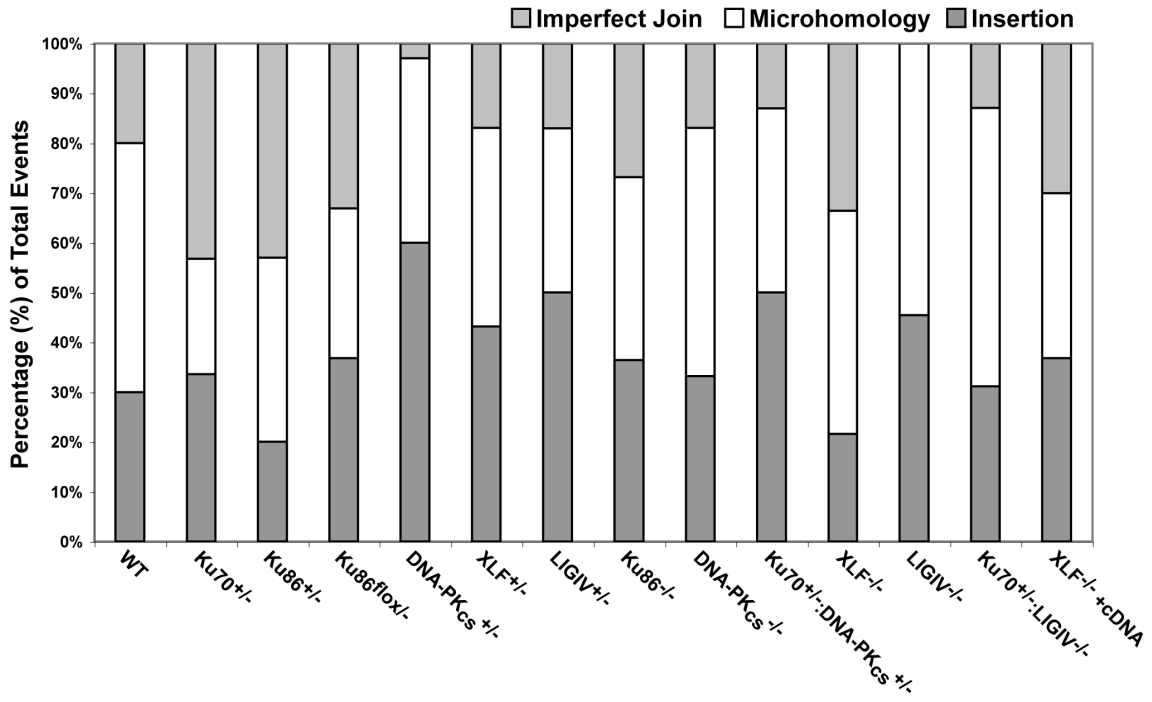
Imperfect Join
Microhomology
Insertion
Percentage (%) of Total Events
100%
90%
80%
70%
60%
50%
40%
30%
20%
10%
0%
WT
Ku70+/-
Ku86+/-
Ku86flox/-
DNA-PKcs +/-
XLF+/-
LIGIV+/-
Ku86-/-
DNA-PKcs -/-
Ku70+/-:DNA-PKcs +/-
XLF-/-
LIGIV-/-
Ku70+/-:LIGIV-/-
XLF-/- +cDNA

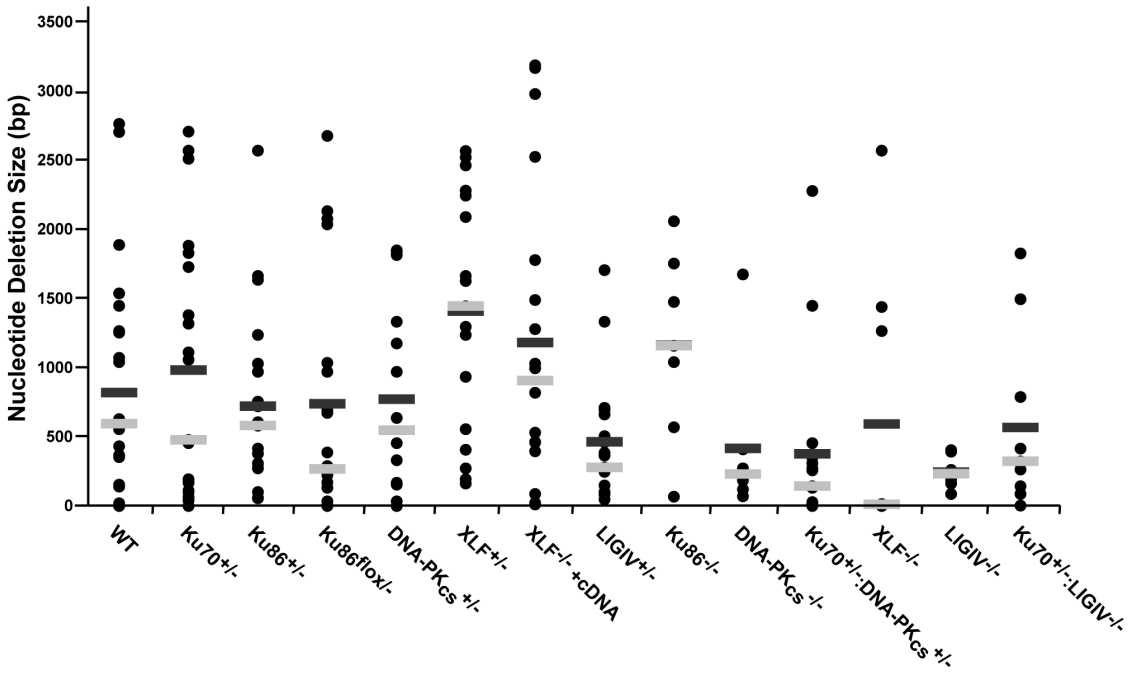
Nucleotide Deletion Size (bp)
3500
3000
2500
2000
1500
1000
500
0
WT
Ku70+/-
Ku86+/-
Ku86flox/-
DNA-PKcs +/-
XLF+/-
XLF-/- +cDNA
LIGIV+/-
Ku86-/-
DNA-PKcs -/-
Ku70+/-:DNA-PKcs +/-
XLF-/-
LIGIV-/-
Ku70+/-:LIGIV-/-

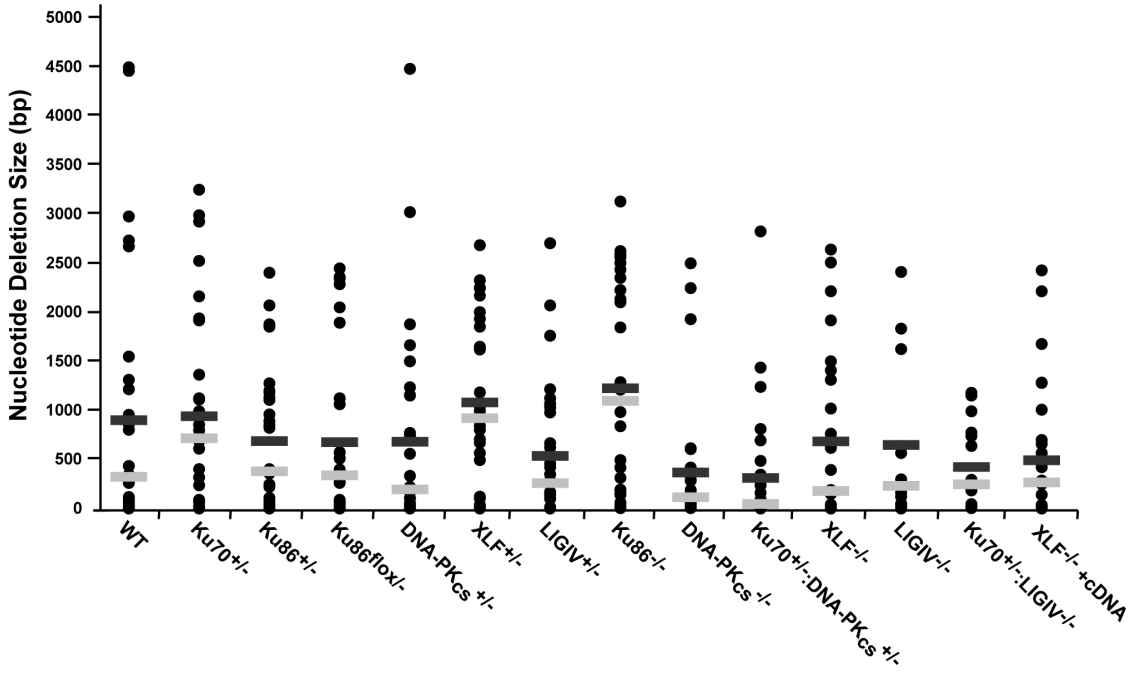
Nucleotide Deletion Size (bp)
5000
4500
4000
3500
3000
2500
2000
1500
1000
500
0
WT
Ku70+/-
Ku86+/-
Ku86flox/-
DNA-PKcs +/-
XLF+/-
LIGIV+/-
Ku86-/-
DNA-PKcs -/-
Ku70+/-:DNA-PKcs +/-
XLF-/-
LIGIV-/-
Ku70+/-:LIGIV-/-
XLF-/- +cDNA

Table S1. Sequence analysis for HindIII-linearized pEGFP-Pem1-Ad2 plasmids recovered from Ku-deficient cells

Supporting Table 1. Sequence analysis for *HindIII*-linearized pEGFP-Pem1-Ad2 plasmids recovered from Ku-deficient cells.

***HindIII* Data:**	del	WT	del	del	Ku70$^{+/-}$	del	del	Ku86$^{+/-}$	del	del	Ku86$^{flox/-}$	del	del	Ku86$^{-/-}$	del
	0	4 bp	0	0	4 bp	0				0	5 bp	0			
	0	5 bp	5	28	...	12				0	3 bp	5			
	6	...	0	14	**AgCAT**	34				9	**TG**	25			
	2	...	4	55	63 bp	12				53	**GG**	79			
	3	...	18	89	...	13	del	Ku86$^{+/-}$	del	109	...	61			
	43	...	97	27	73 bp	76	2	...	55	109	...	61			
	60	...	94	98	8 bp	13	2	...	55	94	**TGGc**	130			
	126	...	228	89	**GGGGG**	79	3	...	55	95	**TGG**	130			
	352	23 bp	17	1	**AAG**	186	34	...	68	61	...	164			
	53	2 bp	379	9	...	185	47	**AGGGgAAAGAg**	226	94	1 bp	133			
	253	**AGG**	304	167	...	287	163	...	140	120	**T**	133			
	256	...	339	177	...	300	197	**A**	111	147	**CTG**	114			
	368	**TT**	246	924	47 bp	134	172	...	207	133	...	156			
	337	3 bp	293	875	**C**	237	349	...	66	267	**CA**	119			
	746	...	296	248	**CC**	1072	149	**C**	431	248	**GCaACC**	427			
	352	18 bp	720	674	...	708	290	**GGATtGtGC**	317	347	11 bp	345	del	Ku86$^{-/-}$	del
	369	5 bp	887	1455	...	274	453	**G**	302	668	...	304	62	...	4
	823	...	443	629	**CC**	1202	668	...	304	361	...	676	234	75 bp	335
	51	**GGG**	698	1878	...	4	1002	...	127	4	**T**	2033	214	...	828
	699	...	838	2368	...	223	881	77 bp	358	410	...	1667	830	**GT**	328
	1884	**TG**	4	2354	**G**	217	1472	...	164	410	...	1667	1441	35 bp	36
	352	93 bp	2355	2354	**G**	217	1569	...	95	334	**A**	1800	0	...	1754
	337	...	2428	353	68 bp	2355	2354	**G**	217	2504	...	175	244	...	1815
AVERAGE:	**325**		**465**	**646**		**341**	**545**		**183**	**286**		**452**	**432**		**729**
Total Deletion Average:		**820**			**984**			**723**			**739**			**1161**	
Total Deletion Median:		*595*			*477*			*498*			*267*			*1158*	
Percent Microhomology:		*13%*			*27%*			*20%*			*33%*			*3%*	
Percent Insertions:		*27%*			*20%*			*3%*			*13%*			*7%*	
Percent Perfect Joins:		**23%**			**23%**			**40%**			**23%**			**77%**	

Samples shown in the table do not include those that perfectly rejoined their ends as determined by *HindIII* restriction enzyme digestion and hence the variation in column entries across the indicated cell lines. The percentage of perfect joins within the 30 samples is shown in the last row. The nucleotide deletions (del) upstream (left column) and downstream (right column) are shown for each sample. The nucleotide deletion data are skewed to the downstream side so both the mean and the median of total nucleotide deletions are summarized below the individual sample data. Bold capital letters in the middle column describe microhomology sequences; the lower case letters show nucleotides that could not be accounted for. Numbers in the middle column represent the number of nucleotide insertions whereas 3 dots indicates that the plasmid was repaired without microhomology or insertions. The percentage of both microhomology and insertions are also summarized below the middle column. The 30 samples shown were randomly collected from three to six independent transfections.

Table S2. Sequence analysis for I-SceI-linearized pEGFP-Pem1-Ad2 plasmids recovered from Ku-deficient cells

Supporting Table 2. Sequence analysis for *I-SceI*-linearized pEGFP-Pem1-Ad2 plasmids recovered from Ku-deficient cells.

***I-SceI* Data:**	del	WT	del	del	Ku70$^{+/-}$	del	del	Ku86$^{+/-}$	del	del	Ku86$^{flox/-}$	del	del	Ku86$^{-/-}$	del
	2	...	0	2	3 bp	0	0	1 bp	0	0	...	0	4	...	0
	2	...	0	3	4 bp	0	1	1 bp	0	3	...	1	4	3 bp	0
	3	...	0	4	...	0	8	12 bp	5	4	4 bp	0	9	**AAGCTT**	5
	4	...	0	4	4 bp	0	9	**AAGCTT**	5	4	5 bp	0	18	**CC**	0
	9	**aAAGCTT**	4	7	7 bp	0	11	...	6	8	8 bp	0	4	...	26
	9	**AAGCTT**	5	16	...	9	26	...	6	17	...	0	44	2 bp	15
	9	155 bp	8	26	1 bp	0	27	33 bp	6	23	5 bp	0	139	...	0
	16	...	8	67	...	1	27	15 bp	8	7	40 bp	33	67	**GG**	85
	16	6 bp	10	8	**T**	67	54	1 bp	12	34	...	15	187	3 bp	0
	22	**TGT**	10	86	19 bp	2	1	1 bp	85	28	**T**	23	192	...	0
	41	**AA**	15	110	...	126	22	103 bp	85	56	...	7	208	**G**	103
	18	**C**	79	26	2 bp	289	204	**AC**	18	66	...	13	413	...	2
	58	97 bp	59	221	...	181	211	**AC**	18	1	3 bp	87	23	2 bp	470
	259	**CC**	1	139	6 bp	470	161	6 bp	85	124	**TG**	87	294	...	546
	168	**T**	145	599	...	85	163	...	195	273	257 bp	1	253	**T**	729
	69	...	260	366	16 bp	375	55	**CTT**	344	190	...	207	706	...	505
	168	**AT**	175	209	**AG**	589	816	**GCTTGTC**	7	286	4 bp	223	693	1 bp	583
	119	**GG**	315	240	1 bp	613	366	18 bp	483	286	**A**	226	693	1 bp	583
	388	35 bp	413	649	...	316	865	57 bp	24	289	**A**	223	1673	**C**	173
	165	**C**	693	87	3 bp	903	172	...	787	271	**CT**	298	1773	...	328
	59	**GGA**	844	92	117 bp	1017	351	...	755	271	**CCT**	298	2107	**G**	27
	681	**T**	275	769	...	353	769	...	353	243	**C**	331	1889	**CAAG**	336
	977	...	236	270	7 bp	1094	769	7 bp	361	228	...	834	994	**TGAAcCCA**	1355
	525	**TCA**	788	1705	**A**	210	276	**G**	908	769	...	353	748	...	1687
	617	...	931	1713	...	225	794	**GG**	405	399	**TCCA**	1492	2501	...	0
	2179	...	491	626	**T**	1534	30	**AC**	1247	227	6 bp	1822	199	63 bp	2361
	2613	...	117	67	**G**	2455	712	**C**	1142	196	...	2089	1436	**TGCTGCTGC**	1137
	1201	**T**	1773	548	**tTTT**	2374	1636	**A**	239	2343	...	0	1457	**TGCTGCTGC**	1137
	145	271 bp	4313	673	...	2315	195	**GG**	1872	61	141 bp	2297	2624	2 bp	0
	218	318 bp	4277	511	**G**	2738	100	130 bp	2302	54	**C**	2393	1283	...	1846
AVERAGE:	**359**		**542**	**328**		**611**	**294**		**392**	**225**		**447**	**755**		**468**
Total Deletion Average:		**900**			**939**			**686**			**672**			**1223**	
Total Deletion Median:		*321*			*713*			*379*			*336*			*1097*	
Percent Microhomology:		*47%*			*23%*			*37%*			*30%*			*37%*	
Percent Insertions:		*20%*			*43%*			*43%*			*33%*			*27%*	

All definitions are as described in Supporting Table 1.

Table S3. Sequence analysis for HindIII-linearized pEGFP-Pem1-Ad2 plasmids recovered from DNA-PKCS-deficient cells

Supporting Table 3. Sequence analysis for *HindIII*-linearized pEGFP-Pem1-Ad2 plasmids recovered from DNA-PK$_{CS}$-deficient cells.

***HindIII* Data:**

WT			DNA-PK$_{CS}^{+/-}$			DNA-PK$_{CS}^{-/-}$			Ku70$^{+/-}$:DNA-PK$_{CS}^{-/-}$		
del		**del**	**del**		**del**	**del**		**del**	**del**		**del**
0	4 bp	0	0	20 bp	0	55	...	15	0	4 bp	0
0	5 bp	5	1	...	0	41	**CCTT**	81	11	4 bp	0
6	...	0	23	...	12	105	**GCCTTG**	80	3	**CA**	9
2	...	4	42	**CT**	112	148	...	41	4	2 bp	12
3	...	18	56	...	100	47	**AGGGaAAAGAG**	226	19	...	9
43	...	97	56	...	100	142	**CCTGGAAAG**	267	92	**CCC**	40
60	...	94	52	**GA**	116	144	**CCTGGAA**	267	80	...	62
126	...	228	177	**CT**	154	676	**AC**	999	73	**GAGTGACC**	69
352	23 bp	17	268	**AGCAC**	187				73	**GAGTGGACC**	69
53	2 bp	379	173	5 bp	464				179	**GGCC**	79
253	**AGG**	304	668	...	304				47	**AGGGgAAAGAg**	226
256	...	339	668	...	304				189	**CA**	119
368	**TT**	246	352	21 bp	823				311	**CCC**	39
337	3 bp	293	698	**G**	302				286	**AGCAC**	187
746	...	296	1030	**G**	302				341	**CACCCCCA**	1108
352	18 bp	720	81	**A**	1735				2186	116 bp	94
369	5 bp	887	90	7 bp	1735						
823	...	443	757	2 bp	1088						
51	**GGG**	698	764	4 bp	1085						
699	...	838									
1884	**TG**	4									
352	93 bp	2355									
337	...	2428									
AVERAGE:	**325**	**465**	**292**		**479**	**170**		**247**	**243**		**133**
Total Deletion Average:	**820**		**771**			**417**			**375**		
Total Deletion Median:	*595*		*546*			*231*			*142*		
Percent Microhomology:	*13%*		20%			*20%*			*33%*		
Percent Insertions:	*27%*		20%			*0%*			*13%*		
Percent Perfect Joins:	**23%**		**43%**			**73%**			**47%**		

All definitions are as described in Supporting Table 1.

Table S4. Sequence analysis for I-SceI-linearized pEGFP-Pem1-Ad2 plasmids recovered from DNA-PK$_{CS}$-deficient cells

Supporting Table 4. Sequence analysis for *I-SceI*-linearized pEGFP-Pem1-Ad2 plasmids recovered from DNA-PK$_{CS}$-deficient cells.

***I-SceI* Data:**	del	WT	del	del	DNA-PK$_{CS}^{+/-}$	del	del	DNA-PK$_{CS}^{-/-}$	del	del	Ku70$^{+/-}$:DNA-PK$_{CS}^{-/-}$	del
	2	...	0	2	...	0	4	...	2	2	...	0
	2	...	0	2	...	0	6	...	1	2	...	0
	3	...	0	4	...	0	5	...	5	2	...	0
	4	...	0	2	...	5	7	162 bp	3	4	...	1
	9	**aAAGCTT**	4	9	**AAGCTT**	5	6	**AG**	6	3	**A**	4
	9	**AAGCTT**	5	15	...	0	9	**aAAGCTT**	4	5	...	3
	9	155 bp	8	17	...	0	9	**AAGCTT**	5	7	**TA**	3
	16	...	8	11	...	7	9	**AAGCTT**	5	4	...	6
	16	6 bp	10	21	...	0	17	...	0	5	...	6
	22	**TGT**	10	19	**C**	15	17	**CA**	13	17	...	0
	41	**AA**	15	21	...	13	23	...	21	17	...	0
	18	**C**	79	32	...	2	39	**AGA**	16	9	4 bp	14
	58	97 bp	59	21	**TT**	35	10	1 bp	67	8	8 bp	18
	259	**CC**	1	57	**CC**	46	60	...	47	22	...	16
	168	**T**	145	163	**C**	0	26	**CATGG**	82	24	...	19
	69	...	260	148	**CTG**	71	64	4 bp	49	19	**C**	28
	168	**AT**	175	193	...	139	55	**T**	67	15	**GTTTCtAAG**	33
	119	**GG**	315	4	...	330	114	**TGGtTTC**	31	48	**C**	19
	388	35 bp	413	397	**A**	159	87	**GAGTGACC**	75	74	...	19
	165	**C**	693	425	...	318	123	...	67	87	**gGGAGTGACC**	74
	59	**GGA**	844	371	**T**	400	60	**G**	223	180	...	57
	681	**T**	275	191	...	570	61	**AGGGgAAAGAc**	232	161	**G**	77
	977	...	236	879	**C**	273	159	1 bp	208	158	**CCTGGaA**	134
	525	**TCA**	788	879	...	274	206	**GCAcAGGGc**	208	288	**GT**	55
	617	...	931	1229	**GCTTG**	7	249	**T**	167	6	4 bp	481
	2179	...	491	1177	**GA**	324	331	...	275	388	**T**	305
	2613	...	117	823	32 bp	835	11	**C**	602	195	...	614
	1201	**T**	1773	754	...	1123	835	...	1093	641	**CTTCCCAC**	597
	145	271 bp	4313	657	...	2361	2038	...	209	148	13 bp	1289
	218	318 bp	4277	47	...	4431	135	92 bp	2361	2614	...	208
AVERAGE:	**359**		**542**	**286**		**391**	**159**		**205**	**172**		**136**
Total Deletion Average:		**900**			**677**			**364**			**308**	
Total Deletion Median:		*321*			*191*			*111*			*45*	
Percent Microhomology:		*47%*			*37%*			*50%*			*37%*	
Percent Insertions:		*20%*			*3%*			*17%*			*13%*	

All definitions are as described in Supporting Table 1.

Table S5. Sequence analysis for HindIII-linearized pEGFP-Pem1-Ad2 plasmids recovered from XLF-deficient cells

Supporting Table 5. Sequence analysis for *HindIII*-linearized pEGFP-Pem1-Ad2 plasmids recovered from XLF-deficient cells.

***HindIII* Data:**

del	WT	del
0	4 bp	0
0	5 bp	5
6	...	0
2	...	4
3	...	18
43	...	97
60	...	94
126	...	228
352	23 bp	17
53	2 bp	379
253	**AGG**	304
256	...	339
368	**TT**	246
337	3 bp	293
746	...	296
352	18 bp	720
369	5 bp	887
823	...	443
51	**GGG**	698
699	...	838
1884	**TG**	4
352	93 bp	2355
337	...	2428
AVERAGE: 325		**465**

del	$XLF^{+/-}$	del
110	**CTTG**	53
138	**GAA**	56
174	...	98
3	**CCA**	405
253	**AGG**	304
309	...	626
352	16 bp	885
255	**TGA**	1041
488	...	958
688	**TTCAaGT**	941
828	32 bp	835
1910	8 bp	181
2242	**C**	2
701	**AACC**	1580
719	4 bp	1745
639	...	1883
274	...	2293
593		**817**

del	$XLF^{-/-}$	del
0	7 bp	0
0	29 bp	9
0	**A**	10
0	29 bp	10
4	11 bp	7
8	**TT**	6
823	...	443
341	**CCA**	1099
2354	**G**	217
392		**200**

del	$XLF^{-/-}$ +cDNA	del
3	**CA**	9
4	1 bp	11
15	**ACA**	8
4	**TGTTTCC**	84
356	...	41
450	**GA**	11
223	**TT**	240
182	**G**	348
515	...	305
23	**A**	972
509	**CTCAgA**	520
1151	**C**	129
1455	49 bp	36
1701	1 bp	79
725	**C**	1801
817	**T**	2164
737	...	2432
751	...	2438
535		**646**

	WT	$XLF^{+/-}$	$XLF^{-/-}$	$XLF^{-/-}$ +cDNA
Total Deletion Average:	**820**	**1410**	**592**	**1181**
Total Deletion Median:	*595*	*1446*	*11*	*908*
Percent Microhomology:	*13%*	*27%*	*13%*	*37%*
Percent Insertions:	*27%*	*13%*	*13%*	*10%*
Percent Perfect Joins:	**23%**	**43%**	**70%**	**40%**

All definitions are as described in Supporting Table 1.

Table S6. Sequence analysis for I-SceI-linearized pEGFP-Pem1-Ad2 plasmids recovered from XLF-deficient cells

Supporting Table 6. Sequence analysis for *I-SceI*-linearized pEGFP-Pem1-Ad2 plasmids recovered from XLF-deficient cells.

I-SceI Data:	del	WT	del	del	$XLF^{+/-}$	del	del	$XLF^{-/-}$	del	del	$XLF^{-/-}$ +cDNA	del
	2	...	0	2	...	0				0	...	0
	2	...	0	4	...	0				2	...	0
	3	...	0	4	...	0				2	...	0
	4	...	0	4	**G**	11	del	$XLF^{-/-}$	del	2	...	0
	9	**aAAGCTT**	4	17	**A**	6	0	2 bp	0	2	...	0
	9	**AAGCTT**	5	36	...	0	1	1 bp	0	2	3 bp	0
	9	155 bp	8	17	**T**	89	4	4 bp	0	4	4 bp	0
	16	...	8	106	**C**	0	9	**AAGCTT**	5	14	1 bp	0
	16	6 bp	10	119	11 bp	0	9	**AAGCTT**	5	18	4 bp	0
	22	**TGT**	10	301	...	191	9	**AAGCTT**	5	4	...	26
	41	**AA**	15	434	...	131	9	**AAGCTT**	5	29	**A**	4
	18	**C**	79	366	16 bp	304	9	**AAGCTT**	5	31	...	4
	58	97 bp	59	554	...	152	9	**AAGCTT**	5	55	**CCTT**	87
	259	**CC**	1	100	**CTGA**	702	17	...	24	105	**CCT**	143
	168	**T**	145	632	...	209	62	3 bp	85	248	**C**	0
	69	...	260	90	6 bp	903	154	**AG**	6	193	2 bp	85
	168	**AT**	175	353	**C**	691	87	**GAGTGACC**	75	192	6 bp	90
	119	**GG**	315	521	**A**	662	187	3 bp	0	3	**A**	279
	388	35 bp	413	1232	**ATAGgC**	387	366	16 bp	27	193	7 bp	90
	165	**C**	693	87	**C**	1552	267	...	350	352	...	68
	59	**GGA**	844	702	**TTCaTGT**	947	2	6 bp	619	194	**AGGC**	310
	681	**T**	275	607	**GG**	1242	259	143 bp	502	356	...	209
	977	...	236	838	3 bp	1093	708	...	311	118	10 bp	538
	525	**TCA**	788	1608	...	391	101	**TGGtCCTgCTG**	1212	548	**T**	149
	617	...	931	542	**gAATA**	1628	1193	361 bp	213	757	3 bp	250
	2179	...	491	2037	...	208	543	...	958	349	...	932
	2613	...	117	1040	3 bp	208	1705	**A**	210	868	...	415
	1201	**T**	1773	193	...	2131	1280	**AA**	935	353	**C**	1324
	145	271 bp	4313	208	...	2119	2292	...	214	2025	**GG**	187
	218	318 bp	4277	787	...	1894	192	**GAGGCCc**	2447	127	**C**	2300
AVERAGE:	**359**		**542**	**451**		**595**	**364**		**316**	**238**		**250**
Total Deletion Average:		**900**			**1080**			**680**			**488**	
Total Deletion Median:		*321*			*917*			*175*			*263*	
Percent Microhomology:		*47%*			*40%*			*40%*			*33%*	
Percent Insertions:		*20%*			*17%*			*30%*			*30%*	

All definitions are as described in Supporting Table 1.

Table S7. Sequence analysis for HindIII-linearized pEGFP-Pem1-Ad2 plasmids recovered from LIGIV-deficient cells

Supporting Table 7. Sequence analysis for *HindIII*-linearized pEGFP-Pem1-Ad2 plasmids recovered from LIGIV-deficient cells.

	del	WT	del	del	LIGIV$^{+/-}$	del	del	LIGIV$^{-/-}$	del	del	Ku70$^{+/-}$:LIGIV$^{-/-}$	del
***HindIII* Data:**	0	4 bp	0							3	...	0
	0	5 bp	5							4	**TGTTTCC**	84
	6	...	0							80	...	62
	2	...	4	42	**T**	6				38	**AGGGAAAAGAG**	226
	3	...	18	31	**T**	54				0	...	320
	43	...	97	39	**GA**	62				274	...	49
	60	...	94	87	**TTCTG**	63				269	**TGAGCA**	145
	126	...	228	46	**gcatAgGGaGAAAGAGg**	202				336	**CCCc**	454
	352	23 bp	17	213	**A**	57				29	**TGCATTCT**	1466
	53	2 bp	379	47	**AGGGgAAAGAg**	226				1100	**CTA**	728
	253	**AGG**	304	48	**AGGGgAAAGA**	226						
	256	...	339	50	**AGGGGAAA**	226						
	368	**TT**	246	47	**AAAGAg**	231						
	337	3 bp	293	140	**aggGgAAAGAg**	226						
	746	...	296	147	...	237	4	**TGTTTCC**	84			
	352	18 bp	720	457	...	3	83	1 bp	79			
	369	5 bp	887	258	**C**	247	70	184 bp	118			
	823	...	443	137	...	525	132	...	79			
	51	**GGG**	698	342	...	355	167	**TTTCCC**	86			
	699	...	838	551	**AT**	158	192	**GCAcAGGGc**	202			
	1884	**TG**	4	1030	**G**	302	192	...	11			
	352	93 bp	2355	333	...	1373						
	337	...	2428									
AVERAGE:	**325**		**465**	**213**		**252**	**127**		**93**	**213**		**353**
Total Deletion Average:		**820**			**464**			**243**			**567**	
Total Deletion Median:		*595*			*278*			*211*			*326*	
Percent Microhomology:		*13%*			*47%*			*10%*			*20%*	
Percent Insertions:		*27%*			*0%*			*7%*			*0%*	
Percent Perfect Joins:		**23%**			**37%**			**77%**			**67%**	

All definitions are as described in Supporting Table 1.

Table S8. Sequence analysis for I-SceI-linearized pEGFP-Pem1-Ad2 plasmids recovered from LIGIV-deficient cells

Supporting Table 8. Sequence analysis for *I-SceI*-linearized pEGFP-Pem1-Ad2 plasmids recovered from LIGIV-deficient cells.

***I-SceI* Data:**

	del	WT	del
	2	...	0
	2	...	0
	3	...	0
	4	...	0
	9	**aAATCTT**	4
	9	**AAGCTT**	5
	9	155 bp	8
	16	...	8
	16	6 bp	10
	22	**TGT**	10
	41	**AA**	15
	18	**C**	79
	58	97 bp	59
	259	**CC**	1
	168	**T**	145
	69	...	260
	168	**AT**	175
	119	**GG**	315
	388	35 bp	413
	165	**C**	693
	59	**GGA**	844
	681	**T**	275
	977	...	236
	525	**TCA**	788
	617	...	931
	2179	...	491
	2613	...	117
	1201	**T**	1773
	145	271 bp	4313
	218	318 bp	4277
AVERAGE:	**359**		**542**

	del	LIGIV$^{+/-}$	del
	0	...	0
	0	...	0
	1	1 bp	0
	1	1 bp	0
	2	...	0
	4	...	0
	4	**G**	7
	4	**G**	11
	3	...	14
	82	**AC**	18
	5	**GG**	103
	88	...	54
	4	...	154
	136	**G**	33
	192	...	65
	191	1 bp	67
	60	**G**	223
	104	3 bp	243
	293	...	129
	366	18 bp	90
	213	...	409
	325	...	339
	228	**CC**	749
	1010	...	19
	890	...	178
	17	**CCA**	1105
	351	**CC**	922
	792	...	967
	1277	...	792
	2320	**TtTAT**	384
AVERAGE:	**299**		**236**

	del	LIGIV$^{-/-}$	del
	2	...	0
	9	**AAGCTT**	5
	22	**TGT**	10
	15	**GTTTCcAAG**	33
	48	...	74
	87	**GAGTGACC**	75
	241	14 bp	57
	356	...	211
	304	...	332
	942	...	681
	108	**TCAgGGC**	1726
	618	**AAGaACT**	1791
AVERAGE:	**229**		**416**

	del	Ku70$^{+/-}$:LIGIV$^{-/-}$	del
	3	...	0
	9	**AAGCTT**	5
	17	...	0
	18	**CC**	1
	0	19 bp	43
	99	**CCTTgTgaC**	87
	104	...	85
	105	**CCCT**	95
	6	**TAG**	285
	61	**AGGGaAAAGAc**	232
	304	...	332
	739	**CcCtAAAGC**	0
	467	**G**	308
	682	...	310
	879	**C**	273
	879	26 bp	300
AVERAGE:	**273**		**147**

	WT	LIGIV$^{+/-}$	LIGIV$^{-/-}$	Ku70$^{+/-}$:LIGIV$^{-/-}$
Total Deletion Average:	**900**	**533**	**646**	**421**
Total Deletion Median:	*321*	*258*	*230*	*246*
Percent Microhomology:	*47%*	*33%*	*50%*	*56%*
Percent Insertions:	*20%*	*17%*	*0%*	*13%*

All definitions are as described in Supporting Table 1.

CHAPTER IV:
Final Discussion and Future Directions

Final Discussion

CtIP, EXO1, and DNA2 are essential genes in human cells

DNA resection is a highly conserved biological process that generates ssDNA from dsDNA, and is catalyzed by nucleases. DNA resection is a critical process that links DNA damage to cell cycle checkpoint activation, which is key to the survival and fitness of an organism[1]. Furthermore, DNA resection is required for HR[2] and for generating the ssDNA that forms protective t-loops at the ends of telomeres[3]. Notably, hypomorphic CtIP mutations in humans have been identified in patients with Seckel or Jawad syndrome who suffer from microcephaly and growth retardation[4]. The majority of studies on human CtIP, EXO1 and DNA2 have depended on siRNA knockdowns and only addressed gene function in the context of DSB repair responding to exogenous DNA damaging agents[5-12]. Although these studies have significantly contributed to the field, they fail to address if these genes are essential in human cells and if so what their essential function(s) in an unperturbed cell may be. Therefore, we constructed CtIP$^{F/-}$:CreERt2, EXO1$^{F/-}$:CreERt2, and DNA2$^{F/-/-}$:CreERt2 conditionally-null human somatic HCT116 cell lines that are also equipped with a CreERt2, tamoxifen-inducible system.

My initial postulation was that CtIP and EXO1 would not be essential genes because humans with hypomorphic CtIP mutations and EXO1 knockout mice are viable. With this information, it seemed safe to assume that human cells would survive without CtIP or EXO1, and I attempted to construct CtIP$^{-/-}$ and EXO1$^{-/-}$ null

human cell lines as models for my study. After targeting the first allele, my attempts to target the second allele of either CtIP or EXO1 only resulted in retargeting of the initially targeted allele such that one WT allele always remained. The strong disequilibrium in favor of retargeting strongly suggested that CtIP and EXO1 were essential. Therefore, I had to reconfigure my approach and construct conditionally-null cell lines for these genes. With the CtIP$^{F/-}$:CreERt2 and EXO1$^{F/-}$:CreERt2 cell lines, I found that these cells could not survive in the presence of tamoxifen. This data was completely consistent with my initial observation that CtIP and EXO1 are essential genes.

We and our collaborators, Dr. Judith Campbell and Sheila Stewart of California Institute of Technology and Washington University in St. Louis, respectively, greatly desired a DNA2-null cell line for similar studies. Learning the fates of my CtIP- and EXO1- gene targeting studies, I decided to directly construct a DNA2 conditionally-null cell line. Unfortunately, I was delayed in generating this cell line because DNA2 turned our to be triploid in the HCT116 cell line. HCT116 is often used for gene targeting studies because it is diploid, but it does carry several small chromosomal duplications. Unfortunately the DNA2 locus falls into one of these intervals.

Ultimately, I constructed a DNA2$^{F/-/-}$:CreERt2 cell line. Like CtIP and EXO1, DNA2 conditionally-null cells did not proliferate in the presence of tamoxifen. Due to the delay in cell line construction, I was not able to investigate DNA2 as extensively as CtIP and EXO1.

The HCT116 cell line is mismatch repair deficient due to a null mutation in MLH1[13]. This raised a concern that the lethality of CtIP and EXO may be synthetic with MLH1, which would mean any data produced from this study would be cell line specific and less generally biologically, relevant. Therefore, I constructed $CtIP^{F/-}$:CreERt2 and $EXO1^{F/-}$:CreERt2 cell lines that stably expressed a complementing wild-type MLH1 cDNA. With these cells, I was able to show that MLH1-expressing HCT116 cells still cannot survive without CtIP and EXO1. Additionally, I have preliminary data demonstrating that DNA2 is also not synthetically lethal with MLH1. In toto, CtIP or EXO1 is clearly not synthetically lethal with the absence MLH1, and consequently any results are not cell line specific.

My novel findings show that CtIP, EXO1, and DNA2 are essential genes in human cells. This data clearly suggest that either DNA resection is an essential activity in human cells or that CtIP, EXO1 and DNA2 have other functions required to keep cells alive. While it is clear that the inactivation of CtIP, EXO1, and DNA2 with tamoxifen results in cell death, an advantage of my experimental system is that the cells die slowly and a generous window of time was available for me to investigate the novel phenotypes.

The inactivation of CtIP and EXO1 with tamoxifen, resulted in very similar severe phenotypes. In general, I acquired data after 1, 3, 5, and/or 7 days after tamoxifen treatment such that a temporal view of the phenotypes could be acquired after the inactivation of expression CtIP or EXO1. Importantly, the findings here were observed in unperturbed cells without any exposure to DNA damaging agents.

The essential functions of CtIP and EXO1

After inactivating CtIP and EXO1, I initially found that p53 levels were highly elevated, which is consistent with many studies that show that CtIP and EXO1 is required for genome stability[5,9,10]. Extending this study, I found elevated levels of chromosomal breaks, fragmentations, radial chromosomes, and extreme aneuploidy in CtIP- and EXO1-null cells. Furthermore, during the analysis we noticed many fusion events but their complex structures were too difficult to analyze and thus they were omitted from the dataset. The more compelling aspect of our study is the $CtIP^{F/-}$:CreERt2 and $EXO1^{F/-}$:CreERt2 cells were never exposed to DNA damaging agents. It is clear that the genetic inactivation of CtIP or EXO1 triggers severe DNA damage in an unperturbed cell.

In unperturbed cells, DNA replication is the major source of DNA damage[14,15], which led me to hypothesize that the loss of CtIP and EXO1 was affecting DNA replication such that it leads to severe DNA damage. Therefore, I carried out several DNA replication assays to test my hypothesis.

With the EdU incorporation assay, I was able to acquire a temporal view of cell-cycle profiles after inactivating CtIP or EXO1 with tamoxifen. I found that the inactivation of CtIP and EXO1 triggered continuous DNA replication initiation and DNA synthesis. The continuous DNA synthesis resulted in extremely high DNA content, which was consistent with the aneuploid cells found in the karyotype analysis. Extending this study, I performed DNA fiber assays on CtIP- and EXO1-null cells to measure DNA replication tract lengths as a measure of DNA replication fork progression or velocity. The inactivation of CtIP and EXO1 resulted in severely

shortened replication tract lengths over time. These findings strongly indicated that CtIP and EXO1 are directly involved in DNA replication. In retrospect, this is probably not surprising since CtIP and EXO1 have a PIP box domain that interacts with PCNA.

From the immunofluorescence and chromatin fractionation experiments, I found that the inactivation of CtIP and EXO1 triggered severe DNA replication fork stalling. These stalled forks eventually collapsed into DSBs that were then repaired by NHEJ. In these cells I found elevated levels of FANCD2 and RPA nuclear foci, and chromatin recruitment. Additionally, I also found that modified PCNA accumulated to extremely high levels over time in the chromatin fractions. Together, these observations indicate that the inactivation of CtIP and EXO1 strongly triggers stalled replication forks that persist over days because they cannot restart. Indeed, the high levels of γH2AX foci is consistent with the conclusion that the stalled replication forks are not resolved and collapse into DSBs. In addition, the persistent 53BP1 nuclear foci and chromatin recruitment strongly suggests that NHEJ is actively repairing these DSBs, which, in turn, that results in the aberrant chromosomes seen in the karyotype analysis. Further corroborating my findings, the loss of CtIP and EXO1 triggered the phosphorylation of $CHK2_{T68}$ and ATM_{S1981}. These modified proteins are hallmarks of an activated checkpoint and strongly suggests that DSBs are activating the ATM-CHK2 pathway, which can be a promoter of NHEJ repair[16].

Finally, I analyzed WCE and chromatin fractions by western analysis. I was able make several novel findings. I found that CtIP and EXO1 are co-regulated such

that inactivating either of these genes results in the down regulation of the other one. Interestingly, the inactivation of CtIP or EXO1 also triggered the degradation of FANCD2, BRCA2, Rad51, and CHK1. The degradation of these proteins is a novel finding, and shows that DNA resection connects the HR and FA pathways. Moreover, this data shows that the lack of DNA resection effectively disables the FA, HR, and ATR-CHK1 pathways.

All of these findings are connected to to each other by previous studies: 1) CHK1-, and BRCA2- deficient cells increase DNA replication initiation and have severely short replication tracts[17]Daboussi:2008kr}, 2) chronic genotoxic stress leads to CHK1 degradation[18], 3) In HR-compromised cells 53BP1 promotes NHEJ repair of DSBs, which leads to aberrant chromosomes[19].

Collectively, the data I have generated show that CtIP and EXO1 are intimately involved in DNA replication. In unperturbed cells, DNA replication forks eventually run into repetitive regions that cause them to stall. The ATR-CHK1 pathway is activated which in turn stabilizes the stalled forks and recruit factors that restart the stalled forks (e.g. FANCD2, BRCA2, and Rad51). CtIP and EXO are closely associated to the replication forks, presumably through docking onto PCNA. The close proximity of CtIP and EXO1 permits swifter end resection on the stalled forks, which creates access for FANCD2, BRCA2 and Rad51 to restart the stalled forks in timely manner.

However, in the absence of CtIP and EXO1, stalled replication forks are unable to restart because the FANCD2, BRCA2 and Rad51 cannot access the stalled forks. As the stalled forks persist over time, CHK1 is under constant activation that

leads to its rapid degradation, with insufficient time for recovery. As a result, ATR cannot stabilize the stalled forks without CHK1 and the forks are now susceptible to collapse. Moreover, since the absence of CtIP and EXO1 lead to degradation of BRCA2 and Rad51, the HR pathway is also essentially non-functional; therefore, the cell is left to repair DSBs with NHEJ as mirrored with the elevated levels of 53BP1 nuclear foci.

DNA2 is also co-regulated with CtIP and EXO1

CtIP initiates DSB resection with minimal processing of the DNA ends, and then EXO1 and DNA2 are recruited for the subsequent extensive resection, which generates the long stretches of ssDNA for HR. It has been clear that these nucleases participate in the same pathway; however, it has never been shown how these three genes genetically interact in human cells.

The CtIP$^{F/-}$:CreERt2 and EXO1$^{F/-}$:CreERt2 cell lines have proven to be powerful human cell genetic models. With them, I was able to determine the fates of cells in the absence of CtIP or EXO1, and to determine the genetic interaction between CtIP and EXO1. However, the addition of the DNA2$^{F/-/-}$:CreERt2 cell line allowed me to shed even more light on how this trio of nucleases genetically interact with each other.

With the DNA2$^{F/-/-}$:CreERt2 cell line, I was able to show that CtIP, EXO1, and DNA2 are co-regulated; the inactivation of any one of the 3 genes results in the downregulation of the other 2 genes. Furthermore, I also found that the inactivation

of DNA2 also results in the degradation of FANCD2, BRCA2, Rad51, and CHK1. Therefore, the 3 nucleases coordinately regulate HR and FA.

Since these phenotypes have never been observed before, we thought that it would important to recapitulate these findings in another cell line. In collaboration with Dr. Jung Eun from the Sobeck laboratory, Dr. Eun knocked down CtIP, EXO1, and DNA2 in the GM637 cell line (immortalized, human fibroblast[20]) with siRNA. She also found that CtIP, EXO1, and DNA2 are co-regulated; and the three nucleases also coordinately regulate FANCD2. These results are consistent with my findings in the HCT116 cell line and emphasize that the coordinate regulation of FANCD2 is not specific to the HCT116 cell line.

In conclusion, I have constructed three genetic models in order to study the roles of DNA resection in human cells. I found that CtIP, EXO1, and DNA2 are epistatic, and that they are essential genes in human cells. Furthermore, I demonstrated that CtIP and EXO1 are required for normal DNA replication fork progression. In their absence, DNA replication forks inevitably stall with no means of restarting and eventually collapse into DSBs. In order to survive, the cell relies on the remaining DSB repair pathway, NHEJ, which results in the formation of aberrant chromosomes.

Collaborating with Dr. Farjana Fattah, a previous graduate student in our laboratory, we utilized a series of isogenic mutant cell lines that were disrupted for Ku, DNA-PK$_{cs}$, XLF, and LIGIV (C-NHEJ factors) to investigate their impact on the spectrum of end-joining repair in human somatic cells. This investigation was facilitated by well-characterized *in vivo* end-joining plasmid assays[21] to determine

the overall end joining competence of a cell; and another end-joining plasmid-based assay, which measured microhomology usage in the repair junction[22]. In the absence of DNA-PKcs, XLF, and LIGIV end-joining activity was severely compromised; and sequencing of the plasmids were rescued from cells revealed that the A-NHEJ pathway predominantly uses microhomology for repair. Furthermore, our experiments showed that Ku is the master regulator of NHEJ pathway choice and is important for protecting DNA ends from degradation. In conclusion, this work helped elucidate how A-NHEJ is regulated in human somatic cells.

Future Directions

Characterization of DNA2-null cells

Since the construction of the $DNA2^{F/-/-}$ cell line was delayed, their characterization is still incomplete and this should be the next priority. The remaining experiments required to achieve a similar depth of characterization as the CtIP- and EXO1-null cells are: 1) growth curves and MLH1 complementation, 2) EdU incorporation assay, 3) karyotype analysis, 4) DNA fiber assays, 5) immunofluorescence, and 6) western analysis of WCE and chromatin fractions. Accomplishing these experiments will paint a stronger picture of how this trio of nucleases functions in a cell.

Complementation

The next experiment for these studies is clearly to rescue the phenotypes of CtIP-, EXO1-, and DNA2-null cells. I have made multiple attempts to complement the CtIP$^{F/-}$:CreERt2 and EXO1$^{F/-}$:CreERt2 cell lines with CtIP and EXO1 either (EXO1a or EXO1b) cDNA expression vectors driven by a CAG promoter, respectively. Unfortunately my efforts have never been successful, as the cells do not survive after inactivating CtIP or EXO1. This is likely due to poor or unregulated expression of the rescuing cDNAs. The next strategy should be to try other expression vectors and/or rescue the mutant cell lines by knocking back in a functional copy of the relevant gene.

Structure: function analyses

There are no known patients with EXO1 or DNA2 mutations. However, there do exist patients with CtIP truncation mutations (Seckel and Jawad syndromes) that suffer from developmental abnormalities[4]. Generating knock-in models of these patient mutations in the HCT116 cell line would potentially allow us to understand the structure and function of CtIP in DNA replication, and its role in human development.

Are CtIP, EXO1, and DNA2 involved in telomeric G-overhang synthesis?

Several studies have implicated CtIP, EXO1, and DNA2 are involved in telomere

maintenance[2,3,23]. In yeast, SAE2 (CtIP in humans), EXO1 and DNA2 have all been implicated in maintaining the length of telomeres. A recent study in mice showed that EXO1 is responsible for generation of G-overhangs that are required in telomeres to form the t-loop complex, which protects the ends of chromosomes[3]. However, there have been no reports of human CtIP, EXO1, and DNA2 being involved in maintaining telomere length or G-overhang derivation.

In collaboration with graduate student in our laboratory, Adam Harvey, we have preliminary data showing that CtIP-, EXO1-, and DNA2-null cells have shortened telomeres; however, these cells also have high levels of DSBs. Since DSBs that occur in the telomeres can present themselves as shortened telomeres, these data must be viewed as very preliminary. Interestingly, however, we also have preliminary data showing that EXO1 (but not CtIP nor DNA2) may generate telomeric 3' G-overhangs in human cells. These findings clearly need to be pursued and if they can be authenticated they would expand the functional repertoire of EXO1 in human cell.

Are CtIP and EXO1 required for DNA replication through repetitive regions?

The genomic landscape of human cell is wrought with obstacles for a moving replication fork. To determine if CtIP and EXO1 are required to restart these stalled replication forks, we will use a technique called single molecule analysis of replicated DNA (SMARD)[27]. SMARD couples Southern blotting techniques with the DNA fiber assay, which allows the visualization of DNA replication tracts at the locus

of interest. If the replication tract lengths of repetitive regions in CtIP- or EXO1-null cells are significantly different from wild-type cells (with the appropriate controls), it would strengthen a model where CtIP and EXO1 are required for proper DNA replication in repetitive regions.

Analysis of protein dynamics of replication forks in the absence of CtIP, EXO1, or DNA2 via iPOND

I have found that the loss of CtIP or EXO1 results in DNA replication-related damage and the rapid degradation of FANCD2, BRCA2, Rad51, and CHK1. To further understand the pattern of recruitment of these factors to the replication forks in CtIP- and EXO1-null cells, I plan to isolate proteins on nascent DNA (iPOND)[24-26] to monitor changes occurring at the replication fork. During DNA replication, EdU will be incorporated into the nascent strand. After a determined EdU incubation time, the cells are fixed with paraformaldehyde to crosslink the proteins on to the nascent strands containing EdU. Subsequently, EdU is covalently linked to alkyne-Biotin molecules via a "click" reaction followed by lysis and sonication[24]. The proteins are then purified through a streptavidin column and can be analyzed by western analysis. Performing iPOND analysis in a time course after inactivating CtIP and EXO1 with tamoxifen will provide insightful data on the evolution of replication forks in the absence of CtIP and EXO1.

References

1. Huertas, P. DNA resection in eukaryotes: deciding how to fix the break. *Nat Struct Mol Biol* **17,** 11–16 (2010).
2. Symington, L. S. & Gautier, J. Double-strand break end resection and repair pathway choice. *Annu Rev Genet* **45,** 247–271 (2011).
3. Wu, P., Takai, H. & de Lange, T. Telomeric 3′ overhangs derive from resection by Exo1 and Apollo and fill-in by POT1b-associated CST. *Cell* **150,** 39–52 (2012).
4. Qvist, P. *et al.* CtIP mutations cause Seckel and Jawad syndromes. *PLoS Genet* **7,** e1002310 (2011).
5. You, Z. *et al.* CtIP links DNA double-strand break sensing to resection. *Mol Cell* **36,** 954–969 (2009).
6. Yuan, J. & Chen, J. N-Terminus of CtIP is critical for homologous recombination-mediated double-strand break repair. *J Biol Chem* **284,** 31746–31752 (2009).
7. Yun, M. H. & Hiom, K. CtIP-BRCA1 modulates the choice of DNA double-strand-break repair pathway throughout the cell cycle. *Nature* **459,** 460–463 (2009).
8. Huertas, P. & Jackson, S. P. Human CtIP mediates cell cycle control of DNA end resection and double strand break repair. *J Biol Chem* **284,** 9558–9565 (2009).
9. Sartori, A. A. *et al.* Human CtIP promotes DNA end resection. *Nature* **450,** 509–514 (2007).
10. Eid, W. *et al.* DNA end resection by CtIP and exonuclease 1 prevents genomic instability. *EMBO Rep* **11,** 962–968 (2010).
11. Karanja, K. K., Cox, S. W., Duxin, J. P., Stewart, S. A. & Campbell, J. L. DNA2 and EXO1 in replication-coupled, homology-directed repair and in the interplay between HDR and the FA/BRCA network. *Cell Cycle* **11,** 3983–3996 (2012).
12. Engels, K., Giannattasio, M., Muzi-Falconi, M., Lopes, M. & Ferrari, S. 14-3-3 Proteins regulate exonuclease 1–dependent processing of stalled replication forks. *PLoS Genet* **7,** e1001367 (2011).
13. Hawn, M. T. *et al.* Evidence for a connection between the mismatch repair system and the G2 cell cycle checkpoint. *Cancer Res* **55,** 3721–3725 (1995).
14. Branzei, D. & Foiani, M. The checkpoint response to replication stress. *DNA Repair (Amst)* **8,** 1038–1046 (2009).
15. Cimprich, K. A. & Cortez, D. ATR: an essential regulator of genome integrity. *Nat Rev Mol Cell Biol* **9,** 616–627 (2008).
16. Smith, J., Tho, L. M., Xu, N. & Gillespie, D. A. The ATM-Chk2 and ATR-Chk1 pathways in DNA damage signaling and cancer. *Adv. Cancer Res.* **108,** 73–112 (2010).
17. Petermann, E. *et al.* Chk1 requirement for high global rates of replication fork progression during normal vertebrate S phase. *Mol Cell Biol* **26,** 3319–3326 (2006).
18. Zhang, Y.-W. *et al.* Genotoxic stress targets human Chk1 for degradation by the ubiquitin-proteasome pathway. *Mol Cell* **19,** 607–618 (2005).
19. Callén, E. *et al.* 53BP1 Mediates Productive and Mutagenic DNA Repair

through Distinct Phosphoprotein Interactions. *Cell* **153,** 1266–1280 (2013).
20. Schwarz, S. B. *et al.* The effect of radio-adaptive doses on HT29 and GM637 cells. *Radiat Oncol* **3,** 12 (2008).
21. Mao, Z., Bozzella, M., Seluanov, A. & Gorbunova, V. DNA repair by nonhomologous end joining and homologous recombination during cell cycle in human cells. *Cell Cycle* **7,** 2902–2906 (2008).
22. Verkaik, N. S. *et al.* Different types of V(D)J recombination and end-joining defects in DNA double-strand break repair mutant mammalian cells. *Eur J Immunol* **32,** 701–709 (2002).
23. Choe, W., Budd, M. E., Imamura, O., Hoopes, L. & Campbell, J. L. Dynamic localization of an Okazaki fragment processing protein suggests a novel role in telomere replication. *Mol Cell Biol* **22,** 4202–4217 (2002).
24. Sirbu, B. M., Couch, F. B. & Cortez, D. Monitoring the spatiotemporal dynamics of proteins at replication forks and in assembled chromatin using isolation of proteins on nascent DNA. *Nat Protoc* **7,** 594–605 (2012).
25. López-Contreras, A. J. *et al.* A proteomic characterization of factors enriched at nascent DNA molecules. *Cell Rep* **3,** 1105–1116 (2013).
26. Sirbu, B. M. *et al.* Analysis of protein dynamics at active, stalled, and collapsed replication forks. *Genes Dev* **25,** 1320–1327 (2011).
27. Gerhardt, J. *et al.* The DNA replication program is altered at the Fmr1 locus in fragile x embryonic stem cells. *Mol Cell* **53,** 1–13 (2013).

Bibliography

1. Goodarzi, A. A. & Jeggo, P. A. The repair and signaling responses to DNA double-strand breaks. *Adv. Genet.* **82,** 1–45 (2013).
2. Bentley, J., Diggle, C. P., Harnden, P., Knowles, M. A. & Kiltie, A. E. DNA double strand break repair in human bladder cancer is error prone and involves microhomology-associated end-joining. *Nucleic Acids Res* **32,** 5249–5259 (2004).
3. Bianconi, E. *et al.* An estimation of the number of cells in the human body. *Ann. Hum. Biol.* **40,** 463–471 (2013).
4. Fouché, N., Ozgür, S., Roy, D. & Griffith, J. D. Replication fork regression in repetitive DNAs. *Nucleic Acids Res* **34,** 6044–6050 (2006).
5. Voineagu, I., Narayanan, V., Lobachev, K. S. & Mirkin, S. M. Replication stalling at unstable inverted repeats: interplay between DNA hairpins and fork stabilizing proteins. *Proc Nat Acad of Sci* **105,** 9936–9941 (2008).
6. Gerhardt, J. *et al.* The DNA replication program is altered at the Fmr1 locus in fragile x embryonic stem cells. *Mol Cell* **53,** 1–13 (2013).
7. Malumbres, M. & Barbacid, M. Cell cycle, CDKs and cancer: a changing paradigm. *Nat Rev Cancer* **9,** 153–166 (2009).
8. DePamphilis, M. L., de Renty, C. M., Ullah, Z. & Lee, C. Y. 'the octet': eight protein kinases that control mammalian DNA replication. *Front Physiol* **3,** 1–20 (2012).
9. Cimprich, K. A. & Cortez, D. ATR: an essential regulator of genome integrity. *Nat Rev Mol Cell Biol* **9,** 616–627 (2008).
10. Lopes, M. *et al.* The DNA replication checkpoint response stabilizes stalled replication forks. *Nature* **412,** 557–561 (2001).
11. San Filippo, J., Sung, P. & Klein, H. Mechanism of eukaryotic homologous recombination. *Annu Rev Biochem* **77,** 229–257 (2008).
12. Lieber, M. R. The mechanism of double-strand DNA break repair by the nonhomologous DNA end-joining pathway. *Annu Rev Biochem* **79,** 181–211 (2010).
13. Longhese, M. P., Bonetti, D., Manfrini, N. & Clerici, M. Mechanisms and regulation of DNA end resection. *EMBO J* **29,** 2864–2874 (2010).
14. You, Z. & Bailis, J. M. DNA damage and decisions: CtIP coordinates DNA repair and cell cycle checkpoints. *Trends in Cell Biology* **20,** 402–409 (2010).
15. Huertas, P. DNA resection in eukaryotes: deciding how to fix the break. *Nat Struct Mol Biol* **17,** 11–16 (2010).
16. Mimitou, E. P. & Symington, L. S. DNA end resection: many nucleases make light work. *DNA Repair (Amst)* **8,** 983–995 (2009).
17. Pierce, A. J. *et al.* Double-strand breaks and tumorigenesis. *Trends in Cell Biology* **11,** S52–59 (2001).
18. Verkaik, N. S. *et al.* Different types of V(D)J recombination and end-joining defects in DNA double-strand break repair mutant mammalian cells. *Eur J Immunol* **32,** 701–709 (2002).
19. Hakem, R. DNA-damage repair; the good, the bad, and the ugly. *EMBO J* **27,** 589–605 (2008).

20. Anand, R. P. *et al.* Overcoming natural replication barriers: differential helicase requirements. *Nucleic Acids Res* **40,** 1091–1105 (2012).
21. Maizels, N. Dynamic roles for G4 DNA in the biology of eukaryotic cells. *Nat Struct Mol Biol* **13,** 1055–1059 (2006).
22. Mirkin, S. M. Expandable DNA repeats and human disease. *Nature* **447,** 932–940 (2007).
23. Branzei, D. & Foiani, M. The checkpoint response to replication stress. *DNA Repair (Amst)* **8,** 1038–1046 (2009).
24. Chaudhury, I., Sareen, A., Raghunandan, M. & Sobeck, A. FANCD2 regulates BLM complex functions independently of FANCI to promote replication fork recovery. *Nucleic Acids Res* **41,** 6444–6459 (2013).
25. Petermann, E., Orta, M. L., Issaeva, N., Schultz, N. & Helleday, T. Hydroxyurea-stalled replication forks become progressively inactivated and require two different RAD51-mediated pathways for restart and repair. *Mol Cell* **37,** 492–502 (2010).
26. Branzei, D. & Foiani, M. Maintaining genome stability at the replication fork. *Nat Rev Mol Cell Biol* **11,** 208–219 (2010).
27. Ragland, R. L. *et al.* RNF4 and PLK1 are required for replication fork collapse in ATR-deficient cells. *Genes Dev* **27,** 2259–2273 (2013).
28. Mahaney, B. L., Meek, K. & Lees-Miller, S. P. Repair of ionizing radiation-induced DNA double-strand breaks by non-homologous end-joining. *Biochem J* **417,** 639–650 (2009).
29. Hendrickson, E. A., Huffman, J. L. & JA, T. Structural aspects of Ku and the DNA-dependent protein kinase complex. New York: Taylor and Francis Group. *DNA damage recognition* 629–684 (2006).
30. Kastan, M. B. & Bartek, J. Cell-cycle checkpoints and cancer. *Nature* **432,** 316–323 (2004).
31. Löbrich, M. & Jeggo, P. A. The impact of a negligent G2/M checkpoint on genomic instability and cancer induction. *Nat Rev Cancer* **7,** 861–869 (2007).
32. Smith, J., Tho, L. M., Xu, N. & Gillespie, D. A. The ATM-Chk2 and ATR-Chk1 pathways in DNA damage signaling and cancer. *Adv. Cancer Res.* **108,** 73–112 (2010).
33. Symington, L. S. & Gautier, J. Double-strand break end resection and repair pathway choice. *Annu Rev Genet* **45,** 247–271 (2011).
34. Méchali, M. Eukaryotic DNA replication origins: many choices for appropriate answers. *Nat Rev Mol Cell Biol* **11,** 728–738 (2010).
35. Errico, A. & Costanzo, V. Mechanisms of replication fork protection: a safeguard for genome stability. *Crit Rev Biochem Mol Bio* **47,** 222–235 (2012).
36. Chini, C. C. S. Human Claspin is required for replication checkpoint control. *J Biol Chem* **278,** 30057–30062 (2003).
37. Chini, C. C. S., Wood, J. & Chen, J. Chk1 is required to maintain claspin stability. *Oncogene* **25,** 4165–4171 (2006).
38. Petermann, E., Helleday, T. & Caldecott, K. W. Claspin promotes normal replication fork rates in human cells. *Mol. Biol. Cell* **19,** 2373–2378 (2008).
39. Mendez, J. Temporal regulation of DNA replication in mammalian cells. *Crit Rev Biochem Mol Bio* **44,** 343–351 (2009).

40. Lange, S. S., Takata, K.-I. & Wood, R. D. DNA polymerases and cancer. *Nat Rev Cancer* **11,** 96–110 (2011).
41. Thu, Y. M. & Bielinsky, A. K. Enigmatic roles of Mcm10 in DNA replication. *Trends Biochem Sci* **38,** 184–194 (2013).
42. Durkin, S. G. & Glover, T. W. Chromosome fragile sites. *Annu Rev Genet* **41,** 169–192 (2007).
43. Cimprich, K. A. Fragile sites: breaking up over a slowdown. *Curr Biol* **13,** R231–R233 (2003).
44. Casper, A. M., Nghiem, P., Arlt, M. F. & Glover, T. W. ATR regulates fragile site stability. *Cell* **111,** 779–789 (2002).
45. Barlow, J. H. *et al.* Identification of early replicating fragile sites that contribute to genome instability. *Cell* **152,** 620–632 (2013).
46. Mao, Z., Bozzella, M., Seluanov, A. & Gorbunova, V. DNA repair by nonhomologous end joining and homologous recombination during cell cycle in human cells. *Cell Cycle* **7,** 2902–2906 (2008).
47. Krogh, B. O. & Symington, L. S. Recombination proteins in yeast. *Annu Rev Genet* **38,** 233–271 (2004).
48. Mazin, A. V., Mazina, O. M., Bugreev, D. V. & Rossi, M. J. Rad54, the motor of homologous recombination. *DNA Repair (Amst)* **9,** 286–302 (2010).
49. Wang, H. *et al.* The interaction of CtIP and Nbs1 connects CDK and ATM to regulate HR-mediated double-strand break repair. *PLoS Genet* **9,** e1003277 (2013).
50. Buis, J., Stoneham, T., Spehalski, E. & Ferguson, D. O. Mre11 regulates CtIP-dependent double-strand break repair by interaction with CDK2. *Nat Struct Mol Biol* **19,** 246–252 (2012).
51. Eid, W. *et al.* DNA end resection by CtIP and exonuclease 1 prevents genomic instability. *EMBO Rep* **11,** 962–968 (2010).
52. You, Z. *et al.* CtIP links DNA double-strand break sensing to resection. *Mol Cell* **36,** 954–969 (2009).
53. Huertas, P. & Jackson, S. P. Human CtIP mediates cell cycle control of DNA end resection and double strand break repair. *J Biol Chem* **284,** 9558–9565 (2009).
54. Mimitou, E. P. & Symington, L. S. Sae2, Exo1 and Sgs1 collaborate in DNA double-strand break processing. *Nature* **455,** 770–774 (2008).
55. Zhu, Z., Chung, W.-H., Shim, E. Y., Lee, S. E. & Ira, G. Sgs1 helicase and two nucleases Dna2 and Exo1 resect DNA double-strand break ends. *Cell* **134,** 981–994 (2008).
56. Huertas, P., Cortés-Ledesma, F., Sartori, A. A., Aguilera, A. & Jackson, S. P. CDK targets Sae2 to control DNA-end resection and homologous recombination. *Nature* **455,** 689–692 (2008).
57. Sartori, A. A. *et al.* Human CtIP promotes DNA end resection. *Nature* **450,** 509–514 (2007).
58. Takeda, S., Nakamura, K., Taniguchi, Y. & Paull, T. T. Ctp1/CtIP and the MRN complex collaborate in the initial steps of homologous recombination. *Mol Cell* **28,** 351–352 (2007).
59. Peng, G. *et al.* Human nuclease/helicase Dna2 alleviates replication stress by promoting DNA end resection. *Cancer Res* 1–12 (2012). doi:10.1158/0008-

5472.CAN-11-3152
60. Nimonkar, A. V. *et al.* BLM-DNA2-RPA-MRN and EXO1-BLM-RPA-MRN constitute two DNA end resection machineries for human DNA break repair. *Genes Dev* **25,** 350–362 (2011).
61. Mimitou, E. P. & Symington, L. S. Ku prevents Exo1 and Sgs1-dependent resection of DNA ends in the absence of a functional MRX complex or Sae2. *EMBO J* **29,** 3358–3369 (2010).
62. Ira, G. *et al.* DNA end resection, homologous recombination and DNA damage checkpoint activation require CDK1. *Nature* **431,** 1011–1017 (2004).
63. Karanja, K. K., Cox, S. W., Duxin, J. P., Stewart, S. A. & Campbell, J. L. DNA2 and EXO1 in replication-coupled, homology-directed repair and in the interplay between HDR and the FA/BRCA network. *Cell Cycle* **11,** 3983–3996 (2012).
64. Hodgson, A. *et al.* Mre11 and Exo1 contribute to the initiation and processivity of resection at meiotic double-strand breaks made independently of Spo11. *DNA Repair (Amst)* **10,** 138–148 (2011).
65. Nicolette, M. L. *et al.* Mre11–Rad50–Xrs2 and Sae2 promote 5′ strand resection of DNA double-strand breaks. *Nat Struct Mol Biol* **17,** 1478–1485 (2010).
66. Marrero, V. A. & Symington, L. S. Extensive DNA end processing by Exo1 and Sgs1 inhibits break-induced replication. *PLoS Genet* **6,** e1001007 (2010).
67. Bolderson, E. *et al.* Phosphorylation of Exo1 modulates homologous recombination repair of DNA double-strand breaks. *Nucleic Acids Res* **38,** 1821–1831 (2010).
68. Wu, P., Takai, H. & de Lange, T. Telomeric 3′ overhangs derive from resection by Exo1 and Apollo and fill-in by POT1b-associated CST. *Cell* **150,** 39–52 (2012).
69. Qvist, P. *et al.* CtIP mutations cause Seckel and Jawad syndromes. *PLoS Genet* **7,** e1002310 (2011).
70. Wu, G. & Lee, W.-H. CtIP, a multivalent adaptor connecting transcriptional regulation, checkpoint control and tumor suppression. *Cell Cycle* **5,** 1592–1596 (2006).
71. Schaeper, U., Subramanian, T., Lim, L., Boyd, J. M. & Chinnadurai, G. Interaction between a cellular protein that binds to the C-terminal region of adenovirus E1A (CtBP) and a novel cellular protein is disrupted by E1A through a conserved PLDLS motif. *J Biol Chem* **273,** 8549–8552 (1998).
72. Meloni, A. R., Smith, E. J. & Nevins, J. R. A mechanism for Rb/p130-mediated transcription repression involving recruitment of the CtBP corepressor. *Proc Natl Acad Sci USA* **96,** 9574–9579 (1999).
73. Li, S. Binding of CtIP to the BRCT repeats of Brca1 involved in the transcription regulation of p21 is disrupted upon DNA damage. *J Biol Chem* **274,** 11334–11338 (1999).
74. Yu, X., Wu, L. C., Bowcock, A. M., Aronheim, A. & Baer, R. The C-terminal (BRCT) domains of BRCA1 interact in vivo with CtIP, a protein implicated in the CtBP pathway of transcriptional repression. *J Biol Chem* **273,** 25388–25392 (1998).
75. Yu, X. & Chen, J. DNA damage-induced cell cycle checkpoint control requires CtIP, a phosphorylation-dependent binding partner of BRCA1 C-terminal domains. *Mol Cell Biol* **24,** 9478–9486 (2004).

76. Lee, W.-H. *et al.* Functional link of BRCA1 and ataxia telangiectasia gene product in DNA damage response : Article : Nature. *Nature* **406,** 210–215 (2000).
77. Dubin, M. J. Dimerization of CtIP, a BRCA1- and CtBP-interacting Protein, Is mediated by an N-terminal coiled-coil Motif. *J Biol Chem* **279,** 26932–26938 (2004).
78. Barber, L. J. & Boulton, S. J. BRCA1 ubiquitylation of CtIP: Just the tIP of the iceberg? *DNA Repair (Amst)* **5,** 1499–1504 (2006).
79. Gu, B. & Chen, P.-L. Expression of PCNA-binding domain of CtIP, a motif required for CtIP localization at DNA replication foci, causes DNA damage and activation of DNA damage checkpoint. *Cell Cycle* **8,** 1409–1420 (2009).
80. Chen, P.-L. *et al.* Inactivation of CtIP leads to early embryonic lethality mediated by G1 restraint and to tumorigenesis by haploid insufficiency. *Mol Cell Biol* **25,** 3535–3542 (2005).
81. Wilson, D. M. *et al.* Hex1: a new human Rad2 nuclease family member with homology to yeast exonuclease 1. *Nucleic Acids Res* **26,** 3762–3768 (1998).
82. Orans, J. *et al.* Structures of human exonuclease 1 DNA complexes suggest a unified mechanism for nuclease family. *Cell* **145,** 212–223 (2011).
83. Nimonkar, A. V., Ozsoy, A. Z., Genschel, J., Modrich, P. & Kowalczykowski, S. C. Human exonuclease 1 and BLM helicase interact to resect DNA and initiate DNA repair. *Proc Natl Acad Sci USA* **105,** 16906–16911 (2008).
84. Richard, D. J. *et al.* hSSB1 rapidly binds at the sites of DNA double-strand breaks and is required for the efficient recruitment of the MRN complex. *Nucleic Acids Res* **39,** 1692–1702 (2011).
85. Tran, P. T., Erdeniz, N., Symington, L. S. & Liskay, R. M. EXO1-A multi-tasking eukaryotic nuclease. *DNA Repair (Amst)* **3,** 1549–1559 (2004).
86. Liberti, S. E. *et al.* Bi-directional routing of DNA mismatch repair protein human exonuclease 1 to replication foci and DNA double strand breaks. *DNA Repair (Amst)* **10,** 73–86 (2011).
87. Marti, T. M., Mansour, A. A., Lehmann, E. & Fleck, O. Different frameshift mutation spectra in non-repetitive DNA of MutSalpha- and MutLalpha-deficient fission yeast cells. *DNA Repair (Amst)* **2,** 571–580 (2003).
88. Sun, X., Zheng, L. & Shen, B. Functional alterations of human exonuclease 1 mutants identified in atypical hereditary nonpolyposis colorectal cancer syndrome. *Cancer Res* **62,** 6026–6030 (2002).
89. Jäger, A. C. *et al.* HNPCC mutations in the human DNA mismatch repair gene hMLH1 influence assembly of hMutLalpha and hMLH1-hEXO1 complexes. *Oncogene* **20,** 3590–3595 (2001).
90. Schmutte, C. *et al.* Human exonuclease I interacts with the mismatch repair protein hMSH2. *Cancer Res* **58,** 4537–4542 (1998).
91. López-Contreras, A. J. *et al.* A proteomic characterization of factors enriched at nascent DNA molecules. *Cell Rep* **3,** 1105–1116 (2013).
92. Sertic, S. *et al.* Human exonuclease 1 connects nucleotide excision repair (NER) processing with checkpoint activation in response to UV irradiation. *Proc Natl Acad Sci USA* **108,** 13647–13652 (2011).
93. Morin, I. *et al.* Checkpoint-dependent phosphorylation of Exo1 modulates the

DNA damage response. *EMBO J* **27,** 2400–2410 (2008).
94. Engels, K., Giannattasio, M., Muzi-Falconi, M., Lopes, M. & Ferrari, S. 14-3-3 Proteins regulate exonuclease 1–dependent processing of stalled replication forks. *PLoS Genet* **7,** e1001367 (2011).
95. Andersen, S. D. *et al.* 14-3-3 checkpoint regulatory proteins interact specifically with DNA repair protein human exonuclease 1 (hEXO1) via a semi-conserved motif. *DNA Repair (Amst)* **11,** 267–277 (2012).
96. Richard, D. J. *et al.* Single-stranded DNA-binding protein hSSB1 is critical for genomic stability. *Nat Rev Mol Cell Biol* **453,** 677–681 (2008).
97. Yang, S.-H. *et al.* The SOSS1 single-stranded DNA binding complex promotes DNA end resection in concert with Exo1. *EMBO J* **9,** 126–139 (2012).
98. Schaetzlein, S. *et al.* Exonuclease-1 deletion impairs DNA damage signaling and prolongs lifespan of telomere-dysfunctional mice. *Cell* **130,** 863–877 (2007).
99. Wei, K. Inactivation of Exonuclease 1 in mice results in DNA mismatch repair defects, increased cancer susceptibility, and male and female sterility. *Genes Dev* **17,** 603–614 (2003).
100. Masuda-Sasa, T., Imamura, O. & Campbell, J. L. Biochemical analysis of human Dna2. *Nucleic Acids Res* **34,** 1865–1875 (2006).
101. Bae, S. H. Coupling of DNA Helicase and Endonuclease Activities of Yeast Dna2 Facilitates Okazaki Fragment Processing. *J Biol Chem* **277,** 26632–26641 (2002).
102. Kao, H. I. Dna2p helicase/nuclease Is a tracking protein, like FEN1, for flap cleavage during Okazaki fragment maturation. *J Biol Chem* **279,** 50840–50849 (2004).
103. Lee, K. H. *et al.* The endonuclease activity of the yeast Dna2 enzyme is essential in vivo. *Nucleic Acids Res* **28,** 2873–2881 (2000).
104. Zheng, L. *et al.* Human DNA2 is a mitochondrial nuclease/helicase for efficient processing of DNA replication and repair intermediates. *Mol Cell* **32,** 325–336 (2008).
105. Cotta-Ramusino, C. *et al.* Exo1 processes stalled replication forks and counteracts fork reversal in checkpoint-defective cells. *Mol Cell* **17,** 153–159 (2005).
106. Mimitou, E. P. & Symington, L. S. DNA end resection- unraveling the tail. *DNA Repair (Amst)* **10,** 344–348 (2011).
107. Kottemann, M. C. & Smogorzewska, A. Fanconi anaemia and the repair of Watson and Crick DNA crosslinks. *Nature* **493,** 356–363 (2013).
108. Kee, Y. & D'Andrea, A. D. Molecular pathogenesis and clinical management of Fanconi anemia. *J Clin Invest* **122,** 3799–3806 (2012).
109. Moldovan, G.-L. & D'Andrea, A. D. How the fanconi anemia pathway guards the genome. *Annu Rev Genet* **43,** 223–249 (2009).
110. Sobeck, A., Stone, S., Landais, I., de Graaf, B. & Hoatlin, M. E. The Fanconi Anemia Protein FANCM Is Controlled by FANCD2 and the ATR/ATM Pathways. *J Biol Chem* **284,** 25560–25568 (2009).
111. Sareen, A., Chaudhury, I., Adams, N. & Sobeck, A. Fanconi anemia proteins FANCD2 and FANCI exhibit different DNA damage responses during S-phase. *Nucleic Acids Res* **40,** 8425–8439 (2012).

112. Garner, E. & Smogorzewska, A. Ubiquitylation and the Fanconi anemia pathway. *FEBS Letters* **585,** 2853–2860 (2011).
113. Roy, R., Chun, J. & Powell, S. N. BRCA1 and BRCA2: different roles in a common pathway of genome protection. *Nat Rev Cancer* **12,** 68–78 (2011).
114. Long, D. T., Räschle, M., Joukov, V. & Walter, J. C. Mechanism of RAD51-dependent DNA interstrand cross-link repair. *Science* **333,** 84–87 (2011).
115. Boboila, C. *et al.* Robust chromosomal DNA repair via alternative end-joining in the absence of X-ray repair cross-complementing protein 1 (XRCC1). *Proc Natl Acad Sci USA* **109,** 2473–2478 (2012).
116. Liang, L. *et al.* Human DNA ligases I and III, but not ligase IV, are required for microhomology-mediated end joining of DNA double-strand breaks. *Nucleic Acids Res* **36,** 3297–3310 (2008).
117. Kramer, K. M., Brock, J. A., Bloom, K., Moore, J. K. & Haber, J. E. Two different types of double-strand breaks in Saccharomyces cerevisiae are repaired by similar RAD52-independent, nonhomologous recombination events. *Mol Cell Biol* **14,** 1293–1301 (1994).
118. Nussenzweig, A. & Nussenzweig, M. C. A backup DNA repair pathway moves to the forefront. *Cell* **131,** 223–225 (2007).
119. Wang, M. *et al.* PARP-1 and Ku compete for repair of DNA double strand breaks by distinct NHEJ pathways. *Nucleic Acids Res* **34,** 6170–6182 (2006).
120. Meek, K., Dang, V. & Lees-Miller, S. P. DNA-PK: the means to justify the ends? *Adv. Immunol.* **99,** 33–58 (2008).
121. Ellenberger, T. & Tomkinson, A. E. Eukaryotic DNA ligases: structural and functional insights. *Annu Rev Biochem* **77,** 313–338 (2008).
122. Bunting, S. F. *et al.* 53BP1 inhibits homologous recombination in Brca1-deficient cells by blocking resection of DNA breaks. *Cell* **141,** 243–254 (2010).
123. Bunting, S. F. *et al.* BRCA1 Functions independently of homologous recombination in DNA interstrand crosslink repair. *Mol Cell* **46,** 125–135 (2012).
124. Patel, A. G., Sarkaria, J. N. & Kaufmann, S. H. Nonhomologous end joining drives poly(ADP-ribose) polymerase (PARP) inhibitor lethality in homologous recombination-deficient cells. *Proc Natl Acad Sci USA* **108,** 3406–3411 (2011).
125. Pace, P. *et al.* Ku70 Corrupts DNA repair in the absence of the Fanconi anemia pathway. *Science* **329,** 219–223 (2010).
126. Fattah, F. *et al.* Ku regulates the non-homologous end joining pathway choice of DNA double-strand break repair in human somatic cells. *PLoS Genet* **6,** e1000855 (2010).
127. McVey, M. & Lee, S. E. MMEJ repair of double-strand breaks (director's cut): deleted sequences and alternative endings. *Trends Genet* **24,** 529–538 (2008).
128. Boulton, S. Identification of a Saccharomyces cerevisiae Ku80 homologue: roles in DNA double strand break rejoining and in telomeric maintenance. *Nucleic Acids Res* **24,** 4639–4648 (1996).
129. Roth, D. B. & Wilson, J. H. Nonhomologous recombination in mammalian cells: role for short sequence homologies in the joining reaction. *Mol Cell Biol* **6,** 4295–4304 (1986).
130. Roth, D. B., Porter, T. N. & Wilson, J. H. Mechanisms of nonhomologous

recombination in mammalian cells. *Mol Cell Biol* **5,** 2599–2607 (1985).
131. Daley, J. M. & Wilson, T. E. Rejoining of DNA double-strand breaks as a function of overhang length. *Mol Cell Biol* **25,** 896–906 (2005).
132. Wang, H. *et al.* Biochemical evidence for Ku-independent backup pathways of NHEJ. *Nucleic Acids Res* **31,** 5377–5388 (2003).
133. Difilippantonio, M. J. *et al.* Evidence for replicative repair of DNA double-strand breaks leading to oncogenic translocation and gene amplification. *J Exp Med* **196,** 469–480 (2002).
134. Zhu, C. *et al.* Unrepaired DNA breaks in p53-deficient cells lead to oncogenic gene amplification subsequent to translocations. *Cell* **109,** 811–821 (2002).
135. Weinstock, D. M. A model of oncogenic rearrangements: differences between chromosomal translocation mechanisms and simple double-strand break repair. *Blood* **107,** 777–780 (2006).
136. Tsai, A. G. *et al.* Human chromosomal translocations at CpG sites and a theoretical basis for their lineage and stage specificity. *Cell* **135,** 1130–1142 (2008).
137. Audebert, M., Salles, B. & Calsou, P. Involvement of poly(ADP-ribose) polymerase-1 and XRCC1/DNA ligase III in an alternative route for DNA double-strand breaks rejoining. *J Biol Chem* **279,** 55117–55126 (2004).
138. Liang, L. *et al.* Modulation of DNA end joining by nuclear proteins. *J Biol Chem* **280,** 31442–31449 (2005).
139. Bunting, S. F. & Nussenzweig, A. End-joining, translocations and cancer. *Nat Rev Cancer* **13,** 443–454 (2013).
140. Haber, J. E. Alternative endings. *Proc Natl Acad Sci USA* **105,** 405–406 (2008).
141. Ma, J.-L., Kim, E. M., Haber, J. E. & Lee, S. E. Yeast Mre11 and Rad1 proteins define a Ku-independent mechanism to repair double-strand breaks lacking overlapping end sequences. *Mol Cell Biol* **23,** 8820–8828 (2003).
142. Ferretti, L. P., Lafranchi, L. & Sartori, A. A. Controlling DNA-end resection: a new task for CDKs. *Front Genet* **4,** 99 (2013).
143. Cerqueira, A. *et al.* Overall Cdk activity modulates the DNA damage response in mammalian cells. *J Cell Biol* **187,** 773–780 (2009).
144. Di Virgilio, M. *et al.* Rif1 prevents resection of DNA breaks and promotes immunoglobulin class switching. *Science* **339,** 711–715 (2013).
145. Callén, E. *et al.* 53BP1 Mediates Productive and Mutagenic DNA Repair through Distinct Phosphoprotein Interactions. *Cell* **153,** 1266–1280 (2013).
146. Escribano-Díaz, C. *et al.* A cell cycle-dependent regulatory circuit composed of 53bp1-Rif1 and Brca1-ctip controls DNA repair pathway choice. *Semin. Cell Dev. Biol.* (2013).
147. Zimmermann, M., Lottersberger, F., Buonomo, S. B., Sfeir, A. & de Lange, T. 53BP1 regulates DSB repair using Rif1 to control 5' end resection. *Science* **339,** 700–704 (2013).
148. Berns, K. I. & Giraud, C. Biology of adeno-associated virus. *Curr. Top. Microbiol. Immunol.* **218,** 1–23 (1996).
149. Chirmule, N. *et al.* Immune responses to adenovirus and adeno-associated virus in humans. *Gene Ther* **6,** 1574–1583 (1999).
150. Lai, C. M., Lai, Y. K. Y. & Rakoczy, P. E. Adenovirus and adeno-associated virus

vectors. *DNA Cell Biol* **21,** 895–913 (2002).
151. Berns, K. I. & Linden, R. M. The cryptic life style of adeno-associated virus. *Bioessays* **17,** 237–245 (1995).
152. Berns, K. I. & Giraud, C. Adenovirus and adeno-associated virus as vectors for gene therapy. *Ann N Y Acad Sci* **772,** 95–104 (1995).
153. Daya, S. & Berns, K. I. Gene therapy using adeno-associated virus vectors. *Clinical Microbiology Reviews* **21,** 583–593 (2008).
154. Russell, D. W. & Hirata, R. K. Human gene targeting by viral vectors. *Nat Genet* **18,** 325–330 (1998).
155. Hendrickson, E. A. Gene targeting in human somatic cells. *Sourcebook of Models for Biomedical Research* 509–525 (2008). doi:10.1007/978-1-59745-285-4_53
156. Kohli, M., Rago, C., Lengauer, C., Kinzler, K. W. & Vogelstein, B. Facile methods for generating human somatic cell gene knockouts using recombinant adeno-associated viruses. *Nucleic Acids Res* **32,** e3 (2004).
157. Topaloglu, O., Hurley, P. J., Yildirim, O., Civin, C. I. & Bunz, F. Improved methods for the generation of human gene knockout and knockin cell lines. *Nucleic Acids Res* **33,** e158 (2005).
158. Bunz, F. *et al.* Requirement for p53 and p21 to sustain G2 arrest after DNA damage. *Science* **282,** 1497–1501 (1998).
159. Aebi, S. *et al.* Loss of DNA mismatch repair in acquired resistance to cisplatin. *Cancer Res* **56,** 3087–3090 (1996).
160. Yuan, J. & Chen, J. N-Terminus of CtIP is critical for homologous recombination-mediated double-strand break repair. *J Biol Chem* **284,** 31746–31752 (2009).
161. Yun, M. H. & Hiom, K. CtIP-BRCA1 modulates the choice of DNA double-strand-break repair pathway throughout the cell cycle. *Nature* **459,** 460–463 (2009).
162. Adamo, A. *et al.* Preventing nonhomologous end joining suppresses DNA repair defects of Fanconi anemia. *Mol Cell* **39,** 25–35 (2010).
163. Fouché, N., Ozgür, S., Roy, D. & Griffith, J. D. Replication fork regression in repetitive DNAs. *Nucleic Acids Res* **34,** 6044–6050 (2006).
164. Mimitou, E. P. & Symington, L. S. DNA end resection: many nucleases make light work. *DNA Repair (Amst)* **8,** 983–995 (2009).
165. Maga, G. Okazaki fragment processing: Modulation of the strand displacement activity of DNA polymerase delta by the concerted action of replication protein A, proliferating cell nuclear antigen, and flap endonuclease-1. *Proc Natl Acad Sci USA* **98,** 14298–14303 (2001).
166. Budd, M. E., Antoshechkin, I. A., Reis, C., Wold, B. J. & Campbell, J. L. Inviability of a DNA2 deletion mutant is due to the DNA damage checkpoint. *Cell Cycle* **10,** 1690–1698 (2011).
167. Nussenzweig, A. *et al.* Requirement for Ku80 in growth and immunoglobulin V(D)J recombination. *Nature* **382,** 551–555 (1996).
168. Li, G., Nelsen, C. & Hendrickson, E. A. Ku86 is essential in human somatic cells. *Proc Natl Acad Sci USA* **99,** 832–837 (2002).
169. Wang, Y., Ghosh, G. & Hendrickson, E. A. Ku86 represses lethal telomere deletion events in human somatic cells. *Proc Natl Acad Sci USA* **106,** 12430–12435 (2009).
170. Duxin, J. P. *et al.* Human Dna2 is a nuclear and mitochondrial DNA maintenance

protein. *Mol Cell Biol* **29,** 4274–4282 (2009).
172. Hawn, M. T. *et al.* Evidence for a connection between the mismatch repair system and the G2 cell cycle checkpoint. *Cancer Res* **55,** 3721–3725 (1995).
173. Liu, F. & Lee, W.-H. CtIP activates its own and cyclin D1 promoters via the E2F/RB pathway during G1/S progression. *Mol Cell Biol* **26,** 3124–3134 (2006).
174. Wu, G. & Lee, W.-H. CtIP, a multivalent adaptor connecting transcriptional regulation, checkpoint control and tumor suppression. *Cell Cycle* **5,** 1592–1596 (2006).
175. Daboussi, F. *et al.* A homologous recombination defect affects replication-fork progression in mammalian cells. *J Cell Sci* **121,** 162–166 (2008).
176. Petermann, E. *et al.* Chk1 requirement for high global rates of replication fork progression during normal vertebrate S phase. *Mol Cell Biol* **26,** 3319–3326 (2006).
177. Moldovan, G.-L., Pfander, B. & Jentsch, S. PCNA, the maestro of the replication fork. *Cell* **129,** 665–679 (2007).
178. Bonner, W. M. *et al.* GammaH2AX and cancer. *Nat Rev Cancer* **8,** 957–967 (2008).
179. Nakamura, A. J., Rao, V. A., Pommier, Y. & Bonner, W. M. The complexity of phosphorylated H2AX foci formation and DNA repair assembly at DNA double-strand breaks. *Cell Cycle* **9,** 389–397 (2010).
180. Dimitrova, N., Chen, Y.-C. M., Spector, D. L. & de Lange, T. 53BP1 promotes non-homologous end joining of telomeres by increasing chromatin mobility. *Nature* **456,** 524–528 (2008).
181. Andreassen, P. R., D'Andrea, A. D. & Taniguchi, T. ATR couples FANCD2 monoubiquitination to the DNA-damage response. *Genes Dev* **18,** 1958–1963 (2004).
182. Zou, L. & Elledge, S. J. Sensing DNA damage through ATRIP recognition of RPA-ssDNA complexes. *Science* **300,** 1542–1548 (2003).
183. Byun, T. S., Pacek, M., Yee, M.-C., Walter, J. C. & Cimprich, K. A. Functional uncoupling of MCM helicase and DNA polymerase activities activates the ATR-dependent checkpoint. *Genes Dev* **19,** 1040–1052 (2005).
184. Petermann, E. & Helleday, T. Pathways of mammalian replication fork restart. *Nat Rev Mol Cell Biol* **11,** 683–687 (2010).
185. Chini, C. C. S. & Chen, J. Claspin, a regulator of Chk1 in DNA replication stress pathway. *DNA Repair (Amst)* **3,** 1033–1037 (2004).
186. Zhang, Y.-W. *et al.* Genotoxic stress targets human Chk1 for degradation by the ubiquitin-proteasome pathway. *Mol Cell* **19,** 607–618 (2005).
187. Peschiaroli, A. *et al.* SCFbetaTrCP-mediated degradation of Claspin regulates recovery from the DNA replication checkpoint response. *Mol Cell* **23,** 319–329 (2006).
188. Mailand, N., Bekker-Jensen, S., Bartek, J. & Lukas, J. Destruction of Claspin by SCFbetaTrCP restrains Chk1 activation and facilitates recovery from genotoxic stress. *Mol Cell* **23,** 307–318 (2006).
189. Ward, I. M., Wu, X. & Chen, J. Threonine 68 of Chk2 is phosphorylated at sites of DNA strand breaks. *J Biol Chem* **276,** 47755–47758 (2001).
190. Bakkenist, C. J. & Kastan, M. B. DNA damage activates ATM through

intermolecular autophosphorylation and dimer dissociation. *Nature* **421,** 499–506 (2003).
191. Lee, D. H. & Goldberg, A. L. Proteasome inhibitors: valuable new tools for cell biologists. *Trends in Cell Biology* **8,** 397–403 (1998).
192. Schwarz, S. B. *et al.* The effect of radio-adaptive doses on HT29 and GM637 cells. *Radiat Oncol* **3,** 12 (2008).
193. Syljuåsen, R. G. *et al.* Inhibition of human Chk1 causes increased initiation of DNA replication, phosphorylation of ATR targets, and DNA breakage. *Mol Cell Biol* **25,** 3553–3562 (2005).
194. Sabatinos, S. A., Green, M. D. & Forsburg, S. L. Continued DNA Synthesis in Replication Checkpoint Mutants Leads to Fork Collapse. *Mol Cell Biol* **32,** 4986–4997 (2012).
195. Wang, B. 53BP1, a Mediator of the DNA Damage Checkpoint. *Science* **298,** 1435–1438 (2002).
196. DiTullio, R. A. *et al.* 53BP1 functions in an ATM-dependent checkpoint pathway that is constitutively activated in human cancer. *Nat. Cell Biol.* **4,** 998–1002 (2002).
197. Rahrmann, E. P. *et al.* Forward genetic screen for malignant peripheral nerve sheath tumor formation identifies new genes and pathways driving tumorigenesis. *Nat Genet* **45,** 756–766 (2013).
198. Rago, C., Vogelstein, B. & Bunz, F. Genetic knockouts and knockins in human somatic cells. *Nat Protoc* **2,** 2734–2746 (2007).
199. Ge, X. Q., Jackson, D. A. & Blow, J. J. Dormant origins licensed by excess Mcm2-7 are required for human cells to survive replicative stress. *Genes Dev* **21,** 3331–3341 (2007).
200. Hamelik, R. M. & Krishan, A. Click-iT assay with improved DNA distribution histograms. *Cytometry A* **75,** 862–865 (2009).
201. Fattah FJ, Lichter NF, Fattah KR, Oh S, Hendrickson EA (2008) Ku70, an essential gene, modulates the frequency of rAAV-mediated gene targeting in human somatic cells. Proc Natl Acad Sci U S A 105: 8703-8708.
202. Wang Y, Ghosh G, Hendrickson EA (2009) Ku86 represses lethal telomere deletion events in human somatic cells. Proc Natl Acad Sci U S A in press.
204. Cahill D, Connor B, Carney JP (2006) Mechanisms of eukaryotic DNA double strand break repair. Front Biosci 11: 1958-1976.
205. Li X, Heyer WD (2008) Homologous recombination in DNA repair and DNA damage tolerance. Cell Res 18: 99-113.
206. Manolis KG, Nimmo ER, Hartsuiker E, Carr AM, Jeggo PA, et al. (2001) Novel functional requirements for non-homologous DNA end joining in *Schizosaccharomyces pombe*. EMBO J 20: 210-221.
207. Gottlich B, Reichenberger S, Feldmann E, Pfeiffer P (1998) Rejoining of DNA double-strand breaks in vitro by single-strand annealing. Eur J Biochem 258: 387-395.
208. Kabotyanski EB, Gomelsky L, Han JO, Stamato TD, Roth DB (1998) Double-strand break repair in Ku86- and XRCC4-deficient cells. Nucl Acids Res 26: 5333-5342.

209. Feldmann E, Schmiemann V, Goedecke W, Reichenberger S, Pfeiffer P (2000) DNA double-strand break repair in cell-free extracts from Ku80-deficient cells: implications for Ku serving as an alignment factor in non-homologous DNA end joining. Nucl Acids Res 28: 2585-2596.
210. Guirouilh-Barbat J, Huck S, Bertrand P, Pirzio L, Desmaze C, et al. (2004) Impact of the KU80 pathway on NHEJ-induced genome rearrangements in mammalian cells. Mol Cell 14: 611-623.
211. Guirouilh-Barbat J, Rass E, Plo I, Bertrand P, Lopez BS (2007) Defects in XRCC4 and KU80 differentially affect the joining of distal nonhomologous ends. Proc Natl Acad Sci U S A 104: 20902-20907.
212. Wu W, Wang M, Wu W, Singh SK, Mussfeldt T, et al. (2008) Repair of radiation induced DNA double strand breaks by backup NHEJ is enhanced in G2. DNA Repair (Amst) 7: 329-338.
213. Soulas-Sprauel P, Le Guyader G, Rivera-Munoz P, Abramowski V, Olivier-Martin C, et al. (2007) Role for DNA repair factor XRCC4 in immunoglobulin class switch recombination. J Exp Med 204: 1717-1727.
214. Yan CT, Boboila C, Souza EK, Franco S, Hickernell TR, et al. (2007) IgH class switching and translocations use a robust non-classical end-joining pathway. Nature 449: 478-482.
215. Corneo B, Wendland RL, Deriano L, Cui X, Klein IA, et al. (2007) Rag mutations reveal robust alternative end joining. Nature 449: 483-486.
216. Ferguson DO, Sekiguchi JM, Chang S, Frank KM, Gao Y, et al. (2000) The nonhomologous end-joining pathway of DNA repair is required for genomic stability and the suppression of translocations. Proc Natl Acad Sci U S A 97: 6630-6633.
217. Difilippantonio MJ, Zhu J, Chen HT, Meffre E, Nussenzweig MC, et al. (2000) DNA repair protein Ku80 suppresses chromosomal aberrations and malignant transformation. Nature 404: 510-514.
218. Morris T, Thacker J (1993) Formation of large deletions by illegitimate recombination in the HPRT gene of primary human fibroblasts. Proc Natl Acad Sci U S A 90: 1392-1396.
219. Nohmi T, Suzuki M, Masumura K, Yamada M, Matsui K, et al. (1999) Spi(-) selection: An efficient method to detect gamma-ray-induced deletions in transgenic mice. Environ Mol Mutagen 34: 9-15.
220. Canning S, Dryja TP (1989) Short, direct repeats at the breakpoints of deletions of the retinoblastoma gene. Proc Natl Acad Sci U S A 86: 5044-5048.
221. Smanik PA, Furminger TL, Mazzaferri EL, Jhiang SM (1995) Breakpoint characterization of the ret/PTC oncogene in human papillary thyroid carcinoma. Hum Mol Genet 4: 2313-2318.
222. Shrivastav M, De Haro LP, Nickoloff JA (2008) Regulation of DNA double-strand break repair pathway choice. Cell Res 18: 134-147.
223. Li G, Nelsen C, Hendrickson EA (2002) Ku86 is essential in human somatic cells. Proc Natl Acad Sci U S A 99: 832-837.
224. Myung K, Ghosh G, Fattah FJ, Li G, Kim H, et al. (2004) Regulation of telomere length and suppression of genomic instability in human somatic cells by Ku86. Mol Cell Biol 24: 5050-5059.

225. Rago C, Vogelstein B, Bunz F (2007) Genetic knockouts and knockins in human somatic cells. Nat Protoc 2: 2734-2746.
226. Seluanov A, Mittelman D, Pereira-Smith OM, Wilson JH, Gorbunova V (2004) DNA end joining becomes less efficient and more error-prone during cellular senescence. Proc Natl Acad Sci U S A 101: 7624-7629.
227. Fattah KR, Ruis BL, Hendrickson EA (2008) Mutations to Ku reveal differences in human somatic cell lines. DNA Repair (Amst) 7: 762-774.
228. Ruis BL, Fattah KR, Hendrickson EA (2008) The catalytic subunit of DNA-dependent protein kinase regulates proliferation, telomere length, and genomic stability in human somatic cells. Mol Cell Biol 28: 6182-6195.
229. Schulte-Uentrop L, El-Awady RA, Schliecker L, Willers H, Dahm-Daphi J (2008) Distinct roles of XRCC4 and Ku80 in non-homologous end-joining of endonuclease- and ionizing radiation-induced DNA double-strand breaks. Nucleic Acids Res 36: 2561-2569.
230. Adachi N, Ishino T, Ishii Y, Takeda S, Koyama H (2001) DNA ligase IV-deficient cells are more resistant to ionizing radiation in the absence of Ku70: Implications for DNA double-strand break repair. Proc Natl Acad Sci U S A 98: 12109-12113.
231. Karanjawala ZE, Adachi N, Irvine RA, Oh EK, Shibata D, et al. (2002) The embryonic lethality in DNA ligase IV-deficient mice is rescued by deletion of Ku: implications for unifying the heterogeneous phenotypes of NHEJ mutants. DNA Repair (Amst) 1: 1017-1026.
232. Lou Z, Chen BP, Asaithamby A, Minter-Dykhouse K, Chen DJ, et al. (2004) MDC1 regulates DNA-PK autophosphorylation in response to DNA damage. J Biol Chem 279: 46359-46362.
233. Ruscetti T, Lehnert BE, Halbrook J, Le Trong H, Hoekstra MF, et al. (1998) Stimulation of the DNA-dependent protein kinase by poly(ADP-ribose) polymerase. J Biol Chem 273: 14461-14467.
234. Ariumi Y, Masutani M, Copeland TD, Mimori T, Sugimura T, et al. (1999) Suppression of the poly(ADP-ribose) polymerase activity by DNA-dependent protein kinase in vitro. Oncogene 18: 4616-4625.
235. Galande S, Kohwi-Shigematsu T (1999) Poly(ADP-ribose) polymerase and Ku autoantigen form a complex and synergistically bind to matrix attachment sequences. J Biol Chem 274: 20521-20528.
236. Pleschke JM, Kleczkowska HE, Strohm M, Althaus FR (2000) Poly(ADP-ribose) binds to specific domains in DNA damage checkpoint proteins. J Biol Chem 275: 40974-40980.
237. Sartorius CA, Takimoto GS, Richer JK, Tung L, Horwitz KB (2000) Association of the Ku autoantigen/DNA-dependent protein kinase holoenzyme and poly(ADP-ribose) polymerase with the DNA binding domain of progesterone receptors. J Mol Endocrinol 24: 165-182.
238. Van Dyck E, Stasiak AZ, Stasiak A, West SC (1999) Binding of double-strand breaks in DNA by human Rad52 protein. Nature 398: 728-731.
239. Finnie NJ, Gottlieb TM, Blunt T, Jeggo PA, Jackson SP (1995) DNA-dependent protein kinase activity is absent in xrs-6 cells: implications for site-specific

recombination and DNA double-strand break repair. Proc Natl Acad Sci U S A 92: 320-324.
240. DeChiara TM (2001) Gene targeting in ES cells. Methods Mol Biol 158: 19-45.
241. Konishi H, Lauring J, Garay JP, Karakas B, Abukhdeir AM, et al. (2007) A PCR-based high-throughput screen with multiround sample pooling: application to somatic cell gene targeting. Nat Protoc 2: 2865-2874.
242. Choe, W., Budd, M. E., Imamura, O., Hoopes, L. & Campbell, J. L. Dynamic localization of an Okazaki fragment processing protein suggests a novel role in telomere replication. *Mol Cell Biol* **22,** 4202–4217 (2002).
243. Sirbu, B. M., Couch, F. B. & Cortez, D. Monitoring the spatiotemporal dynamics of proteins at replication forks and in assembled chromatin using isolation of proteins on nascent DNA. *Nat Protoc* **7,** 594–605 (2012).
244. López-Contreras, A. J. *et al.* A proteomic characterization of factors enriched at nascent DNA molecules. *Cell Rep* **3,** 1105–1116 (2013).
245. Sirbu, B. M. *et al.* Analysis of protein dynamics at active, stalled, and collapsed replication forks. *Genes Dev* **25,** 1320–1327 (2011).
246. Gerhardt, J. *et al.* The DNA replication program is altered at the Fmr1 locus in fragile x embryonic stem cells. *Mol Cell* **53,** 1–13 (2013).